Investigating Radiation in Combination with Oncolytic Vaccinia Virus to Improve the Treatment of Glioblastoma

by

Quinn Taras Storozynsky

A thesis submitted in partial fulfillment of the requirements for the degree of

Doctor of Philosophy

in

Cancer Sciences

Department of Oncology
University of Alberta

Abstract

Glioblastoma (GBM) is a malignant and immune-suppressed brain cancer that remains incurable despite the current standard of care. Radiotherapy is a mainstay of GBM treatment, however invasive cancer cells outside the irradiated field and radioresistance preclude complete eradication of GBM cells. Further, radiation induces cellular senescence in GBM cells. Senescent cells cease proliferation but remain viable and are implicated in promoting tumor progression. Oncolytic virus (OV) therapy harnesses tumor-selective viruses to spread through and destroy tumors while stimulating antitumor immune responses, and thus has potential for use following radiotherapy. We demonstrate that oncolytic Δ*F4L*Δ*J2R* vaccinia virus (VACV) replicates in and induces cytotoxicity of irradiated brain tumor initiating cells *in vitro*. Importantly, a single 10 Gy dose of radiation combined with Δ*F4L*Δ*J2R* VACV produced considerably superior anticancer effects relative to either monotherapy when treating immune-competent orthotopic CT2A-luc mouse models–significantly extending survival and curing the majority of mice. Following intracranial tumor challenges, mice cured by the combination displayed significantly increased survival relative to naïve age-matched controls, with some complete rejections. Further, the combination therapy was associated with an increased ratio of $CD8^+$ effector T cells to regulatory T cells compared to either monotherapy. Moreover, it is unknown how radiation-induced cellular senescence may impact the oncolytic properties of VACV-based OVs used in combination with radiotherapy. The interaction of viruses with senescent cells is nuanced; some viruses exploit the senescent state to their benefit, while others are hampered, indicating senescence-associated antiviral activity. To better understand this, we induced cellular senescence by treating GBM cells with radiation, and then evaluated the growth kinetics, infectivity, and cytotoxicity of oncolytic Δ*F4L*Δ*J2R* VACV, as well as wild-type VACV for comparison, in irradiated senescence-enriched and non-irradiated human GBM cell lines. Our results show that both viruses display attenuated oncolytic activities in irradiated

senescence-enriched GBM cell populations compared to non-irradiated controls. Taken together, these findings validate the use of radiation with an oncolytic Δ*F4L*Δ*J2R* VACV to improve treatment of this malignant brain cancer and indicate that radiation-induced cellular senescence is associated with antiviral activity–highlighting important considerations for the combination of VACV-based oncolytic therapies with senescence-inducing agents such as radiotherapy.

Preface

The research projects, of which this thesis is a part, received ethics approval from the University of Alberta Research Ethics Board, Project Name "Combination radiation and oncolytic vaccinia virus treatment for cancer", ID: AUP00001914. Animal studies were carried out at the Cross Cancer Institute and the University of Alberta, Edmonton, Alberta, and were conducted in accordance with the Canadian Council on Animal Care Guidelines and Policies with approval from the Cross Cancer Institute's Animal Care Committee and the Animal Care and Use Committee: Health Sciences for the University of Alberta.

Sections 1.4.1 and 1.4.2 of this thesis are modified from the following published work: "**Storozynsky, Q.T.,** and Hitt, M.M. (2020). The Impact of Radiation-Induced DNA Damage on cGAS-STING-Mediated Immune Responses to Cancer. *International Journal of Molecular Science*, *21*, 8877. https://doi.org/10.3390/ijms21228877."

Chapter 3 of this thesis has been modified from the following published work: "**Storozynsky, Q.T.,** Agopsowicz, K.C., Noyce, R.S., Bukhari, A.B., Han, X., Snyder, N., Umer, B.A., Gamper, A.M., Godbout, R.G., Evans, D.H., and Hitt, M.M. (2023). Radiation combined with oncolytic vaccinia virus provides pronounced antitumor efficacy and induces immune protection in an aggressive glioblastoma model. *Cancer Letters*, 562, 216169, doi:10.1016/j.canlet.2023.216169."

Chapter 4 of this thesis has been modified from the following published work: "**Storozynsky, Q.T.,** Han, X., Komant, S., Agopsowicz, K.C., Potts, K.G., Gamper, A.M., Godbout, R.G., Evans, D.H., and Hitt, M.M. (2023). Radiation-induced cellular senescence reduces susceptibility of glioblastoma cells to oncolytic vaccinia virus. *Cancers*, *15*, 3341. https://doi.org/10.3390/cancers15133341."

Acknowledgements

I would like to thank my supervisor, Dr. Mary Hitt, for providing me with the opportunity to embark on the challenging path of advancing cancer therapy. This academic experience allowed me to push my boundaries and discover untapped potential, and I am grateful for her support throughout this journey. During my graduate studies, Dr. Hitt provided exceptional support in various ways, including deep guidance for fulfilling requirements, always being readily available to review data, fostering independent thinking, and even assisting with experiments at the bench. I would also like to thank the members of my supervisory committee, Dr. Roseline Godbout and Dr. Armin Gamper for their support and guidance. I am greatly inspired by the immense work ethic, drive, and compassion exhibited by Dr. Godbout, as well as the quick intelligence and profound ability to comprehend and question research displayed by Dr. Gamper. These qualities serve as a model that I aim to emulate in my professional pursuits.

I would like to thank Kate Agopsowicz, Amirali Bukhari, Nicole Favis, Ryan Noyce, Brittany Umer, Shyambabu Chaurasiya, Dan McGinn, Cheryl Santos, and Sarah Samuelson for providing technical support, useful discussions, or experimental guidance throughout my studies. None of this work would have been possible without their assistance and dedication. I am incredibly grateful to Powel Crosley and Kyle Potts for helping lay the foundation of my success in the laboratory. Their guidance, teaching of numerous experimental techniques, responsiveness to my questions, and engaging discussions were invaluable shaping my research journey. I also thank my students, Shae Komant, Xuefei Han, Natalie Snyder, and Sheldon Cannon for their contributions to my projects and for helping me develop invaluable management and leadership skills.

I extend my appreciation to Dr. David Evans and others of the joint laboratory meetings for nurturing my capacity to present difficult scientific information, honing my communication skills, and enhancing my

ability to think on my feet. These gatherings played a pivotal role in the development and success of my research projects, particularly during times when I was the sole remaining member of the Hitt lab.

Flow cytometry was performed at the University of Alberta, Faculty of Medicine and Dentistry with assistance from Dr. Aja Rieger and Francisca Cristi Munoz. Imaging was performed at the University of Alberta, Department of Oncology Cell Imaging Facility with assistance from Dr. Xuejun Sun. I would especially like to extend my appreciation to Dr. Sun, for displaying unmatched dedication to his discipline. His commitment to our work extended beyond regular hours, as he even addressed and resolved imaging issues on several weekends.

I am profoundly grateful of the unwavering support and encouragement provided by my parents and family. I would be nothing without them. I also thank my close circle of friends for always believing in me and being a source of stress relief throughout this pursuit. Finally, I extend a heartfelt thanks to my partner, Tiffany, whose unwavering support, sacrifices, and beautiful soul have made this entire journey possible. Her dedication to my dreams has been a constant source of inspiration, and I truly believe that I wouldn't be the man I am today without her by my side.

This work was supported by a University of Alberta Li Ka Shing Institute of Virology Translational Research Grant (to M.M. Hitt) and a Canadian Institutes for Health Research (CIHR) Operating Grant (to D.H. Evans). Q.T. Storozynsky's stipend was also funded by the Alberta Cancer Foundation's “Antoine Noujaim Graduate Entrance Scholarship,” CIHR's “Frederick Banting and Charles Best Canada Graduate Scholarship,” the University of Alberta's “Walter H. Johns Graduate Fellowship,” “Queen Elizabeth II Graduate Scholarship,” “Doctoral Recruitment Award,” and “Faculty of Medicine and Dentistry Dean's Doctoral Award,” the Government of Alberta's “Alberta Graduate Excellence Scholarship,” the Li Ka Shing Institute of Virology's “Doctoral Student Award,” and the Terry Fox Research Institute's/Cancer Institute of Northern Alberta's “Marathon of Hope Graduate Studentship in Glioblastoma Research.”

Table of Contents

List of Tables

List of Figures

Abbreviations

2-HG	2-hydroxyglutarate
α-KG	α-ketoglutarate
AGMK	African green monkey kidney
ANOVA	Analysis of variance
ATCC	American Type Cell Culture Collection
ATRX	α-thalassemia/mental retardation syndrome X-linked
BiTEs	Bi-specific T-cell engagers
BSL2	Biosafety level 2
BTIC(s)	Brain tumor initiating cell(s)
CAR	Chimeric antigen receptor
cDC1s	Conventional DCs type 1
CDKN2A	Cyclin-dependent kinase inhibitor 2A
CDKN2B	Cyclin-dependent kinase inhibitor 2B
CDKs	Cyclin D-dependent kinases
cDNA	Complementary DNA
CEV	Cell-associated enveloped virus
cGas	Cyclic GMP–AMP synthase
CM	Conditioned media
CNS	Central nervous system
CTV	CellTrace™ Violet
CTV^{hi}	High intensity of CellTrace™ Violet
CTV^{lo}	Low intensity of CellTrace™ Violet
CXCL11	C-X-C motif chemokine ligand 11
dATP	Deoxyadenosine triphosphate
DCs	Dendritic cells
dCTP	Deoxycytidine triphosphate
DDR	DNA damage response

dGTP	Deoxyguanosine triphosphate
DNA-SCARS	DNA segments with chromatin alterations reinforcing senescence
dNDPs	Deoxynucleotide diphosphates
dNTPs	Deoxynucleotide triphosphates
ds	Double-stranded
dT	Deoxythymidine
dTMP	Deoxythymidine monophosphate
dTTP	Deoxythymidine triphosphate
dU	Deoxyuridine
dUMP	Deoxyuridine monophosphate
EBV	Epstein-barr virus
EEV	Extracellular enveloped virus
EFC	Entry-fusion complex
EGF	Epidermal growth factor
EGFR	Epidermal growth factor receptor
ER	Endoplasmic reticulum
FBS	Fetal bovine serum
FDA	Food and Drug Administration
FLASH-RT	FLASH radiotherapy
FMO	Fluorescence minus one
GBM	Glioblastoma
GSCs	Glioblastoma stem cells
HCC	Hepatocellular carcinoma
HG-DMEM	High glucose Dulbecco's modified Eagle's medium
HSV	Herpes simplex virus
hTERT	Human telomerase reverse transcriptase
ICB	Immune checkpoint blockade
ICD	Immunogenic cell death
ICI	Immune checkpoint inhibitor

IDH	Isocitrate dehydrogenase
IEV	Intercellular enveloped virus
IL	Interleukin
IFN	Interferon
IMV	Intracellular mature virus
ITRs	Inverted terminal repeats
IV	Immature virus
IVIS	In Vivo Imaging System
MEM	Minimal essential medium
MDSCs	Myeloid-derived suppressor cells
MGMT	O^6-methylguanine-DNA-methyltransferase
MHC I	Major histocompatibility complex class I
M-MDSCs	Monocytic myeloid derived suppressor cells
MMPs	Matrix metalloproteinases
MOI	Multiplicity of infection
MRI	Magnetic resonance imaging
mRNA	Messenger RNAs
NADPH	Nicotinamide adenine dinucleotide phosphate
NDPs	Nucleotide diphosphates
NDV	Newcastle disease virus
NOS	Not Otherwise Specified
NSC	Neural stem cells
NSG	NOD-*scid*-gamma (NOD.Cg-Prkdcscid Il2rgtm1Wjl/SzJ)
NYCBH	New York City Board of Health
OV(s)	Oncolytic virus(es)
PAMPs	Pathogen-associated molecular patterns
PBK	Protein kinase B
PBS	Phosphate buffered saline
PD1	Programmed cell death protein 1

PD-L1	Programmed death ligand 1
PFU	Plaque-forming units
PI3K	Phosphoinositide 3-kinase
PKR	Protein kinase R
PMN-MDSCs	Polymorphonuclear myeloid derived suppressor cells
PRRs	Pattern recognition receptors
PVDF	Polyvinylidene difluoride
Rb	Retinoblastoma
RR	Ribonucleotide reductase
RRM2	Ribonucleotide reductase small subunit R2
RT-qPCR	Reverse transcription quantitative polymerase chain reaction
SA-β-gal	Senescence-associated-β-galactosidase activity
SAHF	Senescence-associated heterochromatin foci
SARRP	Small animal radiation research platform
SASP	Senescence-associated secretory phenotype
SFRT	Spatially fractionated radiation therapy
SRS	Stereotactic radiosurgery
STR	Stereotactic radiotherapy
STING	Stimulator of interferon genes
SVZ	Subventricular zone
TAM	Tumor-associated macrophage
TAM/Mi	Tumor-associated macrophage and microglia
TCR	T cell receptor
TERT	Telomerase reverse transcriptase
TILs	Tumor infiltrating lymphocytes
TIM-3	T-cell immunoglobulin mucin-3
TK	Thymidine kinase
TME	Tumor microenvironment
TMZ	Temozolomide

TNF	Tumor necrosis factor
TP53	Tumor protein p53
TRAIL	Tumor necrosis factor-related apoptosis-inducing ligand
Tregs	Regulatory T cells
TTF	Tumor-treating fields
T-VEC	Talimogene laherparepvec
VACV	Vaccinia virus
VSV	Vesicular stomatitis virus
WHO	World Health Organization
WR	Western Reserve
WT	Wild-type
YPLL	Years of potential life lost

CHAPTER 1: General Introduction

Preface

Sections 1.4.1 and 1.4.2 of this chapter are modified from the following published work:

"**Storozynsky, Q.T.,** and Hitt, M.M. (2020). The Impact of Radiation-Induced DNA Damage on cGAS-STING-Mediated Immune Responses to Cancer. *International Journal of Molecular Science*, *21*, 8877. https://doi.org/10.3390/ijms21228877."

1.1 Glioblastoma

Glioblastoma (GBM) is a malignant brain cancer that requires an aggressive first line standard of care involving surgery, then concurrent administration of radiotherapy and temozolomide (TMZ; a chemotherapeutic alkylating agent), followed by adjuvant cycles of TMZ[1]. Recently, antimitotic tumor-treating fields (TTFs), a therapy in which alternating electric fields are used to disrupt mitosis of GBM cells, has been approved for treating newly diagnosed GBM. TTFs have been shown to improve overall survival when used to supplement adjuvant administration of TMZ[2,3].

Despite the present standard of care, recurrence within 2 cm of the original tumor border is virtually inevitable[4,5] (**Figure 1.1**). Thus, patient prognosis is dismal; the median survival for GBM patients ranges between 12-16 months[6] and approximately 93-96% of patients are deceased within 5-years[7,8]. In recurrent settings, treatment consensus is absent. Second line treatment remains specific to the institution providing care[1], but progression of disease is still expected. Given the failure of first line and second line treatment regimens to control GBM, novel therapeutic strategies are urgently needed to improve outcomes of this disease.

1.1.1 Epidemiology and risk factors. GBM makes up 14.3% of diagnoses of non-malignant and malignant primary brain and central nervous system (CNS) cancers[7]. Among the deadliest brain and CNS diagnoses, GBM is the most prevalent and subsequently responsible for killing the most patients[7]. The annual incidence rate of GBM is low, at 3.23 per 100,000 population[7]. Furthermore, years of potential life lost (YPLL) is greatest with malignant brain tumors in comparison to other cancers. Malignant brain tumors account for approximately 19.9 YPLL, versus 9.6 YPLL with prostate cancer, 14.5 YPLL with lung/bronchus cancers, and 15.1 YPLL with pancreatic cancers[9].

Increased risk for developing GBM is associated with several features. GBM occurs 1.1 to 2.6 times more frequently in males than females[7,10,11]. Incidence also increases with age; more than half of GBM

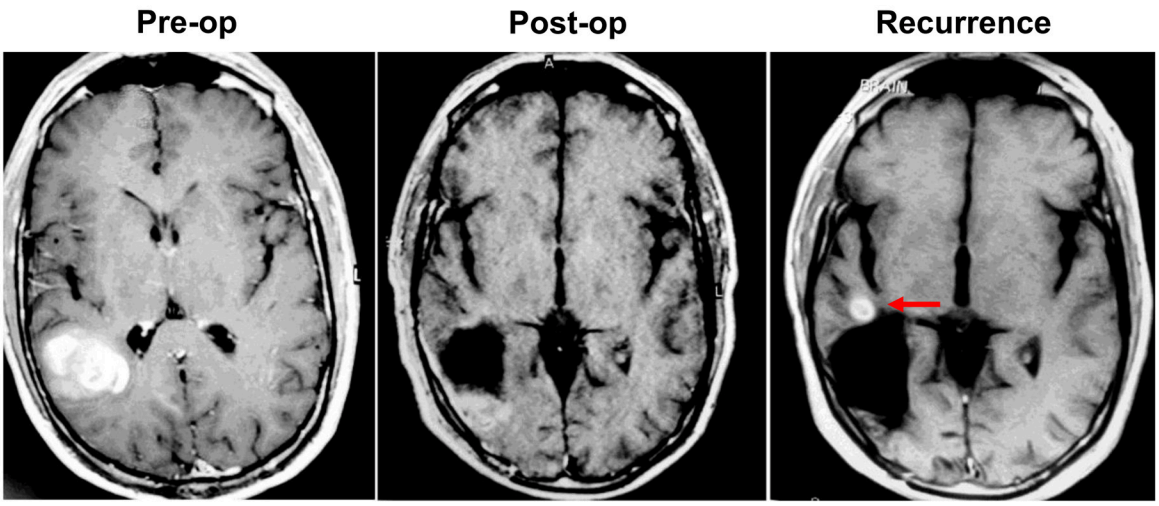

Figure 1.1. Glioblastoma images. Contrast enhanced magnetic resonance imaging of glioblastoma before surgical rection (pre-op), after surgical resection (post-op), and of local recurrence within 2 cm of the original tumor border (indicated by red arrow) 10 months later. Figure adapted from [5] with permission.

diagnoses occur over the age of 65 and the highest incidence rates are between age 75 to 84[7]. Other risk factors include exposure to ionizing radiation, familial genetic disorders, and potentially, certain viral infections. Computed tomography imaging of the brain in children is associated with up to a three-fold increased risk for developing brain cancer[12,13]. Individuals with genetic maladies related to DNA repair processes or cell-cycle regulation, such as Lynch syndrome and Li-Fraumeni syndrome, have an increased risk for developing GBM[14,15]. Interestingly, several reports suggest that cytomegalovirus and epstein-barr virus (EBV) may be associated with GBM tumorigenesis[16–18], though, these observations remain controversial[19,20]. Remarkably, immune hypersensitivities may have a protective role preventing GBM as individuals with allergies/atopy show decreased incidences of high-grade gliomas and GBM[21,22]. Indeed, recent preclinical *in vivo* studies have demonstrated allergic inflammation hinders GBM progression[23].

1.1.2 Presentation, diagnosis, and pathological features. Before GBM is diagnosed, patients present with a variety of symptoms. This can include common symptoms like headache, fatigue, nausea, and seizure, as well as less common motor, sensory and neurological symptoms such as ataxia, speech/visual impairments, dizziness, anxiety, sleeplessness, and cognitive deficit[24]. GBM is first diagnosed using gadolinium-enhanced magnetic resonance imaging (MRI); subsequently, histopathological diagnosis is confirmed from biopsy tissue obtained during surgery[24].

Histology remains the definitive diagnostic tool for GBM. Remarkably, advanced artificial intelligence systems have recently been integrated to aid with histological diagnosis of gliomas with success[25]. Histological hallmarks for GBM include nuclear atypia, a high mitotic index, microvascular hyperplasia, neovascularization, and pseudopalisading necrosis[26,27]. Pseudopalisading necrosis is a unique histological feature associated with GBM, resembling a “picket-fence line” of migrating rows of cells that surround areas of necrosis[27,28]. These dense rows of pseudopalisading migratory cells appear to be fleeing nutrient-deprived areas (necrotic tissue) towards more suitable oxygenated microenvironments[27,28].

1.1.3 Classification. GBM is classified as a grade 4 primary brain tumor by the World Health Organization (WHO)[29]. In the past, Roman numerals were used to represent grades (*i.e.,* grade I, II, III, IV), however the most recent 2021 WHO classification system opted to using Arabic numerals (*i.e.,* grade 1, 2, 3, and 4)[29]. The major characteristic that separates grade 3 and 4 brain tumors from grade 1 and 2 is significant mitotic activity, while necrosis or microvascular proliferation separates grade 4 from 3[26].

The WHO nomenclature system of CNS tumors uses a hybrid taxonomy model, in which histology and molecular features classify tumor types. Formally, under the 2016 WHO nomenclature, GBM was classified in three categories, all of which were designated as grade 4 disease; (1) *GBM, isocitrate dehydrogenase (IDH)-wild-type (WT),* (2) *GBM, IDH-mutant*, or (3) *GBM, NOS (Not Otherwise Specified)*[30]. Under the most recent 2021 WHO nomenclature, *astrocytoma, IDH-mutant, grade 4* replaced the term *GBM, IDH-mutant* from the 2016 WHO nomenclature[29,30], and *GBM, NOS* is no longer a classification[29]. Although, the classification of *GBM, IDH-mutant* was changed to astrocytoma, the molecular distinction between IDH-WT and IDH-mutant is still relevant in GBM literature (more details in section 1.1.6).

Astrocytoma, IDH-mutant, grade 4 (previously termed *GBM, IDH-mutant*) is defined as a diffusely infiltrative astrocytic glioma with one or any combination of the following: microvascular proliferation, necrosis, and/or homozygous deletion of cyclin-dependent kinase inhibitor 2A (*CDKN2A*) or cyclin-dependent kinase inhibitor 2B (*CDKN2B*)[26,29]. GBM*, IDH-WT, grade 4* is defined as an IDH-WT, diffuse astrocytic glioma, with one or more of the following: microvascular proliferation, necrosis, telomerase reverse transcriptase (*TERT*) promoter mutation, epidermal growth factor receptor (*EGFR)* gene amplification, or gain of entire chromosome 7 and loss of entire chromosome 10 (+7/-10)[26,29].

GBM can also be separated into four clinically relevant subtypes; *proneural*, *neural*, *classical*, and *mesenchymal*[31]. These GBM subtypes respond differentially to intense standard of care relative to less aggressive treatment regimens (*i.e.,* non-concurrent chemo- radiotherapy or shorter chemotherapy

courses). Classical and mesenchymal subtypes responded best, followed by neural, while proneural responded poorly[31]. Further, unique immunological profiles are associated with each subtype. Notably, mesenchymal is the most immunologically "hot", which suggests potentially favourable responsiveness with immunotherapy[32,33], whereas proneural is immunologically "cold", suggesting less favourable immunotherapeutic responses[33]. It should be noted that the classification of four GBM subtypes is contested. One study, using a different form of integrated genome analysis than in [[31]], reported only three subtypes–proneural, classical, and mesenchymal[34]. Another study indicated that the original identification of the neural subtype was due to contamination[35]. Lastly, signatures of all four GBM subtypes have been identified within individual patient tumors using singe-cell sequencing[36], indicating that a single tumor can be composed of multiple subtypes.

1.1.4 Origin and glioblastoma stem cells. Two main theories postulate the cellular etiology of GBM. Lee *et al.* (2018) provide evidence that the cell-of-origin for GBM tumorigenesis may result from low-level driver mutations in neural stem cells (NSCs) of the subventricular zone (SVZ)[37], a region in the brain that is rich in NSCs and involved in neurogenesis[38]. Friedmann-Morvinski *et al.* (2012) offer a different cell-of-origin source for GBM initiation, suggesting that differentiated astrocytes or neurons with p53 deficiencies and active Ras signaling can dedifferentiate into a stem-like cells capable of initiating GBM[39]. There is currently no consensus as to which proposed mechanism is responsible for GBM[40].

On a related note, although the GBM cell-of-origin remains to be elucidated, it is generally accepted that GBM tumors contain stem-like and/or progenitor-like cancer cells–colloquially referred to as brain tumor initiating cells (BTICs) or GBM stem cells (GSCs)[41,42]. These cells possess stem cell characteristics such as self-renewal, multilineage differentiation, and expression of NSC markers[43,44]. In addition to having a potential role in GBM initiation, BTICs/GSCs are proposed to be responsible for the maintenance and recurrence of GBM[41,45] and correlate with poorer prognosis[46]. Further, BTICs/GSCs are

resistant to radiotherapy[47,48] and TMZ[49]; as such, elimination of these cell types is an important goal of novel GBM therapies[50].

1.1.5 Common genetic abnormalities. In GBM, the most common genetic aberrations occur in three regulatory pathways: (1) phosphoinositide 3-kinase (PI3K)/protein kinase B (PBK; also called AKT)/RAS (88–90%), (2) p53 (86–87%), and (3) retinoblastoma (Rb; 78–79%)[51,52]. Chiefly, these regulatory networks regulate cell-cycle progression, hence genetic disruptions can distort normal signal transduction and lead to uncontrolled cell division. Specific genetic aberrations common to GBM include perturbations of the *TERT* promoter (55–80%)[53,54], α-thalassemia/mental retardation syndrome X-linked (*ATRX*; 11-80%)[55,56], tumor protein p53 (*TP53*; 28–40%)[51,52,57,58], phosphatase and tensin homolog (*PTEN*; 24–41%)[51,52,57,58], *CDKN2A* (31–61%)[51,52,57,58], *CDKN2B* (47-61%)[51,52], and amplification/mutation of *EGFR* (34-57%)[51,52,57–59] (among others).

TERT and *ATRX* relate to telomere maintenance. *TERT* encodes telomerase, an enzyme that maintains telomere length on chromosome ends that would otherwise be lost over many cycles of DNA replication and trigger inhibitory proliferative signals[60]. Mutations of the *TERT* promoter increase telomerase activity thereby preventing telomere-erosion, which enables continued mitotic rounds[60]. Similarly, perturbations of *ATRX* maintains telomere length through a mechanism independent of telomerase termed alternative lengthening of telomeres[61].

TP53, *PTEN*, *CDKN2A*, and *CDKN2B* are tumor suppressor genes. *TP53* encodes p53, a 53 kDa transcription factor proverbially referred to as the "guardian of the genome[62]." Broadly speaking, p53 responds to genetic damage or oncogene activation by initiating cell-cycle arrest, apoptosis, cellular senescence, or DNA repair[62]. *PTEN* encodes PTEN, a phosphatase that negatively regulates kinase signaling cascades that lead to cell-cycle progression, cell survival, angiogenesis, and migration/invasion (*i.e.,* the PI3K/PBK (AKT) pathway)[63]. *CDKNA2A* encodes two distinct proteins, $p16^{INK4A}$ and $p14^{ARF}$, while

CDKNA2B encodes $p15^{INK4b}$, all of which block cell-cycle progression[64]. $p16^{INK4A}$ and $p15^{INK4b}$ inhibit cyclin D-dependent kinases (CDKs) which coordinate cell-cycle progression[64], while $p14^{ARF}$ facilitates p53-induced cell-cycle arrest by negatively regulating its inhibitor, Mdm2[64].

Lastly, *EGFR* encodes for a receptor tyrosine kinase, EGFR, which upon binding its ligand, epidermal growth factor (EGF), activates signaling cascades involved in cell growth (*i.e.,* PI3K/PKB (AKT) and RAS pathways)[59]. EGFR variant III (EGFRvIII), is a mutated constitutively active version of EGFR that can be co-expressed with normal (but amplified) EGFR or be expressed in the absence of EGFR amplification[59].

1.1.6 Meaningful biomarkers. GBM patients with methylated O^6-methylguanine-DNA-methyltransferase (*MGMT*) promoters have superior treatment outcomes (median survival of 21.7 months *vs*. 15.3 months)[65]. TMZ cytotoxicity is attributed primarily to methylation of O^6-guanine in DNA molecules (but also methylates N^7-guanine and N^3-adenine) which results in cell death if the adduct is left unrepaired[66,67]. MGMT activity disrupts the efficacy of alkylating agents by removing O^6 methylation, hence silencing of *MGMT* expression enhances TMZ therapy[68].

GBM patients with mutant IDH have substantially better treatment outcomes than IDH-WT patients[58,69]. Only 10% of GBM patients are IDH-mutant while 90% are IDH-WT[30]. At the time of diagnosis, IDH-WT patients present with advanced disease, whereas IDH-mutant patients present with a lower grade 2/3 glioma which progresses overtime to grade 4 disease[30]. Enzymatic activity of IDH-WT produces α-ketoglutarate (α-KG) and nicotinamide adenine dinucleotide phosphate (NADPH) within the Krebs Cycle[70]. However, IDH-mutant activity produces an oncometabolite, 2-hydroxyglutarate (2-HG) and less NADPH[70]. Reduced NADPH levels are proposed to enhance oxidative stress induced by radiotherapy and chemotherapy due to impaired scavenging of reactive oxygen species; this may partially account for improved IDH-mutant prognosis[71]. Although IDH-mutant patients have better outcomes, the 2-HG oncometabolite competes to bind α-KG-dependent histone demethylases which results in downstream

epigenetic alterations believed to drive tumorigenesis[72]. This may explain why IDH-mutant GBMs progress from lower grade gliomas.

1.1.7 Standard of care. The "Stupp protocol" forms the basis of present-day first line standard of care for GBM and involves surgery, radiotherapy, and administration of TMZ[27,73]. The protocol was established in 2005 after a successful phase III randomized clinical trial improved median survival from 12.1 months to 14.6 months with the introduction of TMZ to surgery and radiotherapy[73]. Since 2005, the standard of care for GBM has remained unchanged (note: TTFs are recently available, but the technology is seldom used)[27] (**Figure 1.2**).

Surgery is performed first (if possible) to reduce tumor associated mass effects, defer recurrence, and obtain biopsy material for diagnostic purposes[27]. The highly invasive nature of GBM precludes complete resection, therefore additional therapeutic approaches are required to target remaining GBM cells. A total radiation dose of 60 Gy is delivered in 30 fractions (2 Gy per day) over 6 weeks to the resection cavity, gross residual tumor, and an additional 2-3 cm margin–which compose the clinical treatment volume–using pre- and post-operative MRI scans[74]. A further 3-7 mm margin surrounding the clinical treatment volume (i.e., the planning treatment volume) is added to account for day-to-day variations in patient position, setup, and movement[74]. Of note, radiation doses less than 60 Gy produce inferior survival outcomes[75] and doses in excess increase radionecrosis of normal tissue (a major limiting factor)[76,77]. TMZ is administered concurrently with radiotherapy at a dose of 75 mg/m^2 of body surface area per day[73]. Following chemo-radiation, TMZ is further administered at a dose of 150 mg/m^2 of body surface area for 5 days during a 28-day cycle, for up to 6 cycles[73].

For elderly GBM patients a hypofractionated radiation plan (*i.e.,* delivery of fewer, larger doses, usually exceeding 2 Gy) is also used with similar efficacy as conventionally fractionated radiotherapy (60 Gy over 30 fractions) in which a total dose of 40 Gy is administered across 15 fractions (2.67 Gy per fraction)[78].

This hypofractionated treatment was further improved with the addition of TMZ[79], and even higher radiation doses (3.4 Gy per fraction, total dose of 34 Gy) have shown improved outcomes compared with conventional fractionation (60 Gy over 30 fractions) in elderly cohorts[80]. Of note, there is a trend in radiation oncology towards the implementation of hypofractionated over conventionally fractionated regimens, for example, in breast[81], prostate[82], lung[83], rectal[84], liver[85], head and neck[86], and gynecologic cancers[87]. Importantly, part of the efficacy associated with hypofractionated radiotherapy is attributed to the stimulation of antitumor immune responses[88–90]. Further, hypofractionated radiotherapy may also reduce systemic loss of T cells[91]. These reports suggest that higher radiation doses may be superior to conventional dosing in terms of harnessing immune-mediated antitumor effects.

TTFs were recently approved for treating newly diagnosed GBM after a successful phase III randomized clinical trial improved median survival from 16.0 months to 20.9 months with the addition of TTFs to maintenance cycles of TMZ[3]. TTFs are administered using a portable, non-invasive, helmet-like device that delivers cranial alternating electric fields to disrupt mitosis of GBM cells[92]. Despite improved efficacy, use of this modality remains limited (3–12% of patients) due to cost, patient inconvenience (must wear 18 hours per day), and skepticism of the mechanism (despite the clinical trial data)[93].

Lastly, TMZ and radiotherapy delivered as outlined in the Stupp protocol reduces patient tumor infiltrating lymphocytes (TILs) and causes immune-suppression that correlates with worse prognosis[94–101]. Further, patients frequently receive corticosteroids (*i.e.,* dexamethasone) to manage tumor-associated cerebral edema throughout standard of care[1]. Corticosteroids are well-known immune-suppressants also reported to negatively affect treatment outcomes of GBM[102,103]. Notably, elevated TIL levels correlate with a better prognosis in GBM patients[104,105], even despite systemic immune-suppression[106]. In fact, GBM patients with high TIL levels benefited the most from dendritic cell (DC) vaccine immunotherapy[107]. These findings indicate that novel therapeutic approaches capable of breaking immune-suppression may be important to integrate into GBM.

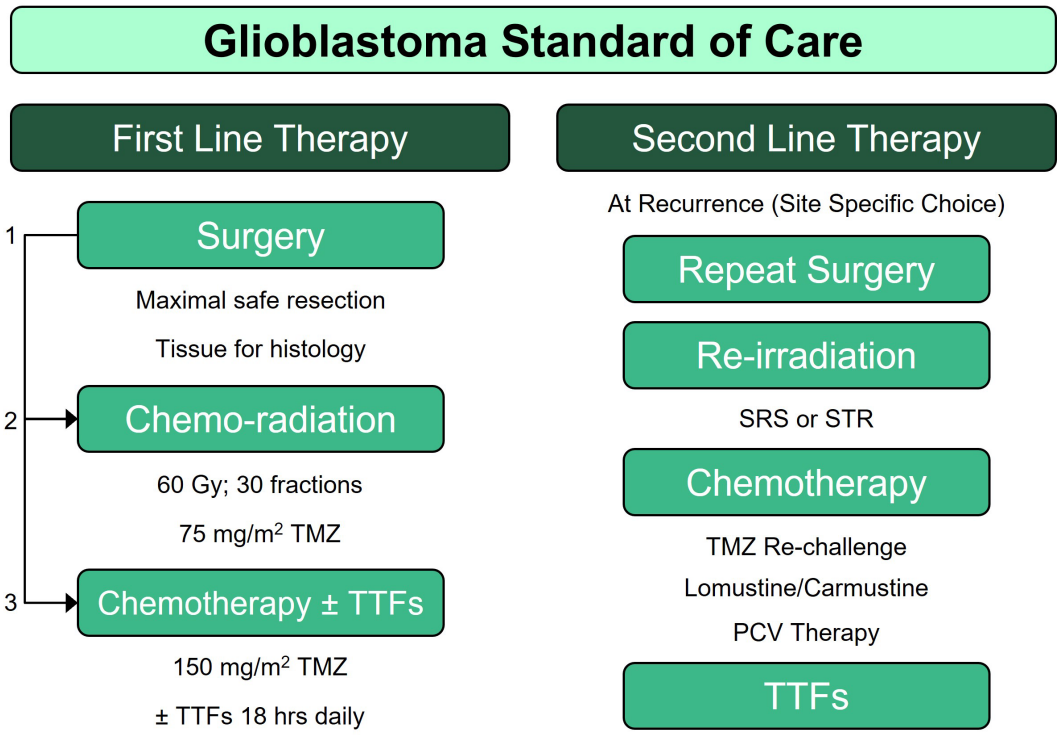

Figure 1.2. Glioblastoma treatment regimens. First line standard of care begins with surgery (1), followed by chemo-radiation (2), then an adjuvant course of chemotherapy, with TTFs if available (3). Established second line therapy is undefined at present; therefore, treatment is specific to the healthcare site evaluating the disease. **Abbreviations**: ± indicates with or without; Gy, grays; PCV, procarbazine, lomustine, and vincristine regimen; SRS, stereotactic radiosurgery; STR, stereotactic radiotherapy; TMZ, temozolomide; TTFs, tumor-treating fields.

1.1.8 Recurrence. Following first line therapy recurrence is expected within only 6 months[108] and there is no established consensus on standard of care in this setting[1], hence, several different therapeutic strategies are used depending on the institution treating the disease (**Figure 1.2**). Repeat operation may be considered and can moderately benefit some patients, but the role of surgery in managing GBM recurrence remains unclear[109]. Alkylating chemotherapy is often used in recurrent settings. Patients with *MGMT* promoter methylation benefit from TMZ rechallenge in comparison to patients without this methylation[110]. Alternative alkylating agents to TMZ, such as carmustine, lomustine, and the combination of procarbazine/lomustine/vincristine (PCV therapy) are other options utilized[111–113]. Interestingly, TTFs have shown equivalent survival outcomes as chemotherapeutic approaches in recurrent settings while also offering substantial reductions in toxicity and improved quality of life (the worst toxicities are skin irritation where electrodes are placed on skull)[114].

Re-irradiation offers a non-invasive, targeted approach that can provide modest control for recurrent GBM[115]. Re-irradiation is usually administered as a high, single-fraction dose (or over a few high-dose fractions) via stereotactic radiosurgery (SRS; typically using a GammaKnife) or over multiple fractions via hypofractionated or conventionally fractionated stereotactic radiotherapy (STR; typically using a LINAC)[116]. The chief difference between SRS and STR is the steep ablative dose gradient associated with SRS. SRS can be used to deliver a single-fraction of 10–22 Gy (sometimes greater) to the tumor site[117], whereas hypofractionated SRT and conventionally fractionated SRT deliver 2.5–5 Gy fractions or 2 Gy fractions, respectively[116]. Of note, several studies that used a high, single-fraction dose to treat preclinical models (mimicking SRS) indicated that efficacy was associated with antitumor immune activation[118–121]. Further, SRS has been proposed as a tool to immunologically stimulate the brain tumor microenvironment[122] and is currently being clinically evaluated to potentiate immunotherapies[123].

Overall, despite available salvage therapies progression of the disease is virtually inevitable–underscoring an urgent need for novel therapeutic strategies. Notably, given an established safety

profile using SRS to treat recurrent GBM[124] and recent promise of modalities harnessing immune-based destruction of GBM[125], high single-fraction radiotherapy may be a solid candidate to investigate in combination with other immunological therapeutics (like oncolytic viruses [OVs], the focus of this thesis).

1.2 Cellular Senescence

Senescence is a near permanent state in which cells cease proliferation but remain metabolically active. The phenotype was initially described by Hayflick and Moorhead in the 1960's after observing that human fibroblasts ceased proliferation after a certain number of cell divisions–this threshold was termed the *Hayflick limit*[126,127]. Since then, a collection of senescence hallmarks have been described that identify senescent cells *in vitro* and *in vivo*[128,129]. Importantly, a number of biological contexts involve senescence including various age-related pathologies (including cancer), developmental processes, immune modulation, and tissue repair[130]. Further, a unique characteristic of cellular senescence is the senescence-associated secretory phenotype (SASP), in which senescent cells secrete a variety of different factors that cause downstream effects[131] (discussed further in section 1.2.3). Of relevance to cancer, factors secreted via the SASP can exacerbate tumor progression and induce pro-tumorigenic events[132,133]. Therefore, identifying potential therapies that clear senescent cells is of great interest for improving cancer outcomes[134].

1.2.1 Induction. Cellular senescence is induced by myriad stimuli including but not limited to, telomere attrition over many cycles of division, oncogenic activation, reduced oxygen levels, dysfunctional mitochondria, and exposure to DNA-damaging agents[135]. These stimuli produce cellular insults which cause signaling networks to coordinate to resolve the issue, leading to cell cycle arrest that is typically p53-mediated. If the insult is repaired, cell cycle arrest is transient, but if unresolved, persistent cell cycle arrest is enforced. To fully engage the senescence program, a prolonged period of

negative cell cycle regulation is required[136]. It is believed that $p21^{WAF1/CIP1}$ participates in the initiation of senescence, but that durable arrest is mediated by sustained $p16^{INK4A}$ signaling[136–138]. However, the senescent state is enforced by many other factors, including heterochromatization which precludes expression of pro-proliferative genes[139], SASP factors reinforcing the senescent state[131,140,141], sustained DNA damage response (DDR) signaling[142,143], and degradation of nuclear laminin B1 which alters the global chromatin landscape and gene expression, as well as releases cytoplasmic chromatin fragments that reinforce senescence through cyclic GMP–AMP synthase (cGAS)/stimulator of interferon genes (STING) cGAS-STING signaling[144–148].

1.2.2 Hallmarks. The paramount marker of senescence is the cessation of cell division[126,127]. However, this single feature is insufficient for distinguishing the senescent phenotype from non-proliferating quiescent, terminally differentiated, or exhausted cells[149]. Therefore, multiple hallmarks are required to identify senescence (**Figure 1.3**). Arguably the most frequently evaluated senescence marker is senescence-associated-β-galactosidase activity (SA-β-gal), which under pH conditions subpar for enzymatic activity, allows detection of β-gal activity in senescent cells but not in non-senescent cells[150]. Importantly, SA-β-gal activity can be evaluated both *in vitro* and *in vivo* contributing to its broad use and application[150,151]. To further characterize cell cycle arrest, the levels of negative cell cycle regulators are also interrogated, of which the most common are $p16^{INK4A}$ and $p21^{WAF1/CIP1}$ [128,129]. Visually, increased cell size and the formation of punctate DNA foci, termed "senescence-associated heterochromatin foci" (SAHF), are other hallmarks of senescence[127,139]. Of note, an increase in cell size drives senescence-associated alterations of the proteome[152] while the formation of SAHF represses expression of pro-proliferative genes[139]. Further, senescent cells form distinct, persistent DNA lesions, termed "DNA segments with chromatin alterations reinforcing senescence" (DNA-SCARS), which associate with DDR proteins and are involved in maintaining the SASP[153,154]. The SASP, being a unique hallmark of senescence, is frequently detected by evaluating the expression levels of established SASP factors[128,129].

Additionally, decreased levels of nuclear lamin B1 is associated with cellular senescence and can be used as a marker[145]. Lastly, other senescence-associated cell surface markers have been proposed[155] and more recently, lipofuscin, which is an aggregate of oxidized lipids that accumulates in lysosomes of senescent cells, has been used as a marker for senescence[156].

1.2.3 Biological effects of senescence and the SASP. Senescent cells are secretory cells which modulate surrounding cells and tissue compartments via their SASP. The SASP is regulated by networks involving mTOR[157], NF-κB[158], and persistent DNA damage signaling[154]. The SASP exerts pleiotropic biological effects in both autocrine and paracrine ways via secretion of pro-inflammatory cytokines/chemokines, as well as other factors such as mitogens, matrix metalloproteinases (MMPs), lipids, and extracellular vesicles[140,141,159]. Several biological activities and therapeutic applications associated with senescence and the SASP are outlined below.

Immune-mediated clearance. SASP-mediated chemokine/cytokine signaling can attract and activate host immune cells such as natural killer cells, macrophages, and CD4+ T cells to coordinate targeted elimination of senescent cells[160–164]. In this way, senescence can be framed as a signaling mechanism for the coordinated removal of dysfunctional, pre-malignant, or injured cells.

Role in developmental processes. Cellular senescence helps to instruct growth, patterning, and remodeling in normal mammalian and avian embryonic developmental processes[165,166]. Interestingly, in the developmental process senescent cells are removed by programmed cell death or macrophages[165,166]. These findings suggest that senescent cells function to transiently modulate certain developmental processes. Further, senescence also plays a role in the development of amphibians and fish (indicating it is a common feature among vertebrates)[167,168].

Tissue repair and remodelling. Senescent fibroblasts accelerate wound healing via secretion of growth factors[169] and also limit fibrosis[170]. The resolution of fibrosis is thought to be aided by the elimination of

senescent cells by natural killer cells and the secretion of MMPs by senescent cells[171]. Further, SASP factors can induce stem-like plasticity in exposed cells enabling tissue regenerative capacities *in vivo*[172]. Collectively, senescent cells play a role in repairing or replenishing tissue compartments.

Disease and cancer. Senescent cells accumulate with age and the pro-inflammatory nature of the SASP contributes to age-related pathologies such as osteoarthritis[173], atherosclerosis[174], neurodegenerative disease[175], and cancer[176]. The role of cellular senescence in cancer is nuanced[176], acting as a tumor-suppressive mechanism in some contexts[177–180], while contributing to tumorigenesis and tumor growth in others[132,133,180–184]. Senescence can both contribute to, or impair, immune-mediated clearance of cancer cells[180]. Additionally, although normal senescent cells can facilitate tissue repair and tissue remodeling, senescent cancer cells exacerbate tumor growth[132,183], induce *de novo* cancer stem cells[133], and acquire an aggressive phenotype following spontaneous bypass of the senescent state[133,184]. These findings highlight the dual nature of senescence and the SASP, having beneficial aspects in the context of normal repair, regeneration, and immune-surveillance, but detrimental aspects in the context of cancer. Furthermore, senescent cancer cells enhance the invasiveness of cancer[131,182] and facilitate cancer relapse[181]. These data indicate that removal of senescent cancer cells could be a fruitful therapeutic strategy.

Targeting senescence and the SASP. Due to the detrimental effects of senescence in cancer and other age-related pathologies, therapeutic strategies to blunt or modulate the SASP are actively being explored[185]. Further, the field of *senolytics* has emerged, which seeks to identify agents that can selectively deplete senescent cells or that harness immune-mediated clearance of senescent cells[186].

1.2.4 A word on antagonistic pleiotropy. Given the detrimental roles of senescence in the health of individuals, why is senescence an evolutionarily preserved phenomenon? This paradox can be resolved by applying the concept of *antagonistic pleiotropy*, which states that a biological process can be

both beneficial and detrimental at different time points in the organisms lifespan[187]. In short, from an evolutionary perspective, aged individuals are scarce, often removed by the fatal hazards of nature; thus, a biological process that confers a benefit to survival and reproduction *early* will be selected for despite that same process having detrimental effects *late* in an organism's lifespan. In a sense, the forces of natural selection "miss" the detrimental late effects of the biological process because the beneficial early effects increase the propensity to survive and reproduce. Hence, senescence both aids in tumor-suppression, tissue repair, and development, while also facilitating a range of age-related pathologies later in life[188].

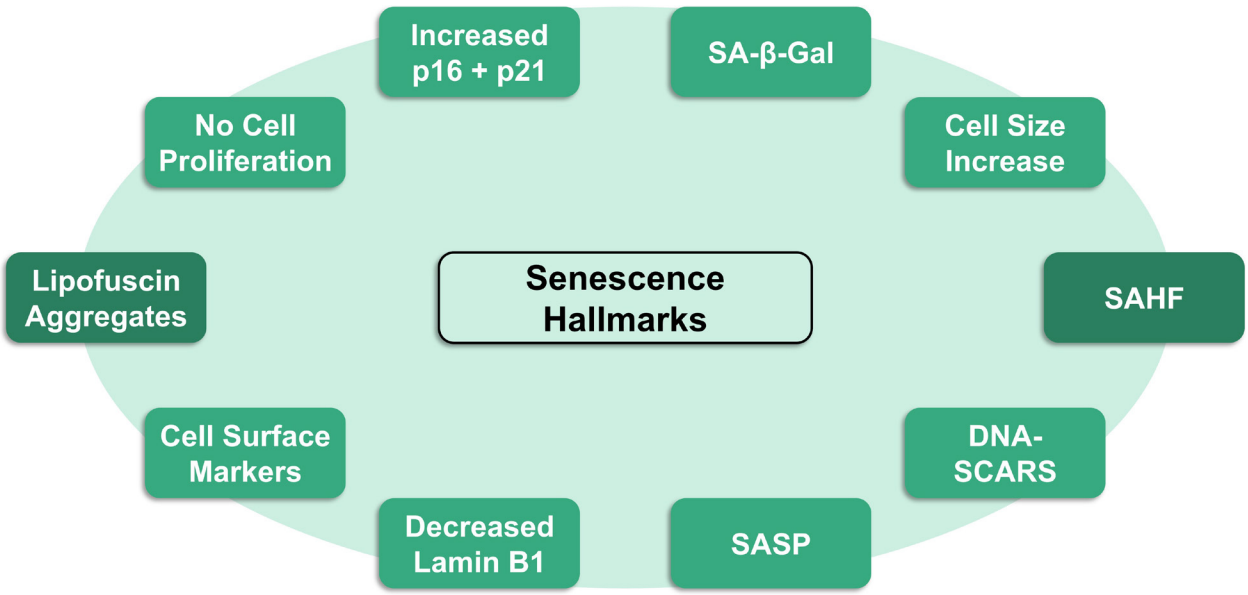

Figure 1.3. Hallmarks and markers of cellular senescence. No single hallmark is sufficient to identify cellular senescence, as such, a collection of hallmarks is typically evaluated. **Abbreviations**: DNA-SCARS, DNA segments with chromatin alterations reinforcing senescence; SA-β-gal, senescence-associated β-galactosidase; SAHF, senescence-associated heterochromatin foci; SASP, senescence-associated secretory phenotype.

1.3 Poxviruses

Poxviridae is composed of two subfamilies called *Chordopoxvirinae* (vertebrate-infecting viruses) and *Entomopoxvirinae* (insect-infecting viruses) which collectively infect a broad host range that includes humans and other mammals, reptiles, birds, fish, and several orders of insects[189]. The most notorious poxvirus, variola virus, is human-specific and linked with immense loss of life as the causative agent of smallpox[190]. The WHO announced in 1980 that smallpox was eradicated after extensive vaccination campaigns involving another noteworthy poxvirus, vaccinia virus (VACV)[190]. VACV is widely regarded as the most effective vaccine in history due to its success eradicating smallpox and has since been studied in several other therapeutic settings. In veterinary contexts, vaccination with recombinant, antigen-encoding vectors based on VACV have protected cattle against rinderpest virus[191] and eradicated rabies virus in areas of Belgium[192] and Ontario, Canada[193]. VACV has also been studied as a gene therapy vector for the delivery of various payloads to treat infectious disease and cancer[194,195]. Lastly, VACV has undergone extensive evaluation as a candidate oncolytic virus (OV) to treat cancer[195]–the focus of this thesis.

1.3.1 Vaccinia Virus Basics

1.3.1.1 Taxonomy, origin, strains. VACV is the most studied virus within the *Poxviridae* family and is a member of the *Orthopoxvirus* genus (within the subfamily *Chordopoxvirinae* of *Poxviridae*). The *Orthopoxvirus* genus also includes the infamous variola virus, as well as other notable poxviruses such as monkeypox virus and cowpox virus[189]. Interestingly, despite the prominence of VACV in poxvirus research, the natural host and origin has not been identified and remains controversial[196]. It was believed Edward Jenner's early bovine-derived pustular smallpox vaccines contained cowpox virus (which conferred cross-reactivity to variola virus), however, several lines of evidence indicate that VACV may have emerged from horsepox virus in horses[197,198]. Additionally, there are many VACV strains used

and studied. Notably for smallpox vaccination, the New York City Board of Health (NYCBH) strain and the Lister strain were widely used; the NYCBH strain concentrating in North America, and the Lister strain throughout Europe, Asia, and Africa[196,199]. The Western Reserve (WR) strain was derived from the NYCBH strain after serial passages intracranially in mice[200]–this WR strain is the backbone of the OV used in this thesis. Other VACV strains include Dryvax (derived from NYCBH, also referred to as Wyeth), Copenhagen (Denmark), Bern (Germany), Ankara (Turkey), Tian Tan (China), and Dairen (Japan)[196,199].

1.3.1.2 Molecular characteristics of the virion. The *Poxviridae* family is a group of linear double-stranded (ds) DNA viruses with large size and genomes, brick- or ovoid-shaped in structure, and that have a life-cycle which occurs entirely in the cytoplasm of infected cells (a feature atypical of DNA viruses)[201]. VACV virions are uniform in shape and size, forming large brick-shaped particles that are approximately 360 × 270 × 250 nm in dimension as indicated by cryo-microscopy and electron tomographic reconstruction techiniques[202]. The virion is packaged with approximately 80 virus-encoded proteins and contains two proteinaceous lateral bodies, one adjacent to each side of an inner dumb-bell-shaped nucleoprotein core which houses a large 190-195 kb, linear, dsDNA genome encoding 218–263 genes[202–207]. 10 kb inverted terminal repeats (ITRs) are located on both ends of the genome and end in incompletely base-paired hairpin termini that covalently link the two strands of the dsDNA genome[206,208,209]. The function of ITRs remains to be fully elucidated but likely serves a role in virion maturation[210]. The VACV genome nomenclature is based on the size of the DNA fragments produced by *Hind*III digestion of the Copenhagen strain[206]. Fragments are labelled A to O from largest to smallest, with the transcription direction indicated as "*R*" (right) or "*L*" (left) for each gene–for example, the *E9L* gene resides within the "E" fragment and is transcribed leftward. The central genomic area among VACV strains and other orthopoxviruses is relatively conserved, containing essential genes for replication, whereas outer genomic regions located towards ITRs are more variable, containing non-essential genes

involved in immune-modulation, host-specificity, and virulence[211–214]. **Figure 1.4** depicts the structure of VACV and **Figure 1.5** depicts the VACV *Hind*III genomic map.

1.3.1.3 Unique infectious forms. The inner nucleoprotein core is enveloped by one or two lipoprotein bilayers which reflects two morphologically distinct forms of infectious virions, a single-enveloped intracellular mature virus (IMV), or a double-enveloped extracellular enveloped virus (EEV), respectively[215–217]. EEV contains the underlying IMV but is surrounded by an additional lipoprotein membrane. The two infectious forms differ in protein composition within their outer membrane[215,218–220], are antigenically distinct[221], as well as make use of different binding and signaling mechanisms to enter cells[222–224]. IMV is the most abundant form of VACV (99% of infectious virions) and is released upon virus-induced cell lysis[215]. Though EEV is far less abundant, its role in transmission is immense. EEV is derived from a triple-enveloped intercellular enveloped virus (IEV) upon fusion with the plasma membrane during egress[217,219,225]. Here, the resulting double-enveloped virion either remains on the cell surface as cell-associated enveloped virus (CEV) and drives cellular actin-tail formation to facilitate cell-to-cell transmission[226–228], or is released extracellularly as EEV, facilitating long-range dissemination *in vivo*[215,229]. EEV resists antibody neutralization and complement-mediated immunity relative to IMV[218,230,231], and is also repelled from VACV-infected cells, facilitating uptake by uninfected cells[232]–all of which enhance systemic spread of the EEV form. It should be mentioned that EEV is difficult to isolate due to its relative scarcity and fragile outer membrane, thus most studies investigating VACV properties have used IMV.

1.3.1.4 Immune-modulation by vaccinia virus. VACV modulates host immune responses in myriad ways to evade immune recognition. In fact, it is estimated that 33%–50% of the VACV genome is dedicated to modulating the host immune response[233]. Within the host organism, the innate immune system is responsible for initial broad detection of threats and subsequently activates an adaptive immune response responsible for targeted clearance of foreign agents. Broadly, immune evasion

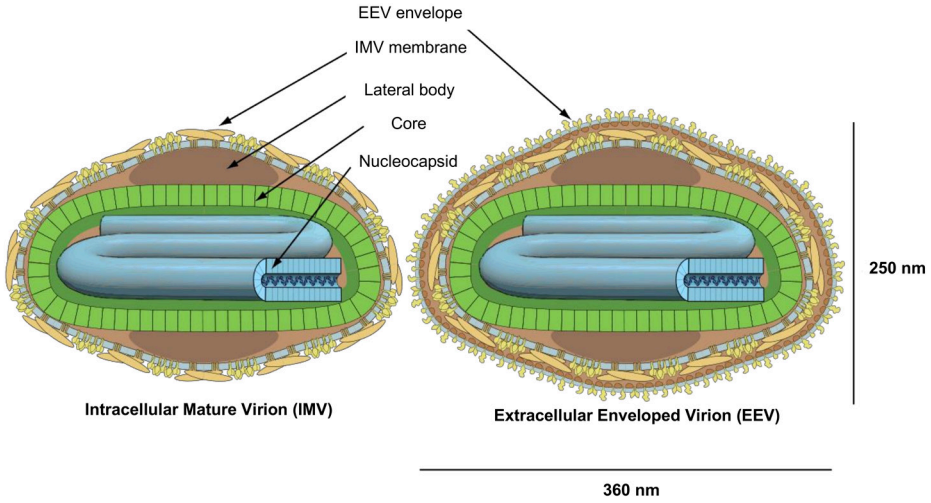

Figure 1.4. General structure and size of vaccinia virus. Two unique infectious forms of vaccinia virus exist, the single-enveloped intracellular mature virion, and the double-enveloped extracellular enveloped virion. Both virions contain two proteinaceous lateral body structures adjacent the nucleoprotein core. The nucleoprotein core encapsulates the vaccinia virus genome. Figure adapted from ViralZone, Swiss Institute of Bioinformatics, www.expasy.org/viralzone (Creative Commons Attribution 4.0 International License).

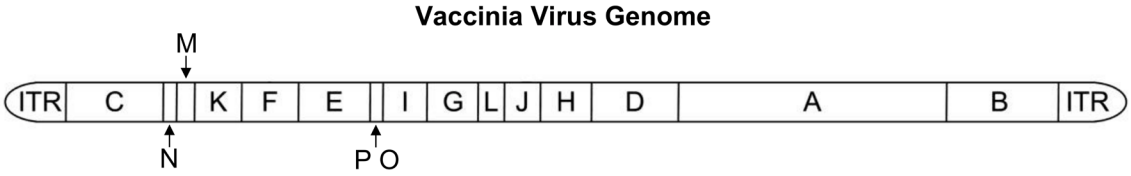

Figure 1.5. *Hind*III genomic map of vaccinia virus. The vaccinia virus genome is organized based on DNA fragments produced by *Hind*III digestion of the Copenhagen strain. Sixteen fragments are labelled A to O from largest to smallest; inverted terminal repeats cap each end of the genome. Viral genes that reside within each fragment are labelled with the corresponding fragment letter. For example, the *E9L* gene resides within the "E" fragment. Figure adapted from [234] (Creative Commons Attribution 4.0 International License). **Abbreviations**: ITR, inverted terminal repeat.

mechanisms implemented by VACV include blocking activation of the complement system[235], hindering prominent innate immune pathways such as NF-κB[236–238], type I interferon (IFN)[239–242], and cGAS/STING circuits[242–244], employing decoy chemokine/cytokine receptors[245–248], and hampering immune cell function[238,249–252]. Overall, the large genome of VACV is well equipped to thwart many host antiviral defenses.

1.3.2 Life-cycle of vaccinia virus

1.3.2.1 Binding and entry. Different mechanisms allow for uptake of IMV or EEV into a host cell. The IMV is proposed to attach to cells in a side-on orientation[253] via cell surface glycosaminoglycans such as heparin sulfate[254], laminin[255], and/or chondroitin sulfate[256], though, other partners are likely[257]. Here, the outer viral lipoprotein envelope of IMV may fuse directly with the cellular plasma membrane at a neutral pH[257], or IMV may be endocytosed and fuse with the engulfed vacuole via a low pH-dependent route[258]; both entry routes liberate the inner nucleoprotein core within the cytoplasm. Engulfment of IMV occurs through apoptotic mimicry, a process that hijacks cellular macropinocytosis to gain entry due to phosphatidyl serine on the virion surface resembling surface-exposed phosphatidyl serine of apoptotic bodies[259,260]. Due to the double-envelope of EEV, a single fusion event will not liberate the inner nucleoprotein core, thus, the outer lipoprotein bilayer must be shed before the remaining virus envelope can fuse with cellular plasma or vacuolar membrane. Like IMV, EEV may also enter at the plasma membrane at a neutral pH, but the outer lipoprotein membrane is first disrupted by an unknown non-fusogenic mechanism at the cell surface (note: this is atypical for enveloped viruses)[261]. EEV also activates macropinocytosis, in which acidification of the engulfed vacuole ruptures the outer membrane[262]. Both mechanisms free the underlying IMV-like particle to fuse and release the nucleoprotein core as normal[261,262].

The entry-fusion complex (EFC) is a complex of 11 proteins located on opposing tips of the IMV in clusters[253]. The EFC is conserved amongst *Chordopoxviridae* and mediates fusion entry events[263]. Lipid-mixing between the outer leaflets of the virus and the cell membrane form a hemifusion intermediate, then subsequent merging of the inner leaflets forms a pore, through which the two lateral bodies and the nucleoprotein core are released into the cytoplasm[264]. Upon release into the cytoplasm, the protein-containing lateral bodies are rapidly disassembled in a proteasome-dependent manner releasing factors which immediately begin to hamper host innate immune defenses[265] and exert antioxidative effects proposed to enhance viral gene expression and assembly[266].

1.3.2.2 Gene expression and DNA replication. Once the nucleoprotein core is liberated, the entire VACV replication process occurs within the cytoplasm. VACV gene expression is temporally regulated–categorized as early, intermediate, and late expression[267]. Early transcription of messenger RNAs (mRNAs) begins within the nucleoprotein core[268] which is trafficked via microtubules to the perinuclear region of the cytoplasm[269]. Capped and polyadenylated mRNAs are released from the core and translated to early proteins[270–272]. Approximately 100 early genes encode proteins required for uncoating of the nucleoprotein core, transcription of intermediate genes, and replication of the VACV genome[273]. Notably, a number of early genes are involved in evading host immune defenses[267]. Uncoating of the nucleoprotein core releases the VACV genome into the cytoplasm, where a subcompartment derived from the endoplasmic reticulum (ER) rapidly forms, termed a *virus replication factory*[270,272,274,275]. A virus factory is derived from a single infectious particle (although, multiple virus factories can combine at late time points to form a virus factory derived from multiple infectious particles). This membrane-encapsulation presumably concentrates factors required for DNA replication while also protecting the VACV genome from degradation and cytoplasmic sensors.

Uncoating of the nucleoprotein core marks the end of early gene expression whereas the onset of VACV DNA replication marks intermediate/late gene expression[273,276,277]. In general, intermediate genes

encode factors that initiate late gene expression, while late genes encode structural components and factors required by the virion for entry and transcription of early genes[267]. Due to the cytoplasmic site of replication, VACV must possess nuclear autonomy and thus encodes an array of its own DNA replication machinery. This includes a DNA polymerase holoenzyme (complex of E9 DNA polymerase and A20/E4 processivity factors), a primase (D5), a single-stranded DNA binding protein (I3), a scaffold protein (H5), a DNA ligase (A50), an endonuclease (G5), a Holliday junction resolvase (A22), and a multitude of deoxynucleotide triphosphate (dNTP) biosynthesis enzymes (J2, F4, I4, A48 – among others)[273]. Within the virus factory, a putative self-priming model describes how replication of VACV genomes occurs (reviewed in [278]).

1.3.2.3 Morphogenesis, assembly, egress. Intermediate and late gene expression begets the complex processes of virion assembly and morphogenesis (the term used for the VACV maturation process). Within the virus factory, the initiation of morphogenesis is distinguished by the formation of ER-derived crescent-shaped membranes associated with viral protein[279–281]. These crescent structures elongate and assemble independently to encapsulate the VACV genome while packaging viroplasm-containing core proteins to form spherical non-infectious immature virus (IV)[280,282–285]. Only approximately one-third of VACV DNA is encapsulated into IVs[286]. Next, IV undergoes a series of morphological transitions facilitated by proteolytic processing, losing its spherical shape and condensing in size, culminating in the formation of the typical infectious brick-shaped IMV[281,287]. The majority of IMV remain in the cytoplasm until the cell is lysed, but a portion are transported along microtubules from factories to cytoplasmic sites[288] where two additional membranes derived from endosomal[289] or trans Golgi cisternae[290] are acquired using a retrograde transport system[291]; these wrapping events form triple-enveloped IEV. IEV is trafficked along microtubules to the inner cell surface where it fuses with the plasma membrane, releasing an EEV particle or remaining on the cell surface as CEV[292,293]. **Figure 1.6** depicts the life-cycle of VACV.

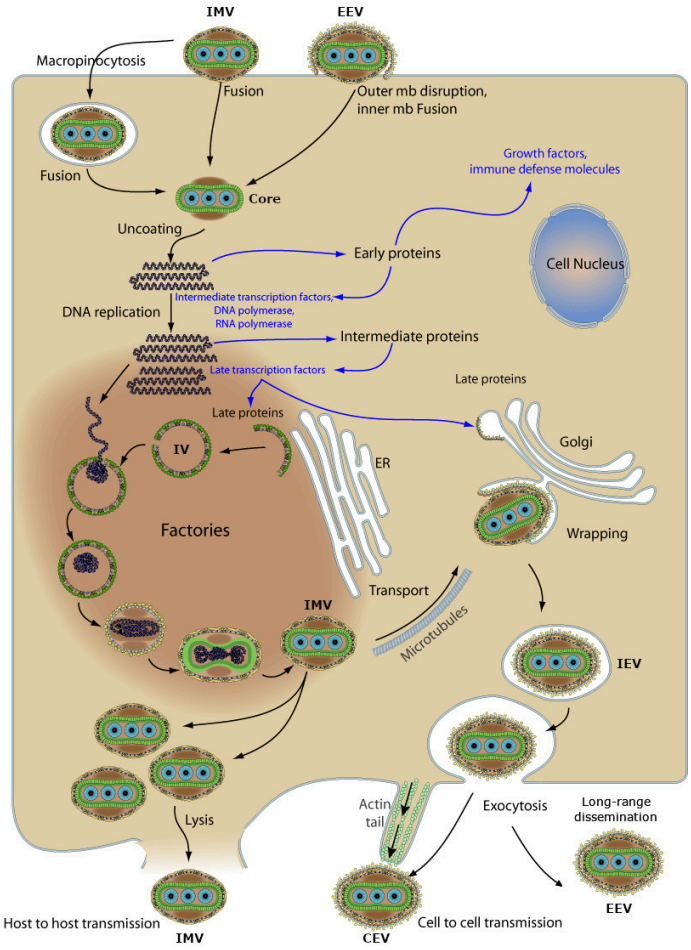

Figure 1.6. Life-cycle of vaccinia virus. Vaccinia virus enters cells by direct fusion or macropinocytosis leading to the release of its nucleoprotein core into the cytoplasm. The coordination of early, intermediate, and late viral genes leads to the production of new virions within virus factories. Intracellular mature virions are released upon cell lysis, or transported and wrapped with an additional envelope resulting in intracellular enveloped virus which egresses and remains as cell-associated virus or is released as extracellular enveloped virus. Figure modified from ViralZone www.expasy.org/viralzone, Swiss Institute of Bioinformatics (Creative Commons Attribution 4.0 International License).

Abbreviations: CEV, cell-associated enveloped virus; EEV, extracellular enveloped virus; ER, endoplasmic reticulum; IEV, intracellular enveloped virus; IMV, intracellular mature virus; IV, immature virus; mb, membrane.

1.3.2.4 Dissemination. Numerous mechanisms mediate dissemination of VACV. In general, IMV is believed to be responsible for host-to-host spread, EEV for systemic spread within the host, and CEV for cell-to-cell spread. IMV properties that facilitate host-to-host transmission are its abundance, ambient temperature stability, and resistance to desiccation[294]. The composition of the EEV virion facilitates long-range spread within the host due to resisting antibody neutralization and complement-mediated immunity relative to IMV[218,230,231]. Superinfection exclusion mechanisms prevent secondary infections by both IMV[295,296] and EEV[232]. For EEV, this process speeds up the rate of spread four-fold due to the increased propensity for virions to encounter uninfected cells[232]. An additional mechanism for VACV dissemination is the formation of actin-tails which force CEV outwards from the infected cell into adjacent cells[226–228]. Further, VACV hijacks cell signaling systems that cause directional migration of infected cells to facilitate cell-to-cell contact with nearby uninfected cells[297].

1.4 Immune Responses to Cancer

1.4.1 Innate and adaptive immunity. Prior to discussing OV therapy in the next section, a primer on how the immune system coordinates antitumor responses is required. The immune system can be broadly categorized into two fundamental components called innate and adaptive immunity that coordinate the clearance of pathogens and malignant cells. Some major distinctions between these two arms of the immune response are the differences in specificity and activation-time; innate immunity involves fast-acting generalized defense mechanisms, whereas adaptive immunity develops much slower and involves highly specific targeting of threats.

A crucial component of innate immunity involves the sensing and communication of threats to the adaptive immune system. Molecular motifs, termed pathogen-associated molecular patterns (PAMPs) or damage-associated molecular patterns (DAMPs), are detected by pattern recognition

receptors (PRRs) of innate immune cells, initiating production of various cytokines or chemokines that function to alert and activate further immune responses[298]. In this way, innate immunity produces early inflammatory events, shaping the intensity and extent of subsequent immune responses.

An important component of the adaptive immune response is the evolutionarily selected class of potent immunological effectors, termed CD8+ cytotoxic T cells, that systemically and specifically destroy pathogen-infected or cancerous cells. All nucleated cells that compose our bodies are decorated with specialized antigen presenting complexes on the cell surface termed major histocompatibility complex class I molecules (MHC I, or human leukocyte antigen I in humans) that serve as signaling devices to the immune system[299]. CD8+ cytotoxic T cells engage infected or transformed cells by recognizing foreign peptide fragments (*i.e.,* peptides produced by intracellular degradation of proteins that are microbial-derived, of different tissue origin, or mutated) bound to MHC I on the target cell surface[299]. In the context of cancer, both neoantigens and tumor-associated-antigens are recognized by T cells. Neoantigens are tumor-specific antigens that arise from mutations in cancer cells and are not present in normal healthy cells, whereas tumor-associated-antigens are present in both cancer and normal cells, but abnormally expressed in cancer cells[300]. When the T cell receptor (TCR) on the surface of a CD8+ T cell possesses specific affinity to a peptide–MHC I complex on the surface of the target cell, the T cell will directly kill the cellular target by triggering apoptosis through release of granzyme B and perforin, or death receptor signaling (*i.e.,* Fas/FasL)[301]. In this way, cells residing in the body harboring harmful infectious agents or that have initiated tumorigenesis display antigens indicative of a compromised cellular state and can be selectively eliminated by the immune system to preserve normal host function.

1.4.2 Coordinating antitumor immune responses. DCs are the cellular bridge connecting innate and adaptive arms of the immune system. DCs sense innate danger signals and cues from the microenvironment, process and present antigens, and provide costimulatory molecular signals to activate adaptive immune effectors—ultimately initiating an adaptive immune response against foreign

(non-self) entities[302]. In the context of antitumor immunity, DC subtypes specialized at cross-presenting tumor antigens (*i.e.,* conventional DCs type 1; cDC1s) to tumor-reactive cytotoxic CD8+ T cells are the most important[303]. Cross-presentation is a mechanism in which DCs process and present extracellular antigens on MHC I molecules to CD8+ cytotoxic T cells (that is, instead of on MHC class II molecules to CD4+ T helper cells). CD8α+ DCs are a subset of conventional DCs that exhibit efficient cross-presentation of viral and tumor antigens enabling CD8+ T cell-mediated defense[303,304].

Optimal immune-mediated tumor destruction requires not only the CD8α+ DC lineage but also type I IFN signaling. Type I IFNs are immunomodulatory factors that mobilize host defenses to counter viral and bacterial pathogens[305], as well as to destroy cancer cells[306,307]. They include IFNα (comprising 13 subtypes), IFNβ, and the other less-characterized IFNε, IFNκ, and IFNω, all of which are secreted and act on a common IFNα/β receptor that is present on all nucleated cells. Binding of type I IFNs to this receptor activates multiple signal transduction pathways inducing diverse responses, including antiviral and antiproliferative activities[308]. Type I IFNs can bridge innate and adaptive immune responses by facilitating DC maturation, increasing DC costimulatory molecule expression, and enhancing migration of DCs to lymph nodes—each of which amplifies DC-mediated stimulation of T cells[306,309]. Studies using highly immunogenic tumor models capable of producing spontaneous antitumor T cell activity revealed that type I IFN is essential for regulating the capacity of CD8α+ DCs to prime CD8+ T cells and facilitate subsequent immune-mediated antitumor responses[310,311]. Type I IFN responsiveness of DCs is also required for induction of tumor-antigen specific CD8+ T cells[312].

Collectively, these data validate the essential roles of type I IFNs, cross-presenting DCs, and CD8+ T cells for maximizing anticancer activity. OV therapy seeks to harness this process and direct the immune system to destroy cancer.

1.4.3 Immune-suppression in glioblastoma. In part, a major obstacle to the successful treatment of GBM is the highly immune-suppressive landscape of its unique tumor microenvironment (TME). GBM cells have evolved numerous mechanisms to strongly limit antitumor immune responses[313,314]. Some of these immune-suppressive mechanisms include recruiting macrophage and microglia (specialized resident "macrophage-like" cells of the brain) to the GBM microenvironment through the release of chemo-attractive factors[315,316]. GBM cells convert these tumor-associated macrophage and microglia (TAM/Mi) to an immune-suppressive and tumor-promoting phenotype through secretion of various cytokines that can further potentiate suppression and tumorigenesis[315]. Other immune-suppressive cell types common to the GBM microenvironment include regulatory T cells (Tregs) and myeloid-derived suppressor cells (MDSCs)[317,318]. Tregs and MDCSs are recruited to the TME via chemo-attractive molecules released from GBM cells and support tumor growth by directly and indirectly countering antitumor immune responses[319,320]. Further, expression of inhibitory immune checkpoint surface molecules such as programmed death ligand 1 (PD-L1) also restrict immune-mediated cancer cell killing and correlate with worse prognosis[321]. Overall, GBM recruits distinct immune cell types that contribute to the maintenance of an immunosuppressed TME that limits immune-mediated cancer killing. Therefore, strategies aimed at ameliorating GBM immune-suppression may improve therapeutic outcomes by unlocking potent antitumor immune responses. **Figure 1.7** outlines a subset of GBM immune-suppressive mechanisms.

1.4.4 Novel immunotherapeutic approaches for treating glioblastoma. Harnessing antitumor immunological responses is a major focus in oncology and is actively explored for GBM[125]. Traditionally the brain was considered an immune-privileged site, however, recent understandings and discovery of CNS lymphatic systems challenge this notion[322,323] and suggest that immunotherapy may have a role for treating GBM. Several approaches have been tried clinically to treat GBM with varying levels of success

such as autologous DC vaccines[324], immune checkpoint blockade (ICB)[325], chimeric antigen receptor (CAR) T cell therapy[326], and OV therapy[327].

Autologous DC vaccines (DCVax-L) have shown particular promise for the improvement of GBM therapy. In a recent phase III randomized clinical trial the addition of DCVax-L to standard of care improved median survival of newly diagnosed GBM patients from 16.5 months to 19.3 months, and of recurrent GBM patients from 7.8 months to 13.2 months[324]. Importantly, the 5-year survival rate increased from 5.7% to 13.0%, indicating improved long-term durable efficacy[324]. Although ICB has revolutionized the treatment of certain cancers, with GBM, ICB has failed to provide survival benefits in all completed phase III clinical trials to date[325]. Certain subsets of GBM patients have shown marginal benefits[325]. The role for ICB likely will be in combination with other modalities capable of priming antitumor responses to potentiate ICB-related efficacy[328]. Like ICB, CAR T cell therapy also has failed to produce substantial benefits treating GBM patients clinically, although it has shown promise treating some patients[326]. Many OVs are being investigated in phase I/II trials for GBM[327]. With GBM, only one OV progressed to phase III, Toca 511 (vocimagene amiretrorepvec), but the trial was unsuccessful[329]. Notably, a recombinant oncolytic poliovirus (called PVS-RIPO) received Food and Drug Administration (FDA) breakthrough therapy status for treating recurrent GBM after a phase I clinical trial demonstrated a 21% overall survival rate at 2-years that remained through 3-years (which was superior to historical controls)[330]. Additionally, after a small phase II clinical trial, ΔG47, a modified herpes simplex virus (HSV), was conditionally approved within Japan for treating malignant gliomas, including recurrent GBM[331].

The use of novel immunotherapeutic approaches for treating GBM is still in its infancy. It should be re-stated that the current standard of care and supportive care regimens are highly immune-suppressive[94–98,102,103]. The magnitude that this therapy-associated immune-suppression may hamper efficacy of immunotherapeutic modalities is unclear, but it remains an important consideration for the successful integration of these modalities.

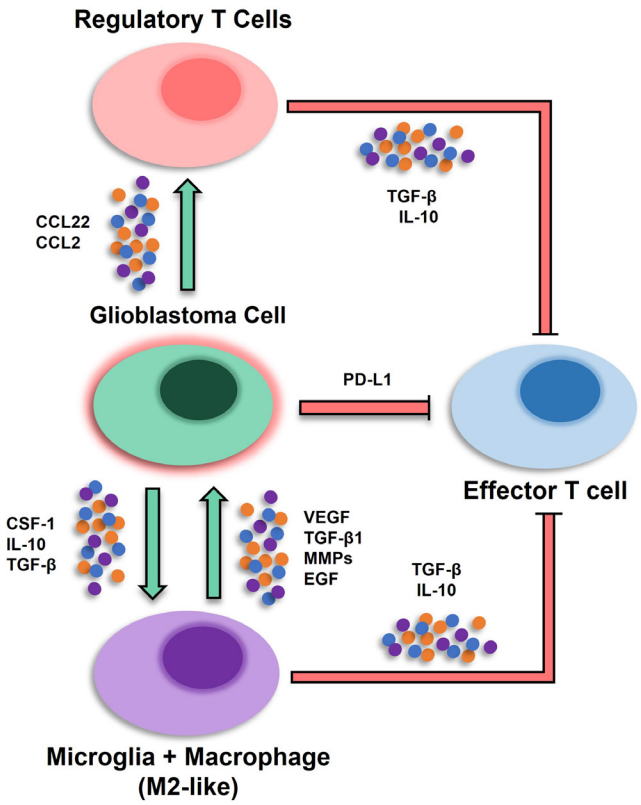

Figure 1.7. Examples of immune-suppressive mechanisms of glioblastoma. T cell-mediated cancer cell killing is repressed in the glioblastoma microenvironment by various cell types and signaling. Glioblastoma cells recruit immune-suppressive cell types such as regulatory T cells and tumor-associated macrophage and microglia via chemokine secretion. Tumor-associated macrophage and microglia are reprogrammed by immune-suppressive cytokines in the microenvironment towards a more immune-suppressive phenotype (M2-like) that also exacerbates tumor growth. Glioblastoma cells also directly impair T cells via inhibitory immune checkpoint signaling. **Abbreviations**: CCL22, C-C motif chemokine 22; CCL2, chemokine (C-C motif) ligand 2; CSF-1, colony stimulating factor 1; EGF, epidermal growth factor; IL-10, Interleukin 10; MMPs, matrix metalloproteinases; PD-L1, programmed death-ligand 1; TGF-β, transforming growth factor β; VEGF, vascular endothelial growth factor.

1.5 Oncolytic Viruses

1.5.1 History. Virus infection coinciding with clinical cancer remission was noted over 100 years ago[332]. Several other notable clinical case reports were published between 1940-1980[333–337]. These early observations sparked interest in the therapeutic application of viruses for cancer, which began to be studied more broadly using animal models and in human clinical trials throughout the same time period (reviewed in [338]). However, due to the inherent pathogenicity and virulence of many viruses towards humans, the safety of non-attenuated virotherapy was questionable and faced regulatory barriers, marking declined interest in the field[338]. Furthermore, this time period coincided with the development of chemotherapy, once thought to be the "cure" for cancer. In the 1990's, the standardization of common molecular recombination techniques enabled scientists to engineer tumor selectivity of viruses, greatly enhancing their safety profile. Together with the realization that chemotherapy was far from curing cancer, there was renewed interest in the field–begetting the modern era of OV therapy[338]. Of note, the first preclinically tested recombinant OV was an oncolytic HSV used to treat GBM mouse models[339]. Since, a large number of different viruses have been investigated for OV therapy including adenovirus, other HSVs, VACV, reovirus, Newcastle disease virus (NDV), reovirus, measles virus, vesicular stomatitis virus (VSV), and myxoma virus (among others)[340].

1.5.2 Definition and anticancer mechanisms of action. OV therapy is an advancing treatment option harnessing normal-tissue-sparing, tumor-selective viruses to kill cancer cells while also stimulating the host immune system to destroy cancer[341,342]. Direct destruction of infected cancer cells occurs when virus replication results in cell lysis or cell death mediated by apoptotic, necrotic, or autophagic pathways[343]. Newly produced virions are subsequently released and infect adjacent tumor cells–in this way, OVs induce an amplifying therapeutic effect. Direct oncolysis of cancer cells was initially proposed to be the chief anticancer mechanism of OV therapy. However, it is now widely

recognized that viral oncolysis triggers potent adaptive antitumor immune responses[343]. OV therapy increases the immunogenicity of dying cancer cells by facilitating immunogenic cell death (ICD)[343,344], a process which exposes DAMPs and tumor antigens (both derived from dying cancer cells), as well as PAMPs (derived from virus) that alert the innate immune system, activate type I IFNs, and lead to DC-mediated display of tumor-antigen on MHC I to CD8+ cytotoxic T cells–facilitating the establishment of adaptive antitumor immunity[345,346]. **Figure 1.8** outlines the dual anticancer mechanisms of OV therapy. Further, OVs acutely counter immune-suppression within TMEs by modulating the proportion of tumor-reactive lymphocytes and immune-suppressive cell types[347]. Briefly within TMEs, OVs have been associated with reducing immune-suppressive Tregs[348–351], reversing tumor-associated macrophage (TAM) immune suppression[348,352,353], and recruiting antitumor CD8+ cytotoxic T cells[350,351,354]. Lastly, it should be mentioned that virus-associated destruction of tumor vasculature, which prevents cancer cells from acquiring nutrients, is another proposed anticancer mechanism associated with OV therapy[355,356]. Overall, although OV therapy was initially investigated as a direct cancer killing agent, studies over the last several decades have positioned this modality as a prominent, emerging cancer immunotherapy[340].

1.5.3 Tumor selectivity. Tumor selectivity is paramount for safe execution of OV therapy. Two main categories of OVs exist: naturally tumor-selective viruses and genetically engineered tumor-selective viruses. NDV, reovirus, and measles virus (the Edmonston B vaccine strain) are examples of viruses with natural tropisms for cancer cells without modifications. NDV is an avian virus that preferentially replicates in cancer cells due to low type I IFN responsiveness relative to normal cells[357]. Reovirus is asymptomatic in humans and preferentially replicates in RAS-activated cancer cells[358]. The live Edmonston B vaccine strain of measles virus preferentially infects cancer cells due to increased surface levels of the entry receptor CD46[359] and impaired type I IFN signaling relative to normal cells[360].

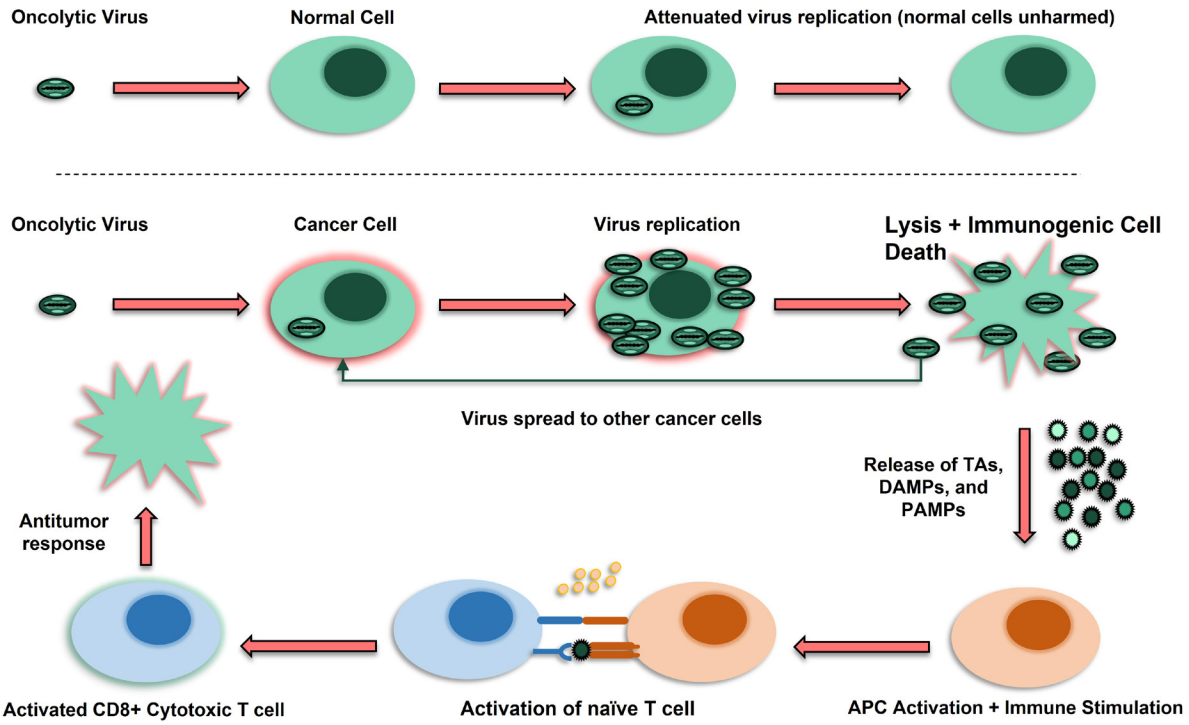

Figure 1.8. Tumor selectivity and anticancer mechanisms of oncolytic virotherapy. Oncolytic virus tumor selectivity is either inherent (natural) or genetically engineered. Within normal cells, oncolytic virus replication is absent or negligible (upper panel), whereas in cancer cells virus replication is robust (lower panel). Oncolytic virus replication leads to cell lysis and immunogenic cell death, releasing newly produced virions that can infect adjacent cancer cells while also exposing immune-stimulatory factors and tumor antigens (neoantigens or tumor-associated antigens). Specialized immune cells, such as dendritic cells, provide activation signals and present tumor-antigen to naïve CD8+ cytotoxic T cells, which become activated and expand, mounting an antitumor immune response to destroy cancer cells. **Abbreviations**: APC, antigen-presenting cell; DAMPs, danger-associated molecular patterns; PAMPs, pathogen-associated molecular patterns.

Genetic engineering techniques greatly expand the repertoire of OVs beyond those that naturally possess tumor selectivity. One prominent strategy is to remove viral genes that are required for optimal replication in normal cells, but that are redundant in malignant cells due to various mutations or aberrations in signaling pathways–a *redundancy-exploitation* approach. For example, cancer cells exhibit impaired activation of protein kinase R (PKR is an inhibitor of protein translation–detrimental for viral protein production), therefore the *$\gamma_1$34.5* gene in HSV, which encodes an enzyme that impairs PKR, becomes redundant in cancer cells (but not normal cells) and its deletion produces a tumor-selective HSV[361]. This principle will be detailed further for oncolytic VACV tumor selectivity in later sections. *Transcriptional targeting* places essential viral genes under the regulation of a tumor-specific promoter. For example, human telomerase reverse transcriptase (*hTERT*) expression is upregulated in different cancers, therefore engineering the *hTERT* promoter to drive expression of essential adenovirus genes renders the modified adenovirus tumor-selective[362]. *Transductional targeting* restricts OVs to entering cancer cells that express a particular surface molecule at elevated levels relative to normal cells. For example, an oncolytic measles virus was designed to target $CD133^+$ cells, a marker of GSCs[363].

1.5.4 Enhancing efficacy. Potentiating antitumor efficacy is crucial to improve treatment outcomes and adoption of OV therapy. As such, OVs are engineered to encode factors that enhance antitumor activity beyond the inherent OV anticancer mechanisms–proverbially referred to as *arming* OVs. One approach is to encode cytotoxic proteins in the viral genome which enables delivery of cancer-killing payloads to the tumor site. For example, some OVs have been armed to express tumor necrosis factor (TNF)-related apoptosis-inducing ligand (TRAIL)[364]. Another approach is to arm OVs with immune-stimulating factors such as cytokines, chemokines, and co-stimulatory molecules to potentiate immune-mediated antitumor responses[365]. This strategy has received immense attention following FDA approval of T-VEC, which encodes a cytokine called granulocyte-macrophage colony-stimulating factor (GM-CSF)[366]. Notably, Pexa-Vec, an oncolytic VACV furthest along clinically, also encodes GM-CSF[367,368]. A

more recent strategy is arming OVs with bi-specific T-cell engagers (BiTEs), an approach that uses bi-specific antibodies to bind T cells and malignant cells to one another, improving T cell-mediated tumor cell destruction[369].

Other efficacy enhancing approaches exist that do not include arming OVs. Shielding OVs from detection of the innate immune system can also increase the potency of OV therapy. Cellular vehicles with natural tumor-homing properties safeguard virus from being sequestered or neutralized, improving efficacy compared to direct delivery[370]. Finally, using OVs in combination with other approved therapies, like radiotherapy, or other immunotherapies, like ICB, is frequently investigated[371]. In particular, the capacity of OVs to acutely modulate the TME away from an immune-supressed state, as well as recruit tumor-antigen specific CD8+ cytotoxic T cells to the TME, has positioned OV therapy to pair well with ICB[350,372,373], something increasingly being investigated clinically[374].

1.5.5 Approved and notable oncolytics. A variety of OVs have been engineered and studied extensively for a wide range of cancers. The world's first approved OV therapy was granted by Chinese regulators in 2005 for the treatment of head and neck cancer using a genetically modified adenovirus (referred to as H101; trade name Oncocrine)[375]. A decade later in 2015, the FDA approved talimogene laherparepvec (T-VEC; trade name IMLYGIC), a genetically modified HSV to treat metastatic melanoma[366]. Also in 2015, a recombinant poliovirus (PVS-RIPO) received FDA breakthrough status for treatment of recurrent GBM[330], a status with the aim to expedite progress of therapies demonstrating substantial promise. In 2021 Japanese regulators conditionally approved Deyltact (formally called ΔG47), another genetically modified HSV, for the treatment of malignant gliomas and recurrent GBM[331,376]. Although these approvals mark important milestones for OV therapy, the field is still in its infancy, and many viruses are still under clinical investigation.

Clinically, the most frequently studied OVs are based on adenovirus, HSV, and VACV (in that order; see **Table 1.1** for a selection of clinically tested OVs)[340]. A notable adenovirus-based OV is DNX-2401, which is being investigated to treat GBM[377]. Of relevance to this thesis, this virus is being studied clinically in combination with radiotherapy to treat pediatric diffuse intrinsic pontine glioma[378]. G207 is a prominently studied HSV-based OV[379]. G207 has been evaluated clinically treating GBM[380], and is being explored for the treatment of pediatric brain tumors in combination with radiotherapy[381,382]. Further, several notable oncolytic VACVs are under clinical investigation. Pexastimogene devacirepvec (Pexa-Vec; formally called JX-594) is the furthest along clinically. Pexa-Vec initially showed dose-related efficacy while being well-tolerated for treatment of advanced HCC[367] but failed to improve overall survival in phase III clinical trials[368]. In phase I clinical trials, the VACV-based GL-ONC1 was safely administered for the treatment of peritoneal carcinomatosis[383] and used in combination with chemoradiotherapy for advanced head and neck cancer[384]. In another phase I study, administration of vvDD was well-tolerated in patients with advanced solid tumors, infecting both injected and noninjected tumors, and providing some indication of antitumor activity[385]. Of relevance to the treatment of GBM, the combination of TG6002 and 5-flucytosine is also being investigated (ClinicalTrials.gov Identifier: NCT03294486).

1.5.6 Why use vaccinia virus? A major barrier for uniform treatment outcomes is the immense heterogeneity among, and within, tumor types. Therefore, a repertoire of clinically-relevant OVs is likely required to optimize virotherapy for different cancers and combinational strategies. As such, although numerous other viruses are studied as oncolytic agents, further exploration and development of VACV-based OVs is warranted. Importantly, VACV possesses several inherent biological properties ideal for OV therapy.

First, the virus has an established safety profile. Knowledge of how VACV behaves, potential risk factors, and how to respond to rare adverse events are well-defined due to the deliberate infection of humans

Table 1.1. Clinically approved oncolytic viruses or notable clinically-tested oncolytic viruses relating to glioblastoma, radiotherapy, or vaccinia virus.

Refs	Oncolytic Name	Characteristics	Status
[375,386]	H101 (Oncocrine)	Adenovirus based *E1B* gene deleted *78.3-85.8 μm* gene segment deleted	Approved for head and neck cancer in China
[377,378]	DNX-2401	Adenovirus based *E1A* gene deletion (24 bps) RGD-4C peptide inserted	Phase I: Treatment of recurrent GBM; treatment of DIPG in combination with radiotherapy
[387]	T-VEC (IMLYGIC)	HSV type 1 based *ICP34.5* and *ICP47* genes deleted *GM-CSF* transgene inserted	FDA approved for metastatic melanoma
[331,376]	ΔG47 *(*Delytact*)*	HSV type 1 based *α47*, *γ34.5*, and *ICP6* genes deleted	Conditionally approved for malignant glioma and recurrent GBM in Japan
[380–382]	G207	HSV (type 1) based *γ34.5* gene deleted *ICP6* gene disrupted by *lacZ* insertion	Phase I: Treatment of GBM; treatment of pediatric brain tumors in combination with radiotherapy
[330]	PSV-RIPO	Based on live attenuated poliovirus type 1 (Sabin) vaccine Internal ribosome entry site replaced Uses CD155 as entry receptor	FDA breakthrough status for recurrent GBM
[368]	JX-594 (Pexa-Vec)	Vaccinia virus based (Wyeth strain) *J2R* gene deleted (viral TK) *GM-CSF* and *lacZ* transgenes inserted	Phase III: Treatment of advanced HCC (failed)
[367,384]	GL-ONC1	Vaccinia virus based (Lister strain) *J2R* (viral TK), *A56R*, and *F14.5L* genes deleted	Phase I: Treatment of peritoneal carcinomatosis; head and neck cancer in combination with chemoradiotherapy
[385]	vvDD (JX-929)	Vaccinia virus based (Western Reserve strain) *J2R* (viral TK) and *VGF* genes deleted	Phase I: Treatment of advanced solid tumors
[388]	TG6002	Vaccinia virus based (Copenhagen strain) *J2R* (viral TK) and *I4L* genes deleted *FCU1* suicide gene inserted	Phase I: Treatment of GBM (NCT03294486)

Abbreviations: DIPG, diffuse intrinsic pontine glioma; FDA, Food and Drug Administration; GBM, glioblastoma; HCC, hepatocellular carcinoma; HSV, herpes simplex virus; TK, thymidine kinase.

with VACV during the smallpox eradication campaign[389,390]. Further, VACV replication occurs in the cytoplasm completely separated from host cellular DNA[270], a feature which precludes the risk of viral DNA integration within host chromosomes. From an anticancer efficacy perspective, VACV rapidly lyses infected host cells relative to several other viruses–an important metric for virus distribution within the tumor and subsequent tumor control[391]. Distinct cellular surface receptors are not required by VACV for entry into cells[257–259], rendering the virus able to broadly infect different tumor types and tumor cell clones that may lack distinct receptors required by other viruses. Further, different morphological forms of VACV (*i.e.,* IMV and EEV) enter cells differently[222–224] which contributes to the broad tissue tropism of VACV. The antigenic distinction between IMV and EEV also enables resistance to host antiviral responses[218,230,231] which facilitates systemic spread of virus to non-local tumor cells[392]. Additionally, VACV is known to induce ICD that facilitates antitumor immune responses by exposing immune-stimulatory DAMPs such as heat-shock proteins[393], high mobility group box 1[344,394], calreticulin[344], and adenosine triphosphate[395]. Lastly, from an oncolytic engineering perspective, VACV is extremely amenable to genetic alterations due to its large genome and coding capacity. VACV can incorporate 25,000 bps of foreign DNA[396]. Furthermore, many sites in the VACV genome are attractive for insertional inactivation, as when deleted, the resulting mutant VACVs exhibit improved antitumor efficacy[354] or tumor selectivity[234,397]. These features open myriad possibilities for equipping VACV with transgenes that can enhance antitumor efficacy or modulate the TME in desired ways[349,398–401].

1.5.7 Oncolytic Δ*F4L*Δ*J2R* vaccinia virus. Cellular thymidine kinase (TK; also called TK1) and ribonucleotide reductase (RR) are critical nucleotide biosynthesis enzymes involved in the production of four distinct dNTPs that serve as building blocks for cellular DNA synthesis and repair[402]. TK is involved in synthesizing deoxythymidine triphosphate (dTTP) through the "salvage" and "*de novo*" pathways of nucleotide biosynthesis[403]. Primarily, TK catalyzes phosphorylation of deoxythymidine (dT) to deoxythymidine monophosphate (dTMP) in salvage pathways, but also catalyzes phosphorylation of

deoxyuridine (dU) to deoxyuridine monophosphate (dUMP) in *de novo* pathways. Both dTMP and dUMP are precursors of dTTP[403]. RR catalyzes the reduction of nucleotide diphosphates (NDPs) to deoxynucleotide diphosphates (dNDPs), which are the precursor molecules for dNTPs[402,404]. RR is involved in the rate-limiting step of the *de novo* pathway for synthesis of all four dNTPs, but largely is associated with synthesizing the precursor molecules of deoxyadenosine triphosphate (dATP), deoxyguanosine triphosphate (dGTP), and deoxycytidine triphosphate (dCTP)[402,404]. Structurally, two large R1 subunits (encoded by the *RRM1* gene) and two small R2 subunits (encoded by the *RRM2* gene) form an active RR heterotetrametric complex ($R1_2R2_2$)[397]. R1 and R2 subunits are both synthesized during S-phase of the cell cycle[405–407]. Importantly, the half lives of R1 and R2 differ substantially–15 hours *vs.* 3 hours, respectively–therefore R1 levels remain relatively constant throughout the cell cycle whereas R2 levels subside, and consequently, R2 is the rate-limiting factor for R1-R2 complex formation[406].

As referenced in above sections, redundancies between cellular and viral protein homologues can be exploited to promote tumor-selectivity and safety. VACV requires the production of dNTPs to replicate its genome, as such, the virus encodes several viral protein homologues of cellular nucleotide biosynthesis enzymes. Some viral genes involved in nucleotide biosynthesis are *J2R* (encodes J2, a viral TK)[408], *I4L* (encodes I4, a viral R1)[409], and *F4L* (encodes F4, a viral R2)[410]. Of note, viral R2 and cellular R1 can associate to form enzymatically-active chimeric virus-host RR complexes[397]. Importantly, cellular TK and R2 are upregulated in many cancer cells[402,411], including GBM[412,413], creating redundancies for the viral homologues of these cellular proteins. The unique oncolytic VACV used in this thesis, designated herein as Δ*F4L*Δ*J2R* VACV, possesses mutations in viral nucleotide biosynthesis genes *J2R* (viral TK) and *F4L* (viral R2–the small subunit of viral RR) that render the virus tumor-selective[397,414] (**Figure 1.9**). Due to these deletions, cancer cells provide a better environment for Δ*F4L*Δ*J2R* VACV replication than normal cells.

Figure 1.10 outlines these nucleotide biosynthesis pathways and relevant cellular/viral enzymes exploited to confer tumor selectivity.

Additionally, Δ*F4L*Δ*J2R* VACV can activate antitumor immune responses. The virus induced antitumor immunity in preclinical bladder cancer models[414] and recruited tumor-antigen specific CD8+ T cells to the TME of treated breast cancer models[354]. Of note, the safety profile of Δ*F4L*Δ*J2R* VACV is enhanced relative to virus deleted only in *J2R* in bladder cancer models[414]. It is important to emphasis that high expression of cellular TK or R2 is associated with worse prognosis for GBM patients[412,413]; this positions Δ*F4L*Δ*J2R* VACV as an attractive therapeutic that may be well-suited suited for this patient population.

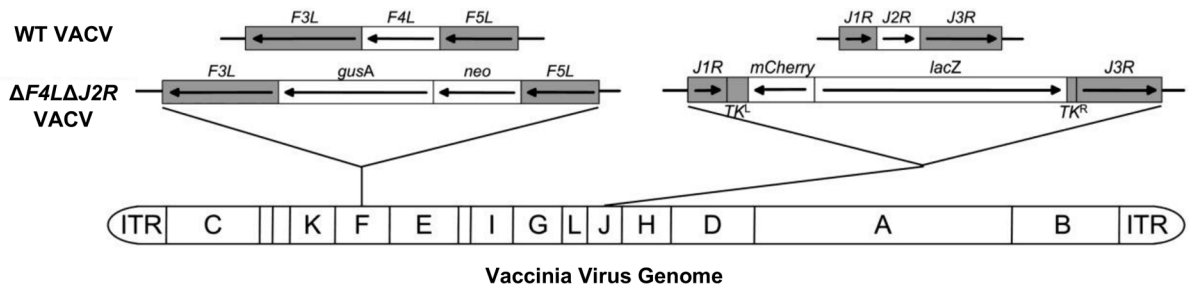

Figure 1.9. Genetic map of wild-type and *ΔF4LΔJ2R* vaccinia viruses. In comparison to wild-type (Western Reserve strain), the mutant *ΔF4LΔJ2R* vaccinia virus possesses *neo*/*gusA* and *mCherry*/*lacZ* insertions in the *F4L* and *J2R* loci respectively. Figure adapted from [414] (Creative Commons Attribution 4.0 International License). **Abbreviations**: ITR, inverted terminal repeat; TK, thymidine kinase; VACV, vaccinia virus; WT, wild-type.

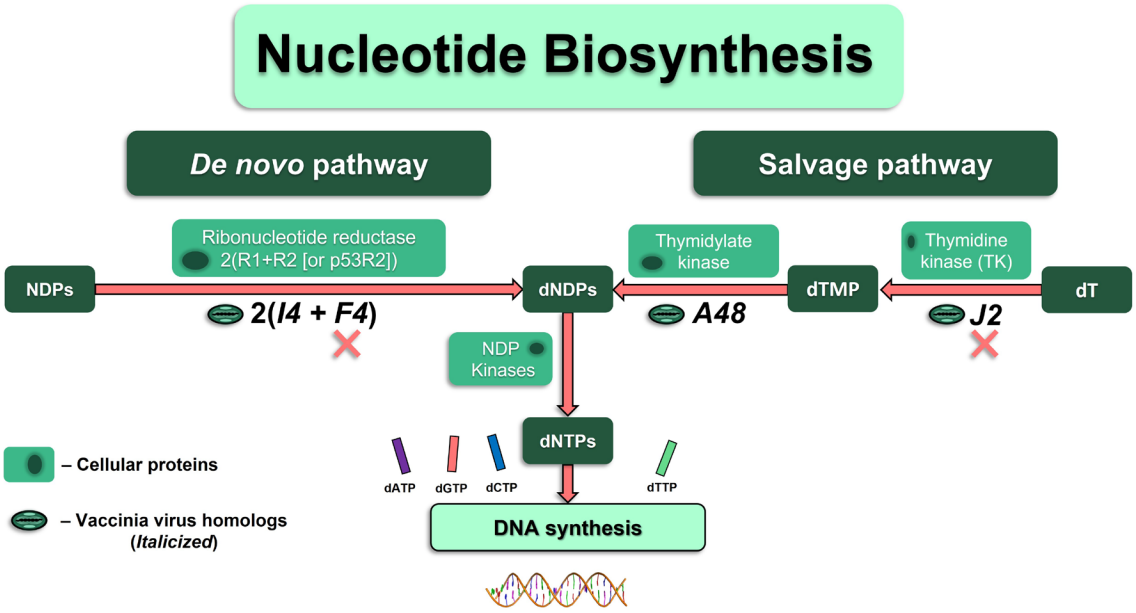

Figure 1.10. Nucleotide biosynthesis pathways are exploited to generate tumor selectivity of *ΔF4LΔJ2R* vaccinia virus. Cellular ribonucleotide reductase converts NDPs to dNDPs in the *de novo* nucleotide biosynthesis pathway, whereas cellular thymidine kinase phosphorylates dT to dTMP in the *salvage* nucleotide biosynthesis pathway–both products are precursor molecules required for creating the building blocks of DNA. *F4L* and *J2R* vaccinia virus genes encode F4 and J2, which are viral homologues of cellular R2 (the small subunit of the ribonucleotide reductase holoenzyme) and cellular thymidine kinase, respectively. Deletion of *F4L* and *J2R* renders the mutant Δ*F4LΔJ2R* vaccinia virus dependent on cellular expression of nucleotide biosynthesis protein homologues, which are upregulated in cancer cells. Hence, cancer cells provide a better environment for Δ*F4LΔJ2R* replication compared to normal cells, conferring tumor selectivity. **Abbreviations**: dATP, deoxyadenosine triphosphate; dCTP, deoxycytidine triphosphate; dGTP, deoxyguanosine triphosphate, dNDPs, deoxynucleotide diphosphates; dNTPs, deoxythymidine triphosphates; dT, deoxythymidine; dTMP, deoxythymidine monophosphate; dTTP, deoxythymidine triphosphate; NDPs, nucleotide diphosphates; R1, large subunit of ribonucleotide reductase; R2, small subunit of ribonucleotide reductase; p53R2, alternative small subunit of ribonucleotide reductase.

1.6 Project Rationales, Hypotheses, and Summaries

1.6.1 Radiation Combined with Oncolytic Vaccinia Virus (Chapter 3)

Rationale. GBM is a highly invasive and aggressive brain tumor with an abysmal prognosis despite the current standard of care[1,6–8,73]–highlighting a need for novel therapeutic strategies. Radiotherapy is a staple GBM treatment[116,415] but can miss invasive cancer cells[416,417] or fail to clear radioresistant GBM cells[418]; both of which contribute to recurrence. Further, some of the difficulties associated with GBM are due to GBM-mediated immune-suppression which strongly limits antitumor immune responses[314,317]. Several lines of evidence suggest that a heightened immune response is beneficial for GBM patient outcomes[94,104–107]. Therefore, treatments with the capability to ameliorate immune-suppression may further improve outcomes by unlocking potent immune-mediated cancer cell killing.

Hypothesis. Both radiation and oncolytic VACV are tools for facilitating antitumor immune responses[195,344,419–422], hence, we hypothesize that combining radiation with Δ*F4L*Δ*J2R* VACV, an OV rendered tumor-selective due to key mutations in viral nucleotide biosynthesis genes[397,414], would improve outcomes for GBM better than either modality alone; reasoning that virus-associated killing and spread would clear GBM cells remaining post-radiation, either through direct oncolysis, or indirectly via antitumor immune activation.

Summary. We showed that Δ*F4L*Δ*J2R* VACV has the capacity to infect, replicate in, and destroy a large panel of non-irradiated and irradiated GBM cells. Further, Δ*F4L*Δ*J2R* VACV spread through invasive tumor extensions and impaired the expansion of GBM spheroids in three-dimensional invasion assays. Δ*F4L*Δ*J2R* VACV was well-tolerated intracranially *in vivo*, in both tumor-bearing GBM models, and non-tumor-bearing severely immune-compromised mice. Importantly, radiation in concert with Δ*F4L*Δ*J2R* VACV produced vastly superior survival outcomes relative to either monotherapy–curing the majority of

mice–and inducing antitumor immunological memory in a portion of cured animals. Lastly, the combination uniquely modulated the brain TME in a way deemed favourable for antitumor immune responses, increasing the CD8+:Treg ratio greater than either monotherapy.

1.6.2 Radiation-Induced Senescence and Vaccinia Virus (Chapter 4)

Rationale. To improve GBM treatment, OV therapy is being explored in combination with radiotherapy in preclinical and clinical settings[327,419,423–425]. One consequence of radiotherapy is the induction of senescence in a portion of exposed cells. Importantly, radiation-induced senescent GBM cells possess tumor-promoting effects[426,427] and removal of senescent GBM cells improves outcomes in preclinical GBM models[427]. Thus, clearance of radiation-induced senescent GBM cells may improve therapeutic outcomes, although it is unclear whether or how OV therapy may contribute to eradicating senescent tumor cells. Further, studies on virus interactions with senescent cells are relatively scarce and offer conflicting conclusions[428–434]. Given limited and inconsistent reports, we sought to better understand how a VACV-based OV, Δ*F4L*Δ*J2R* VACV, as well as WT VACV interact with radiation-induced senescent GBM cells.

Hypothesis. We hypothesize that radiation can induce senescence in GBM cells *in vitro*, and that these senescent GBM cells can be effectively infected and killed by both Δ*F4L*Δ*J2R* VACV and WT VACV.

Summary. We demonstrate that ionizing radiation reliably generates radiation-induced senescent GBM cells 7 days post-irradiation. At this senescence-enriched 7-day time point, the growth, infectivity, and cytotoxicity of both Δ*F4L*Δ*J2R* VACV and WT VACV were impaired in irradiated GBM cells relative to non-irradiated controls suggesting senescence-associated antiviral activity. Interestingly, under the same conditions, the growth of VSV was not impaired but reovirus was–indicating that radiation-induced senescence impacts virus activity in a non-uniform manner. Further, we show that decreased levels of cellular nucleotide biosynthesis enzymes do not explain the attenuated phenotype

of Δ*F4L*Δ*J2R* VACV. Activation of the NF-κB pathway, but not the type I IFN system may in part explain the impaired VACV phenotype in irradiated senescence-enriched conditions. Lastly, irradiated senescence-enriched GBM cell populations secrete factors that induce bystander cells to impair VACV amplification.

CHAPTER 2: Materials and Methods

Preface

This chapter has been modified from the following published works:

"**Storozynsky, Q.T.,** Agopsowicz, K.C., Noyce, R.S., Bukhari, A.B., Han, X., Snyder, N., Umer, B.A., Gamper, A.M., Godbout, R.G., Evans, D.H., and Hitt, M.M. (2023). Radiation combined with oncolytic vaccinia virus provides pronounced antitumor efficacy and induces immune protection in an aggressive glioblastoma model. *Cancer Letters*, 562, 216169, doi:10.1016/j.canlet.2023.216169."

"**Storozynsky, Q.T.,** Han, X., Komant, S., Agopsowicz, K.C., Potts, K.G., Gamper, A.M., Godbout, R.G., Evans, D.H., and Hitt, M.M. (2023). Radiation-induced cellular senescence reduces susceptibility of glioblastoma cells to oncolytic vaccinia virus. *Cancers*, 15, 3341. https://doi.org/10.3390/cancers15133341."

2.1 Cell lines and culture conditions. The human GBM cell lines U87, U138 (obtained from Jorgen Fogh, Sloane Kettering Institute, Rye, NY, USA), U118 (American Type Cell Culture Collection [ATCC]; HTB-15), and T98 (obtained from Walter Nelson-Rees, Naval Biomedical Research Station, Oakland, CA, USA) and mouse GBM cell line CT2A-luc (Sigma-Aldrich; SCC195) were maintained in high glucose Dulbecco's modified Eagle's medium (HG-DMEM) supplemented with 5% (Chapter 4) or 10% (Chapter 3) fetal bovine serum (FBS), 2 mM L-glutamine, 100 U/mL penicillin, and 100 µg/mL streptomycin (Gibco). The African green monkey kidney (AGMK) cell line BSC-40 (CRL-2761) was maintained in minimal essential medium (MEM) supplemented as above, with 5% FBS. Vero (CCL-81), another AGMK cell line, was cultured in HG-DMEM supplemented with 10% FBS, plus glutamine, penicillin, and streptomycin as above. L929 mouse fibroblast cells [kindly provided by M. Shmulevitz (University of Alberta)], were maintained in MEM supplemented with 1X nonessential amino acids (Millipore Sigma) and 1 mM sodium pyruvate (Millipore Sigma). The patient-derived GBM cell lines ED501, ED511, ED512 [established by Hua Chen (University of Alberta)][435], and 12EF, 48EF, 25m, 50m, and 53m brain tumor initiating cell (BTIC) lines [kindly provided by D. Senger and S. Weiss (University of Calgary)][43,436] as well as mouse mBTIC0309 BTIC line [kindly provided by P. Forsyth (Moffit Cancer Center)][437,438] were maintained in serum-free DMEM/F12 medium supplemented with 20 ng/mL recombinant human epidermal growth factor (Gibco), 10 ng/mL human basic fibroblast growth factor (Cedarlane), 0.2% heparin (Sigma-Aldrich), and 1X B-27® Supplement (Gibco). The mouse BTIC line, 005-GFP [kindly provided by S. Rabkin (Harvard Medical School)][439,440], was cultured as described for other BTIC lines, but using 1X N-2 Supplement (Gibco) instead of B-27® Supplement. For the ED501, ED511, and ED512 cell lines, consent for patient GBM tissue was obtained prior to surgery under Health Research Ethics Board of Alberta Cancer Committee Protocol #HREBA CC-14-0070. For the 12EF, 48EF, 25m, 50m, and 53m BTIC lines, patient brain tumor samples were obtained by informed consent under protocols approved by institutional ethics boards as described in Zemp et al. (2013)[436]. BTIC lines were

passaged using Accutase (Gibco); all other cell lines were passaged using trypsin (Gibco). Cells were cultured at 37ºC in a humidified 5% CO_2 environment. Cells were tested for mycoplasma contamination using either DAPI (Sigma-Aldrich) staining and fluorescence microscopy[441], or a *Mycoplasma* PCR Detection Kit (Applied Biological Materials).

2.2 Viruses. The "WT" WR strain VACV used in these studies was originally obtained from the ATCC. The mutant VACV, Δ*F4L*Δ*J2R*, was derived from a clonal isolate of WT VACV and constructed using homologous recombination techniques as described elsewhere[414]. This mutant encodes *gusA* and *neo* in place of *F4L*, and mCherry and *lacZ* in place of *J2R*[414]. Virus stocks were produced as previously described[354]. Serotype 3 Dearing ($T3D^{PL}$) reovirus kindly provided by M. Shmulevitz (University of Alberta, Edmonton, AB, Canada) was originally from P. Lee (Dalhousie University, Halifax, Nova Scotia, Canada). Reovirus stocks were produced as previously described[442]. VSVΔM51-GFP (Indiana strain) was engineered as described by Stojdl et al. (2003)[443] and was kindly provided by Doug Mahoney (University of Calgary, Calgary, AB, Canada). VSVΔM51-GFP was propagated in monolayer cultures of Vero cells and purified using standard protocols[444].

2.3 Virus growth curves. For experiments in Chapter 3, cells were infected with VACV at a multiplicity of infection (MOI) of 0.03 plaque-forming units (PFU) or 1.0 PFU per cell, as indicated, in 12-well plates. At the indicated time points post-infection, cells and media were collected and subjected to three rounds of freeze-thawing to lyse cells, then titered in duplicate on BSC-40 cells as described[414], except without carboxymethylcellulose.

For experiments in Chapter 4, non-irradiated and irradiated GBM cells were cultured for 7 days to allow the induction of senescence. Using cultures prepared in parallel to experimental cultures, the cells were counted using trypan blue to confirm viability, to ensure that equal numbers of cells had been plated in 12-well plates, and for the MOI calculations. The cells were then infected with the virus at an MOI of

0.03 PFU or 3.0 PFU per cell, as indicated, in 12-well plates and growth assays were performed as outlined above. Reovirus growth experiments were performed similarly and titered on L929 cells as previously described[442]. VSVΔM51-GFP growth experiments were performed similarly and titered as described for VACV, except using Vero cells overlaid with DMEM supplemented with 5% FBS and 1% carboxymethyl cellulose.

2.4 Fluorescence imaging of virus growth. VACV-encoded mCherry fluorescence was imaged at the indicated time points post-infection using an EVOS® FL Cell Imaging System (Thermo Fisher Scientific).

2.5 Cytotoxicity assays. Triplicate wells of cells on 48-well plates were infected with VACV at the indicated MOIs and incubated for a total of 72 hours at 37°C. For experiments in Chapter 3, resazurin (Sigma-Aldrich) was added to a final concentration of 44 µM during the last 2-12 hours of incubation as needed for sufficient color development. Fluorescence was measured using a FLUOstar plate reader (BMG Labtech) with 560 nm excitation/590 nm emission filters. For experiments in Chapter 4, neutral red uptake assays were performed to assess cell viability as previously outlined[445]. Briefly, medium was replaced with culture medium containing 40 µg/mL of neutral red (Sigma-Aldrich) during the last 1-2 hours of incubation. Next, neutral red medium was removed, the cells were washed with 1X phosphate buffered saline (PBS), neutral red destain solution (50% ethanol, 49% deionized water, 1% glacial acetic acid) was added, and plates were incubated/shaken for 10 minutes at room temperature. Fluorescence was measured using a FLUOstar plate reader (BMG Labtech) with 544 nm excitation/620 nm emission filters. Cell viability was calculated from fluorescence of treated samples minus background fluorescence of completely non-viable cells (treatment with 2% Triton X-100 (BioRad)), and is reported as a percent value relative to the fluorescence of mock infected cells (100% cell viability).

2.6 Spheroid invasion assays. Cells were seeded at $2x10^4$ cells per well in duplicate in round bottom ultra-low attachment 96-well plates and cultured for 96 hours to allow the formation of spheroids. Plates were then placed on ice and growth medium was replaced with a 1:1 mixture of medium to Matrigel™ (Corning). Plates were incubated for 1 hour at 37ºC to solidify the medium-Matrigel™ mixture after which a layer of growth medium was added and maintained on top of the solid matrix.

For virus dissemination assays, invasive structures were allowed to form for 48 hours following Matrigel™-embedding, then invasive spheroid structures were infected with Δ*F4L*Δ*J2R* VACV (3.0 PFU per cell in 2 µL 1X PBS) using a stereotaxic instrument (Stoelting Co.) and 10 µL microliter™ syringe (Hamilton) with flat 25s needle (Hamilton). Starting at 48 hours post-infection, brightfield and fluorescence images were taken every 15-20 minutes over a period of 48 hours using a ImageXpress®Micro High-Content System (Molecular Devices). For virus invasion interference assays, 24 hours post-Matrigel™-embedding, spheroids were infected with Δ*F4L*Δ*J2R* VACV (at the indicated MOIs in 2 µL 1X PBS), then imaged immediately following infection (0 hour) and every 24 hours for 7 days. MetaXpress 6.5.5.559 software (Molecular Devices) was used to create overlays of images and videos, as well as quantify invasive area. To calculate MOIs, spheroids cultured in parallel (in medium without Matrigel™) were mechanically dissociated using Accutase or trypsin into single cell suspensions and counted.

2.7 *In vitro* irradiation and induction of senescence-enriched cell cultures. GBM cells, including parallel cultures for later use in cell counting, were irradiated with the indicated doses using a MultiRad 160 X-ray irradiator (Faxitron) or non-irradiated (0 Gy control cells) before mock or VACV infections. For senescence induction, GBM cells were cultured in a growth medium appropriate for the cell line in a humidified 5% CO2 environment at 37 ◦C for 7 days.

2.8 Sources and housing of mice used in studies. Studies were conducted in accordance with the Canadian Council on Animal Care Guidelines and Policies with approval from the Cross Cancer Institute's Animal Care Committee and/or the University of Alberta Health Sciences Animal Care and Use Committee. 6–8-week-old male C57Bl/6 mice or NOD-*scid*-gamma (NOD.Cg-Prkdcscid Il2rgtm1Wjl/SzJ; NSG) mice were obtained, respectively, from Charles River Laboratories or a breeding colony in the University of Alberta Health Sciences Laboratory Animal Services facility (L. Postovit, principal investigator). Mice were acclimatized for at least 7 days upon arrival at the animal housing facilities. For *in vivo* radiation experiments, mice were initially housed in the Cross Cancer Institute Vivarium (location of Small Animal Radiation Research Platform; SARRP) before being transported to a biosafety level 2 (BSL2) containment facility at the University of Alberta Health Sciences Laboratory Animal Services Facility for virus administration. All other mouse experiments not requiring the SARRP occurred at the latter facility. Mice were housed in ventilated cages (1-5 mice per cage) with access to water and food *ad libitum*.

2.9 Intracranial tumor establishment and intracranial injection. To generate syngeneic orthotopic brain tumors, mice were anesthetized (2-3% isoflurane), then a burr hole (2.0 mm diameter) was drilled in the skull 2.0 mm lateral from bregma using a K.1070 High Speed Rotary Micromotor Kit (Foredom). CT2A-luc cells ($1x10^4$ cells in 3 µL 1X PBS) were implanted using a stereotaxic instrument and 10 µL microliter™ syringe with flat 25s needle into the right striatum (2.5 mm depth) at a rate of 1 µL per minute. Following administration, the injection was allowed to set for 1 minute, then the needle was removed 0.5 mm every 0.5 minutes. Tumor bioluminescence was confirmed 6-7 days post-implantation using an In Vivo Imaging System (IVIS) Lumina XRMS (PerkinElmer) or an IVIS Spectrum (PerkinElmer). Mice were sorted so that tumor bioluminescence was evenly distributed among treatment groups.

Δ*F4L*Δ*J2R* VACV stock was sonicated before injection. On the indicated day, varying doses of Δ*F4L*Δ*J2R* VACV in a volume of 4.1 µL were administered intracranially as described above at the same stereotactic

coordinates as tumor implantation into mice that had been either previously injected with tumor cells (for the syngeneic model) or not (for the NSG model). 1X PBS was used as an injection control for all mouse studies.

2.10 *In vivo* radiation treatment. A SARRP (Xstrahl Inc.) was used to administer radiation. Mice were anesthetized (2-3% isoflurane), secured to the treatment stage of the SARRP, and a 360° high resolution (1440 slices) computed tomography scan was performed to identify the burr hole from tumor implantation. Using the burr hole as a fiducial marker, an isocenter was defined 2.5 mm beneath the burr hole center (same depth as tumor implantation), and 10 Gy of radiation was delivered directly overhead to the isocenter (tumor site) in a single 3 x 3 mm beam. The next day, mice were transported to the BSL2 facility at the University of Alberta and acclimatized for 24 hours before receiving virus/PBS treatments.

2.11 Tumor challenges. 45 days post-median-survival of PBS treated groups (approximately 76 days after tumor implantation), cured and naïve age-matched control mice were challenged with fresh CT2A-luc cells either intracranially in the contralateral hemisphere as described above, or subcutaneously in the flank with $4x10^5$ cells in 50 µL 1X PBS.

2.12 Tumor growth measurements. Mouse cranial tumor bioluminescence was measured using an IVIS Lumina XRMS or IVIS Spectrum. Before imaging, mice were subcutaneously injected in the back with 200 µL 15 mg/mL D-luciferin (GoldBio) dissolved in 1X PBS. Tumor bioluminescence was quantified using Living Image 4.5.2 software. Flank tumor growth was measured with calipers. Tumor volume was calculated using the equation: Volume = $Length^2$ x Width/2.

2.13 Flow cytometry. 8-color flow cytometric analysis was performed as described elsewhere[446]. Briefly, tumor-bearing brain quadrants were collected, finely minced (< 0.5 mm pieces), and dissociated using Accutase and DNase I (10 U/ml; Promega) into a single cell suspension. CD45+ cells were isolated

via positive magnetic selection using a MagniSort™ Mouse CD45 kit (Invitrogen). Fc receptors were blocked with TruStain FcX anti-mouse CD16/32 antibody (BioLegend). Dead cells were stained with eFluor 506 fixable viability dye (Invitrogen). Cells were immunostained with anti-mouse antibodies described in **Table 2.1**, then fixed and permeabilized according to the manufacturer's instructions using IC Fixation and Permeabilization Buffers (Invitrogen), before intracellularly staining for FoxP3. Fluorescence minus one (FMO) gating controls were used for each antibody (FMO is a control in which all but one antibody is added to enable appropriate gate setting in subsequent analysis). For each antibody, UltraComp eBeads™ (Invitrogen) were used for single-color compensation controls; a portion of pooled cells were used as compensation controls for eFluor 506 viability dye (Invitrogen). Samples were run using a Fortessa X20 Flow Cytometer (BD Biosciences) and analyzed using FlowJo™ v10 software.

2.14 Cell proliferation assays. For proliferation assays, duplicate wells in 6-well plates were seeded with $1x10^4$ cells. 24 hours later, GBM cells were either irradiated or not irradiated. At the indicated time points post-irradiation, cells were washed with 1X PBS, detached by trypsinization, and diluted 1:1 in trypan blue (Lonza). Total cells per well were counted using a hemacytometer (Hausser Scientific). For assays to assess proliferation of serum-starved cells, duplicate wells in 12-well plates were seeded with $4x10^4$ cells into medium containing either 0.1% FBS or 5% FBS. At the indicated time points post-seeding, total cells per well were calculated as described above.

2.15 Reverse transcription quantitative polymerase chain reaction (RT-qPCR). Total RNA was isolated from non-irradiated and irradiated GBM cells 7 days post-irradiation using the illustra™ RNAspin Mini Kit (GE Healthcare) according to the manufacturer's instructions. Isolated RNA (2 μg) was used as a template to synthesize complementary DNA (cDNA) using the High-Capacity cDNA Reverse Transcription Kit (Applied Biosystems) according to the manufacturer's instructions. RT-qPCR analysis was performed using diluted cDNA (1:30) and Fast SYBR™ Green Master Mix (Applied Biosystems) in Optical 96-Well

Table 2.1. Antibodies used in flow cytometry studies.

Antibody	**Clone**	**Company**
CD3-FITC	145-2C11	Invitrogen
CD4-BUV737	RM4-5	BD Bioscience
CD8-BUV395	53-6.7	BD Bioscience
FoxP3-AF647 (intracellular)	FJK-16S	Invitrogen
CD11b-APCeFluor780	M1/70	Invitrogen
Ly6C-eFluor450	HK1.4	Invitrogen
Ly6G-biotin	IA8	BioLegend
Streptavidin-BV711 (used with Ly6G-biotin)	Not applicable	BD Bioscience

Fast Thermal Cycling Plates (Applied Biosystems). Target gene expression levels were normalized to 18S rRNA. Primer sequences are listed in **Table 2.2**.

2.16 Senescence-associated β-galactosidase activity. Non-irradiated and irradiated GBM cells were assessed for SA-β-gal activity 7 days post-irradiation using the Senescence Beta-Galactosidase Staining Kit (Cell Signaling) according to the manufacturer's instructions. Briefly, cells were washed with 1X PBS, incubated at room temperature for 15 minutes in fixative solution, washed twice with 1X PBS, then incubated at 37°C in a dry incubator (no CO_2) in β-galactosidase staining solution for 12-30 hours as needed for sufficient color development. Next, cells were washed twice with 1X PBS, overlaid with 70% glycerol, and imaged using an Olympus IX70 microscope (Olympus Life Sciences). SA-β-gal positive (blue-colored) cells were quantified manually using ImageJ software (Version 1.51w).

2.17 Immunoblotting. Whole cell lysates were prepared from non-irradiated and irradiated GBM cells 7 days post-irradiation using RIPA lysis buffer [150 mM sodium chloride, 1% Triton X-100 (BioRad), 0.5% sodium deoxycholate, 0.1% sodium dodecyl sulfate, 50 mM Tris-HCl (pH 8.0), 0.1 mg/mL phenylmethylsulfonyl fluoride, 1X Halt™ protease inhibitor cocktail (Thermo Fisher)]. Protein concentration was quantified using the Pierce™ BCA Protein Assay Kit (Thermo Fisher) according to the manufacturer's instructions. Next, protein was resolved by SDS-PAGE and transferred to Immobilon-FL polyvinylidene difluoride (PVDF) membranes (EMD Millipore). The PVDF membranes were blocked using Odyssey blocking buffer (Li-COR Biosciences), washed, then incubated overnight at 4°C with the following primary antibodies diluted at the indicated concentrations in blocking buffer containing 0.2% Tween 20 (Fisher Scientific): anti-p21 [1:1000; ab109520 (Abcam)], anti-TK1 [1:500; ab59271 (Abcam)], anti-RRM2 [1:500; ab57653 (Abcam)], anti-p53R2 [1:1000; ab8105 (Abcam)], anti-β-tubulin [1:1000; 2146 (Cell Signaling Technologies)], or anti-β-actin [1:1000; 926-42210 (Li-COR Biosciences)]. Next, the PVDF membranes were washed and then incubated at room temperature for 1 hour with the following

Table 2.2. Primers used in RT-qPCR studies.

Target Gene (human)	Forward Primer	Reverse Primer
GROα	5'- GAA AGC TTG CCT CAA TCC TG -3'	5'- CAC CAG TGA GCT TCC TCC TC -3'
GROβ	5'- AAC TGC GCT GCC AGT GCT -3'	5'- CCC ATT CTT GAG TGT GGC TA -3'
GM-CSF	5'- GGC CCC TTG ACC ATG ATG -3'	5'- TCT GGG TTG CAC AGG AAG TTT -3'
IL-6	5'- CCG GGA ACG AAA GAG AAG CT -3'	5'- GCG CTT GTG GAG AAG GAG TT -3'
IL-8	5'- CTT TCC ACC CCA AAT TTA TCA AAG -3'	5'- CAG ACA GAG CTC TCT TCC ATC AGA -3'
IFNβ	5'- AGG ACA GGA TGA ACT TTG AC -3'	5'- TGA TAG ACA TTA GCC AGG AG -3'
MX1	5'- TTC AGC ACC TGA TGG CCT A -3'	5'- AAA GGG ATG TGG CTG GAG AT -3'
ISG15	5'- GCG AAC TCA TCT TTG CCA GTA -3'	5'- CCA GCA TCT TCA CCG TCA G -3'
IκBα	5'- GCT GAA GAA GGA GCG GCT ACT -3'	5'- TCG TAC TCC TCG TCT TTC ATG GA -3'
IL1β	5'- CCC AAC TGG TAC ATC AGC AC -3'	5'- GGA AGA CAC AAA TTG CAT GG -3'
TNFα	5'- CCC GAG TGA CAA GCC TGT AG -3'	5'- GAT GGC AGA GAG GAG GTT GAC -3'
18S rRNA	5'- CCC TAT CAA CTT TCG ATG GTA GTC G -3'	5'- CCA ATG GAT CCT CGT TAA AGG ATT T -3'

fluorescent-dye conjugated secondary antibodies diluted at the indicated concentrations in blocking buffer containing 0.2% Tween 20 (Fisher Scientific) and 0.01% sodium dodecyl sulfate: IRDye® 680RD Goat anti-Mouse [1:20,000; 926-68070 (Li-COR Biosciences)] or IRDye® 800CW Donkey anti-Rabbit [1:20,000; 926-32213 (Li-COR Biosciences)]. PVDF membranes were washed and then scanned using an Odyssey Infrared Imaging System (Li-COR Biosciences) and analyzed using Image Studio version 2.0 software (Li-COR Biosciences).

2.18 Quantification of virus infection and cellular senescence. Retention of the fluorescent dye, CellTrace™ Violet (CTV), was used as a surrogate marker for cellular senescence. Cells were stained using the fluorescent CellTrace™ Violet Cell Proliferation Kit (Invitrogen) according to the manufacturer's instructions. Mock-stained cells (with or without VACV-infection) were used as controls for background CTV fluorescence. Briefly, a single-cell suspension of $1x10^6$ cells in 0.5 mL of 5-10 µM CTV-staining solution was incubated for 20 minutes at 37°C. A volume of culture medium (HG-DMEM supplemented as described above) that was 5-6 times the staining solution volume was added, and the cell solution was incubated for 5 minutes at room temperature to quench free CTV. Cells were pelleted, resuspended in cell line specific culture medium, and treated with the indicated radiation doses (0 or 10 Gy). 7 days post-irradiation, cells in duplicate wells of black 96-well plates (Greiner) were infected with the indicated VACVs at 3.0 PFU per cell. 24 hours post-infection, cell monolayers were analyzed for expression of the late VACV protein, A27, as a marker for productive infection. Mock-infected cells (with or without CTV-staining) were used as controls for background antibody fluorescence. Briefly, cell monolayers were fixed for 20 minutes at room temperature using 4% paraformaldehyde, washed thrice with 1X PBS, blocked/permeabilized for 30 minutes using Odyssey blocking buffer (Li-COR Biosciences) containing 0.1% Triton-X100 (BioRad), and then incubated for 1 hour at room temperature with primary anti-A27 VACV antibody [ab117453 (Abcam)] diluted 1:500 in blocking buffer. Cells were washed thrice with 1X PBS and then incubated for 30 minutes at room temperature with fluorescent-dye conjugated

secondary Goat anti-Rabbit antibody [ab150077 (Abcam)] diluted 1:2000 in blocking buffer. Next, cells were washed thrice with 1X PBS and the plates were imaged for both CTV fluorescence and anti-A27 VACV antibody fluorescence using an ImageXpress®Micro High-Content System (Molecular Devic-es). MetaXpress 6.5.5.559 software (Molecular Devices) was used to analyze and create overlays of fluorescent images. The fluorescence intensity of images displaying non-irradiated CTV-stained cells (with or without VACV-infection) was used as a reference for low CTV intensity values; fluorescence intensities above this reference were deemed high CTV intensity. An example of CTV-stained cells that are non-irradiated (mostly low CTV intensity – grey cells) and irradiated (mostly high CTV intensity – blue cells) is shown in **Figure 2.1**. Cells were quantified manually using GIMP 2.10.18 software to view the images. Whenever feasible, cells were protected from light.

2.19 Conditioned medium experiments. GBM cells were either irradiated or non-irradiated. 7 days post-irradiation, medium was exchanged with fresh culture medium, and irradiated or non-irradiated cells were incubated for 48 hours under normal growth parameters to condition the medium. Conditioned medium (CM) was collected, filtered using the 0.22 µm Steriflip® Vacuum-driven Filtration System (Millipore), and used to culture fresh radiation-naïve GBM cells for 24 hours in 12-well plates. Next, virus growth curves were generated by infecting cells with VACVs at 0.03 PFU per cell, allowing virus growth in the presence of CM, collecting lysates at the indicated times and titering lysates in duplicate on BSC-40 cells as above.

2.20 Statistics and analysis. Data were analyzed using GraphPad Prism 9.4.1 software. Nonlinear regression was used to fit curves to data and calculate ED_{50} values; curves generated by nonlinear regression were compared using extra sum-of-square F test. To compare multiple groups, one-way analysis of variance (ANOVA) followed by Šidák's multiple comparisons test was used; where appropriate, area under the curve analysis was performed first. Survival data were analyzed by log-rank

Mantel-Cox testing. To compare two groups, unpaired t test was used. Two-way ANOVA was used to compare growth curves.

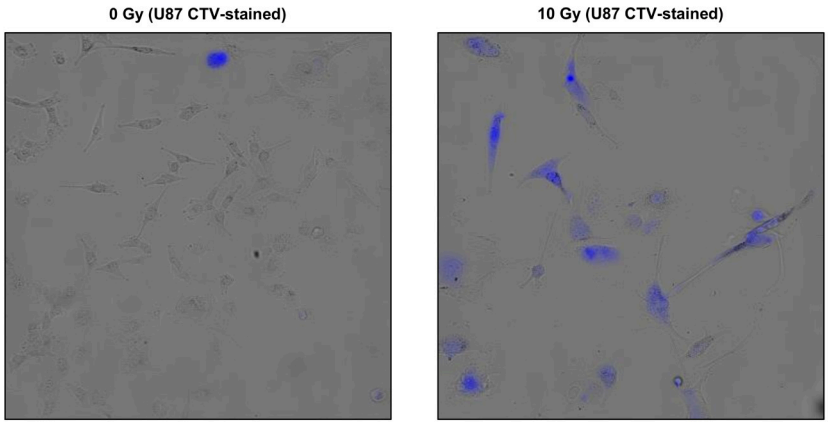

Figure 2.1. Representative images of non-irradiated and irradiated CellTrace™ Violet stained U87 human glioblastoma cells (also treated with wild-type vaccinia virus in this case). Human U87 glioblastoma cells were stained with a fluorescent cell proliferation marker (CellTrace™ Violet; CTV) then were either non-irradiated (0 Gy) or treated with a radiation dose of 10 Gy. 7 days later, cells were infected with 3.0 PFU per cell of wild-type vaccinia virus. 24 hours post-infection, cells were fixed then immunostained with an antibody against the late A27 VACV protein and imaged the next day using fluorescence microscopy. Blue cells in the images were scored as high CTV intensity (CTV^{h}). Grey cells in the images were scored as low CTV intensity (CTV^{lo}).

CHAPTER 3:

Radiation combined with oncolytic vaccinia virus provides pronounced antitumor efficacy and induces immune protection in an aggressive glioblastoma model

Preface

This chapter has been modified from the following published work:

"Storozynsky, Q.T., Agopsowicz, K.C., Noyce, R.S., Bukhari, A.B., Han, X., Snyder, N., Umer, B.A., Gamper, A.M., Godbout, R.G., Evans, D.H., and Hitt, M.M. (2023). Radiation combined with oncolytic vaccinia virus provides pronounced antitumor efficacy and induces immune protection in an aggressive glioblastoma model. *Cancer Letters*, 562, 216169, doi:10.1016/j.canlet.2023.216169."

Contributions:

QTS – Designed and performed experiments, analyzed and interpreted the data, generated the figures, and prepared/revised the manuscript.

KCA, RSN, & ABB – Assisted with animal experiments and contributed to experimental design.

BAU – Designed flow cytometry panel.

XH & NS – Contributed to some virus growth and cytotoxicity experiments and data analysis.

AMG, RG, DHE, & MMH – Provided guidance in experimental design, data interpretation, and manuscript preparation/revision.

*Experiments assisted or performed by other authors have been identified in figure legends.

3.1 Introduction

GBM is a highly invasive and malignant brain tumor requiring an aggressive standard of care regimen involving surgical resection, radiotherapy, and administration of temozolomide[447]. Despite treatments, prognosis is abysmal; median survival is 15.6 months and approximately 95% of patients are deceased within 5 years[6]. These dismal statistics highlight an urgent need for novel therapeutic strategies.

Radiotherapy is a staple part of first-line care for treating GBM and is also used in recurrent settings[116,415]. Despite the precision and efficacy modern radiotherapy offers, invasive cancer cells are still missed[416,417], and a subset of GBM cells are radioresistant[418]. These factors contribute to local recurrence, which often is within 2 cm of the original tumor border[4].

OV therapy is an advancing class of immunotherapy that harnesses tumor-selective viruses to spread through tumors killing cancer cells, while simultaneously stimulating antitumor immune responses[421]. Thus, we hypothesized that these dual anticancer properties of OV therapy would facilitate elimination of GBM cells that remain following radiotherapy.

VACV, a large double-stranded DNA virus used to vaccinate against smallpox[199], has undergone extensive studies as an oncolytic agent for a variety of cancers[195]. Pexa-Vec, an oncolytic VACV furthest along clinically, has been well-tolerated and has shown antitumor immune activation in patients[448,449]. At present, the FDA has approved a single OV, an oncolytic herpesvirus (T-Vec), for treatment of advanced melanoma[387]; no OVs have been approved to date for the treatment of GBM. The oncolytic VACV used here, Δ*F4L*Δ*J2R*, is deleted in viral nucleotide biosynthesis genes *J2R* (*i.e.,* viral thymidine kinase), and *F4L* (*i.e.,* viral R2–the small subunit of viral ribonucleotide reductase), rendering the virus dependent on host cell production of dNTPs required for virus replication[397]. Previously we have shown that Δ*F4L*Δ*J2R* VACV is confined to tumors, displays enhanced safety, and demonstrates antitumor efficacy and

immunity in bladder cancer models[414]. Further, in breast cancer models, Δ*F4L*Δ*J2R* VACV recruits tumor-antigen specific CD8+ T cells to the TME[354].

Though OVs have shown promise with other cancers, as single modalities OVs have had limited success treating malignant brain cancers in the clinic[450] and may be better suited as adjuvants for enhancing other therapies[451]. We hypothesized that combining radiation with Δ*F4L*Δ*J2R* VACV would improve outcomes for GBM better than either modality alone using immune-competent orthotopic CT2A-luc models; speculating that infectious spread of virus would facilitate removal of cancer cells remaining after radiotherapy, either through direct oncolysis, or indirectly via antitumor immune activation.

3.2. Results

3.2.1 ΔF4LΔJ2R vaccinia virus infects, replicates in, and kills glioblastoma cells in vitro

We first evaluated the anticancer potential of Δ*F4L*Δ*J2R* VACV alone *in vitro*. Our initial experiments compared the growth kinetics of WT and Δ*F4L*Δ*J2R* VACVs in a panel of GBM cells consisting of patient-derived GBM and BTIC lines, established human GBM cell lines, and several mouse GBM/BTIC lines. BTICs display cancer stem cell characteristics such as self-renewal, multilineage differentiation, and expression of NSC markers and BTIC lines grown in serum-free, neural stem cell culture conditions maintain stem-like properties[43,44]. Importantly, BTICs are proposed responsible for GBM initiation, maintenance, and recurrence[41,45]. As such, BTIC lines have been a valuable resource for the study and modeling of GBM[43,452]. Virus growth curves indicated that both viruses replicated effectively in our panel of GBM cell lines, though in most cases the growth of Δ*F4L*Δ*J2R* VACV was attenuated relative to WT VACV (**Figure 3.1**). Additionally, we observed Δ*F4L*Δ*J2R* VACV-encoded mCherry fluorescence increase in GBM cultures over time (**Figure 3.2**).

We next evaluated the cytotoxicity of WT and Δ*F4L*Δ*J2R* VACVs using a resazurin-based metabolic viability assay. Virus-mediated cell killing was evident in all GBM cell lines tested, though ED511 and

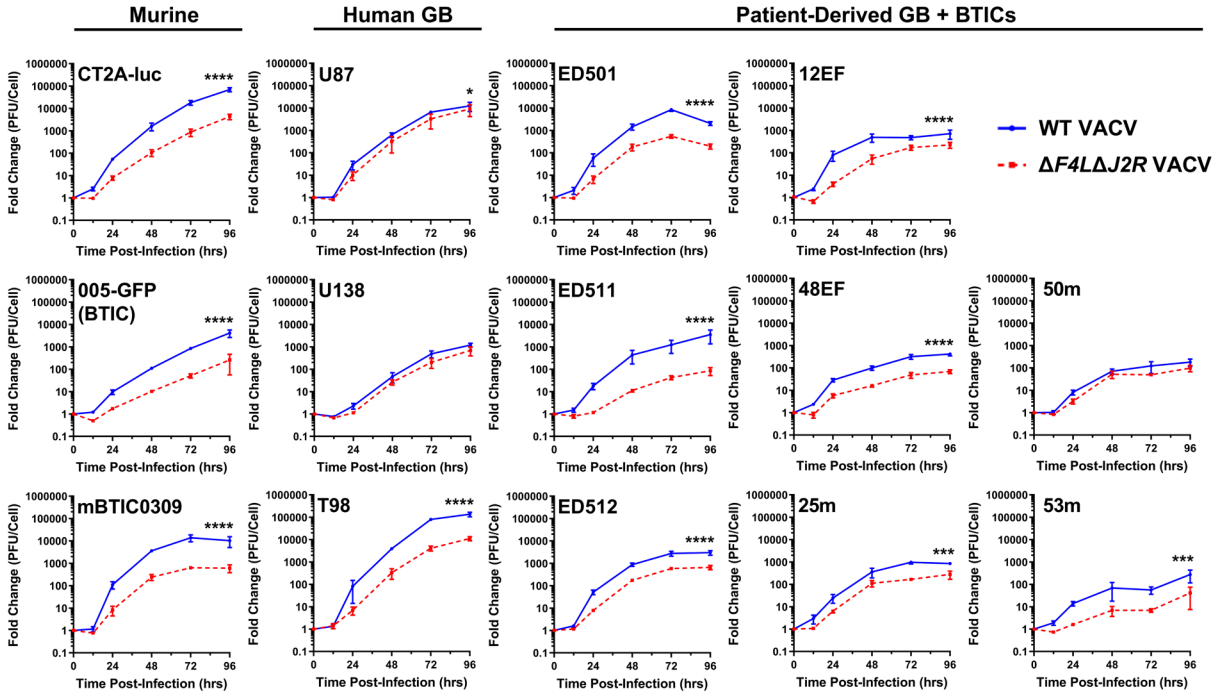

Figure 3.1. Wild-type and Δ*F4L*Δ*J2R* vaccinia viruses replicate in glioblastoma and brain tumor initiating cell lines *in vitro*. Growth curves showing amplification of wild-type (solid blue line) and Δ*F4L*Δ*J2R* (dashed red line) vaccinia viruses in murine/human glioblastoma and brain tumor initiating cell lines. Cells were infected with 0.03 PFU per cell of indicated viruses. Lysates were harvested at the indicated times and titered by plaque assay to assess virus amplification**. Data information:** Data analyzed by nonlinear regression and extra sum-of-square F test (* = $p < 0.05$; *** = $p < 0.001$; **** = $p < 0.0001$). Graphs show fold change relative to lysates taken at t = 0. Data represent 3 independent lysates titered in duplicate. Mean ± SEM is shown. *XH performed experiments with the U138 and T98 cell lines.

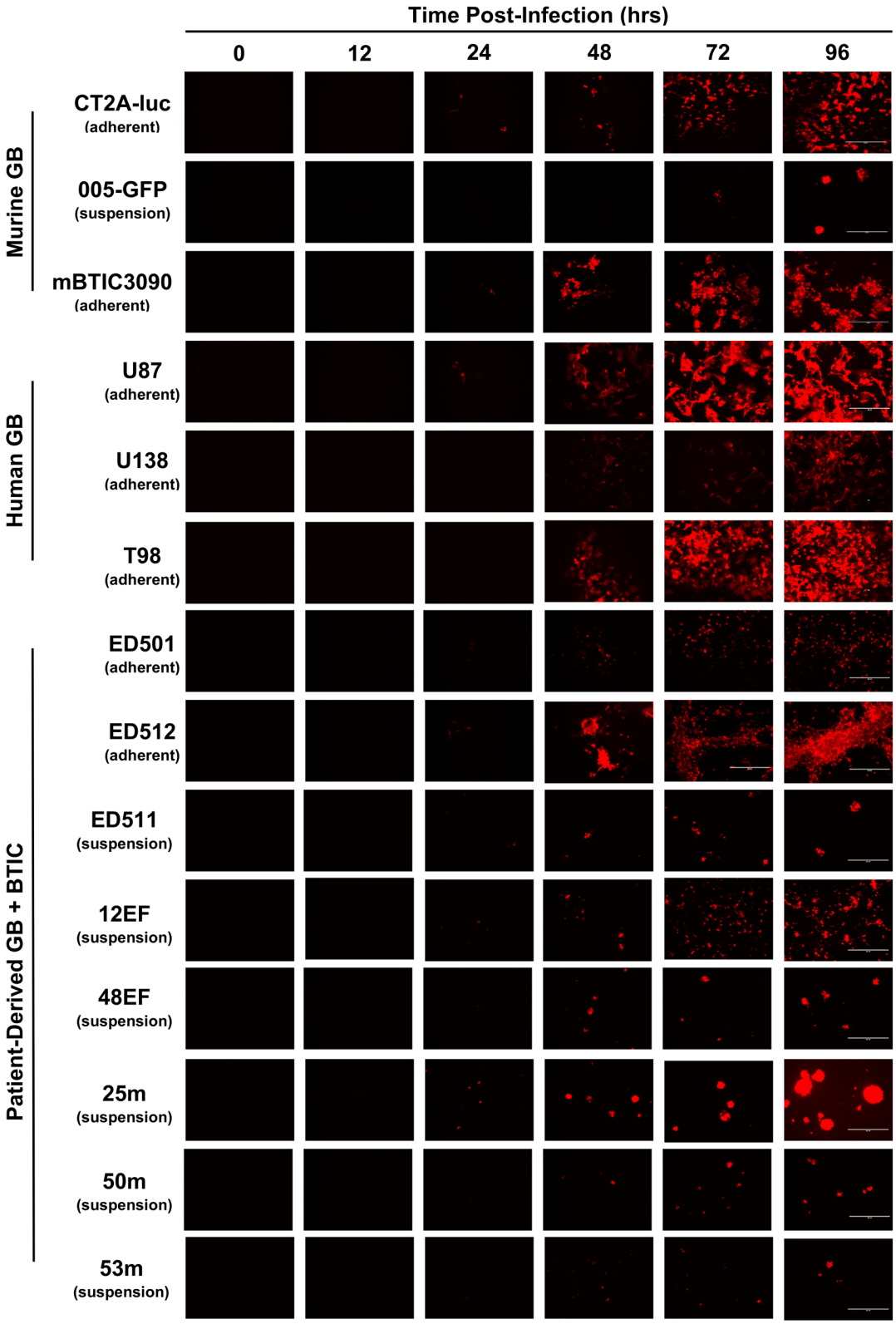
Time Post-Infection (hrs)
0
12
24
48
72
96
Murine GB
CT2A-luc
(adherent)
005-GFP
(suspension)
mBTIC3090
(adherent)
Human GB
U87
(adherent)
U138
(adherent)
T98
(adherent)
Patient-Derived GB + BTIC
ED501
(adherent)
ED512
(adherent)
ED511
(suspension)
12EF
(suspension)
48EF
(suspension)
25m
(suspension)
50m
(suspension)
53m
(suspension)

Figure 3.2. Δ*F4L*Δ*J2R* vaccinia virus infects and replicates in glioblastoma and brain tumor initiating cell lines *in vitro*. Representative images of cells post-infection with 0.03 PFU per cell of Δ*F4L*Δ*J2R* vaccinia virus encoding mCherry. **Data information:** Adherent and suspension cell lines are indicated; suspension cell lines grow as tumor-spheres. Images acquired from 1 experimental repeat in Figure 3.1. Scale bar = 400 μm. *XH performed experiments with the U138 and T98 cell lines.

mBTIC3090 cell lines were less sensitive than the other cell lines to both viruses (**Figure 3.3A, 3.3B**). Importantly, despite the attenuated growth of Δ*F4L*Δ*J2R* VACV relative to WT VACV, both viruses were similarly cytotoxic towards most GBM cell lines. While the growth curves and cytotoxicity data may at first seem inconsistent, it is important to consider that a susceptible cell is killed whether it is infected with 5 infectious virus particles or 500 infectious virus particles, so the number of dead cells and number of infectious particles present do not necessarily correlate in a linear fashion. For 10 of 12 cell lines, dose-response curves evaluating cell viability were not significantly different between WT and Δ*F4L*Δ*J2R* VACVs (**Figure 3.3A**) and the majority of ED_{50} values were comparable (**Figure 3.3B**). Further, in 2 of 12 cell lines, 12EF and ED512, in which WT VACV was more cytotoxic than Δ*F4L*Δ*J2R* VACV, cancer cell killing converged at the highest doses (**Figure 3.3B**). Collectively, these data indicate that Δ*F4L*Δ*J2R* VACV has the capacity to infect, replicate in, and destroy GBM cells. Further studies in this report will focus on the Δ*F4L*Δ*J2R* VACV mutant to determine its suitability as an OV, since use of WT VACV *in vivo* is precluded due to its lethality following intracranial injection[453].

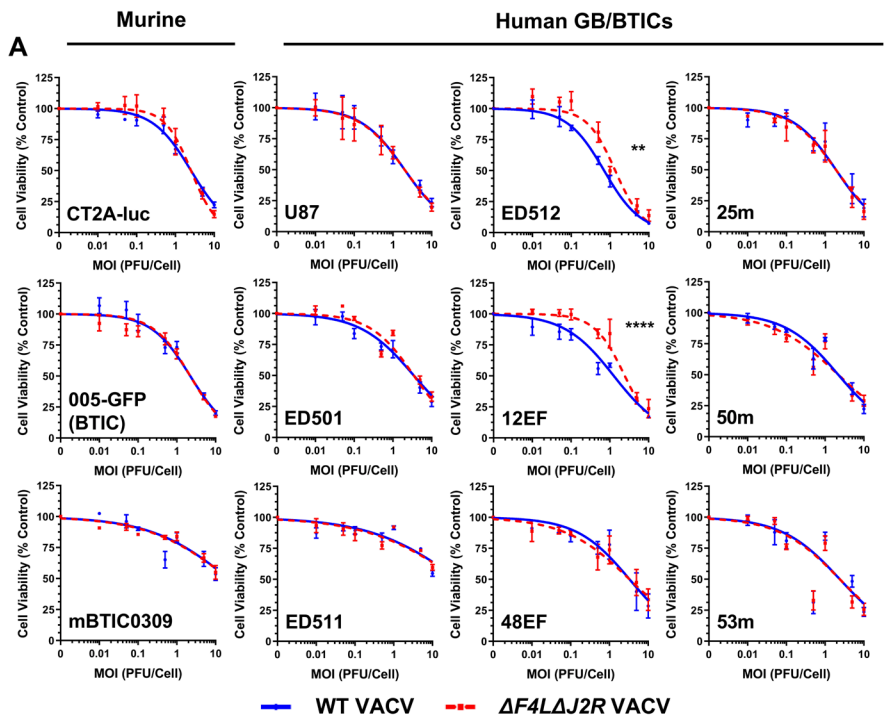

B

ED$_{50}$ (PFU/Cell)		
Cell Line	WT	Δ*F4L*Δ*J2R*
CT2A-luc	2.42 (1.93 to 3.03)	2.61 (1.96 to 3.48)
005-GFP	2.30 (1.83 to 2.89)	2.16 (1.86 to 2.51)
mBTIC0309	15.4 (8.80 to 37.2)	42.2 (20.7 to 123)
U87	2.20 (1.41 to 3.43)	1.84 (1.09 to 3.10)
ED501	2.81 (2.05 to 3.84)	4.07 (2.90 to 5.73)
ED511	33.8 (11.7 to 97.6)	60.2 (13.5 to 268)
ED512	0.706 (0.567 to 0.878)	1.37 (0.989 to 1.89)
12EF	1.27 (1.07 to 1.51)	2.44 (2.06 to 2.88)
48EF	3.09 (1.77 to 5.39)	3.67 (1.86 to 7.24)
25m	2.19 (1.36 to 3.51)	1.66 (1.07 to 2.59)
50m	2.35 (1.57 to 3.50)	2.00 (1.20 to 3.33)
53m	3.27 (1.71 to 6.24)	1.75 (0.935 to 3.27)

Figure 3.3. Wild-type and Δ*F4L*Δ*J2R* vaccinia viruses are cytotoxic towards glioblastoma and brain tumor initiating cell lines in vitro. (A) Dose-response curves showing the viability of murine/human glioblastoma and brain tumor initiating cell lines infected with increasing doses of wild-type (solid blue line) or Δ*F4L*Δ*J2R* (dashed red line) vaccinia viruses based on metabolic resazurin assays. Viability evaluated 72 hours post-infection. **(B)** ED_{50} values of wild-type or Δ*F4L*Δ*J2R* vaccinia viruses for the indicated cell lines. **Data information:** For (A), curves fit to data points using nonlinear regression and analyzed by extra sum-of-square F test (** = $p < 0.01$; **** = $p < 0.0001$). Data is normalized to mock-infected control (0 PFU per cell = 100% cell viability). Data represent 3 independent experiments. Mean ± SEM is shown for data points. For (B), ED_{50} values calculated from curves in (A). 95% confidence intervals are shown in brackets.

3.2.2 ΔF4LΔJ2R vaccinia virus interferes with expansion of glioblastoma spheroids in three-dimensional invasion assays

The highly invasive nature of GBM is a key factor for standard of care failure, therefore therapies that interfere with GBM invasiveness are desired[454]. Using a subset of GBM cell lines from our panel, we generated three-dimensional Matrigel™-embedded GBM structures *in vitro*. Left untreated, these GBM structures invade into Matrigel™ and form spherical invasive patterns that can be imaged and quantified over time (**Figure 3.4A**). Using this system, we assessed the ability of Δ*F4L*Δ*J2R* VACV to disseminate through invasive GBM extensions or to interfere with the expansion of GBM invasive spheroid structures *in vitro* over a one-week period.

As evidenced by virus-encoded mCherry fluorescence, Δ*F4L*Δ*J2R* VACV infected GBM structures and disseminated through invasive GBM extensions (**Figure 3.4B; Figure 3.5; Video S1**). Furthermore, GBM structures infected with Δ*F4L*Δ*J2R* VACV exhibited decreased invasive area in comparison to untreated counterparts (**Figure 3.4C; Video S2**). Virus-mediated interference with the expansion of GBM spheroids in the invasion assays was first detectable by 72 to 96 hours post-infection and was most evident at the highest dose tested (30 PFU per cell) (**Figure 3.4C**). Curiously, time-lapse imaging revealed a unique observation with one BTIC line, 53m. In addition to invasive tumor extensions protruding from the spherical core, untreated 53m cells displayed a diffuse, discontinuous invasive pattern consisting of rapidly-moving single cells detached from the primary spherical structure (**Video S3**). Unexpectedly, this diffuse invasion was nearly absent in Δ*F4L*Δ*J2R* VACV treated conditions (**Video S3**). Together, these data show that Δ*F4L*Δ*J2R* VACV spreads through invasive tumor extensions and limits the expansion of GBM spheroids in three-dimensional invasion assays. Furthermore, Δ*F4L*Δ*J2R* VACV can interfere with diffuse GBM invasion patterns, though this effect was cell line dependent.

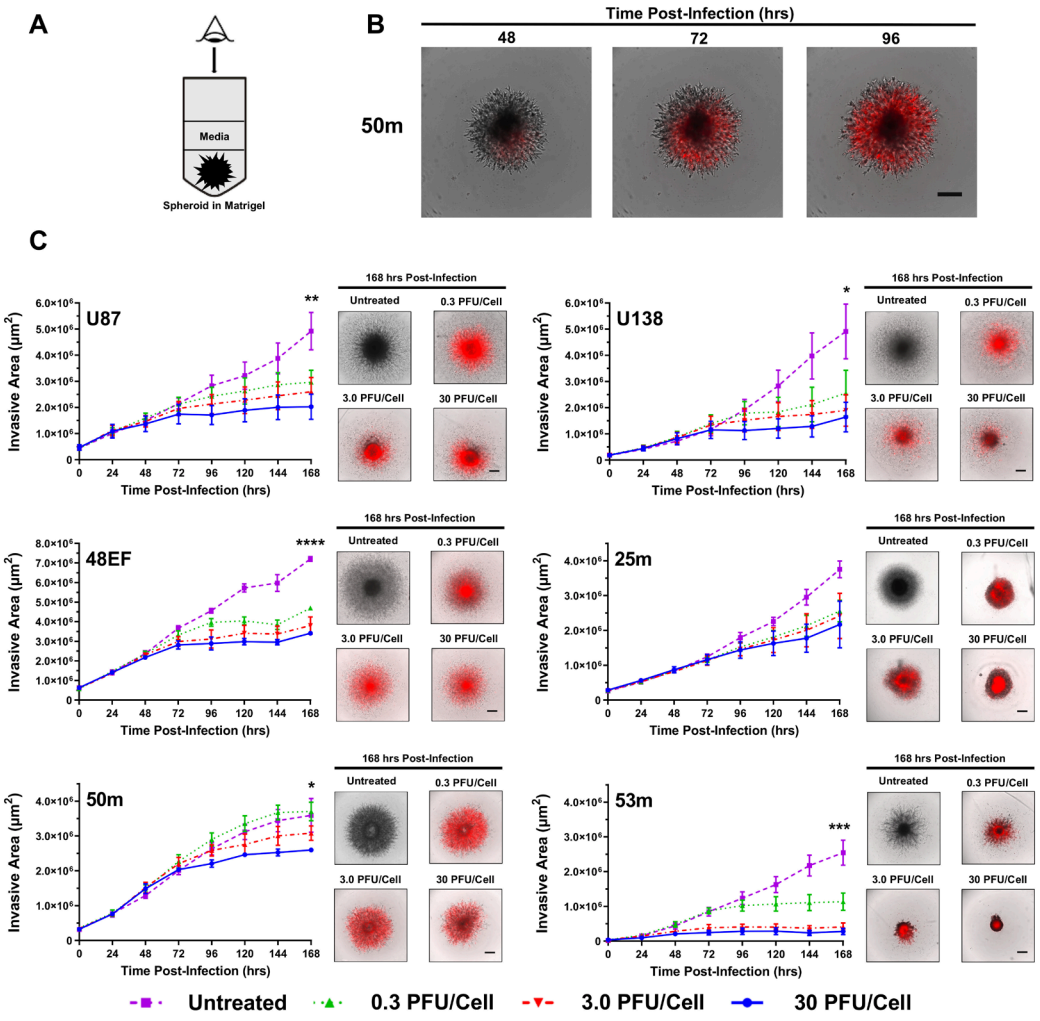

Figure 3.4. Δ*F4L*Δ*J2R* vaccinia virus interferes with expansion of glioblastoma spheroids in three-dimensional invasion assays *in vitro*. (A) Schematic of invasive spheroid structure in well of virus invasion assay. Cartoon eye indicates imaging point of view. **(B)** Virus dissemination assay; representative images of mCherry-encoding Δ*F4L*Δ*J2R* vaccinia virus spreading through invasive glioblastoma extensions after infection with 3.0 PFU per cell. **(C)** Virus invasion interference assay; quantification of invasive area (µm^2) of spheroid structures left untreated or infected with the indicated doses of Δ*F4L*Δ*J2R* vaccinia virus (left panels). Representative images of invasive glioblastoma spheroid structures 168 hours after indicated treatments (right panels). **Data information:** For (B) and (C–right

panels), scale bar = 500 µm. For (C), At least 3 independent experiments were performed, with mean ± SEM shown. Asterisks indicating significance compare untreated to MOI of 30 PFU per cell. Area under the curve analysis followed by one-way ANOVA and Šidák's multiple comparisons test was used (* = $p < 0.05$; ** = $p < 0.01$; *** = $p < 0.001$; **** = $p < 0.0001$).

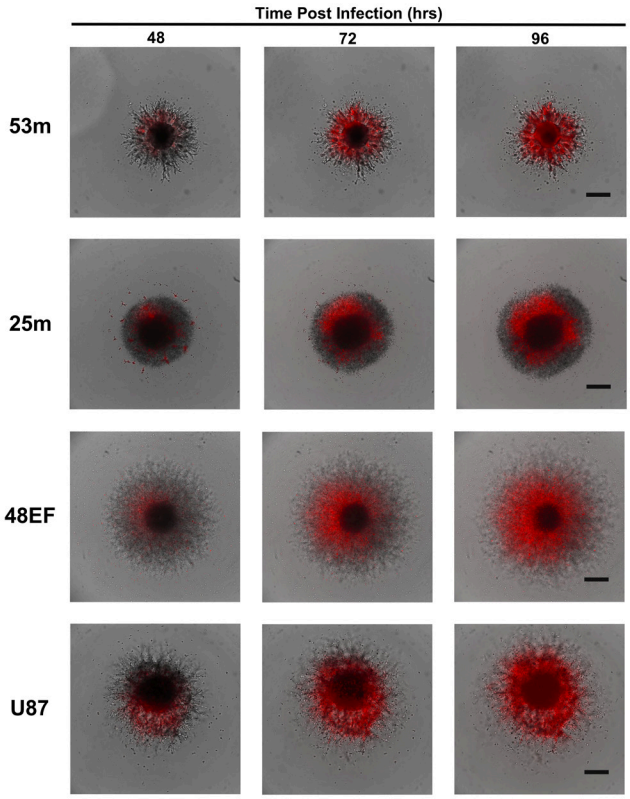

Figure 3.5. Δ*F4LΔJ2R* vaccinia virus disseminates through invasive glioblastoma extensions *in vitro*. Representative images of mCherry-encoding Δ*F4LΔJ2R* vaccinia virus spreading through invasive glioblastoma extensions in the virus dissemination assay. Invasive glioblastoma spheroid structures were infected with 3.0 PFU per cell. **Data information:** Images acquired from 2-3 independent experiments. Scale bar = 500 µm.

3.2.3 Irradiated glioblastoma cells support ΔF4LΔJ2R vaccinia virus replication and are killed post-infection in vitro

Having evaluated Δ*F4LΔJ2R* VACV as a single modality for GBM therapy *in vitro*, we next investigated this virus in combination with radiation. Cells were treated with either 0 Gy (non-irradiated), 4 Gy, or 8 Gy of radiation using a Faxitron X-ray irradiator, then infected with Δ*F4LΔJ2R* VACV 24 hours post-radiation. Plaque assays revealed that the growth kinetics of Δ*F4LΔJ2R* VACV were similar among non-irradiated and irradiated GBM cells, the exception being 12EF cells, where virus growth was inhibited in irradiated cells (**Figure 3.6A**).

Next, the susceptibility of irradiated cells to Δ*F4LΔJ2R* VACV-mediated killing was evaluated using a resazurin-based metabolic viability assay. For all of the cell lines except ED501 and 53m, radiation alone reduced cell viability (see data at MOI = 0 PFU/Cell) (**Figure 3.6B**). Survival of all irradiated and non-irradiated GBM cell lines was consistently reduced at higher doses of Δ*F4LΔJ2R* VACV (**Figure 3.6B**). Of note, irradiated 53m cells displayed increased cell viability (that was not observed with any other cell line) (**Figure 3.6B**); this could have been due to radiation-induced increases in metabolism of GBM cells that survived radiation[455,456] which would be detected by the metabolic viability assay used here. Nonetheless, the highest dose of Δ*F4LΔJ2R* VACV reduced the viability of irradiated 53m cells to 0%—indicating that GBM cells capable of surviving radiation can still be killed by the virus. Overall, these results indicate that Δ*F4LΔJ2R* VACV replicates in, and kills irradiated GBM cells.

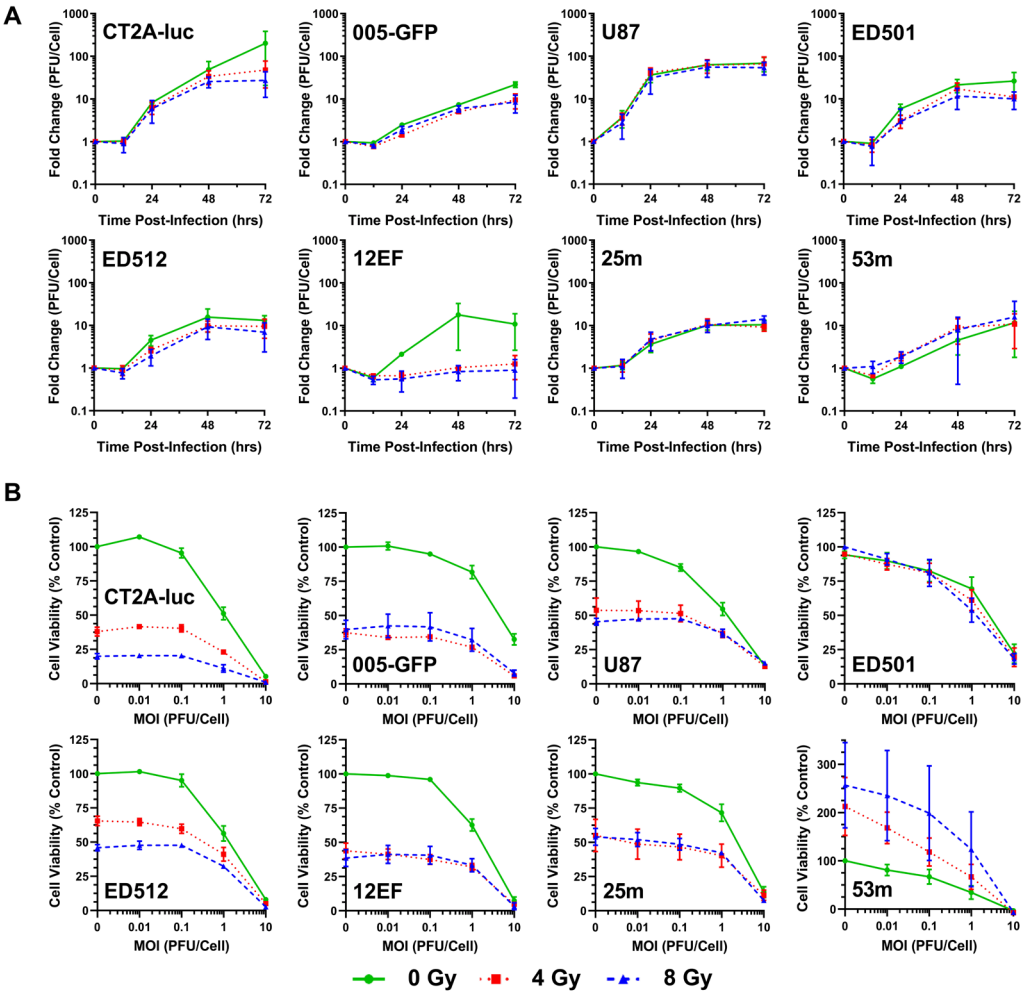

Figure 3.6. Δ*F4L*Δ*J2R* vaccinia virus replicates in and kills irradiated glioblastoma and brain tumor initiating cell lines *in vitro*. (A) Growth curves showing amplification of Δ*F4L*Δ*J2R* vaccinia virus in murine (CT2A-luc, 005-GFP) or human (U87, ED501, ED512, 12EF, 25m, 53m) glioblastoma and brain tumor initiating cell lines treated with radiation doses of 0 Gy (non-irradiated; solid green line), 4 Gy (dotted red line), or 8 Gy (dashed blue line). Cells were infected 24 hours post-radiation with 1.0 PFU per cell. **(B)** Dose-response curves showing cell viability based on metabolic resazurin assay post-infection with the indicated doses of Δ*F4L*Δ*J2R* vaccinia virus. Cells were infected 24 h post-radiation and viability was evaluated 72 h post-infection. **Data information:** For (B), data are normalized to mock-infected control (0 PFU per cell = 100% cell viability). At least 3 independent experiments were performed, with mean ± SEM shown. *NS performed experiments with the ED501 and ED512 cell lines in (B).

3.2.4 ΔF4LΔJ2R vaccinia virus is tolerated and demonstrates efficacy treating a syngeneic orthotopic mouse glioblastoma model

Previous studies have shown that both WT and mutant Δ*J2R* VACVs (single deletion of viral *J2R* gene) are lethal when administered intracranially to mice; the LD_{50} a mere 10 PFU for WT VACV and $4x10^4$ PFU for Δ*J2R* VACV in immune-competent mice[453]. To ensure the safety and feasibility of using our oncolytic VACV intracranially, we injected up to $1x10^7$ PFU of Δ*F4L*Δ*J2R* VACV (approaching the highest feasible intracranial dose) or phosphate buffered saline (PBS; as an injection control) directly into the right striatum of non-tumor-bearing, severely immune-compromised, NSG mice. No concerning weight loss (**Figure 3.7A**) or signs of neurological distress (**Table 3.1**) were noted among treatments. Further, virus recovered from mouse brain homogenates was absent or substantially less than input (**Figure 3.7B**). These findings indicate that Δ*F4L*Δ*J2R* VACV is well-tolerated intracranially *in vivo*, even in mice without adaptive immunity.

We next performed dose-escalation experiments to determine the optimal therapeutic dose of Δ*F4L*Δ*J2R* VACV in syngeneic orthotopic CT2A-luc mouse models. CT2A mouse cells are derived from a carcinogen-induced brain tumor[457] and possess stem-like characteristics[458]. It has been reported that brain tumors formed by CT2A cells recapitulate GBM features such as vascularity, invasiveness, central areas of necrosis, and immune-suppression within the brain TME[458–460]. Of note, the CT2A model is the most aggressive of commonly studied orthotopic syngeneic GBM models[460]. Tumor cells were implanted into the right striatum of male 6–8-week-old C57Bl/6 mice (**Figure 3.8A**). 8 days after tumor injection, mice intracranially received either PBS (as an injection control) or increasing doses of Δ*F4L*Δ*J2R* VACV (10^4, 10^5, 10^6, or 10^7 PFU) at the same stereotaxic coordinates as tumor implantation. Survival was assessed using weight loss and signs of neurological stress as humane endpoints. Tumor bioluminescence was monitored as a surrogate for tumor growth.

Survival was not significantly improved at any dose of Δ*F4L*Δ*J2R* VACV relative to PBS-treated controls (**Figure 3.8B**). However, indications of virus-associated efficacy were observed in some mice. In each of the 10^5, 10^6, or 10^7 PFU cohorts, one mouse was cleared of tumor (cured) based on tumor bioluminescence imaging (**Figure 3.8C**). Furthermore, multiple responders—defined as mice with tumor bioluminescence that dropped below the limit of detection—were noted in each of the 10^5, 10^6, and 10^7 PFU cohorts; the 10^7 PFU treatment possessed the greatest number of responders (**Figure 3.8D**). A transient decrease in weight was noted in a portion of mice administered the 10^7 PFU dose that was not observed with the other lower doses (**Figure 3.8E**). These data indicate that among the doses of Δ*F4L*Δ*J2R* VACV tested, 10^7 PFU produces superior antitumor responses with acceptable transient weight loss.

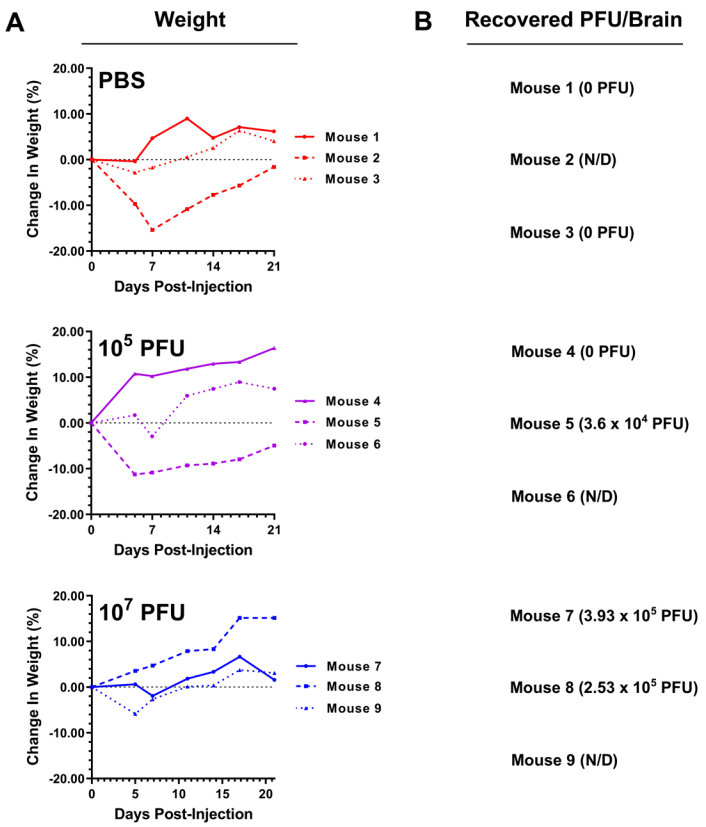

Figure 3.7. Intracranial administration of Δ*F4L*Δ*J2R* vaccinia virus does not cause concerning weight loss in severely immune compromised NOD-*scid*-gamma mice and recovered virus is less than input. Mice were intracranially injected in the right hemisphere striatum with PBS or the indicated doses of Δ*F4L*Δ*J2R* vaccinia virus. **(A)** Change in weight of mice post-treatment. **(B)** PFU recovered from whole brain homogenates of mice 21 days post-treatment. **Data information:** For (A), individual mice are shown. For (B), N/D = not determined.

Table 3.1. List of symptoms used to assess signs of neurological stress post-injection of ∆*F4L*∆*J2R* vaccinia virus in severely immune compromised NOD-*scid*-gamma mice.

Symptoms of Neurological Stress
Ruffled fur
Hunched posture
Impaired mobility
Lack of response to external stimuli
Lethargy
Huddling
Tremors
Listing to one side
Paralysis

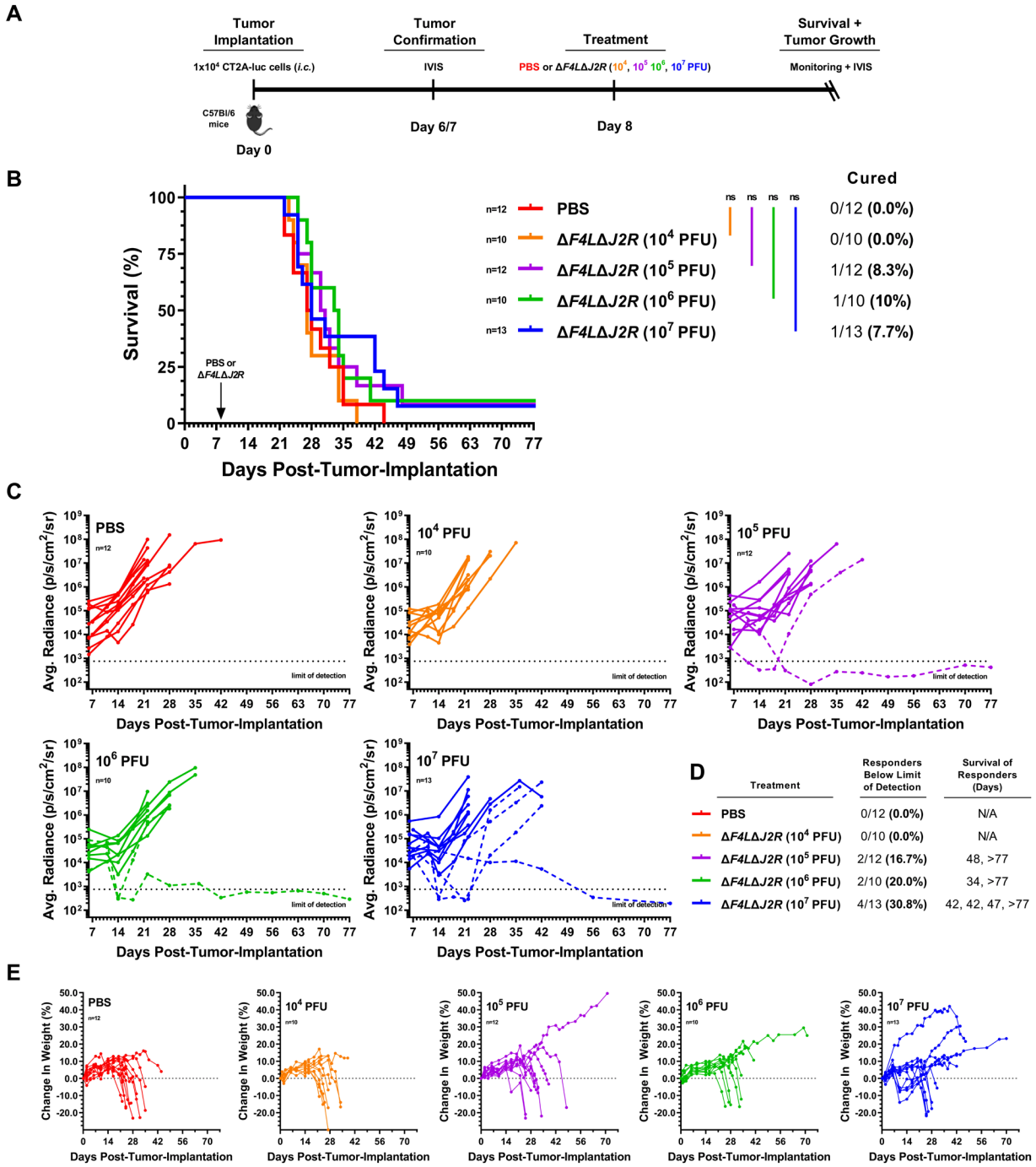

Figure 3.8. Δ*F4LΔJ2R* vaccinia virus is tolerated and exhibits anticancer effects in orthotopic CT2A-luc glioblastoma models. (A) Experimental outline: 1x10^4 CT2A-luc cells were injected into the right striatum of C57Bl/6 mice on Day 0. Tumor implantation was verified by imaging tumor bioluminescence on Day 6/7. On Day 8, PBS or the indicated doses of Δ*F4LΔJ2R* vaccinia virus were intracranially injected.

(B) Kaplan-Meier survival curves of mice administered PBS or the indicated doses of Δ*F4L*Δ*J2R* vaccinia virus; percentage of cured mice from each treatment cohort is shown. **(C)** Quantification of cranial tumor bioluminescence (average radiance; p/sec/cm^2/sr) of individual mice from (B). Dotted line indicates the limit of detection. Dashed lines indicate individual mice with tumor bioluminescence falling below the limit of detection. **(D)** Percentage of mice from (C) with tumor bioluminescence falling below the limit of detection at any time-point post-treatment and corresponding survival. **(E)** Percent change in weight of individual mice post-treatment. **Data information:** For (C) and (D), note: the last bioluminescence imaging session is not necessarily the time of tumor burden endpoint; hence some mice survive longer than the last imaging data point. Data shown in (B–E) are pooled from 3 independent experiments. For (B), survival was analyzed by log-rank Mantel-Cox test (ns = $p > 0.05$).

3.2.5 Radiation combined with ΔF4LΔJ2R vaccinia virus displays superior efficacy relative to either monotherapy

Having observed some evidence of anticancer efficacy with Δ*F4L*Δ*J2R* VACV, we next wanted to determine if outcomes could be improved in combination with radiation. 8 days after tumor implantation, mice were treated with a single 10 Gy beam of radiation directed to the tumor cell injection site using a SARRP (**Figure 3.9A**). The following day, mice were transported to the BSL2 vivarium and acclimatized overnight before administration of 10^7 PFU of Δ*F4L*Δ*J2R* VACV, or PBS as an injection control, the next day. Of note, access to an IVIS imager for one of the experimental repeats was not feasible due to COVID-associated shutdowns. Therefore, bioluminescence data in **Figure 3.9C** were pooled from only two experimental repeats, whereas data for survival and weights in **Figures 3.9B and 3.9D** were pooled from all three experimental repeats.

Radiation alone, Δ*F4L*Δ*J2R* VACV alone, and the combination treatment all significantly increased survival relative to PBS controls (**Figure 3.9B**). However, the combination was significantly superior relative to either monotherapy; further extending survival and curing the majority of mice (**Figure 3.9B**). The median survival was 29 days for PBS, 39.5 days for radiation, 41 days for Δ*F4L*Δ*J2R* VACV, and undefined (but > 76 days) for the combination. Importantly, there was a striking increase in the proportion of cured mice in the combination (66.7%) versus radiation (21.4%) or Δ*F4L*Δ*J2R* VACV (13.3%) alone (**Figure 3.9B**). In these experiments, mice were deemed cured if (1) survival persisted 45 days longer than median survival time for the PBS-treated cohort and remained without neurological symptoms or weight loss, and (2) when imaging data were available, tumor bioluminescence fell below the limit of detection and remained undetectable for the duration of the experiment. The former was necessary given that access to the IVIS to measure tumor bioluminescence was not feasible for all experimental repeats.

As expected, tumor bioluminescence increased rapidly over time in PBS-treated controls (**Figure 3.9C; red panel**). Most mice treated with Δ*F4L*Δ*J2R* VACV alone exhibited a sharp, transient decline in tumor bioluminescence 7 days after virus injection, but ultimately tumor growth resumed; one Δ*F4L*Δ*J2R* VACV-treated mouse was cured (**Figure 3.9C; purple panel**). Following radiation alone, tumor growth persisted but was delayed in most mice relative to PBS-treated controls; a minority of mice were cured (**Figure 3.9C; green panel**). Impressively, radiation in combination with Δ*F4L*Δ*J2R* VACV cleared tumors from the vast majority of mice (**Figure 3.9C; blue panel**). Lastly, as observed in the previous dose-escalation studies, Δ*F4L*Δ*J2R* VACV-treated groups exhibited transient decreases in weight (**Figure 3.9D; purple and blue panels**). One unexpected mortality was observed 72 hours following administration of Δ*F4L*Δ*J2R* VACV alone in one experimental repeat. Collectively, these data strongly indicate that radiation used in concert with Δ*F4L*Δ*J2R* VACV is therapeutically superior relative to either treatment alone.

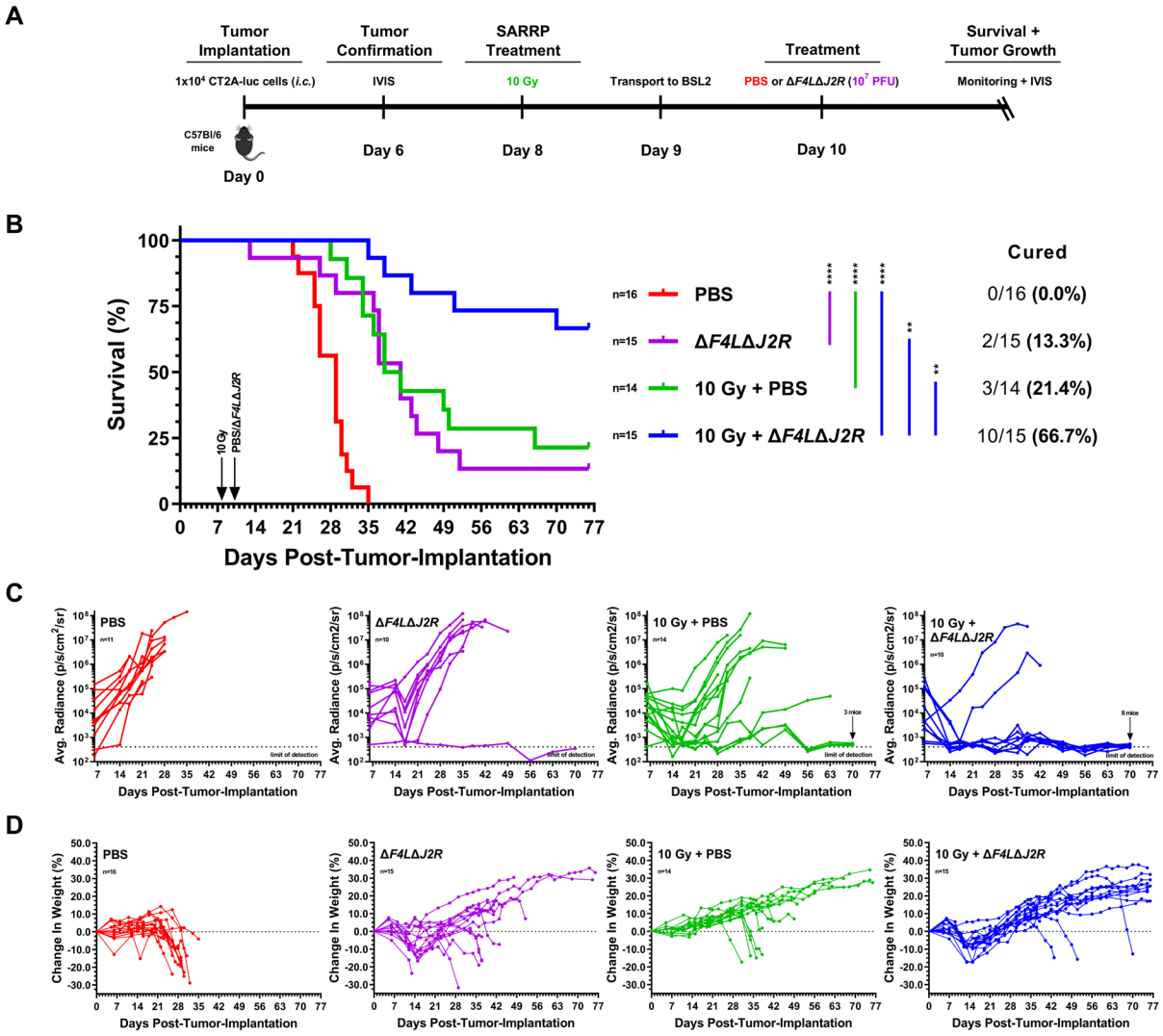

Figure 3.9. Radiation in concert with Δ*F4LΔJ2R* vaccinia virus displays superior anticancer efficacy relative to monotherapies in orthotopic CT2A-luc glioblastoma models. (A) Experimental outline: 1x10^4 CT2A-luc cells were injected into the right striatum of C57Bl/6 mice on Day 0. Tumor implantation was verified by imaging tumor bioluminescence on Day 6. On Day 8, the tumor site was irradiated with a single 10 Gy beam using a Small Animal Radiation Research Platform (SARRP). Mice were transported to a BSL2 facility on Day 9 and intracranially administered PBS or Δ*F4LΔJ2R* vaccinia virus (10^7 PFU) on Day 10. **(B)** Kaplan-Meier survival curves of mice administered the indicated treatments; percentage of cured mice in each treatment cohort is shown. **(C)** Quantification of cranial tumor bioluminescence (average radiance; p/sec/cm^2/sr) of individual mice from (B). Dotted line indicates the limit of detection. **(D)**

Change in weight of individual mice post-treatment. **Data information:** Data shown in (B) and (D) are pooled from 3 independent experiments. Data shown in (C) are pooled from 2 independent experiments. For (B), survival was analyzed by log-rank Mantel-Cox test (** = $p < 0.01$; **** = $p < 0.0001$).

3.2.6 A portion of mice cured by radiation combined with ΔF4LΔJ2R vaccinia virus reject tumor challenge

We next assessed whether cured mice from our previous experiments possessed antitumor immunological memory by performing intracranial tumor challenge experiments. At least 76 days after initial tumor implantation (approximately 45 days after the median survival time of PBS-treated controls), fresh CT2A-luc cells were implanted into the contralateral hemisphere of cured mice from the experiment shown in **Figure 3.9C** and into the same site in naïve age-matched controls.

Relative to naïve age-matched controls, survival after intracranial tumor challenge was significantly increased in mice cured by the combination or by radiation alone (**Figure 3.10A**). Additionally, the one mouse cured by Δ*F4L*Δ*J2R* VACV alone survived longer than all naïve age-matched controls (**Figure 3.10A**). While tumors grew rapidly in all naïve age-matched controls, a portion of cured mice from the combination (3/8 mice; 37.5 %) and all mice cured by radiation alone (3/3 mice; 100 %), rejected intracranial tumor challenge and remained tumor-free for greater than 100 days following tumor challenge (**Figure 3.10A, 3.10B; blue and green panels**). Furthermore, some cured mice from the combination (2/8 mice; 25 %) and one cured mouse from Δ*F4L*Δ*J2R* VACV alone (1/1; 100 %) exhibited delayed tumor growth relative to naïve age-matched controls; resisting, but not rejecting, intracranial tumor challenge (**Figure 3.10A, 3.10B; blue and purple panels**). Lastly, cured mice from one of the three experimental repeats shown in **Figure 3.9B** and a naïve age-matched control were challenged with fresh tumor cells injected subcutaneously in the flank to assess induction of systemic, as opposed to local (intracranial), immunological memory. One of two mice cured by the combination rejected flank tumor challenge (**Figure 3.11**). These data show that radiation in concert with Δ*F4L*Δ*J2R* VACV can induce local, as well as systemic antitumor immunological memory in a portion of cured mice, indicating that the anticancer efficacy associated with the combination may in part be immune-mediated.

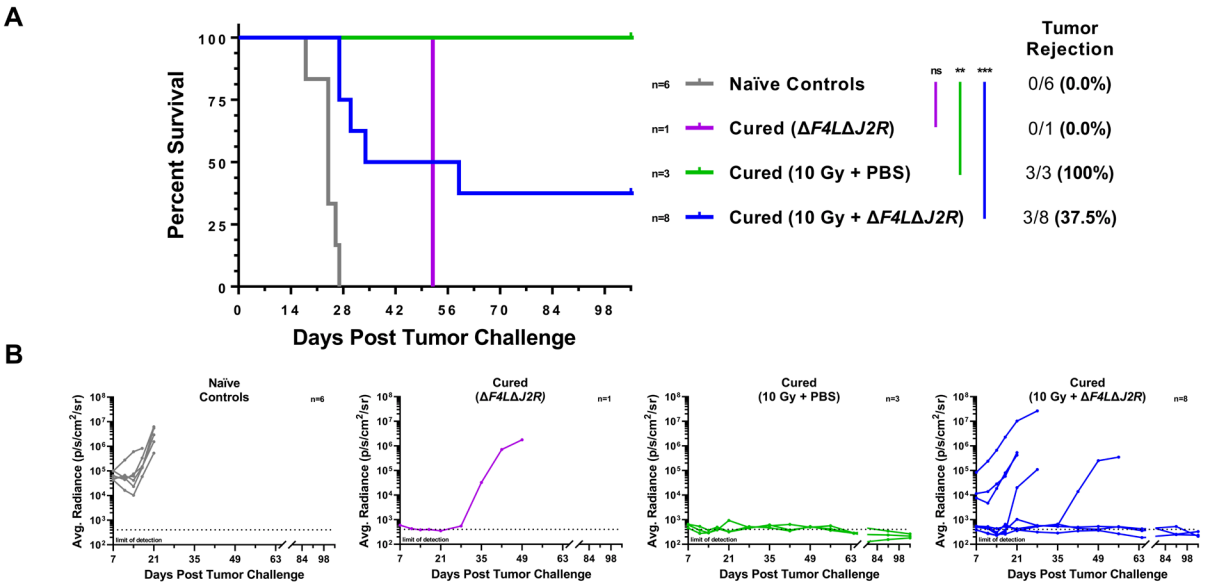

Figure 3.10. Mice cured by radiation alone, Δ*F4L*Δ*J2R* vaccinia virus alone, or the combination resist or reject intracranial CT2A-luc tumor challenge. 12 of the 15 cured mice from the experiment shown in Figure 3.9C and naïve age-matched controls were challenged intracranially with fresh CT2A-luc cells ($1x10^4$ cells) in the contralateral hemisphere. **(A)** Kaplan-Meier survival curves and percentage of mice rejecting tumor following intracranial tumor challenge. **(B)** Quantification of cranial bioluminescence (average radiance; p/sec/cm^2/sr) of individual mice from (A) following intracranial tumor challenge. **Data information:** Data shown in (A–B) are pooled from 2 independent experiments. For (A), survival was analyzed by log-rank Mantel-Cox test (ns = $p > 0.05$; ** = $p < 0.01$; *** = $p < 0.001$).

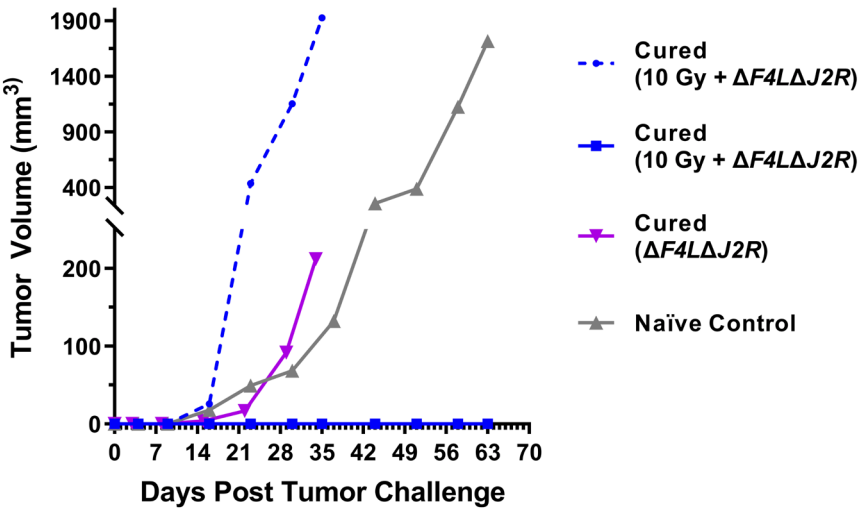

Figure 3.11. Mouse cured by radiation in combination with Δ*F4L*Δ*J2R* vaccinia virus rejects flank CT2A-luc tumor challenge. Tumor growth (measured by caliper) in 3 cured mice and a naïve age-matched control mouse challenged with fresh CT2A-luc cells ($4x10^5$) injected subcutaneously in the flank**. Data information:** Cured mice from 1 of the independent experimental repeats shown in Figure 3.9B.

3.2.7 The brain tumor microenvironment is augmented by radiation combined with ΔF4LΔJ2R vaccinia virus

The superior efficacy of radiation in concert with Δ*F4LΔJ2R* VACV and evidence of antitumor immune responses prompted us to next investigate how treatments may augment the immunological milieu of the brain TME. Mice were treated with either radiation, Δ*F4LΔJ2R* VACV, the combination, or PBS as previously described, then 7 days following virus/PBS injections, tumor-bearing brain quadrants were harvested and assessed by multicolor flow cytometry for immune analysis (**Figure 3.12A**).

CD3+ and CD8+ infiltration is associated with better prognosis in GBM patients[104,106]. Δ*F4LΔJ2R* VACV alone and in combination with radiation significantly increased the proportion of CD3+ cells (TILs; **Figure 3.12B**) and CD3+/CD8+ cells (CD8+ cytotoxic T cells; **Figure 3.12C**) recovered from the brain TME relative to PBS controls. Interestingly, radiation alone did not significantly differ from PBS controls in any of the aforementioned parameters (**Figure 3.12B, 3.12C**). These data indicate that radiation alone is inadequate for altering CD3+ or CD8+ T cell compositions in this model, whereas addition of Δ*F4LΔJ2R* VACV increases proportions of both.

Δ*F4LΔJ2R* VACV alone significantly increased the proportion of CD3+/CD4+/FoxP3- cells (CD4+ helper T cells) relative to PBS, while neither the combination nor radiation alone were significantly different from PBS controls (**Figure 3.12D**). Interestingly, a higher ratio of CD4+ to CD8+ T cells is associated with poorer prognosis in GBM patients[461]. The combination displayed the lowest CD4+:CD8+ ratio among treatments and was the only treatment significantly altered relative to PBS controls (**Figure 3.12E**).

Tregs are a barrier for durable antitumor immune responses[462] and are present in GBM patients at increased levels[317]. The proportion of CD3+/CD4+/FoxP3+ cells (Tregs) was significantly increased by Δ*F4LΔJ2R* VACV alone, whereas the proportion of Tregs recovered from the combination or radiation alone was not significantly different compared to PBS controls (**Figure 3.12F**). A higher ratio of CD8+

cytotoxic T cells to Tregs is a meaningful parameter for immunotherapy efficacy[463] and associated with a favorable prognosis in GBM patients[464]. In our experiments, the CD8+:Treg ratio was significantly increased by the combination relative to PBS controls, but not significantly changed by radiation alone or Δ*F4L*Δ*J2R* VACV alone (**Figure 3.12G**). These data suggest that the proportion of immune cells in the brain TME treated with the combination has less immune-suppressive Tregs than Δ*F4L*Δ*J2R* VACV alone, and more CD8+ cytotoxic T cells than radiation alone, resulting in a superior CD8+:Treg ratio relative to either monotherapy.

Within the GBM microenvironment, TAM/Mi, as well as monocytic and polymorphonuclear MDSCs (M-MDSCs and PMN-MDSCs) contribute to an immune-suppressed landscape, precluding optimal anticancer immune responses[320,465]. The proportion of CD11b+ cells (TAM/Mi and MDSCs; **Figure 3.12H**), CD11b+/Ly6G-/Ly6C- (TAM/Mi; **Figure 3.12I**), CD11b+/Ly6C+/Ly6G- cells (M-MDSCs; **Figure 3.12J**) and CD11b+/Ly6G+ (PMN-MDSCs; **Figure 3.12K**) were not significantly changed compared to PBS controls.

In comparison to monotherapies, these data collectively indicate that radiation combined with Δ*F4L*Δ*J2R* VACV best alters the brain TME towards conditions favorable for antitumor immune responses. That is, increased CD3+ TILs and CD8+ cytotoxic T cells relative to radiation alone, in parallel with an increased CD8+:Treg ratio relative to either monotherapy.

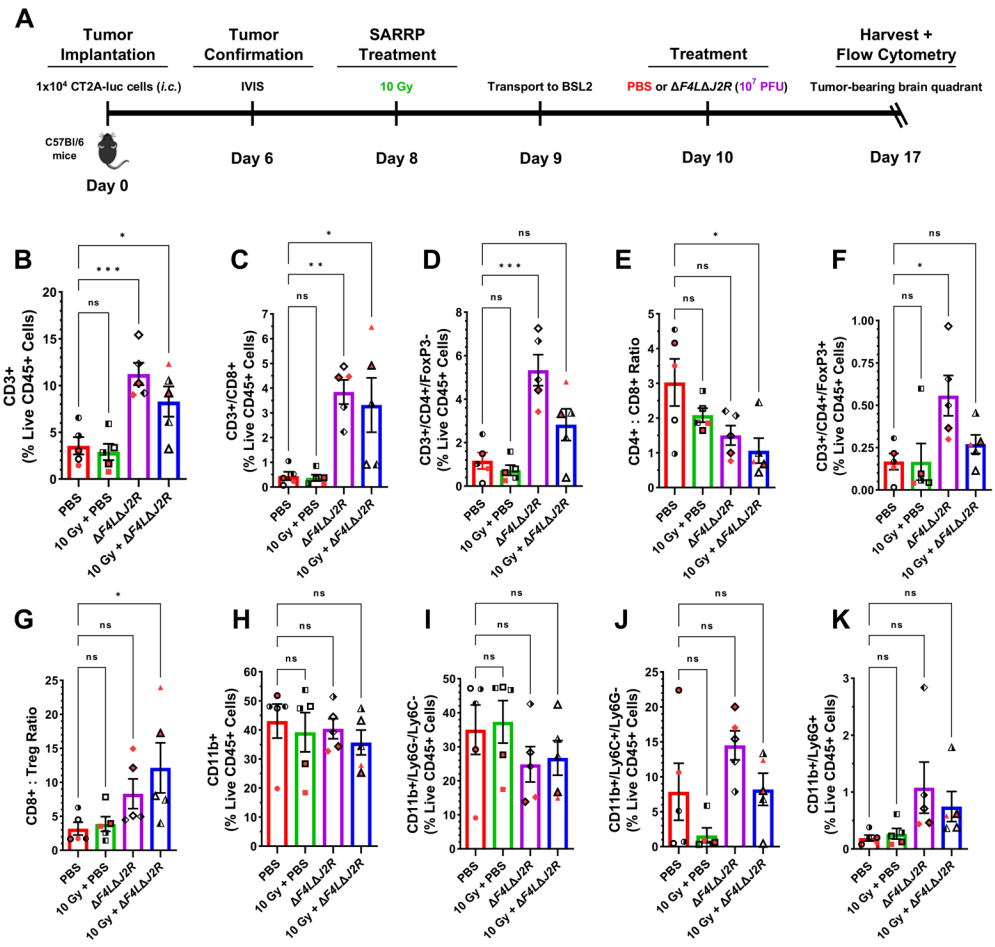

Figure 3.12. The brain tumor microenvironment is uniquely augmented by radiation in combination with Δ*F4LΔJ2R* vaccinia virus relative to either monotherapy in orthotopic CT2A-luc glioblastoma models. (A) Experimental outline: Models established and treated as indicated. 7 days post-virus/PBS treatments (Day 17), brain tumor quadrants were harvested, dissociated into single-cell suspensions, magnetically enriched for CD45+ cells (= total live cells in calculations), stained with fluorochrome-conjugated anti-mouse antibodies, and analyzed by flow cytometry. Immune subsets are shown as the percentage of live CD45+ cells: **(B)** CD3+ tumor infiltrating lymphocytes (TILs); **(C)** CD3+/CD8+ cytotoxic T cells; **(D)** CD3+/CD4+/FoxP3- helper T cells; **(E)** Ratio of CD3+/CD4+ cells to CD3+/CD8+ cells (CD4+:CD8+ ratio); **(F)** CD3+/CD4+/FoxP3+ regulatory T cells (Tregs); **(G)** Ratio of CD3+/CD8+ cells to CD3+/CD4+/FoxP3+ cells (CD8+:Treg ratio); **(H)** CD11b + tumor-associated macrophage and microglia

(TAM/Mi), myeloid-derived suppressor cells (MDSCs); **(I)** CD11b+/Ly6G-/Ly6C- TAM/Mi; **(J)** CD11b+/Ly6C+/Ly6G- monocytic-MDSCs (M-MDSCs); **(K)** CD11b+/Ly6G + polymorphonuclear-MDSCs (PMN-MDSCs). **Data information:** Mean ± SEM is shown. Data shown are pooled from 2 independent experiments (red symbols = 1 independent experiment; black/clear symbols = 1 independent experiment). Each unique data point represents cells from an individual mouse, consistent across all graphs. (B–K) analyzed by one-way ANOVA and Šidák multiple comparison test (ns = $p > 0.05$; * = $p < 0.05$; ** = $p < 0.01$; *** = $p < 0.001$).

3.4. Discussion

As a single agent *in vitro*, Δ*F4L*Δ*J2R* VACV displayed promising anticancer properties. The virus infected, replicated in, and killed an extensive panel of human/mouse GBM and BTIC lines, as well as disseminated through invasive GBM extensions and interfered with the expansion of GB spheroids in three-dimensional invasion assays. Further, radiation did not impact Δ*F4L*Δ*J2R* VACV growth or cytotoxicity towards the vast majority of cell lines. These *in vitro* results over a large GBM panel highlight the potential broad applicability of Δ*F4L*Δ*J2R* VACV alone or in combination with radiation for treating this disease. *In vivo* Δ*F4L*Δ*J2R* VACV alone was well-tolerated, with significant improvements in safety over the reported unmodified or *J2R*-deleted VACVs[453,466], and most effective at the highest feasible dose (10^7 PFU). However, as a single modality the virus offered only modest therapeutic efficacy in our model—a finding echoed clinically where many OVs used alone to treat GBM, despite promise, are insufficient for disease clearance[450]. As such, OVs are frequently explored clinically in combination with other modalities (including radiotherapy) to improve treatment of GBM[327]. Thus, we next investigated using radiation in combination with Δ*F4L*Δ*J2R* VACV *in vivo* to improve efficacy.

A single 10 Gy dose of radiation in combination with oncolytic Δ*F4L*Δ*J2R* VACV produced considerably superior therapeutic outcomes relative to either monotherapy when treating immune-competent orthotopic CT2A-luc mouse models. The aggressiveness of the CT2A model should be noted; compared with other frequently studied orthotopic syngeneic GBM models (*i.e.,* GL261, 005, and Mut3), the CT2A model progresses the fastest to tumor burden endpoint[460]. Strikingly, despite the aggressiveness of this model, the majority of mice in our study were cured following treatment with the combination (66.7%; 10/15).

Importantly, use of the CT2A-luc model in the present study addresses several drawbacks of past studies assessing radiation in concert with oncolytic VACVs for treating GBM. Radiation combined with different

oncolytic VACVs yielded enhanced anticancer efficacy in several subcutaneous GBM xenografts[423–425]. However, subcutaneous GBM models fail to recapitulate critical features of the human pathology as well as the brain TME, reducing translational significance. Advani *et al.* (2012)[423] reported increased survival of orthotopic U87 GBM xenografts following systemic delivery of an oncolytic VACV (GLV-1h68) combined with 12 Gy of radiation delivered over two fractions. However, use of an immune-compromised model precludes determination of immunological contributions to anticancer efficacy. Further, orthotopic U87 models do not recapitulate prototypical characteristics of human GBM including infiltrative invasion[467] and areas of necrosis[468]. The combination of radiation with different oncolytic VACVs has been investigated in preclinical models of other types of cancer such as head and neck cancer[469], pancreatic cancer[470], sarcoma[471,472], $^{V600D/E}$BRAF mutant melanoma[473], and lung cancer[474]. Again, many of the models used in these investigations have similar limitations, including use of immune-compromised models, or in studies that did utilize immune-competent models, use of subcutaneous tumor implantation. In contrast, our study employed an aggressive orthotopic immune-competent model that recapitulates key features of human GBM[458,459] and brain tumor immunology[460], thus strongly bolstering confidence that radiation combined with Δ*F4L*Δ*J2R* VACV has a high degree of translational potential as a multimodal strategy for treating GBM.

The poor response of GBM to treatment is in part due to the highly immune-suppressive landscape of the brain TME[314]. Like human GBM, the CT2A model is highly immune-suppressed; CT2A cells reprogram immune cells towards an immune-suppressive state[475], tumor-suppressive cell types such as Tregs are recruited to the CT2A-tumor microenvironment[460], and CD8+ T cells extracted from the CT2A-TME display severely exhausted phenotypes[476]. Consequently, compared with other syngeneic GBM models, the CT2A model is less responsive to several immunotherapeutic strategies[477–479]. Despite the immune-suppression associated with the CT2A model, our tumor challenge studies indicated that efficacy of the combination was likely mediated in part by the immune system. When challenged intracranially with

fresh tumor cells, mice cured by the combination displayed significantly increased survival relative to naïve age-matched controls, with some of the combination-treated mice completely rejecting or displaying resistance to tumor challenge. Tumor challenge in the flank was also rejected by one combination-cured mouse, suggesting that the combination may induce systemic as well as local antitumor immunity. These findings suggest that radiation in concert with Δ*F4L*Δ*J2R* VACV has the capacity to break immune tolerance in the GBM microenvironment and induce antitumor immunological memory.

The immune-suppressive properties of CT2A cells/tumors may also explain the varying survival outcomes of Δ*F4L*Δ*J2R* VACV treatment between **Figure 3.9** and **Figure 3.10**. Given that Δ*F4L*Δ*J2R* VACV was administered at a later time point in **Figure 3.10** compared to **Figure 3.9**, it is possible that the larger tumor burden would condition and immunologically suppress the TME, facilitating increased virus infection, replication, and/or spread; as the ability of the host immune system to respond and eliminate virus is dampened in the immune-suppressed TME. Indeed, anticancer therapies with immune-suppressive properties can improve oncolytic VACV therapy for GBM[466].

Interestingly, although only a minority of mice in our study were cured by radiation alone (21.4%; 3/14), all of these cured mice rejected tumor challenge. Following treatment with a single ablative dose of radiation, immune-mediated anticancer efficacy has been demonstrated in the B16 melanoma model[118], as well as induction of antitumor immunological memory in the CT26 colon cancer model[119]. Recently, antitumor immunity was also demonstrated in mice cured of subcutaneous NS1 GBM tumors by treatment with 12.5 Gy delivered over two fractions[480]. However, to our knowledge, the present study is the first to report rejection of intracranial tumor challenge in orthotopic GBM models that were cured by radiation alone.

Though radiation has been traditionally categorized as a direct cytocidal agent through induction of dsDNA breaks that lead to cell death[481], it is increasingly appreciated for stimulating antitumor immune effects[419,482]. Likewise, in addition to the direct cytotoxicity of OV therapy via oncolysis of infected cancer cells, activation of antitumor immunity is well-established[195]. Taken together, the capacity for radiation and OV therapy to activate antitumor immune responses likely contributed to the antitumor activity observed in our study. Several other studies corroborate this. Stereotactic body radiation combined with another oncolytic VACV (WR-GS) enhanced anticancer efficacy while also inducing pro-immunogenic effects greater than either modality alone[474]. Further, radiation combined with an oncolytic VSV controlled tumors better than either treatment alone and induced antitumor immune protection[483].

Increased levels of T cells within the TME following treatment with radiation combined with other OVs has been noted in other preclinical brain cancer models[484]. Our investigation of T cells within the CT2A-luc brain TME agrees with these observations. After treatment with the combination, the brain TME displayed greater proportions of CD3+ TILs and CD8+ cytotoxic T cells than when treated with radiation alone and was on par with that following Δ*F4L*Δ*J2R* VACV treatment alone. Additionally, Δ*F4L*Δ*J2R* VACV alone had the greatest proportion of immune-suppressive Tregs, thus an inferior CD8+:Treg ratio, while the combination displayed the highest CD8+:Treg ratio. This favorable balance of pro-immune versus inhibitory immune T cell types is likely to have played a role in the antitumor activity of the combination therapy.

Changes in the myeloid immunological milieu (CD11+ cells) of the brain TME were less apparent. The proportions of TAM/Mi, as well as M-MDSCs and PMN-MDSCs were similar for all treatments in our study. Within the myeloid compartment of immune cells present in GBM, TAM/Mi are major players associated with immune-suppression and compose a substantial proportion of the brain TME (~40%)[485]. Given high levels of TAM/Mi present at baseline with GBM, it is perhaps reasonable that following Δ*F4L*Δ*J2R* VACV treatment proportions remained similar, as many of these cells are already present

within the brain TME (as opposed to being recruited) to respond to virus infection. Unsurprisingly, immune cells recovered from the CT2A-luc brain TME were mostly TAM/Mi among all treatments. Interestingly, despite the abundance of TAM/Mi in GBM, Treg-mediated immune-suppression is more potent within the brain TME[486], which is consistent with our finding of superior efficacy with the combination of radiation and Δ*F4L*Δ*J2R* VACV compared to single modalities, since the combination had the most favorable CD8+:Treg ratio. Overall, following treatment with the combination, the immunological state within the brain TME could be more permissive for antitumor immunity than either treatment alone. However, firmer conclusions will have to await data on the functional status or antigen specificity of T cells within the brain TME.

Factors other than immune activation may also have contributed to the superior efficacy of the combination of radiation and Δ*F4L*Δ*J2R* VACV in our GBM model. First, radioresistant GBM cells that otherwise would have survived radiation could have been directly destroyed by Δ*F4L*Δ*J2R* VACV infection. Further, spatial cooperation could be at play, in which invasive GBM cells outside the radiation field were within the area infected by Δ*F4L*Δ*J2R* VACV; indeed, our *in vitro* invasion assays suggest Δ*F4L*Δ*J2R* VACV can spread through invasive GBM extensions. Taken together, these factors as well as immune activation are likely to have played a role in clearance of tumors in our orthotopic model system.

Lastly, this research has several possible applications. For patients with recurrent GBM, no standard of care is established. As a salvage therapy, re-irradiation via SRS is a non-invasive option that precisely delivers a large dose of radiation to the tumor site[116]. However, despite modest benefits for some patients treated with SRS, the disease remains lethal. Our preclinical research suggests that combining a large dose of radiation with Δ*F4L*Δ*J2R* VACV could improve therapeutic outcomes in this clinical setting. Furthermore, a promising area of investigation to improve GBM treatment involves modifying immunologically “cold” TMEs into “hot” ones, with the intention of reversing immune-suppression and

unleashing antitumor immune responses[125]. The induction of antitumor immunological memory and unique T cell alterations of the CT2A-luc brain TME after treatment with radiation combined with Δ*F4L*Δ*J2R* VACV indicates this multimodal therapy may be effective for reversing immune-suppression and harnessing the immune system. This feature may potentiate other immune-based therapies, allowing further improvements for GBM therapy. Indeed, patients with recurrent GBM treated with ICB lacked meaningful therapeutic outcomes due to low T cell levels and high levels of immune-suppressive cells in the TME[487]. In such clinical settings, perhaps radiation combined with oncolytic VACV therapy could potentiate ICB effectiveness while also offering additional direct cytocidal effects.

In conclusion, we demonstrate that radiation in concert with oncolytic Δ*F4L*Δ*J2R* VACV generates superior anticancer efficacy relative to monotherapies. This multimodal therapy eliminated tumors from an aggressive immune-suppressed GBM model that recapitulates human disease. Further, the combination uniquely alters the brain TME and induces immunological memory. These outcomes indicate the capacity for this combinational strategy to reverse immune-suppression, a desirable feature for treating GBM. Novel therapeutic combinations will likely be required to conquer GBM. This study validates the use of radiation with an oncolytic Δ*F4L*Δ*J2R* VACV to improve treatment of this malignant brain cancer.

CHAPTER 4:

Radiation-induced cellular senescence reduces susceptibility of glioblastoma cells to oncolytic vaccinia virus

Preface

This chapter has been modified from the following published work:

"**Storozynsky, Q.T.,** Han, X., Komant, S., Agopsowicz, K.C., Potts, K.G., Gamper, A.M., Godbout, R.G., Evans, D.H., and Hitt, M.M. (2023). Radiation-induced cellular senescence reduces susceptibility of glioblastoma cells to oncolytic vaccinia virus. *Cancers*, *15*, 3341. https://doi.org/10.3390/cancers15133341."

Contributions:

QTS – Designed and performed experiments, analyzed and interpreted the data, generated the figures, and prepared/revised the manuscript.

XH and SK – Contributed to executing experiments and data analysis.

KCA – Performed and assisted with reovirus related experiments.

KGP – Manuscript revision, prepared the mutant vesicular stomatitis virus, VSVΔM51-GFP, used in this study and contributed to VSVΔM51-GFP related experimental design.

AMG, RG, and DHE – Provided guidance in experimental design, data interpretation, and manuscript preparation/revision.

MMH – Contributed to executing VSVΔM51-GFP experiments and data analysis, provided guidance in experimental design, data interpretation, and manuscript preparation/revision.

*Experiments assisted or performed by other authors have been identified in figure legends.

4.1 Introduction

GBM is a malignant and incurable brain cancer with dismal prognosis despite an aggressive standard of care involving surgery, radiotherapy, and TMZ administration[447]—thus, the development of novel strategies is required to treat this disease. OV therapy is one such developing anticancer strategy being explored clinically to improve GBM outcomes[450]. OVs infect and spread throughout tumors eliminating cancer cells both directly via oncolysis, and indirectly through the activation of anticancer immune responses[488]. Despite its promise for GBM treatment in the clinic, OV therapy as a single modality is unable to achieve complete disease clearance[450] and therefore is increasingly being explored in combination with other established anticancer modalities[327].

Many approved therapies induce cellular senescence in cancer cells[489]. Cellular senescence is a state in which cells cease to proliferate but remain viable and metabolically active[490]. Several features that characterize senescent cells *in vitro* include altered morphology (enlarged size), SA-β-gal activity, upregulation of negative regulators of the cell-cycle such as $p21^{CIP1}$ and $p16^{INK4a}$, and the SASP (a phenotype in which senescent cells secrete a variety of defined factors which can have pro-tumorigenic downstream effects)[128,490]. Both TMZ[491] and radiation[426]—staple parts of GBM standard of care—as well as GBM salvage therapies such as lomustine[492], can induce cellular senescence of GBM cells. Further, radiation is often investigated in combination with OV therapy to improve therapeutic outcomes[493]; therefore, we focused our investigations on radiation-induced senescence. Previous studies have demonstrated that the interaction of viruses with senescent cells is nuanced and complex[433]. Some lines of evidence suggest that cellular senescence can benefit or be exploited by viruses[428,429], whereas other reports indicate that cellular senescence is associated with antiviral activity[430–432]. Thus, we were interested in evaluating how OV activity may be impacted by radiation-induced senescence of GBM cells.

Several oncolytic agents are based on VACV, a large DNA virus used to vaccinate against smallpox[199]. VACV-based oncolytic therapies have been investigated in human clinical trials[384,449] and have demonstrated efficacy treating a variety of preclinical cancer models [reviewed in [195]], including several GBM models[466,494,495]. Further, radiation combined with VACV-based oncolytic therapies has been studied in a broad range of preclinical cancer models[469–474], and several preclinical GBM models[120,423–425]; however, VACV interaction with radiation-induced senescent cancer cells has not been evaluated.

The OV VACV used here, Δ*F4L*Δ*J2R*, is rendered dependent on host cell production of dNTPS via two viral nucleotide biosynthesis gene deletions, *F4L* (*ie.,* viral R2—the small subunit of viral ribonucleotide reductase), and *J2R* (*i.e.,* viral thymidine kinase [TK])[397]. This oncolytic Δ*F4L*Δ*J2R* VACV previously demonstrated anticancer efficacy treating bladder cancer models[414] and an aggressive GBM model when used in combination with radiotherapy[120].

Using oncolytic Δ*F4L*Δ*J2R* VACV, as well as WT VACV for comparison, we investigated the growth kinetics, infectivity, and cytotoxicity of these viruses following infection of radiation-induced senescent GBM cell populations and non-irradiated controls *in vitro*. We show that both oncolytic Δ*F4L*Δ*J2R* VACV and WT VACV display attenuated phenotypes in irradiated senescence-enriched GBM cell populations—indicating that, at least *in vitro*, radiation-induced cellular senescence impairs VACV. These findings underscore important considerations for the combination of VACV-based oncolytic therapies with senescence-inducing agents and provide evidence that cellular senescence induces antiviral properties.

4.2 Results

4.2.1 Radiation induces senescence in glioblastoma cells

The established U87 GBM cell line, as well as a patient-derived GBM cell line, ED501, were employed to assess a panel of different markers evaluating the induction of cellular senescence following radiation exposure. Cellular senescence typically takes 3-7 days to develop in GBM cells after radiation exposure, with increased numbers of radiation-induced senescent GBM cells present at late relative to early time points (5-14 days versus 1-3 days)[426,496–499]. Thus, we chose to perform our analyses 7 days post-irradiation.

Cell proliferation ceased in irradiated U87 and ED501 cell lines while non-irradiated controls continued to proliferate over a 7-day period based on trypan blue assays (**Figure 4.1A**). Additionally, 7 days after radiation treatments, transcription of SASP-associated genes was significantly increased in irradiated GBM cells compared to non-irradiated controls (**Figure 4.1B**). At this same 7-day time point, irradiated GBM cells were larger in size (**Figure 4.1C; left panels**) and had significantly increased SA-β-gal activity compared to non-irradiated controls, with the vast majority of irradiated U87 and ED501 cells staining positive for SA-β-gal activity (~80%) (**Figure 4.1C; right panels**). The same trends were observed using two additional human GBM cells lines, T98 and U118 (**Figure 4.2A–C**). There was a trend towards increased levels of p21, a negative regulator of the cell-cycle, in irradiated U87 and ED501 cells relative to non-irradiated controls 7 days after treatments (**Figure 4.1D**), and no increase was observed in irradiated T98 and U118 cells (**Figure 4.2D**). Collectively, these data indicate that radiation-induced senescent GBM cells are reliably generated 7 days following ionizing radiation exposure.

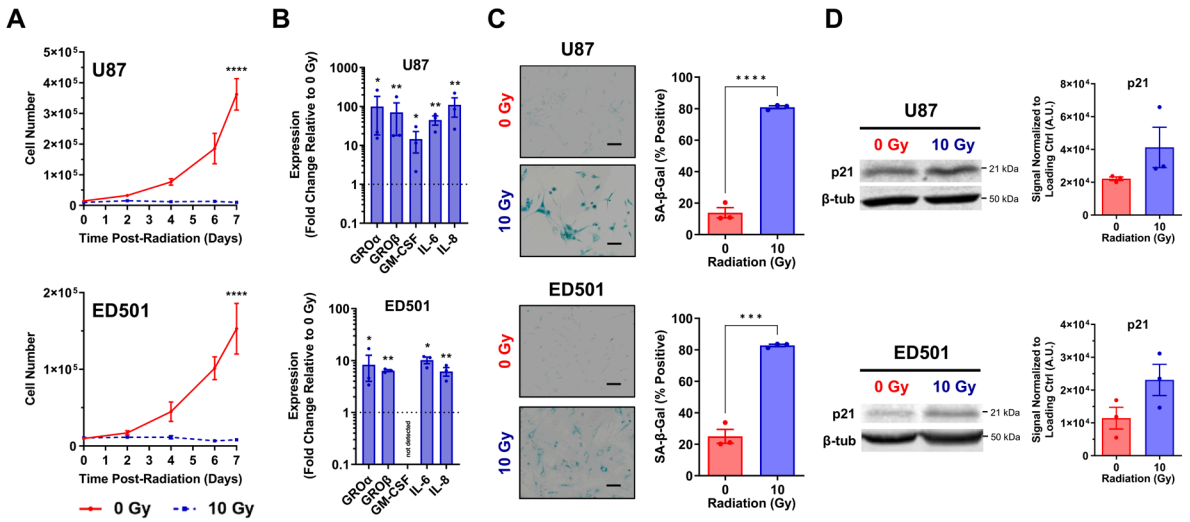

Figure 4.1. Verification of radiation-induced senescence in irradiated glioblastoma cells. Human U87, ED501, T98, and U118 glioblastoma cell lines were either non-irradiated (0 Gy) or treated with a radiation dose of 10 Gy then evaluated for markers of cellular senescence. **(A)** Cellular growth curves showing the change in cell number over time following the indicated radiation treatments. Trypan blue assays were performed to quantify total live cells at the indicated time points. **(B)** Fold change in expression of senescence-associated secretory phenotype (SASP) genes in 10 Gy treated cells relative to 0 Gy treated cells 7 days following radiation treatments, based on RT-qPCR analysis. 18S rRNA levels were used for normalization. **(C)** Representative images of cells assessed for senescence-associated-β-galactosidase activity (left panels) and quantification of cells positive for senescence-associated-β-galactosidase activity (right panels) 7 days following the indicated radiation treatments. **(D)** Representative immunoblots showing p21 protein levels (left panels) and quantification of band signals (arbitrary units; A.U.) normalized to β-tubulin loading controls (right panels) 7 days following radiation treatments. **Data information:** Data represent 3 independent experiments, mean ± SEM is shown. For (A), significance was determined by two-way ANOVA. For (B), asterisks indicate significance of unpaired t-test comparing ΔCt values (**Figure 4.3**). For (C), unpaired t-test was used to determine significance and scale bar = 100 µm. (* = $p < 0.05$; ** = $p < 0.01$; *** = $p < 0.001$; **** = $p < 0.0001$). *SK contributed to (B–D).

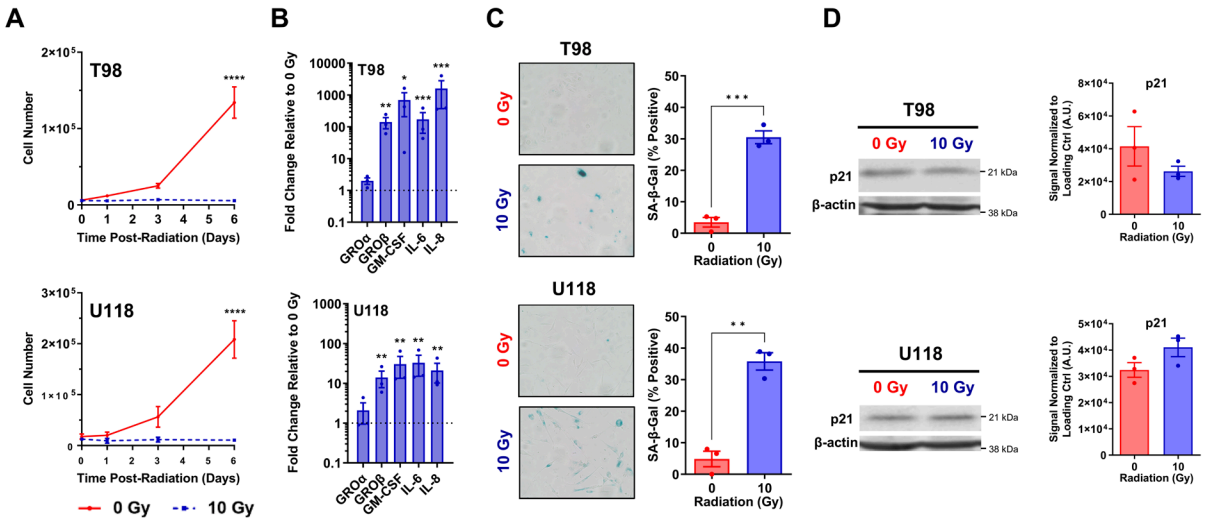

Figure 4.2. Additional verification of radiation-induced senescence in other irradiated glioblastoma cells. Human T98 and U118 glioblastoma cell lines were either non-irradiated (0 Gy) or treated with a radiation dose of 10 Gy then evaluated for markers of cellular senescence. **(A)** Cellular growth curves showing the change in cell number over time following the indicated radiation treatments. Trypan blue assays were performed to quantify total live cells at the indicated time points. **(B)** Fold change in expression of senescence-associated secretory phenotype (SASP) genes in 10 Gy treated cells relative to 0 Gy treated cells 7 days following radiation treatments, based on RT-qPCR analysis. 18S rRNA levels were used for normalization. **(C)** Representative images of cells assessed for senescence-associated-β-galactosidase activity (left panels) and quantification of cells positive for senescence-associated-β-galactosidase activity (right panels) 7 days following the indicated radiation treatments. **(D)** Representative immunoblots showing p21 protein levels (left panels) and quantification of band signals (arbitrary units; A.U.) normalized to β-tubulin loading controls (right panels) 7 days following radiation treatments. **Data information:** Data represent 3 independent experiments, mean ± SEM is shown. For (A), significance was determined by two-way ANOVA. For (B), asterisks indicate significance of unpaired t-test comparing ΔCt values (**Figure 4.3**). For (C), unpaired t-test was used to determine significance and scale bar = 100 µm. (* = $p < 0.05$; ** = $p < 0.01$; *** = $p < 0.001$; **** = $p < 0.0001$). * XH performed experiments in (A–D).

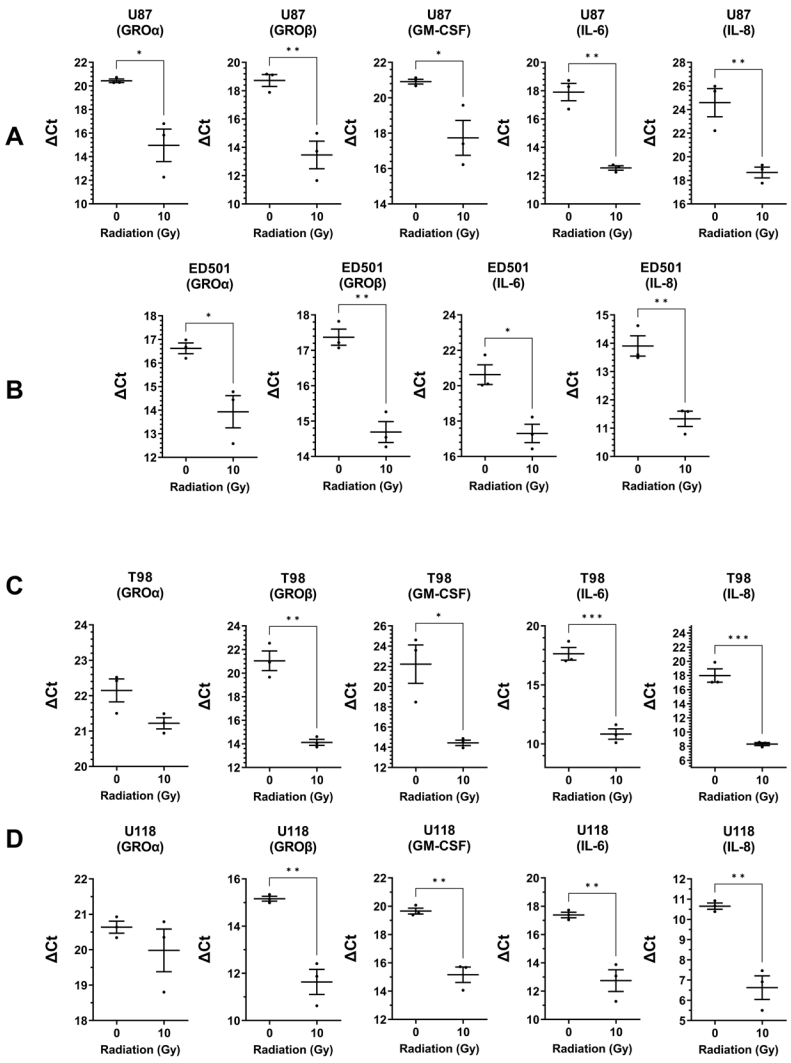

Figure 4.3. ΔCt values used to calculate significant differences of SASP gene expression between non-irradiated and irradiated human glioblastoma cell lines. ΔCt values of the indicated senescence-associated secretory phenotype (SASP) genes based on RT-qPCR analysis of 0 Gy (non-irradiated) or 10 Gy treated human glioblastoma cell lines 7 days post-irradiation. 18S rRNA levels were used for normalization. The glioblastoma cell lines are indicated: **(A)** U87, **(B)** ED501, **(C)** T98, and **(D)** U118. **Data information**: Data represent 3 independent experiments, mean ± SEM is shown. ΔCt values calculated by subtracting the Ct value of the 18S gene from the Ct value of the target gene within the same treatment condition. Significance determined using unpaired t-test (* = $p < 0.05$; ** = $p < 0.01$; *** = $p < 0.001$).

4.2.2 Vaccinia virus growth is attenuated in irradiated senescence-enriched glioblastoma cell populations

We next investigated the growth kinetics of oncolytic *ΔF4LΔJ2R* VACV and WT VACV in U87 and ED501 cell lines under the same treatment conditions as above. Virus growth was assessed as outlined in **Figure 4.4A**. Briefly, GBM cells were irradiated to induce cellular senescence (or not), then infected 7 days later with virus at a low multiplicity of infection (MOI; 0.03 PFU per cell) and virus yields were determined over a 72-hour growth period. Virus growth curves indicated that amplification of oncolytic *ΔF4LΔJ2R* VACV and WT VACV was significantly reduced in irradiated senescence-enriched U87 and ED501 cell lines compared to non-irradiated controls (**Figure 4.4B; left panels**). This effect was most pronounced with the patient-derived ED501 cell line, with no virus growth observed under irradiated senescence-enriched conditions (**Figure 4.4B; left panels**). Additionally, attenuated growth of oncolytic *ΔF4LΔJ2R* VACV and WT VACV was observed using T98 and U118 GBM cell lines treated the same way (**Figure 4.5A, 4.5B**). We extended our analysis of virus growth kinetics by treating GBM cells as above, except using a 100-fold higher MOI (3.0 PFU per cell) to ensure that all cells were infected at t = 0 hours. Again, oncolytic *ΔF4LΔJ2R* VACV was attenuated in both irradiated senescence-enriched U87 and ED501 cell lines versus non-irradiated controls, however WT VACV was only attenuated in the ED501 cell line, not the U87 cell line (**Figure 4.4B; right panels**). These data suggest that at a high MOI, attenuation of WT VACV growth is cell line dependent.

Next, we cultured U87 cells under low-serum conditions to restrict cellular proliferation. Serum-starved U87 cells did not proliferate over 72 hours but did under normal-serum conditions (**Figure 4.6A**). Using low-serum culture conditions we assessed the growth of oncolytic *ΔF4LΔJ2R* VACV and WT VACV in irradiated and non-irradiated U87 cells infected 7 days post-irradiation with a low MOI (0.03 PFU per cell). Again, growth of oncolytic *ΔF4LΔJ2R* VACV was significantly attenuated in the irradiated senescence-enriched condition compared to non-irradiated (non-proliferating) controls (**Figure 4.6B**).

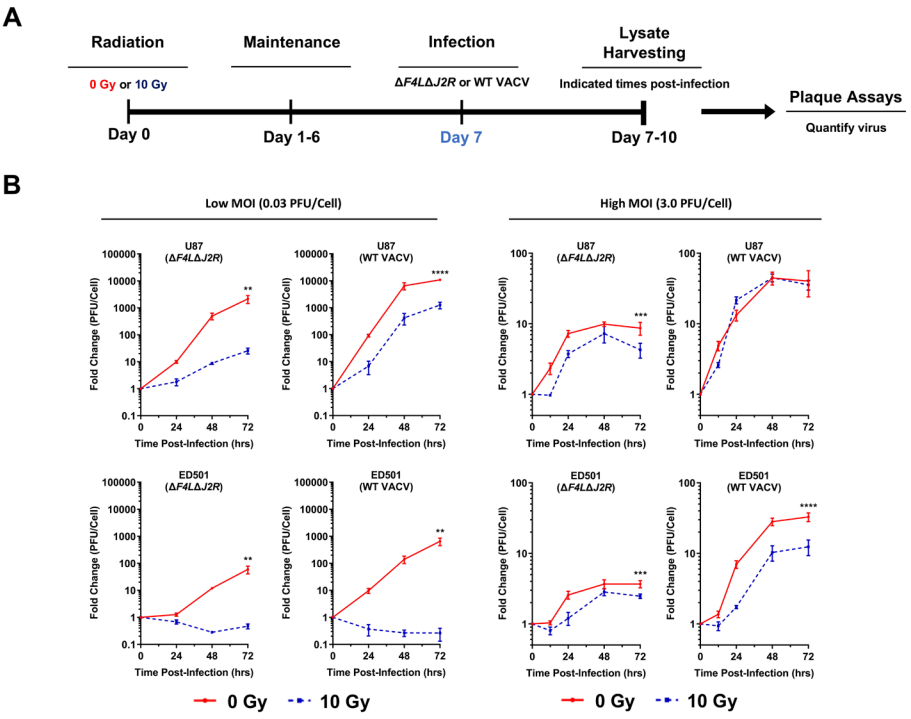

Figure 4.4. Vaccinia virus replication is attenuated in irradiated senescence-enriched human glioblastoma cell lines. (A) Experimental outline: Human U87 and ED501 glioblastoma cell lines were either non-irradiated (0 Gy) or treated with a radiation dose of 10 Gy. 7 days later, cells were infected with the indicated vaccinia viruses. Lysates were harvested at the indicated times and titered by plaque assay to assess virus yield. **(B)** Amplification of oncolytic Δ*F4LΔJ2R* and wild-type (WT) vaccinia viruses in 0 Gy (non-irradiated; solid red lines) and 10 Gy (dashed blue lines) treated human U87 and ED501 glioblastoma cell lines. Cells were infected with 0.03 PFU per cell (left panels) or 3.0 PFU per cell (right panels). **Data information:** Data represent 3 independent lysates titered in duplicate, mean ± SEM is shown. Graphs show fold change relative to lysates taken at t = 0. Significance determined by two-way ANOVA analysis (** = $p < 0.01$; *** = $p < 0.001$; **** = $p < 0.0001$). *SK contributed to (B; left panel).

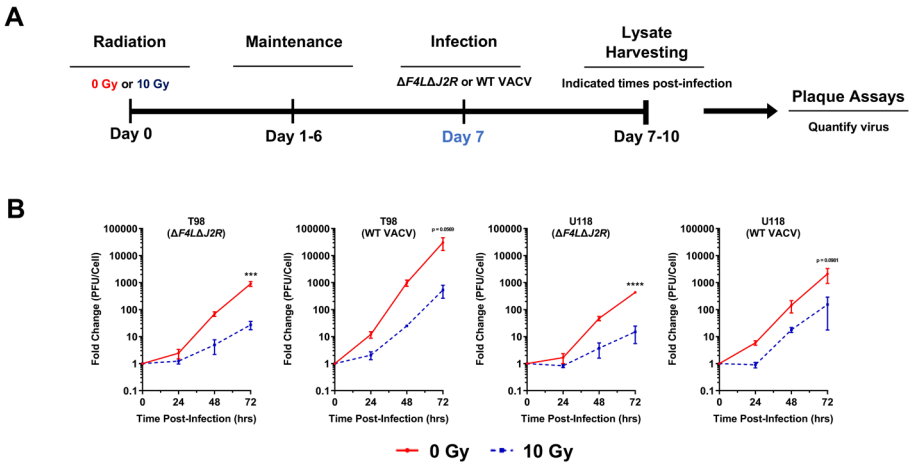

Figure 4.5. Growth attenuation of vaccinia virus occurs in additional irradiated senescence-enriched human glioblastoma cell lines. (A) Experimental outline. Human T98 and U118 glioblastoma cell lines were either non-irradiated (0 Gy) or treated with a radiation dose of 10 Gy. 7 days later, cells were infected with 0.03 PFU per cell of the indicated vaccinia viruses. Lysates were harvested at the indicated times and titered by plaque assay to assess virus yield. **(B)** Growth curves showing amplification of oncolytic Δ*F4LΔJ2R* and wild-type (WT) vaccinia viruses in 0 Gy (non-irradiated; solid red lines) and 10 Gy (dashed blue lines) treated human T98 and U118 glioblastoma cell lines. **Data information:** Data represent 3 independent lysates titered in duplicate. Mean ± SEM is shown. Graphs show fold change relative to lysates taken at t = 0. Significance determined by two-way ANOVA analysis (*** = $p < 0.001$; **** = $p < 0.0001$). *XH performed these experiments.

Growth of WT VACV was also reduced by ~45% 72 hours post-infection in the irradiated senescence-enriched condition versus non-irradiated (non-proliferating) controls, though non-significantly (**Figure 4.6B**). These data indicate that the decreased VACV growth observed in irradiated senescence-enriched conditions compared to non-irradiated controls is not solely due to increased proliferation of non-irradiated control cells.

Lastly, to better understand whether this attenuated virus growth was specific to VACV or applicable to other viruses used for OV therapy, we performed additional experiments using reovirus and the VSV mutant, VSVΔM51-GFP. Reovirus growth was also attenuated in irradiated senescence-enriched U87 cells relative to non-irradiated controls (**Figure 4.7**). Of note, growth of reovirus was blocked in both irradiated and non-irradiated patient-derived ED501 cells, suggesting that pathways other than those implicated in senescence must restrict reovirus infection of these cells (**Figure 4.7**). Interestingly, unlike VACV, growth of VSVΔM51-GFP was unchanged between irradiated senescence-enriched ED501 cells and non-irradiated controls in both low MOI (0.03 PFU per cell) and high MOI (3.0 PFU per cell) conditions (**Figure 4.8**). VSVΔM51-GFP growth was also unchanged between irradiated senescence-enriched cells and non-irradiated controls with the U87 cell line infected using a high MOI (3.0 PFU per cell); however, using a low MOI (0.03 PFU per cell), the growth of VSVΔM51-GFP was slightly, but statistically, attenuated in the irradiated senescence-enriched condition (**Figure 4.8**).

Overall, these data indicate that VACV growth is attenuated in irradiated senescence-enriched GBM cell lines. Further, virus growth attenuation in irradiated senescence-enriched conditions is virus-dependent.

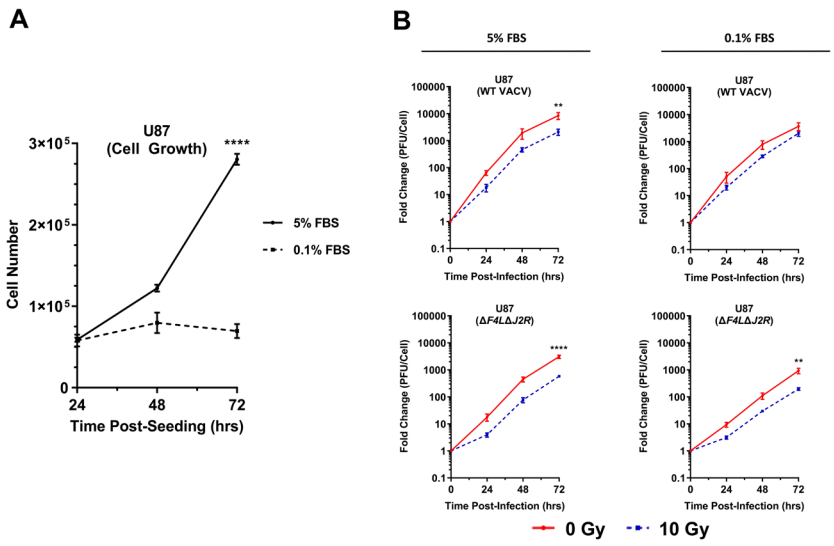

Figure 4.6. Growth of vaccinia virus is attenuated in irradiated senescence-enriched U87 human glioblastoma cells cultured in normal-serum or low-serum conditions. (A) Cellular growth curves showing the change in cell number over time of human U87 glioblastoma cells cultured in normal-serum (5% FBS; solid line) or low-serum (0.1% FBS; dashed line) conditions. Trypan blue assays were performed to quantify total cells at the indicated time points. **(B)** Growth curves showing amplification of oncolytic Δ*F4L*Δ*J2R* and wild-type (WT) vaccinia viruses in non-irradiated (0 Gy; red solid lines) and 10 Gy (dashed blue lines) treated human U87 glioblastoma cells. Cells were infected 7 days after radiation treatments with 0.03 PFU per cell and cultured in normal-serum (5% FBS; left panels) or low-serum (0.1% FBS; right panels) conditions. Lysates were harvested at the indicated times and titered in duplicate by plaque assay to assess virus yield. **Data information:** Data represent 3 independent experiments. Mean ± SEM is shown. For (B), graphs show fold change relative to lysates taken at t = 0. Significance determined by two-way ANOVA analysis (** = $p < 0.01$; **** = $p < 0.0001$).

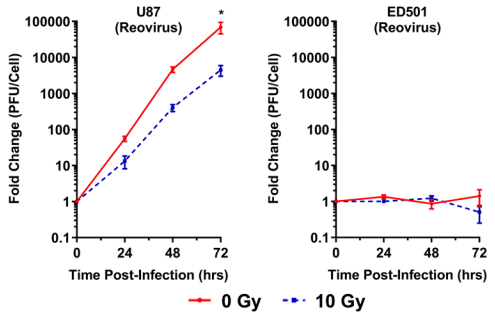

Figure 4.7. Reovirus growth is absent or attenuated in irradiated senescence-enriched human glioblastoma cell lines. Growth curves showing amplification of reovirus (T3Dearing) in non-irradiated (0 Gy; solid red lines) and 10 Gy (dashed blue lines) treated human U87 and ED501 glioblastoma cell lines. 7 days following radiation treatments, cells were infected with reovirus (0.03 PFU per cell). Lysates were harvested at the indicated times and titered by plaque assay to assess virus yield. **Data information:** Data represent 3 independent lysates titered in duplicate. Mean ± SEM is shown. Graphs show fold change relative to lysates taken at t = 0. Significance determined by two-way ANOVA analysis (* = $p < 0.05$). *KCA contributed to these experiments.

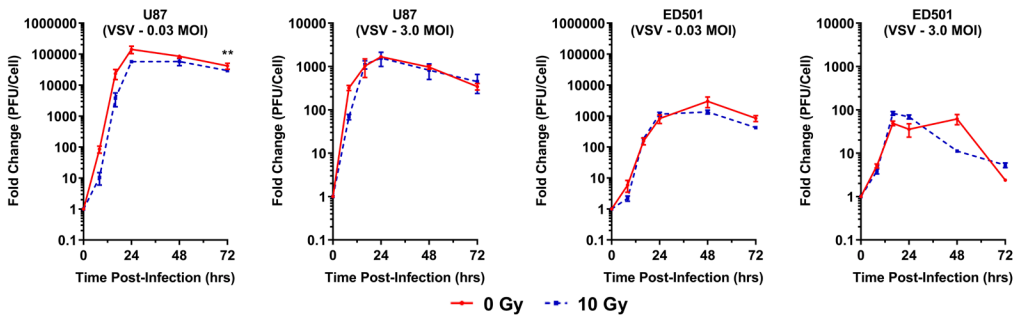

Figure 4.8. Oncolytic vesicular stomatitis virus growth in irradiated senescence-enriched human glioblastoma cell lines and non-irradiated controls. Growth curves showing amplification of VSVΔM51-GFP in non-irradiated (0 Gy; solid red lines) and 10 Gy (dashed blue lines) treated human U87 and ED501 glioblastoma cell lines. 7 days following radiation treatments, cells were infected with VSVΔM51-GFP (0.03 PFU per cell or 3.0 PFU per cell). Lysates were harvested at the indicated times and titered by plaque assay to assess virus yield. **Data information:** Data represent 3 independent lysates titered in duplicate. Mean ± SEM is shown. Graphs show fold change relative to lysates taken at t = 0. Significance determined by two-way ANOVA analysis (** = $p < 0.01$). *MMH contributed to these experiments.

4.2.3 Infectivity of vaccinia virus is reduced in irradiated senescence-enriched glioblastoma cell populations

To better understand the attenuated phenotype of VACV in irradiated senescence-enriched cells, we stained U87 and ED501 cells with a fluorescent proliferation marker, CTV, to label radiation-induced senescent cells. Non-proliferating cells retain high fluorescence intensities whereas proliferating cells lose fluorescence intensity at each division. As outlined in **Figure 4.9A**, 7 days following radiation treatments and CTV-staining, we infected GBM cells with oncolytic Δ*F4L*Δ*J2R* VACV or WT VACV and evaluated the number of $VACV^{+}$ infected cells by staining with an antibody against the late A27 VACV protein 24 hours post-infection.

In comparison to non-irradiated controls, the percentage of $VACV^{+}$ cells 24 hours post-infection with oncolytic Δ*F4L*Δ*J2R* VACV and WT VACV was significantly reduced in irradiated senescence-enriched conditions (**Figure 4.9B; left panels**). These data indicate that VACV is less infectious in GBM cell populations that are enriched with senescent cells post-irradiation. To better understand the interaction of VACV with radiation-induced senescent cells, we analyzed 10 Gy-$VACV^{+}$ cells to determine whether these cells displayed high CTV intensity (CTV^{hi}) or low CTV intensity (CTV^{lo}). The majority (~85-95%) of 10 Gy-$VACV^{+}$ cells were CTV^{hi} (**Figure 4.9B; right panels**) suggesting that VACV is indeed capable of productively infecting radiation-induced senescent cells, as opposed to being restricted to irradiated CTV^{lo} cells.

In agreement with our senescence marker analysis in **Figure 4.1**, the majority (~80-95%) of irradiated GBM cells were CTV^{hi} compared to non-irradiated controls (**Figure 4.9C**) indicating enrichment for senescent cells post-irradiation, but also a sparse population of CTV^{lo} cells (~5-20%; **Figure 4.9D; left panels**). We analyzed the population of virus-treated irradiated cells to determine the percentage of $VACV^{+}$ cells within CTV^{hi} and CTV^{lo} categories. Interestingly, there was no significant difference between

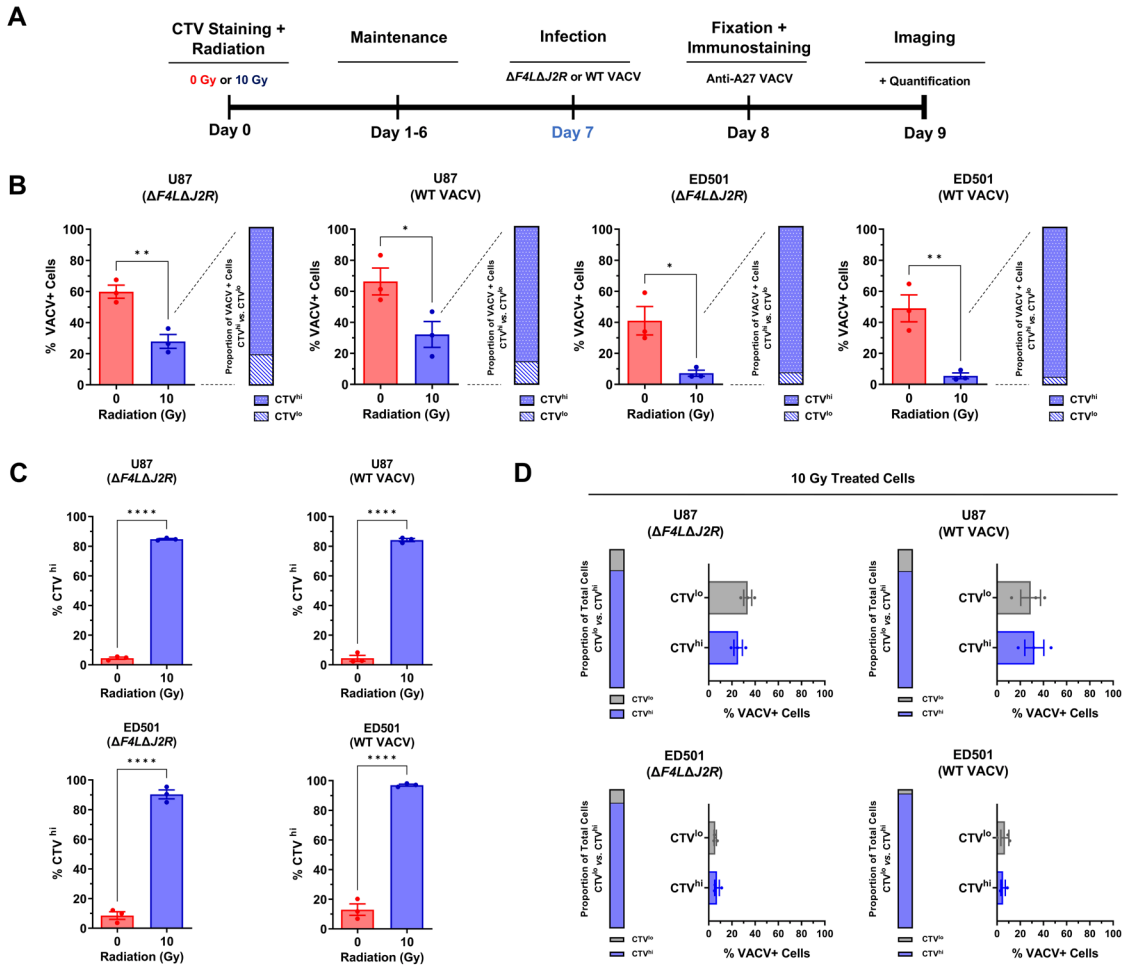

Figure 4.9. Vaccinia virus infectivity is reduced in irradiated senescence-enriched human glioblastoma cell lines. (A) Experimental outline: Human U87 and ED501 glioblastoma cell lines were stained with a fluorescent cell proliferation marker (CellTrace™ Violet; CTV) then were either non-irradiated (0 Gy) or treated with a radiation dose of 10 Gy. 7 days later, cells were infected with 3.0 PFU per cell of oncolytic Δ*F4LΔJ2R* or wild-type (WT) vaccinia viruses. 24 hours post-infection, cells were fixed then immunostained with an antibody against the late A27 VACV protein and imaged the next day using fluorescence microscopy. **(B)** Left panels: percent VACV$^+$ cells 24 hours post-infection of 0 Gy or 10 Gy treated cells (Note: all cells were also treated with CTV). Right panels: Proportion of VACV$^+$ irradiated cells that were scored as high CTV fluorescence (CTV^{hi}, indicating few or no cell divisions) *vs*. those that were scored as low CTV fluorescence (CTV^{lo}). **(C)** Percent of cells scored as CTV^{hi} 8 days following CTV-

staining and treatment with 0 Gy or 10 Gy (Note: all cells were treated with virus as indicated). **(D)** Left panels: proportion of irradiated cells that were CTV^{hi} *vs*. those that were CTV^{lo} 8 days following CTV-staining (Note: all cells were treated with virus as indicated). Right panels: percentage of irradiated cells that were $VACV^{+}$ in the CTV^{hi} population and in the CTV^{lo} population from the same cultures. **Data information:** Data represent 3 independent experiments, mean ± SEM is shown for (B; left panels), (C), and (D; right panels). For (B ; right panels, and D; left panels), the mean value from 3 independent experiments is shown. For (B; left panels), (C), and (D; right panels), significance determined using unpaired t-test (* = $p < 0.05$; ** = $p < 0.01$; **** = $p < 0.0001$).

the percentage of VACV^{+} cells within the CTV^{hi} category and that in the CTV^{lo} category (**Figure 4.9D; right panels**). Put another way, following a 10 Gy dose of radiation, both radiation-induced senescent GBM cells (CTV^{hi}) and a sparse population of proliferating GBM cells (CTV^{lo}) are equally likely to be infected, albeit both at lower percentages than non-irradiated controls.

All together, these data indicate that in the irradiated senescence-enriched condition, both radiation-induced senescent GBM cells and a sparse proliferating population of GBM cells are resistant to VACV infection relative to non-irradiated controls.

4.2.4 Reduced vaccinia virus cytotoxicity in irradiated senescence-enriched glioblastoma cell populations

We next evaluated the cytotoxicity of oncolytic Δ*F4L*Δ*J2R* VACV and WT VACV towards irradiated senescence-enriched U87 and ED501 cell lines using the neutral red viability assay. As depicted in **Figure 4.10A**, GBM cells were irradiated to induce cellular senescence (or left untreated), then infected 7 days later with increasing concentrations of virus and assessed for cell viability 72 hours post-infection.

Dose-response curves evaluating cell viability indicated that both oncolytic Δ*F4L*Δ*J2R* VACV and WT VACV were significantly less cytotoxic towards irradiated senescence-enriched U87 and ED501 cell lines compared to non-irradiated controls (**Figure 4.10B**). These data indicate that irradiated senescence-enriched GBM cell populations are less susceptible to VACV-mediated cell killing consistent with our data on virus growth in these cells.

4.2.5 Oncolytic ΔF4LΔJ2R vaccinia virus attenuation is not explained by reduced cellular nucleotide biosynthesis machinery

VACV requires the production of dNTPs to construct new virus genomes during the viral replication process. To this end, VACV triggers host cells to accumulate in S-phase[500,501], a point in the cell-cycle in

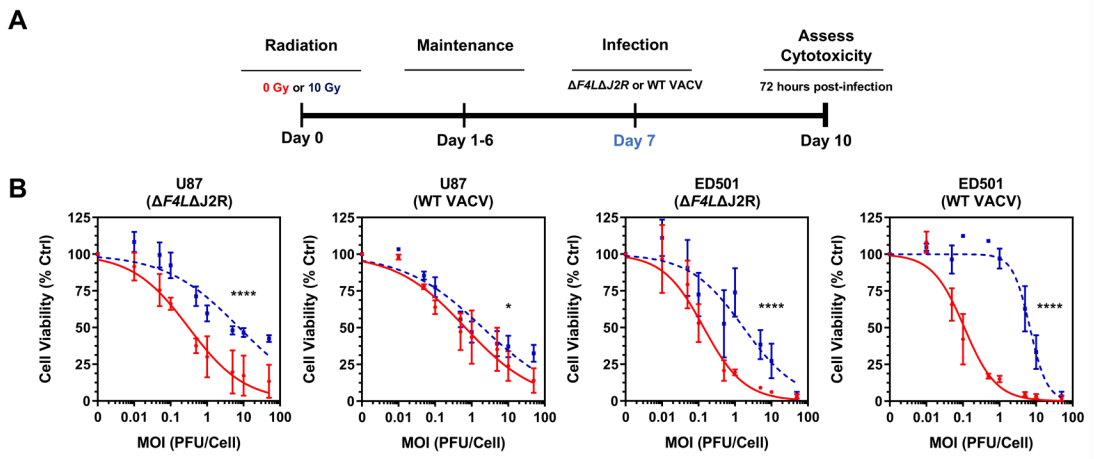

Figure 4.10. Vaccinia virus is less cytotoxic to irradiated senescence-enriched human glioblastoma cell lines than to non-irradiated cell lines. (A) Experimental outline: Human U87 and ED501 glioblastoma cell lines were either non-irradiated (0 Gy) or treated with a radiation dose of 10 Gy. 7 days later, cells were infected with the indicated vaccinia viruses. 72 hours post-infection, neutral red cell viability assays were performed to assess cytotoxicity. **(B)** Dose-response curves showing cell viability 72 hours post-infection with the indicated vaccinia viruses in 0 Gy (non-irradiated; solid red lines) and 10 Gy (dashed blue lines) treated glioblastoma cell lines. **Data information:** Data represent 3 independent experiments. Mean ± SEM is shown for data points. For (B), data is normalized to mock-infected control (0 PFU per cell = 100% cell viability) and curves fit to data points using nonlinear regression and analyzed by extra sum-of-square F test (* = $p < 0.05$; **** = $p < 0.0001$).

which cellular proteins involved in nucleotide biosynthesis are upregulated, such as cellular TK and cellular ribonucleotide reductase small subunit R2 (RRM2)[502–504]. Additionally, VACV encodes a plethora of its own viral nucleotide biosynthesis machinery to ensure dNTP production[402].

A possible explanation for the attenuated phenotype of oncolytic Δ*F4L*Δ*J2R* VACV in irradiated cells is that irradiated cells are deficient in cellular nucleotide biosynthesis enzymes necessary to compensate for the deleted viral genes *J2R* (viral TK) and *F4L* (viral R2). Previous studies have demonstrated that downregulation of cellular TK reduces *J2R*-deleted VACV growth[505], and downregulation of cellular R2 reduces *F4L*-deleted VACV and Δ*F4L*Δ*J2R* VACV growth (but not *J2R*-deleted growth)[414]. Furthermore, cellular p53R2 is a R2-related enzyme that is upregulated following radiation exposure[506]. Thus, to better understand the attenuated phenotype of Δ*F4L*Δ*J2R* VACV, we used immunoblotting to evaluate protein levels of cellular TK1, RRM2, and p53R2 in irradiated senescence-enriched GBM cell lines and non-irradiated controls, expecting that a decrease in levels of these proteins might explain attenuation of the virus in senescence cells.

TK1 levels were significantly reduced in irradiated senescence-enriched U87 cells compared to non-irradiated controls, but significantly increased in the ED501 cell line (**Figure 4.11A**). U87 and ED501 cell lines displayed either slightly, but significantly, increased RRM2 levels (U87), a trend towards increased p53R2 levels (U87), or unchanged RRM2 and p53R2 levels (ED501) in the irradiated senescence-enriched condition compared to non-irradiated controls (**Figure 4.11B, 4.11C**). Overall, TK1 in U87 cells was the only cellular nucleotide biosynthesis enzyme downregulated by radiation treatment.

As further evidence that nucleotide biosynthesis was not a determining factor for growth of Δ*F4L*Δ*J2R* VACV in irradiated senescence-enriched conditions, we examined growth of singly mutated VACVs under this condition. One might predict that a *J2R*-deleted VACV would display attenuated growth in irradiated senescence-enriched U87 cells and that an *F4L*-deleted VACV would not (given cellular TK1,

but not cellular RRM2, downregulation following radiation treatment). However, both *J2R*-deleted VACV and *F4L*-deleted VACV displayed attenuated growth post-infection of irradiated senescence-enriched U87 cells compared to non-irradiated controls (**Figure 4.12**). Of note, *J2R*-deleted VACV, *F4L*-deleted VACV, Δ*F4L*Δ*J2R* VACV, and WT VACV (**Figure 4.12; Figure 4.4B, 4.4C**) all displayed growth attenuation following radiation-induced senescence of the ED501 cell line compared to non-irradiated controls, yet no downregulation of cellular nucleotide biosynthesis enzymes following radiation treatment was observed with the ED501 cell line. In summary, decreased levels of cellular nucleotide biosynthesis enzymes does not explain the attenuated phenotype of Δ*F4L*Δ*J2R* VACV.

4.2.6 Radiation-induced senescence of human glioblastoma cells increases expression of NF-κB-associated genes, but not type I interferon related genes

The type I IFN system and the NF-κB pathway are established antiviral players[507,508]. Further, radiation-induced DNA damage is implicated in activating the type I IFN system[419], and activation of the NF-κB pathway promotes cellular senescence[509,510]. Thus, we hypothesized that these antiviral-associated pathways could be active in irradiated senescence-enriched GBM cell populations and potentially responsible for VACV attenuation.

To elucidate whether these pathways were active, we assessed expression of several genes associated with the type I IFN system (IFNβ, MX1, and ISG15) and the NF-κB pathway (IκBα, IL1β, and TNFα) in irradiated senescence-enriched GBM cell populations and non-irradiated controls 7 days following radiation treatments. IFNβ is a prototypical type I IFN that activates a plethora of IFN-stimulated genes (ISGs)[308,511]. MX1 and ISG15 are well-characterised ISGs[512,513]. IκBα is a cytoplasmic inhibitor of NF-κB that participates in a negative feedback loop to suppress NF-κB activity; its gene expression is activated by NF-κB[514]. As well, NF-κB induces expression of genes encoding the pro-inflammatory factors IL1β and TNFα[515].

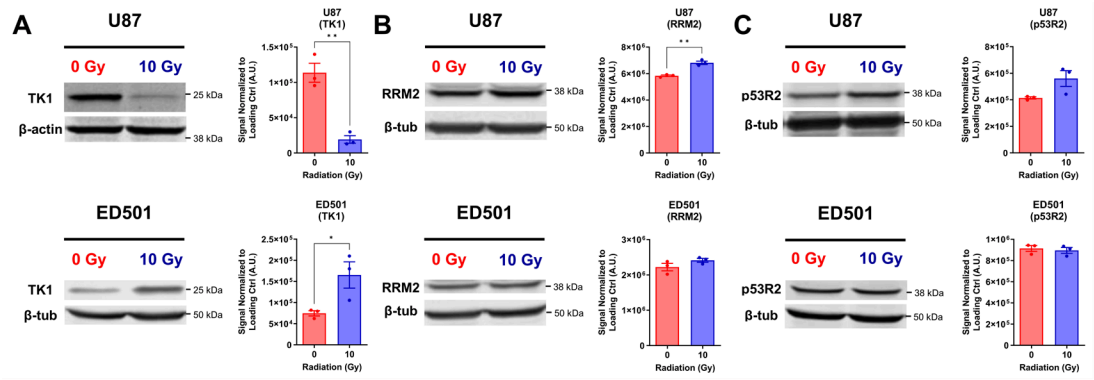

Figure 4.11. Protein levels of cellular nucleotide biosynthesis enzymes in irradiated senescence-enriched human glioblastoma cell lines and non-irradiated controls. Human U87 and ED501 glioblastoma cell lines were either non-irradiated (0 Gy) or treated with a radiation dose of 10 Gy. 7 days later, whole cellular lysates were isolated and analyzed by immunoblotting. Representative images of immunoblots (left panels) and quantified band signals (arbitrary units, A.U.; right panels) show expression of nucleotide biosynthesis enzymes: **(A)** thymidine kinase 1 (TK1); **(B)** ribonucleotide reductase regulatory subunit M2 (RRM2); **(C)** p53 inducible small subunit of ribonucleotide reductase (p53R2). β-actin or β-tubulin were used as loading controls. **Data information:** Data represent 3 independent experiments. Quantified band signal was determined by normalizing probed signal with loading control signal. For (A–C; right panels), mean ± SEM is shown, and unpaired t-test was used to determine significance (* $p < 0.05$; ** $p < 0.01$). *SK contributed to these experiments.

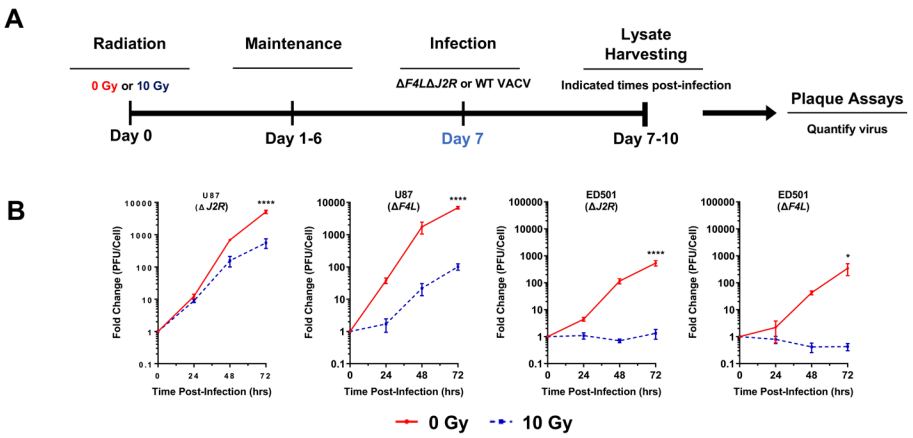

Figure 4.12. *J2R*- and *F4L*-deleted vaccinia viruses display attenuated growth in irradiated senescence-enriched human glioblastoma cell lines. (A) Human U87 and ED501 glioblastoma cell lines were either non-irradiated (0 Gy) or treated with a radiation dose of 10 Gy. 7 days later, cells were infected with 0.03 PFU per cell of the indicated vaccinia viruses. Lysates were harvested at the indicated times and titered by plaque assay to assess virus yield. **(B)** Growth curves showing amplification of *J2R*-deleted and *F4L*-deleted vaccinia viruses in non-irradiated (0 Gy; solid red lines) and 10 Gy (dashed blue lines) treated human U87 and ED501 glioblastoma cell lines. **Data information:** Data represent 3 independent lysates titered in duplicate. Mean ± SEM is shown. Graphs show fold change relative to lysates taken at t = 0. Significance determined by two-way ANOVA analysis (* = $p < 0.05$; **** = $p < 0.0001$).

Expression of IFNβ, MX1, and ISG15 was not significantly different between irradiated and non-irradiated controls (**Figure 4.13A**). These data suggest that the type I IFN system is not upregulated in irradiated senescence-enriched GBM cell populations. However, expression of IκBα and IL1β was significantly upregulated in irradiated senescence-enriched U87 and ED501 cell lines compared to non-irradiated controls (**Figure 4.13B**). Further, with the U87 cell line, expression of TNFα was upregulated in the irradiated senescence-enriched condition compared to non-irradiated controls (**Figure 4.13B**). Collectively, these data suggest that the NF-κB pathway may be activated in irradiated senescence-enriched GBM cell populations, but not the type I IFN system.

4.2.7 Irradiated senescence-enriched human glioblastoma cell populations secrete factors that can attenuate vaccinia virus in non-irradiated bystander cells

The SASP is a unique characteristic of senescent cells in which a variety of factors including cytokines, chemokines, mitogens, and proteases are secreted and can cause various downstream effects[131]. Secreted factors from radiation-induced senescent cells generate bystander effects in nearby non-senescent cells[516–518]. These reports coupled with the observation that, 7 days following irradiation, the senescent cell population in the culture was equally resistant to VACV infection as the proliferating population in the same culture (**Figure 4.9D**), led us to hypothesize that radiation exposure may induce secretion of antiviral factors that might affect virus replication in nearby non-senescent cells. To assess induction of potential antiviral bystander effects we performed CM experiments as outlined in **Figure 4.15A**. Briefly, cellular senescence was induced by irradiating U87 and ED501 cell lines and incubating for 7 days (non-irradiated cells were used as controls), then cell culture medium was replaced with fresh medium and conditioned for 48 hours. Virus growth assays were performed with fresh radiation-naïve GBM cells using CM from irradiated and non-irradiated cells. The growth of oncolytic Δ*F4L*Δ*J2R* VACV and WT VACV was assessed 72 hours post-infection.

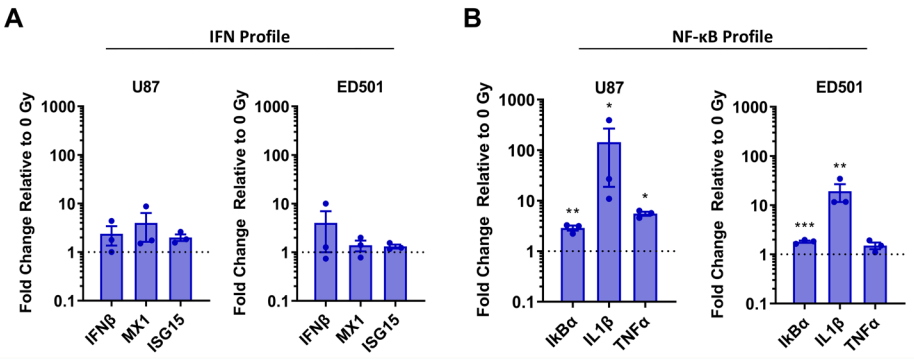

Figure 4.13. Radiation-induced senescence of human glioblastoma cells increases expression of NF-κB-associated genes, but not type I interferon related genes. Human U87 and ED501 glioblastoma cell lines were either non-irradiated (0 Gy) or treated with a radiation dose of 10 Gy. 7 days later, RNA was isolated and gene expression analyzed by RT-qPCR with 18S rRNA used for normalization. Shown is the increase in expression in 10 Gy treated relative to non-irradiated (0 Gy) glioblastoma cells of the following gene panels: **(A)** Type I interferon (IFN) related genes; **(B)** NF-κB-associated genes. **Data information:** Data represent 3 independent experiments, mean ± SEM is shown. Asterisks indicate unpaired t-test comparing ΔCt values (* = $p < 0.05$; ** = $p < 0.01$; *** = $p < 0.001$; ΔCt values are shown in **Figure 4.14**).

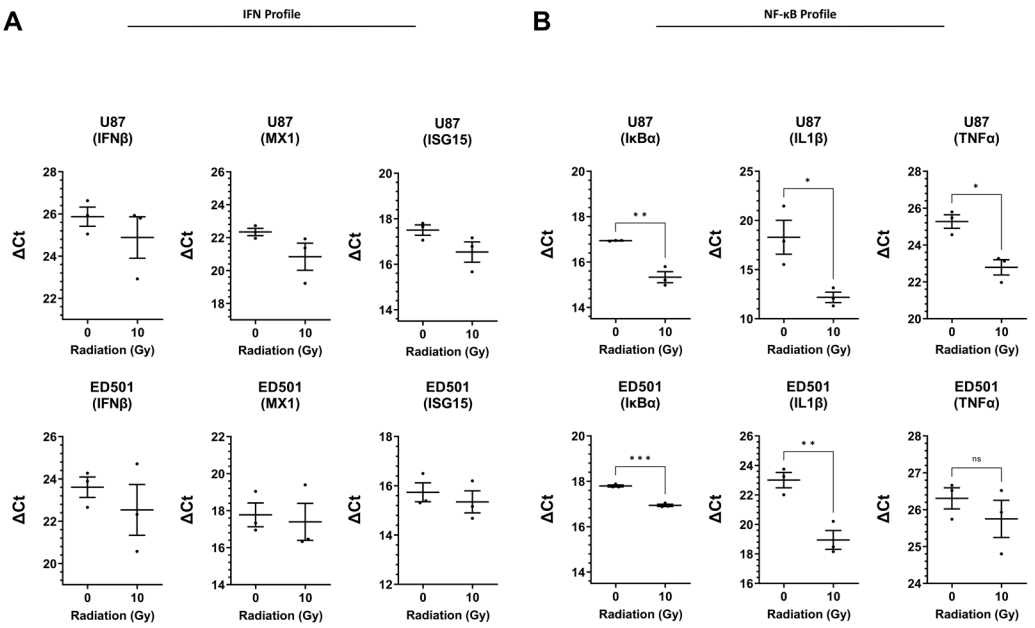

Figure 4.14. ΔCt values used to calculate significant differences of IFN- and NF-κB-associated gene expression between non-irradiated and irradiated human glioblastoma cell lines. ΔCt values of: **(A)** type I interferon (IFN) related genes, **(B)** NF-κB-associated genes; based on RT-qPCR analysis of non-irradiated (0 Gy) and 10 Gy treated human U87 and ED501 glioblastoma cell lines 7 days following radiation treatments. 18S rRNA levels were used for normalization. **Data information:** Data represent 3 independent experiments, mean ± SEM is shown. ΔCt values calculated by subtracting the Ct value of the 18S gene from the Ct value of the target gene within the same treatment condition. Significance determined using unpaired t-test (* = $p < 0.05$; ** = $p < 0.01$; *** = $p < 0.001$).

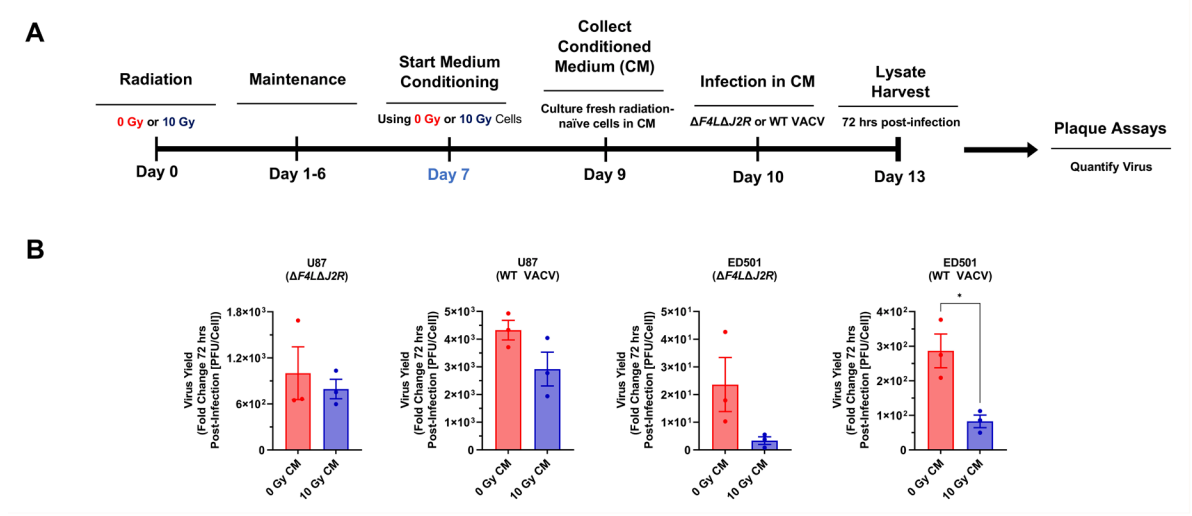

Figure 4.15. Irradiated senescence-enriched human glioblastoma cell populations secrete factors that can attenuate vaccinia virus growth. (A) Experimental outline: Human U87 and ED501 glioblastoma cell lines were either non-irradiated (0 Gy) or treated with a radiation dose of 10 Gy. 7 days later, culture medium was replaced, and conditioned for 48 hours. Fresh radiation-naïve glioblastoma cell lines were cultured in this conditioned medium during subsequent virus growth assays. Lysates were harvested immediately after infection (0 hour) and 72 hours post-infection, then titered in duplicate by plaque assay to assess virus yield. **(B)** Graphs showing fold change in virus yield of oncolytic Δ*F4LΔJ2R* or wild-type (WT) vaccinia viruses 72 hours post-infection in fresh radiation-naïve glioblastoma cells cultured using conditioned medium from either non-irradiated (0 Gy) or 10 Gy treated glioblastoma cells (the cell type infected was matched to the cell type used to condition the media). Cells were infected with 0.03 PFU per cell. **Data information:** Data represent 3 independent experiments, mean ± SEM is shown. Graphs show fold change relative to lysates taken at t = 0. Significance determined by unpaired t-test (* = $p < 0.05$).

To varying extents, decreases in virus yield were observed in radiation-naïve U87 and ED501 cells cultured using CM from irradiated senescence-enriched sources compared with cells cultured using CM from non-irradiated controls (**Figure 4.15B**). Decreased virus yield was particularly apparent with the ED501 cell line. The mean yield of oncolytic Δ*F4L*Δ*J2R* VACV and WT VACV was reduced by ~86% and ~71%, respectively, in radiation-naïve cells cultured using CM from irradiated senescence-enriched sources compared with radiation-naïve cells cultured using CM from non-irradiated controls (**Figure 4.15B**), though, only the reduction in WT VACV was significant. With the U87 cell line, the mean yield of oncolytic Δ*F4L*Δ*J2R* VACV and WT VACV was reduced by ~21% and ~33%, respectively, in radiation-naïve cells cultured using CM from irradiated senescence-enriched sources compared to radiation-naïve cells cultured using CM from non-irradiated controls (**Figure 4.15B**), although reductions in virus yield were non-significant. These data indicate that irradiated senescence-enriched GBM cell populations may secrete factors that induce bystander cells to impair VACV amplification.

4.3 Discussion

Senescence is a stable growth-arrested cellular state that exhibits unique secretory characteristics. Cellular senescence is not only induced by ionizing radiation, but by a broad range of stimuli including telomere attrition from repeated replicative cycles, upregulated oncogenes, hypoxia, dysfunctional mitochondria, oxidative stress, and genotoxic agents (among others)[135]. Further, senescent cells are implicated in a spectrum of biological processes including developmental activities[165], tissue repair[169,519], inflammation and alerting host immunological systems[160,520,521], age-related pathology[522,523], and cancer[524].

In the context of cancer, the effects of cellular senescence are nuanced, inducing both desirable tumor-suppressive effects[177–179] and undesirable tumor progression in a plethora of ways, such as by facilitating cancer relapse[181], enhancing invasiveness[182], contributing to tumor growth[132,183], inducing *de novo*

cancer stem cells[133], and inducing heightened aggressiveness in a subset of cancer cells that escape the senescent state[133,184]. Specific to GBM and radiotherapy, several studies have demonstrated detrimental tumor-promoting effects of GBM cells induced to senesce by ionizing radiation[426,525], and removal of senescent GBM cells was shown to improve outcomes in preclinical GBM models[427]. Hence, eradication of radiation-induced senescent cancer cells may optimize therapeutic outcomes, although it is unclear whether or how OV therapy may contribute to destruction of senescent tumor cells. Despite myriad studies on cellular senescence, reports on virus interactions with senescent cells are limited and the data are conflicting. Some studies indicate that viruses exploit cellular senescence to their benefit[428,429], while others indicate that cellular senescence is associated with antiviral properties[430–432,526]. Further, some evidence that OV therapy may offer enhanced killing of senescent cancer cells exists, such as that reported in a study of an oncolytic measles vaccine virus[434]. It is unknown how VACV-based OVs interact with radiation-induced senescent cancer cells. Given that OV therapy is being investigated in combination with radiotherapy (a senescence inducing agent) to advance the treatment of GBM[327], in conjunction with inconsistent and limited reports regarding VACV interactions with senescent cells, we were interested in better understanding how a VACV-based OV interacts with radiation-induced senescent GBM cells.

We observed that both a VACV-based OV, Δ*F4L*Δ*J2R*, and WT VACV displayed an attenuated phenotype towards irradiated senescence-enriched GBM cell populations. Both viruses exhibited impaired growth kinetics (**Figure 4.4; Figure 4.5; Figure 4.6**), were less infectious (**Figure 4.9**), and showed decreased cytotoxic capabilities (**Figure 4.10**) towards irradiated senescence-enriched GBM cell populations compared to non-irradiated GBM cells *in vitro*. The attenuation of Δ*F4L*Δ*J2R* VACV in irradiated senescence-enriched conditions is not explained by a lack of cellular nucleotide biosynthesis proteins required to compensate the viral gene deletions of *F4L* and *J2R* (**Figure 4.11; Figure 4.12**). Further, attenuation was also observed with WT VACV, which encodes these genes that are deleted in the

mutant. These findings indicate that the senescent state is associated with VACV attenuation and not simply changes in cellular nucleotide biosynthesis levels. Primarily, these data are consistent with the idea that cellular senescence is associated with antiviral activity and highlight an important consideration for optimizing treatment plans that combine VACV-based OVs with radiation. Perhaps treating first with VACV-based OVs—before radiation induces cellular senescence—may optimize the therapeutic potential of the OV treatment because the OV is able to infect more tumor cells and replicate more effectively, enabling greater amounts of viral progeny to infect/spread through adjacent tumor cells than there would otherwise be in senescence-enriched conditions. Further investigation of this concept is an obvious next step. Of note, treating GBM mouse models with 10 Gy of radiation followed by Δ*F4L*Δ*J2R* VACV 48 hours later produced vastly superior tumor control relative to either modality alone while also inducing immune protection[120]. Therefore, it may also be the case that using OV therapy shortly after radiotherapy (also before radiation induces senescence) avoids senescence-associated antiviral activity.

Our data also indicate that WT VACV is more efficient at producing infectious virions than mutant Δ*F4L*Δ*J2R* VACV as WT VACV yields were higher throughout virus growth assays (**Figures 4.4 and 4.15**). This observation likely reflects the inherent deficiencies of Δ*F4L*Δ*J2R* VACV relative to WT VACV due to the deletion of virus-encoded nucleotide biosynthesis machinery. Interestingly, the percentage of VACV-infected cells was similar between WT VACV and Δ*F4L*Δ*J2R* VACV at 24 hours, suggesting that the uptake of the two viruses is similar (**Figure 4.9**). It should be emphasized that WT VACV is not suitable as an anti-GBM therapeutic due to toxicities—the LD_{50} in mice is a mere 10 PFU[453]—whereas Δ*F4L*Δ*J2R* VACV was safe and effective at a dose of 10,000,000 PFU when used to treat GBM mouse models[120].

Though our studies with VACV/reovirus reinforce the hypothesis that cellular senescence is associated with antiviral activity, this is not an absolute and likely depends on the virus in question. We observed that reovirus, which is a naturally tumor-selective OV, also displayed attenuated growth kinetics in irradiated senescence-enriched U87 cells compared to non-irradiated controls (**Figure 4.7**)—corroborating the notion of senescence-associated antiviral activity. In contrast, we did not see attenuation of VSVΔM51-GFP growth in irradiated senescence-enriched GBM cell populations, except marginally, at a low MOI infection with U87 cells (**Figure 4.8**)—indicating that radiation-induced senescence had little to no impact on the growth of VSVΔM51-GFP. Of note, the deletion of methionine 51 in the M protein of VSVΔM51-GFP prevents this mutant virus from blocking IFN responses, therefore this virus is attenuated in normal IFN-responsive cells and not in malignant cells (which often have compromised IFN signaling)[443]. Therefore, the fact that VSVΔM51-GFP grew similarly in irradiated and non-irradiated GBM cells is consistent with our data indicating that the type I IFN system is not upregulated in irradiated senescence-enriched GBM cell populations (**Figure 4.13**). Further, cellular senescence can promote virus activities. Viral replication of influenza virus and varicella zoster virus was enhanced, respectively, in senescent human bronchial epithelial cells and senescent human dermal cells versus non-senescent cells due to a decreased IFN response in senescent cells relative to non-senescent cells following virus infections[428]. The infectivity of dengue virus was enhanced in senescent human monocytic THP-1 cells relative to non-senescent cells due to increased levels of the viral entry receptor, DC-SIGN, on senescent cells relative to non-senescent cells[429]. Lastly, an oncolytic measles vaccine virus displayed enhanced killing of chemotherapy-induced cancer cells—interestingly, although the mechanism was not elucidated, it was determined to not involve a senescence-associated decrease in IFN responsiveness following virus infection or a senescence-associated upregulation of a virus entry receptor[434]. In conjunction with our data, these studies highlight the nuances of virus interactions with

senescent cells and underscore another important consideration for optimizing the combination of OVs with senescence inducers like radiation: the choice of virus may matter.

Importantly, although VSV was not the focus of our studies, it should be mentioned that some of our data with VSVΔM51-GFP conflicts with previous studies investigating WT VSV. Other studies showed that WT VSV was attenuated towards replication-induced, chemotherapy-induced, and oncogene-induced senescent human tumor cells and/or primary mouse cells[432], whereas we observed little to no attenuation of VSVΔM51-GFP in radiation-induced senescence conditions. The contradiction between our study and that done by Baz-Martinez *et al*. (2016)[432], indicates that different senescence-inducing stimuli may induce different types of senescence-associated antiviral activity. The protein contents of the SASP secretome exhibit large variations depending on the stimuli used to induce senescence[527] and factors associated with the SASP have been implicated in partially inducing antiviral properties in exposed cells[432]. It is tempting to speculate that different senescence-inducing stimuli may induce senescence-associated antiviral activity to varying extents due to differing SASP secretomes depending on the senescence-inducer.

We observed increased expression of NF-κB associated genes but not genes associated with the type I IFN system in irradiated senescence-enriched GBM cell populations compared to non-irradiated controls (**Figure 4.13**). NF-κB is a master regulator of the SASP, and SASP-factors can reinforce senescence in an autocrine manner while also inducing senescence of adjacent cells in a paracrine manner[140,141,509]. Given the relevance of NF-κB signaling with senescence, it is not surprising that radiation-induced senescent GBM cells exhibited increased expression of NF-κB-associated genes. Further, activation of NF-κB is a well established antiviral signaling system[508] and VACV encodes a plethora of viral inhibitors to thwart host NF-κB activation in order to operate optimally[237,528–530]. Given the role NF-κB plays in antiviral signaling, our findings suggest that activation of NF-κB pathways may have contributed to the decreased susceptibility of radiation-induced senescent GBM cells to VACV.

Lastly, CM experiments revealed suppression of Δ*F4L*Δ*J2R* VACV and WT VACV growth in non-irradiated GBM cells cultured in media taken from irradiated senescence-enriched GBM cell populations versus media from non-irradiated controls (**Figure 4.15**). This finding indicates that factors secreted by irradiated senescence-enriched GBM cell populations induce an antiviral bystander effect in non-irradiated GBM cells. At least one other study using WT VSV corroborates the notion of a senescence-associated antiviral bystander effect. The cytotoxicity of WT VSV towards A549 lung cancer cells and primary mouse embryo fibroblast cells was impaired when cultured using CM from senescent versus non-senescent cells[432]. Our data also suggest that the SASP is implicated in bystander paracrine antiviral activation. Further investigation should include cytokine arrays to identify the specific SASP components that may be involved in this senescence-associated antiviral activity.

In conclusion, we show that both oncolytic Δ*F4L*Δ*J2R* VACV and WT VACV display less productive infectivity, attenuated growth, and decreased cytotoxic capabilities in irradiated senescence-enriched GBM cell populations. The resistance of radiation-induced senescent GBM cells to VACV may be in part mediated by NF-κB signaling and SASP-associated bystander effects. This research implicates radiation-induced cellular senescence as an antiviral state that impairs VACV. Further, our findings underscore important treatment planning considerations for the combination of VACV-based oncolytic therapies with senescence-inducing agents like radiotherapy.

CHAPTER 5: General Discussion and Future Directions

5.1 General summaries and key findings

5.1.1 Radiation combined with oncolytic vaccinia virus. GBM is an incurable brain cancer that requires novel therapeutic approaches to improve outcomes. The primary objective of this dissertation was to assess whether radiation used in concert with oncolytic VACV therapy may improve treatment of GBM. We initially evaluated the growth kinetics and cytotoxicity of Δ*F4L*Δ*J2R* VACV *in vitro* using up to 14 different GBM cell lines that consisted of established human GBM cell lines, patient-derived GBM and BTIC lines, and mouse GBM/BTIC lines–with or without irradiation. A subset of GBM cell lines were used to generate three-dimensional Matrigel™-embedded GBM structures *in vitro* to assess Δ*F4L*Δ*J2R* VACV dissemination through, or interference with, invasive GBM extensions. Overall, Δ*F4L*Δ*J2R* VACV displayed broad anti-GBM activity as the virus replicated in and killed non-irradiated and irradiated GBM cells, as well as spread through and interfered with GBM spheroids in the three-dimensional invasion assays. It should be noted that the infection of three-dimensional GBM structures utilized a novel, precise, delivery procedure that was developed during these investigations. These promising *in vitro* findings with oncolytic Δ*F4L*Δ*J2R* VACV encouraged further *in vivo* investigations.

Intracranial administration of Δ*F4L*Δ*J2R* VACV was safe and well-tolerated up to 10^7 PFU (approaching the highest feasible dose) in non-tumor-bearing, severely immune-compromised, NSG mice or in syngeneic orthotopic CT2A-luc mouse models as demonstrated by dose-escalation experiments–greenlighting further studies to evaluate the efficacy of radiation in combination with Δ*F4L*Δ*J2R* VACV. We next treated CT2A-luc mouse models with a single 10 Gy dose of radiation and 10^7 PFU of Δ*F4L*Δ*J2R* VACV. Strikingly, the combination cured the majority of mice and significantly enhanced survival relative to either monotherapy. Importantly, a portion of cured mice also rejected or resisted intracranial tumor challenges indicating induction of antitumor immunological memory. Moreover, the CD8+:Treg ratio within the brain TME was increased most by the combination relative to the other therapies used alone,

indicating that radiation in concert with Δ*F4L*Δ*J2R* VACV may alter the immunological milieu towards a state favorable for antitumor immune responses. Key results are summarized in **Figure 5.1**.

5.1.2 Radiation-induced senescence and vaccinia virus. The interaction of viruses with senescent cells is an understudied area. Given senescence is an outcome following irradiation of cancer cells, and OV therapy is investigated in combination with radiotherapy, we sought to better understand how VACV interacts with radiation-induced senescent GBM cells. First, we established that radiation consistently induced senescence in several human GBM cell lines *in vitro*. Next, we evaluated the growth kinetics, productive infectivity, and cytotoxicity of oncolytic Δ*F4L*Δ*J2R* VACV, as well as WT VACV for comparison, using irradiated senescence-enriched GBM cell lines and non-irradiated controls *in vitro*. We discovered that both oncolytic Δ*F4L*Δ*J2R* VACV and WT VACV exhibited attenuated phenotypes in irradiated senescence-enriched conditions based on the metrics mentioned above. Interestingly, under the same conditions when we assessed the growth kinetics of two other OVs, reovirus and VSVΔM51-GFP, we observed that reovirus was attenuated, but VSVΔM51-GFP was not, indicating non-uniform senescence-associated antiviral activity. A decrease in cellular nucleotide biosynthesis enzymes–cellular proteins which are required to compensate Δ*F4L*Δ*J2R* VACV gene deletions–did not explain this attenuation in irradiated senescence-enriched conditions. To better understand the observed VACV attenuation we evaluated two established antiviral pathways and observed increased expression of NF-κB-associated genes, but not type I IFN related genes. Lastly, CM experiments revealed that irradiated senescence-enriched GBM cell populations may release factors which prime bystander cells to resist VACV amplification. Key results are summarized in **Figure 5.2**.

Overall, our work provides substantial justification for the clinical evaluation of radiation in combination with oncolytic VACV therapy, as well as provides an improved understanding of how senescence impacts VACV activity. These findings reveal a set of novel applications and possible opportunities for future exploration that will be outlined over the next several sections.

In vitro

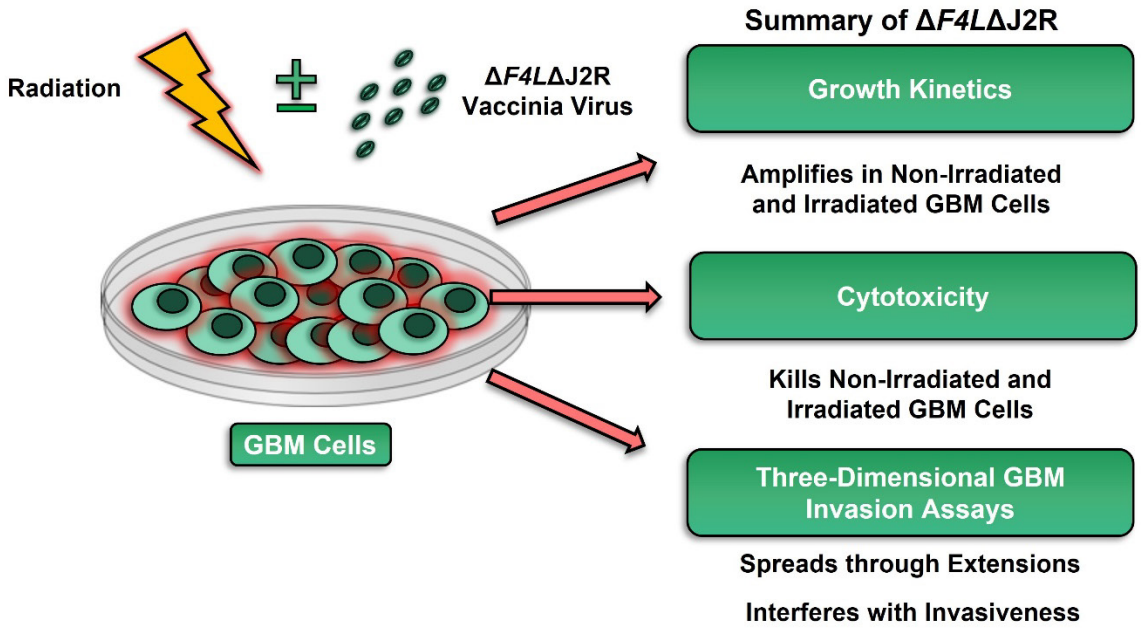

In vivo

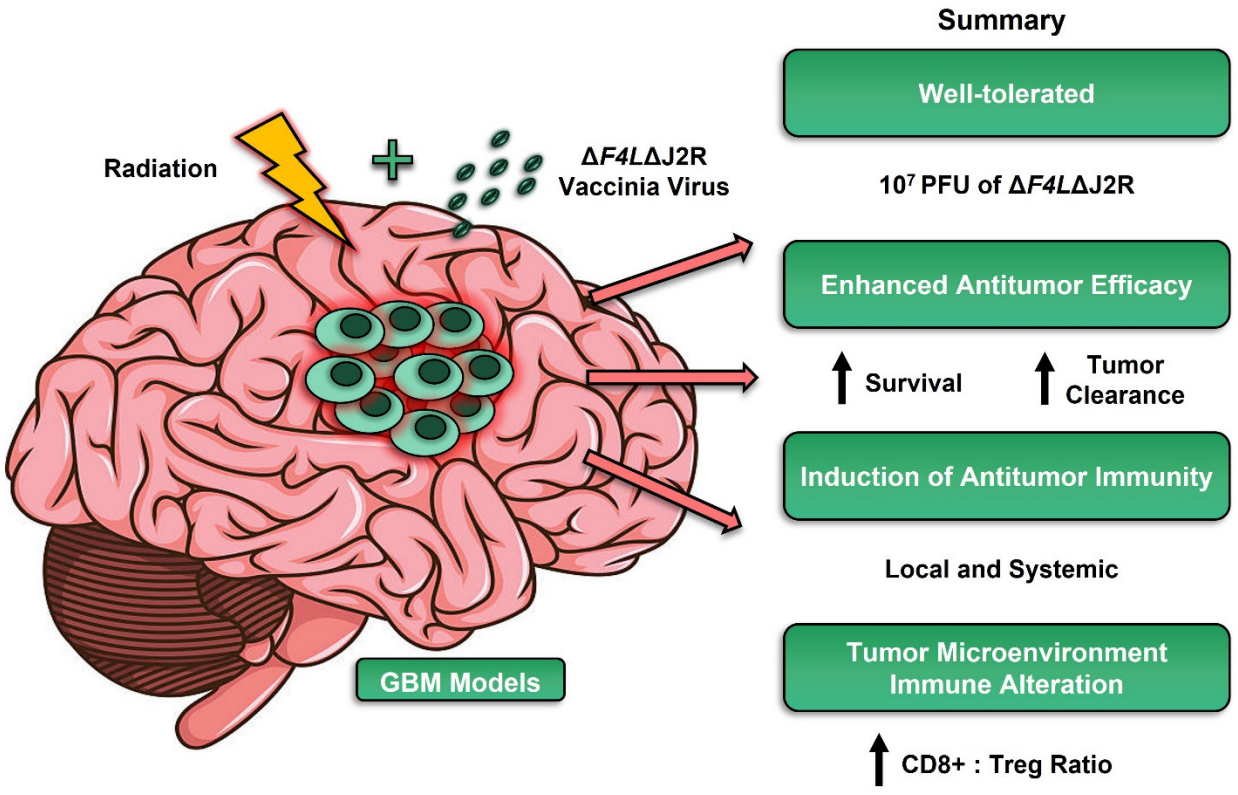

Figure 5.1. Summary of studies investigating the applicability and efficacy of radiation in combination with oncolytic Δ*F4L*Δ*J2R* vaccinia virus for the treatment of glioblastoma. *In vitro* (top panel): Oncolytic Δ*F4L*Δ*J2R* vaccinia virus replicated in and killed a panel of non-irradiated and irradiated human and mouse glioblastoma/brain tumor initiating cell lines. The virus spread through invasive tumor extensions and limited the expansion of glioblastoma spheroids in three-dimensional invasion assays. *In vivo* (bottom panel): The virus was safe and well-tolerated up to the highest feasible dose (10^7 PFU). A single 10 Gy dose of radiation combined with Δ*F4L*Δ*J2R* vaccinia virus significantly extended survival of orthotopic CT2A-luc mouse models relative to either treatment alone and cured the majority of mice. Antitumor immunological memory was induced in a portion of cured mice treated with the combination. The brain tumor microenvironment of combination-treated mice exhibited the highest CD8+ to regulatory T cell ratio. **Abbreviations/symbols**: CD8+, cytotoxic CD8+ T cells; GBM, glioblastoma; PFU, plaque-forming units; Tregs, regulatory T cells. Upward orientated arrows indicate an increase.

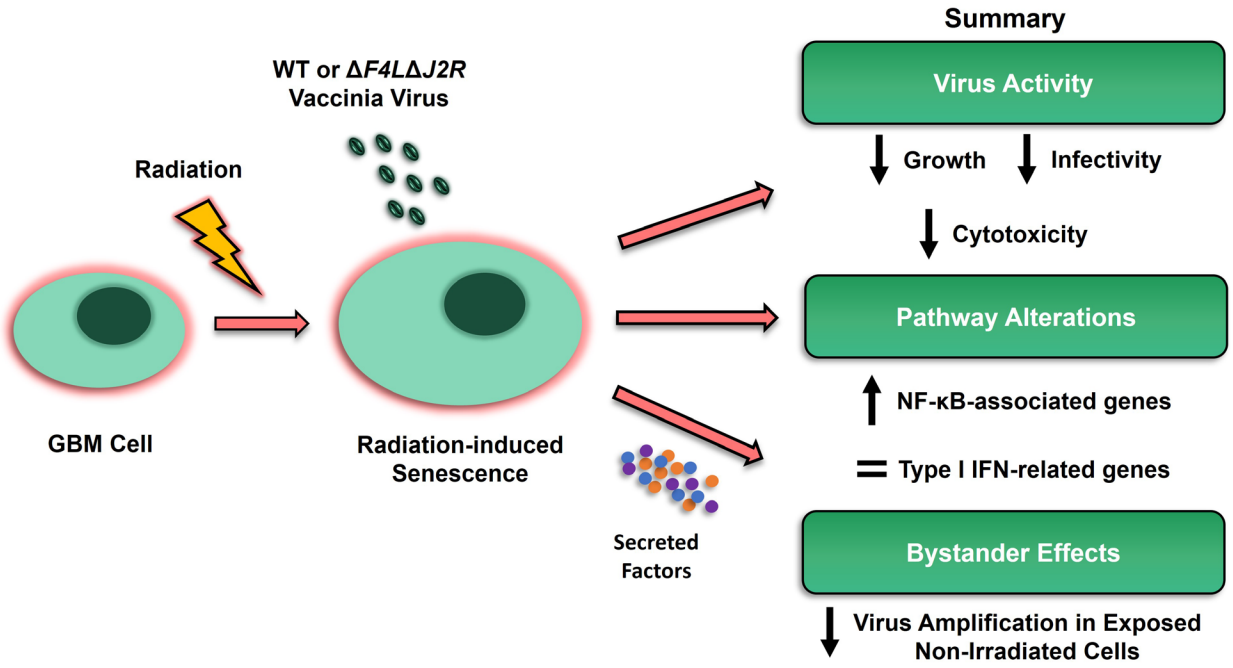

Figure 5.2. Summary of studies investigating the interaction of wild-type and oncolytic Δ*F4LΔJ2R* vaccinia viruses with irradiated senescence-enriched glioblastoma cell populations. The growth kinetics, productive infectivity, and cytotoxicity of both oncolytic Δ*F4LΔJ2R* VACV and WT VACV were attenuated in irradiated senescence-enriched glioblastoma cell populations relative to non-irradiated controls *in vitro*. The senescence-enriched condition displayed increased expression of NF-κB-associated genes but not type I interferon-related genes. Conditioned media experiments indicated that irradiated senescence-enriched GBM cells released factors that made non-irradiated bystander cells resistant to VACV amplification. **Abbreviations/symbols**: GBM, glioblastoma; IFN, interferon; WT, wild-type. Downward orientated arrows indicate a decrease, upward orientated arrows indicate an increase. Equals sign indicates no change.

5.2 Radiotherapy and Oncolytic Vaccinia Virus

5.2.1 Applications

Our preclinical validation of the therapeutic benefits of combining radiation with Δ*F4L*Δ*J2R* VACV suggests several opportunities for its practical application.

5.2.1.1 Stereotactic radiosurgery. SRS can be used as a salvage therapy for recurrent GBM, offering a non-invasive treatment option that delivers a precise and high radiation dose to the tumor site[116]. However, even though some patients may experience modest benefits, virtually all succumb to the disease. Based on our preclinical research, we propose that the addition of Δ*F4L*Δ*J2R* VACV following a high dose of radiation could enhance therapeutic benefits for patients in this clinical scenario. On an added note, patients' lymphocyte and other leukocyte counts begin increasing at later timepoints following TMZ withdrawal (although, the counts still remain below the pre-treatment baseline)[100,101]. Boosted by this increasing immunological baseline post-chemotherapy, there is potential for the OV-radiation combination to exhibit immune-mediated efficacy and improve therapeutic outcomes in the recurrent setting.

5.2.1.2 Modulation of tumor microenvironments. An exciting area of research for enhancing GBM treatment involves transforming immunologically "cold" TMEs into "hot" ones with the goal of reversing immune-suppression to trigger robust antitumor immune responses[125]. Our data demonstrate that combining radiation with Δ*F4L*Δ*J2R* VACV can lead to the development of antitumor immunological memory and distinct augmentations within the T cell compartment in the brain TME, suggesting that this therapeutic combination could be effective overcoming immune-suppression and activating the immune system against GBM cells. By exploiting this property, this multimodal therapy has the potential to enhance other immune-based treatments for GBM, paving the way for further improvement of GBM

therapy by utilizing unique "triple combination" strategies (*i.e.,* radiation, Δ*F4L*Δ*J2R* VACV, plus any one of several promising immunotherapies, two of which are discussed here).

5.2.1.3 Immune checkpoint blockade. Within the realm of immunotherapy, ICB is an obvious approach to induce potential synergy when used in combination with radiation and oncolytic VACV. ICB is a revolutionary form of cancer immunotherapy that utilizes monoclonal antibodies designed to unleash antitumor immune responses by blocking activation of specific inhibitory receptors found on the surface of T cells[531]. Though ICB has exhibited impressive results treating other cancers, in cases where patients with recurrent GBM have been treated with ICB (*i.e.,* anti-programmed cell death protein [PD-1]), the therapy has not significantly improved responses, likely due to low levels of T cells and an abundance of immune-suppressive cells in the TME. Therefore, in this clinical situation the combination of radiation with Δ*F4L*Δ*J2R* VACV may enhance the effectiveness of ICB by recruiting increased levels of CD8+ cytotoxic T cells and reducing Tregs. Furthermore, radiotherapy and OV therapy offer supplementary direct mechanisms to kill cancer cells, which ICB lacks. These direct cancer killing features have the potential to decrease the tumor burden, reducing the number of remaining cancer cells for ICB-activated T cells to eliminate.

Lending support to the addition of radiation and OV therapy to ICB, several studies investigating GBM treatments have reported promising results combining ICB with either radiation alone or several different oncolytic VACVs alone. A radiation dose of 10 Gy in combination with antibodies against PD-1 yielded improved outcomes relative to monotherapies when treating orthotopic GL261-luc mouse GBM models[532]. The addition of another immune checkpoint inhibitor (ICI), anti-T-cell immunoglobulin mucin-3 (TIM-3), to radiation/anti-PD-1 therapy resulted in complete clearance of GL261 brain tumors in mice[533]. Several different oncolytic VACVs used in combination with anti-PD-1 have also shown improved preclinical outcomes treating MC38 colorectal cancer[534,535] and GL261 brain tumors[536]. One very recent study assessed an oncolytic HSV, radiation, and ICB against preclinical melanoma and found that the

triple combination was superior to oncolytic HSV and radiation[537]. Interestingly, this preclinical study also reported one clinical case of a patient with cutaneous squamous carcinoma and pulmonary metastases that showed near complete resolution of disease 44 months following administration of the triple combination[537]. Lastly, given the propensity for immune-related adverse events (IRAEs) with ICB[538], the addition of oncolytic VACV to radiation-ICB protocols, or radiation to oncolytic VACV-ICB protocols may enable lower doses of ICIs to be used, mitigating IRAEs, while hopefully still offering similar therapeutic benefits. These various reports in conjunction with our studies support the notion of investigating the addition of radiation and oncolytic VACV therapy to ICB as a novel therapeutic approach to improve GBM treatment.

5.2.1.4 Chimeric antigen receptor T cell therapy. CAR-T cell therapy is an emerging immunotherapy that uses synthetic transmembrane receptors engineered to redirect T cells to recognize cancer cells expressing a specified target antigen in an MHC-independent manner. This recognition leads to robust CAR-T cell activation and potent antitumor responses[539]. EGFRvIII is a prevalent target antigen present on the surface of GBM cells. Some CAR-T cells are engineered to bind to EGFRvIII which triggers subsequent CAR-T-cell-mediated destruction of these cancer cells. EGFRvIII-directed CAR-T cell therapy for the treatment of recurrent GBM, although showing some promise, resulted in increased infiltration of immune-suppressive Tregs and decreased EGFRvIII target antigen expression[540]–both of which are limiting factors for optimal CAR-T cell therapeutic effects[539]. Our study indicated that radiation in combination with Δ*F4L*Δ*J2R* VACV may reduce the burden of Tregs in the brain TME by increasing the CD8+:Treg ratio, which could benefit CAR-T cell therapy by creating a less immune-suppressive TME. Moreover, the addition of radiation and OV therapy to CAR-T cell therapy might provide a more comprehensive approach to better tackle GBM heterogeneity, potentially compensating the antigen escape associated with CAR-T cell therapy. This can be achieved through

either immune-mediated antitumor responses induced by the combined therapy or by the direct non-specific cell-killing effects of radiation and OV therapy.

Furthermore, though not the focus of our studies, radiation and OV therapy may benefit CAR-T cell therapy in several ways. In a preclinical study, radiation enhanced the susceptibility of antigen-negative tumor cells (those not recognized by CAR-T cells) to TRAIL, which was released by activated CAR-T cells as they engaged with antigen-positive tumor cells[541]. In this way, radiation enabled CAR-T-cell-mediated killing independent of the designed target antigen, a characteristic desirable for overcoming antigen escape[541]. Additionally, an oncolytic VACV designed to express C-X-C motif chemokine ligand 11 (CXCL11) enhanced recruitment of infused CAR-T cells to the tumor site and improved antitumor efficacy[542]. The findings from these studies, along with our own validation of radiation combined with an oncolytic VACV, provide support for pursuing further investigations into this triple combination as a potential means to enhance GBM treatment.

5.2.2 Improving efficacy of the combination

Given the likelihood that the antitumor efficacy of radiation combined with Δ*F4L*Δ*J2R* VACV is partially driven by immune-mediated processes, it is important to explore and implement strategies that could further enhance this effect. Some strategies are highlighted next.

5.2.2.1 Virus-encoded transgenes. Δ*F4L*Δ*J2R* VACV, encodes several transgenes, but does not include any intended to enhance antitumor efficacy. However, VACV can accommodate large genetic insertions and is often equipped with transgenes to boost its antitumor effectiveness. There are many candidate transgenes that could be employed to potentiate oncolytic VACV antitumor immune responses. Some fruitful candidates are interleukin (IL)-12, IL-2, and IL-7 (among others). It should be mentioned that early clinical trials using systemic cytokine therapies, such as IL-2 and IL-12, observed adverse life-threatening toxicities[543,544]. However, it is worth noting that the implementation of novel

"membrane-tethered" cytokines used in conjunction with OVs offers improved safety by confining cytokines within the TME[398,535], potentially mitigating the issues associated with systemic cytokine administration. IL-12 promotes the development of a Th1 immune response and activates CD8+ cytotoxic T cells[545], both of which are important in the context antitumor immunity. Indeed, the use of an oncolytic VACV expressing tethered-IL-12 profoundly altered the TME when treating colon cancer models. The virus resulted in enhanced activation of CD4+ and CD8+ T cells and a reduction in exhausted CD8+ T cells. Additionally, there was a decrease in immune-suppressive cytokines, Tregs, and MDSCs. Similar TME alterations such as increased activation of CD4+ and CD8+ T cells, less CD8+ T cell exhaustion, and reduced Tregs were observed using an oncolytic VACV expressing tethered-IL-2, a T cell growth factor that can enhance CD8+ T cell antitumor activity[398,546]. IL-7 is involved in T cell survival and supporting memory T cells[547]. Interestingly, the use of an oncolytic VACV expressing both IL-7 and IL-12 demonstrated enhanced recruitment of CD4+ and CD8+ T cells to the TME compared to viruses expressing only one of the cytokines. This study suggests that strategically combining multiple transgenes using an oncolytic VACV platform can synergistically modulate the TME and optimize therapeutic impact. Considering this, Umer *et al*. (2020)[354] reported enhanced responses treating 4T1 breast cancer models with oncolytic VACVs that had deletions of genes that disrupt IFN signaling (*i.e., B8R*, *B18R*, *C6L*, and *N1L*). In addition to the sites deleted in Δ*F4L*Δ*J2R* VACV already, these gene deletion sites are promising candidates for inserting the above-mentioned transgenes, potentially creating an oncolytic VACV with superior antitumor immune modulating capacities to be used in combination with radiation. Lastly, it is important to mention that apart from incorporating cytokine transgenes, other transgenes such as chemokines[548], Toll-like receptor activators[549], and T cell engagers[369] also enhance the efficacy of oncolytic VACVs–these approaches could also be explored to produce a superior virus.

5.2.2.2 Alternative radiotherapeutic methods. Numerous methods to enhance antitumor immune responses using radiotherapy can be explored. In this section, three specific techniques will be

discussed: hypofractionated radiotherapy, FLASH radiotherapy (FLASH-RT), and spatially fractionated radiation therapy (SFRT).

Hypofractionated radiotherapy. Hypofractionated radiotherapy, as opposed to conventionally fractionated radiotherapy, involves administering higher doses less frequently. In preclinical studies using GL261 and CT2A GBM mouse models, hypofractionated radiation was far superior compared to conventionally fractionated radiation[550]. Furthermore, radiation-driven immune responses were blunted when single doses exceeded 12 Gy, but hypofractionated delivery of multiple high doses with each dose beneath this threshold (*i.e.,* 3 fractions of 8 Gy) circumvented this issue[551]. It would be highly intriguing to compare hypofractionated, conventionally fractionated, and single-fraction SRS regimens in combination with Δ*F4L*Δ*J2R* VACV. It could be reasoned that an appropriate hypofractionated protocol may enable delivery of the same biologically effective dose to the tumor site as conventionally fractionated and single-fraction SRSs, but without hampering radiation-associated antitumor immune activation. Indeed, a study comparing these three regimens in combination with ICB found that the hypofractionated regimen was superior to conventionally fractionated and single-fraction radiation using the same biologically effective doses[552], indicating that hypofractionated radiotherapy may pair well with immunotherapies.

FLASH-RT and SFRT. FLASH-RT is a novel radiotherapeutic approach that involves the delivery of radiation using ultra-high dose rates which, impressively, enables high radiation doses to be delivered in less than 200 ms[553]. Importantly, this treatment also reduces radiation-related toxicities without compromising antitumor efficacy[553,554]. SFRT delivers radiation to the tumor site using a non-uniform radiation dose in which some regions receive high doses, referred to as peaks, and other regions receive low doses, referred to as valleys[555]. Peaks correspond to the path of radiation beams, while valleys correspond to areas between beams[555]. Some propose that SFRT-mediated tumor killing at peaks releases DAMPs and tumor-antigens, while immune cells and vasculature remain preserved in valleys,

which ultimately facilitates antitumor immune responses[553]. Importantly, both FLASH-RT and SFRT have the potential to activate antitumor immune responses while also reducing normal tissue toxcity[553]. FLASH-RT remodels the TME by reducing Treg levels at early timepoints and increasing CD8+ T cell levels at late timepoints in ovarian cancer models[556]. Further, FLASH-RT has been recently used to treat preclinical GBM models, where it exhibited antitumor efficacy, recruitment of TILs, and induction of antitumor immunological memory[480,557]. Treating orthotopic GBM rat models, SFRT resulted in CD8+ T cell infiltration of the TME, faster CD4+ and CD8+ T cell recruitment relative to conventional radiotherapy, and induction of antitumor immunological memory[558]. Furthermore, SFRT used in combination with ICB resulted in antitumor immune responses at distant tumor sites whereas conventional radiation therapy did not[559]–highlighting that SFRT may pair well with immune-based therapies. While these radiation techniques can elicit antitumor immune responses, research in these areas remains sparse, and additional immune adjuvants will likely be necessary to achieve robust immune-mediated tumor clearance. Therefore, exploring the combination of these radiotherapeutic approaches with an oncolytic VACV could potentially lead to improved antitumor responses while also exploiting the capacity for FLASH-RT and SFRT to mitigate radiation-related toxicities.

5.2.3 Radiation-induced senescence

5.2.3.1 Senescence, the DNA damage response, and antiviral activity. Viruses may exploit or be hindered by the senescent state[428–432,526,560]. Our studies show that radiation-induced senescence of GBM cells hinders VACV activities suggesting senescence-associated antiviral activity. We postulated that the decreased susceptibility of radiation-induced senescent GBM cells towards VACV could be attributed to increased NF-κB activity, a signaling network associated with antiviral activity[508]. However, other concurrent factors are likely at play.

Having immense overlap with DDR machinery and signaling, cellular senescence can be described as a sustained or permanent DDR[142,561]. Many viruses throughout their replication cycles interact with DDR machinery in nuanced ways–some benefiting from the activation of the DDR, while others possess mechanisms to circumvent the DDR, presumably because it interferes with optimal virus replication[562,563]. Considering that a similar trend is true of viruses and senescence, and the DDR is associated with senescence, the involvement of the DDR in VACV attenuation is highly intriguing. Furthermore, the propagation of several other DNA viruses is impaired by DDR machinery. For example, components of the Mre11–Rad50–NBS1 complex play an inhibitory role during adenovirus replication by inducing large concatemers of viral DNA that are too big to be packaged[564]. During EBV infection, virus-induced cell proliferation triggers an ATM/Chk2-dependent DDR promoting growth arrest and cell death[565]–limiting factors for virus spread. Overall, it is possible that a persistent DDR within radiation-induced senescent GBM cells is also responsible for impaired VACV activities. In line with this reasoning, both damaged self-DNA and foreign DNA can be sensed by DDR machinery and activate downstream signaling networks[566]. DNA-PK (a DDR protein) is activated in response to dsDNA breaks[567] and plays a role in senescence and the maintenance of SASP[568]. Additionally, DNA-PK serves as a cytoplasmic DNA sensor capable of recognizing DNA viruses, including VACV, and in this way contributes to innate immune activation[569]. In fact, VACV encodes two proteins, C4 and C16, that inhibit DNA-PK which leads to decreased innate immune activation and immune cell recruitment[570,571]. Taken together, it is reasonable to suspect that radiation-induced senescent GBM cells may be primed to sense VACV via DNA-PK. Future studies looking into senescence, the DDR, and VACV are warranted. It should be noted that VACV also exploits and recruits a number of nuclear DDR proteins to aid in viral DNA replication in the cytoplasm[572]–underscoring the complexities of virus-DDR interactions.

Other, less complex, reasons can be postulated for senescence-associated antiviral activity. For instance, VACV encodes proteins that drive the cell cycle to accumulate in S-phase to optimize

availability of DNA building blocks[500,501]. Given the permanent growth-arrest of radiation-induced senescent GBM cells, this feature of VACV may be impaired resulting in less availability of dNTPs for new virus genomes.

5.2.3.2 Radiation immuno-modulation and senescence. Our studies investigating radiation-induced senescence and VACV were exclusively done *in vitro*. This precludes any understanding of how immune responses elicited by the combination of radiation and Δ*F4L*Δ*J2R* VACV might affect radiation-induced senescent cells *in vivo*. An underappreciated aspect of radiation therapy is its ability to modulate surviving cancer cells in ways that increase their susceptibility to T cell-mediated destruction[573]. Following irradiation, this effect involves amplification of MHC I[574–576], Fas[576,577], ICAM[575,576], and calreticulin[575,578] on the surface of surviving cancer cells. Amplified MHC I increases the probability for T cell receptors to interact with tumor-antigen-loaded MHC I molecules resulting in enhanced recognition and killing[574]. Upregulation of ICAM-1 enhances T cell killing by increasing the formation of immunological synapses between T cells and their targets[579]. Increased Fas expression increases the susceptibility of cancer cells to apoptosis induction by FasL on T cells[577]. Lastly, calreticulin is a well-characterized DAMP exposed during ICD, but also has a direct (but still undefined) role in enhancing T cell-mediated tumor cell killing following radiation[575,578]. Importantly, these studies investigating increased susceptibility of surviving irradiated cancer cells did not investigate the induction of senescence following radiation. It is tempting to speculate that radiation-induced senescent GBM cells may also be rendered susceptible to T cell-mediated killing. Furthermore, this susceptibility might be exploited by the antitumor immune responses elicited by the combination of radiation and Δ*F4L*Δ*J2R* VACV. Hence, in a broader context of antitumor efficacy, the impairment of VACV towards killing radiation-induced senescent GBM cells *in vitro*, might not necessarily translate *in vivo* because radiation-

induced senescent GBM cells may be rendered susceptible to tumor-specific CD8+ T cells induced by the radiation-oncolytic treatment. This notion presents a fascinating future direction.

5.3 Conclusions

This research demonstrates that the combination of radiation with oncolytic Δ*F4L*Δ*J2R* VACV offers superior anticancer efficacy compared to either therapy alone. This potent multimodal approach proved highly effective in eradicating brain tumors from an aggressive immune-suppressed GBM model that closely mimics human disease. The combination therapy exerts unique, favorable effects on the brain TME and induces antitumor immunological memory highlighting its potential to reverse immune-suppression–a feature sought after for successful GBM treatment. Given the challenges posed by this malignant brain cancer, novel therapeutic combinations are vital to improve outcomes. This research validates the use of radiation in concert with oncolytic Δ*F4L*Δ*J2R* VACV as a promising strategy. Moreover, our findings reveal insights into the behavior of oncolytic Δ*F4L*Δ*J2R* VACV and WT VACV within irradiated senescence-enriched GBM cell populations. Both viruses exhibit reduced infectivity, growth, and cytotoxic capabilities in this context. The resistance of radiation-induced senescent GBM cells to VACV may be partially attributed to NF-κB signaling and SASP-associated bystander effects, offering an improved understanding of the antiviral state associated with radiation-induced senescence. Overall, this research contributes valuable insights towards advancing more effective therapeutic approaches for this challenging brain cancer.

Literature Cited

1. Tan, A. C., Ashley, D. M., López, G. Y., Malinzak, M., Friedman, H. S. & Khasraw, M. Management of glioblastoma: State of the art and future directions. *CA: A Cancer Journal for Clinicians* **70,** 299–312 (2020).
2. Stupp, R., Taillibert, S., Kanner, A. A., Kesari, S., Steinberg, D. M., Toms, S. A., Taylor, L. P., Lieberman, F., Silvani, A., Fink, K. L., Barnett, G. H., Zhu, J.-J., Henson, J. W., Engelhard, H. H., Chen, T. C., Tran, D. D., Sroubek, J., Tran, N. D., Hottinger, A. F., Landolfi, J., Desai, R., Caroli, M., Kew, Y., Honnorat, J., Idbaih, A., Kirson, E. D., Weinberg, U., Palti, Y., Hegi, M. E. & Ram, Z. Maintenance Therapy With Tumor-Treating Fields Plus Temozolomide vs Temozolomide Alone for Glioblastoma: A Randomized Clinical Trial. *JAMA* **314,** 2535–2543 (2015).
3. Stupp, R., Taillibert, S., Kanner, A., Read, W., Steinberg, D. M., Lhermitte, B., Toms, S., Idbaih, A., Ahluwalia, M. S., Fink, K., Di Meco, F., Lieberman, F., Zhu, J.-J., Stragliotto, G., Tran, D. D., Brem, S., Hottinger, A. F., Kirson, E. D., Lavy-Shahaf, G., Weinberg, U., Kim, C.-Y., Paek, S.-H., Nicholas, G., Bruna, J., Hirte, H., Weller, M., Palti, Y., Hegi, M. E. & Ram, Z. Effect of Tumor-Treating Fields Plus Maintenance Temozolomide vs Maintenance Temozolomide Alone on Survival in Patients With Glioblastoma: A Randomized Clinical Trial. *JAMA* **318,** 2306–2316 (2017).
4. Piper, R. J., Senthil, K. K., Yan, J.-L. & Price, S. J. Neuroimaging classification of progression patterns in glioblastoma: a systematic review. *Journal of Neuro-Oncology* **139,** 77–88 (2018).
5. De Bonis, P., Anile, C., Pompucci, A., Fiorentino, A., Balducci, M., Chiesa, S., Lauriola, L., Maira, G. & Mangiola, A. The influence of surgery on recurrence pattern of glioblastoma. *Clinical Neurology and Neurosurgery* **115,** 37–43 (2013).
6. Marenco-Hillembrand, L., Wijesekera, O., Suarez-Meade, P., Mampre, D., Jackson, C., Peterson, J., Trifiletti, D., Hammack, J., Ortiz, K., Lesser, E., Spiegel, M., Prevatt, C., Hawayek, M., Quinones-

Hinojosa, A. & Chaichana, K. L. Trends in glioblastoma: outcomes over time and type of intervention: a systematic evidence based analysis. *Journal of Neuro-Oncology* **147,** 297–307 (2020).

7. Ostrom, Q. T., Cioffi, G., Waite, K., Kruchko, C. & Barnholtz-Sloan, J. S. CBTRUS Statistical Report: Primary Brain and Other Central Nervous System Tumors Diagnosed in the United States in 2014-2018. *Neuro Oncol* **23,** iii1–iii105 (2021).
8. Brodbelt, A., Greenberg, D., Winters, T., Williams, M., Vernon, S. & Collins, V. P. Glioblastoma in England: 2007-2011. *Eur J Cancer* **51,** 533–542 (2015).
9. Rouse, C., Gittleman, H., Ostrom, Q. T., Kruchko, C. & Barnholtz-Sloan, J. S. Years of potential life lost for brain and CNS tumors relative to other cancers in adults in the United States, 2010. *Neuro-Oncology* **18,** 70–77 (2016).
10. Dobec-Meić, B., Pikija, S., Cvetko, D., Trkulja, V., Pažanin, L., Kudelić, N., Rotim, K., Pavliček, I. & Kostanjevec, and R. Intracranial tumors in adult population of the Varaždin County (Croatia) 1996–2004: a population-based retrospective incidence study. *Journal of Neuro-Oncology* **78,** 303–310 (2006).
11. Ghosh, M., Shubham, S., Mandal, K., Trivedi, V., Chauhan, R. & Naseera, S. Survival and prognostic factors for glioblastoma multiforme: Retrospective single-institutional study. *Indian Journal of Cancer* **54,** (2017).
12. Pearce, M. S., Salotti, J. A., Little, M. P., McHugh, K., Lee, C., Kim, K. P., Howe, N. L., Ronckers, C. M., Rajaraman, P., Craft, A. W., Parker, L. & Berrington de González, A. Radiation exposure from CT scans in childhood and subsequent risk of leukaemia and brain tumours: a retrospective cohort study. *The Lancet* **380,** 499–505 (2012).
13. Meulepas, J. M., Ronckers, C. M., Smets, A. M. J. B., Nievelstein, R. A. J., Gradowska, P., Lee, C., Jahnen, A., van Straten, M., de Wit, M.-C. Y., Zonnenberg, B., Klein, W. M., Merks, J. H., Visser, O.,

van Leeuwen, F. E. & Hauptmann, M. Radiation Exposure From Pediatric CT Scans and Subsequent Cancer Risk in the Netherlands. *JNCI: Journal of the National Cancer Institute* **111,** 256–263 (2019).

14. Therkildsen, C., Ladelund, S., Rambech, E., Persson, A., Petersen, A. & Nilbert, M. Glioblastomas, astrocytomas and oligodendrogliomas linked to Lynch syndrome. *European Journal of Neurology* **22,** 717–724 (2015).
15. Orr, B. A., Clay, M. R., Pinto, E. M. & Kesserwan, C. An update on the central nervous system manifestations of Li–Fraumeni syndrome. *Acta Neuropathologica* **139,** 669–687 (2020).
16. Peredo-Harvey, I., Rahbar, A. & Söderberg-Nauclér, C. Presence of the Human Cytomegalovirus in Glioblastomas—A Systematic Review. *Cancers* **13,** (2021).
17. Söderberg-Nauclér, C. & Johnsen, J. I. Cytomegalovirus in human brain tumors: Role in pathogenesis and potential treatment options. *World J Exp Med* **5,** 1–10 (2015).
18. Role of Epstein-Barr Virus in Glioblastoma. *Critical Reviews™ in Oncogenesis* **24,** 307–338 (2019).
19. Lawler, S. E. Cytomegalovirus and glioblastoma; controversies and opportunities. *Journal of Neuro-Oncology* **123,** 465–471 (2015).
20. Akhtar, S., Vranic, S., Cyprian, F. S. & Al Moustafa, A.-E. Epstein–Barr Virus in Gliomas: Cause, Association, or Artifact? *Frontiers in Oncology* **8,** (2018).
21. Schwartzbaum, J., Ahlbom, A., Malmer, B., Lönn, S., Brookes, A. J., Doss, H., Debinski, W., Henriksson, R. & Feychting, M. Polymorphisms Associated with Asthma Are Inversely Related to Glioblastoma Multiforme. *Cancer Research* **65,** 6459–6465 (2005).
22. Amirian, E. S., Zhou, R., Wrensch, M. R., Olson, S. H., Scheurer, M. E., Il'yasova, D., Lachance, D., Armstrong, G. N., McCoy, L. S., Lau, C. C., Claus, E. B., Barnholtz-Sloan, J. S., Schildkraut, J., Ali-Osman, F., Sadetzki, S., Johansen, C., Houlston, R. S., Jenkins, R. B., Bernstein, J. L., Merrell, R. T., Davis, F. G., Lai, R., Shete, S., Amos, C. I., Melin, B. S. & Bondy, M. L. Approaching a Scientific

Consensus on the Association between Allergies and Glioma Risk: A Report from the Glioma International Case-Control Study. *Cancer Epidemiology, Biomarkers & Prevention* **25,** 282–290 (2016).

23. Poli, A., Oudin, A., Muller, A., Salvato, I., Scafidi, A., Hunewald, O., Domingues, O., Nazarov, P. V., Puard, V., Baus, V., Azuaje, F., Dittmar, G., Zimmer, J., Michel, T., Michelucci, A., Niclou, S. P. & Ollert, M. Allergic airway inflammation delays glioblastoma progression and reinvigorates systemic and local immunity in mice. *Allergy* **78,** 682–696 (2023).
24. McKinnon, C., Nandhabalan, M., Murray, S. A. & Plaha, P. Glioblastoma: clinical presentation, diagnosis, and management. *BMJ* **374,** n1560 (2021).
25. Jin, L., Shi, F., Chun, Q., Chen, H., Ma, Y., Wu, S., Hameed, N. U. F., Mei, C., Lu, J., Zhang, J., Aibaidula, A., Shen, D. & Wu, J. Artificial intelligence neuropathologist for glioma classification using deep learning on hematoxylin and eosin stained slide images and molecular markers. *Neuro-Oncology* **23,** 44–52 (2021).
26. Komori, T. Grading of adult diffuse gliomas according to the 2021 WHO Classification of Tumors of the Central Nervous System. *Laboratory Investigation* **102,** 126–133 (2022).
27. Oronsky, B., Reid, T. R., Oronsky, A., Sandhu, N. & Knox, S. J. A Review of Newly Diagnosed Glioblastoma. *Frontiers in Oncology* **10,** (2021).
28. Rong, Y., Durden, D. L., Van Meir, E. G. & Brat, D. J. 'Pseudopalisading' Necrosis in Glioblastoma: A Familiar Morphologic Feature That Links Vascular Pathology, Hypoxia, and Angiogenesis. *Journal of Neuropathology & Experimental Neurology* **65,** 529–539 (2006).
29. Louis, D. N., Perry, A., Wesseling, P., Brat, D. J., Cree, I. A., Figarella-Branger, D., Hawkins, C., Ng, H. K., Pfister, S. M., Reifenberger, G., Soffietti, R., von Deimling, A. & Ellison, D. W. The 2021 WHO Classification of Tumors of the Central Nervous System: a summary. *Neuro-Oncology* **23,** 1231–1251 (2021).

30. Louis, D. N., Perry, A., Reifenberger, G., von Deimling, A., Figarella-Branger, D., Cavenee, W. K., Ohgaki, H., Wiestler, O. D., Kleihues, P. & Ellison, D. W. The 2016 World Health Organization Classification of Tumors of the Central Nervous System: a summary. *Acta Neuropathologica* **131,** 803–820 (2016).

31. Verhaak, R. G. W., Hoadley, K. A., Purdom, E., Wang, V., Qi, Y., Wilkerson, M. D., Miller, C. R., Ding, L., Golub, T., Mesirov, J. P., Alexe, G., Lawrence, M., O'Kelly, M., Tamayo, P., Weir, B. A., Gabriel, S., Winckler, W., Gupta, S., Jakkula, L., Feiler, H. S., Hodgson, J. G., James, C. D., Sarkaria, J. N., Brennan, C., Kahn, A., Spellman, P. T., Wilson, R. K., Speed, T. P., Gray, J. W., Meyerson, M., Getz, G., Perou, C. M. & Hayes, D. N. Integrated Genomic Analysis Identifies Clinically Relevant Subtypes of Glioblastoma Characterized by Abnormalities in PDGFRA, IDH1, EGFR, and NF1. *Cancer Cell* **17,** 98–110 (2010).

32. Doucette, T., Rao, G., Rao, A., Shen, L., Aldape, K., Wei, J., Dziurzynski, K., Gilbert, M. & Heimberger, A. B. Immune Heterogeneity of Glioblastoma Subtypes: Extrapolation from the Cancer Genome Atlas. *Cancer Immunology Research* **1,** 112–122 (2013).

33. Martinez-Lage, M., Lynch, T. M., Bi, Y., Cocito, C., Way, G. P., Pal, S., Haller, J., Yan, R. E., Ziober, A., Nguyen, A., Kandpal, M., O'Rourke, D. M., Greenfield, J. P., Greene, C. S., Davuluri, R. V. & Dahmane, N. Immune landscapes associated with different glioblastoma molecular subtypes. *Acta Neuropathologica Communications* **7,** 203 (2019).

34. Shen, R., Mo, Q., Schultz, N., Seshan, V. E., Olshen, A. B., Huse, J., Ladanyi, M. & Sander, C. Integrative Subtype Discovery in Glioblastoma Using iCluster. *PLOS ONE* **7,** e35236 (2012).

35. Wang, Q., Hu, B., Hu, X., Kim, H., Squatrito, M., Scarpace, L., deCarvalho, A. C., Lyu, S., Li, P., Li, Y., Barthel, F., Cho, H. J., Lin, Y.-H., Satani, N., Martinez-Ledesma, E., Zheng, S., Chang, E., Sauvé, C.-E. G., Olar, A., Lan, Z. D., Finocchiaro, G., Phillips, J. J., Berger, M. S., Gabrusiewicz, K. R., Wang, G., Eskilsson, E., Hu, J., Mikkelsen, T., DePinho, R. A., Muller, F., Heimberger, A. B., Sulman, E. P., Nam,

D.-H. & Verhaak, R. G. W. Tumor Evolution of Glioma-Intrinsic Gene Expression Subtypes Associates with Immunological Changes in the Microenvironment. *Cancer Cell* **32,** 42-56.e6 (2017).

36. Patel, A. P., Tirosh, I., Trombetta, J. J., Shalek, A. K., Gillespie, S. M., Wakimoto, H., Cahill, D. P., Nahed, B. V., Curry, W. T., Martuza, R. L., Louis, D. N., Rozenblatt-Rosen, O., Suvà, M. L., Regev, A. & Bernstein, B. E. Single-cell RNA-seq highlights intratumoral heterogeneity in primary glioblastoma. *Science* **344,** 1396–1401 (2014).
37. Lee, J. H., Lee, J. E., Kahng, J. Y., Kim, S. H., Park, J. S., Yoon, S. J., Um, J.-Y., Kim, W. K., Lee, J.-K., Park, J., Kim, E. H., Lee, J.-H., Lee, J.-H., Chung, W.-S., Ju, Y. S., Park, S.-H., Chang, J. H., Kang, S.-G. & Lee, J. H. Human glioblastoma arises from subventricular zone cells with low-level driver mutations. *Nature* **560,** 243–247 (2018).
38. Beiriger, J., Habib, A., Jovanovich, N., Kodavali, C. V., Edwards, L., Amankulor, N. & Zinn, P. O. The Subventricular Zone in Glioblastoma: Genesis, Maintenance, and Modeling. *Frontiers in Oncology* **12,** (2022).
39. Friedmann-Morvinski, D., Bushong, E. A., Ke, E., Soda, Y., Marumoto, T., Singer, O., Ellisman, M. H. & Verma, I. M. Dedifferentiation of neurons and astrocytes by oncogenes can induce gliomas in mice. *Science* **338,** 1080–1084 (2012).
40. Habib, A., Hoppe, M., Beiriger, J., Kodavali, C. V., Edwards, L. & Zinn, P. O. Letter: Glioblastoma Cell of Origin. *Stem Cell Reviews and Reports* **18,** 691–693 (2022).
41. Singh, S. K., Hawkins, C., Clarke, I. D., Squire, J. A., Bayani, J., Hide, T., Henkelman, R. M., Cusimano, M. D. & Dirks, P. B. Identification of human brain tumour initiating cells. *Nature* **432,** 396–401 (2004).
42. Heddleston, J. M., Li, Z., McLendon, R. E., Hjelmeland, A. B. & Rich, J. N. The hypoxic microenvironment maintains glioblastoma stem cells and promotes reprogramming towards a cancer stem cell phenotype. *Cell Cycle* **8,** 3274–3284 (2009).

43. Cusulin, C., Chesnelong, C., Bose, P., Bilenky, M., Kopciuk, K., Chan, J. A., Cairncross, J. G., Jones, S. J., Marra, M. A., Luchman, H. A. & Weiss, S. Precursor States of Brain Tumor Initiating Cell Lines Are Predictive of Survival in Xenografts and Associated with Glioblastoma Subtypes. *Stem Cell Reports* **5,** 1–9 (2015).

44. Kelly, J. J. P., Stechishin, O., Chojnacki, A., Lun, X., Sun, B., Senger, D. L., Forsyth, P., Auer, R. N., Dunn, J. F., Cairncross, J. G., Parney, I. F. & Weiss, S. Proliferation of Human Glioblastoma Stem Cells Occurs Independently of Exogenous Mitogens. *Stem Cells* **27,** 1722–1733 (2009).

45. Kameda-Smith, M. M., Manoranjan, B., Bakhshinyan, D., Adile, A. A., Venugopal, C. & Singh, S. K. Brain tumor initiating cells: with great technology will come greater understanding. *Future Neurology* **12,** 223–236 (2017).

46. Pallini, R., Ricci-Vitiani, L., Banna, G. L., Signore, M., Lombardi, D., Todaro, M., Stassi, G., Martini, M., Maira, G., Larocca, L. M. & De Maria, R. Cancer Stem Cell Analysis and Clinical Outcome in Patients with Glioblastoma Multiforme. *Clinical Cancer Research* **14,** 8205–8212 (2008).

47. Bao, S., Wu, Q., McLendon, R. E., Hao, Y., Shi, Q., Hjelmeland, A. B., Dewhirst, M. W., Bigner, D. D. & Rich, J. N. Glioma stem cells promote radioresistance by preferential activation of the DNA damage response. *Nature* **444,** 756–760 (2006).

48. Cheng, L., Wu, Q., Huang, Z., Guryanova, O. A., Huang, Q., Shou, W., Rich, J. N. & Bao, S. L1CAM regulates DNA damage checkpoint response of glioblastoma stem cells through NBS1. *The EMBO Journal* **30,** 800–813 (2011).

49. Eramo, A., Ricci-Vitiani, L., Zeuner, A., Pallini, R., Lotti, F., Sette, G., Pilozzi, E., Larocca, L. M., Peschle, C. & De Maria, R. Chemotherapy resistance of glioblastoma stem cells. *Cell Death & Differentiation* **13,** 1238–1241 (2006).

50. Cho, D.-Y., Lin, S.-Z., Yang, W.-K., Lee, H.-C., Hsu, D.-M., Lin, H.-L., Chen, C.-C., Liu, C.-L., Lee, W.-Y. & Ho, L.-H. Targeting cancer stem cells for treatment of glioblastoma multiforme. *Cell Transplant* **22,** 731–739 (2013).

51. Comprehensive genomic characterization defines human glioblastoma genes and core pathways. *Nature* **455,** 1061–1068 (2008).

52. Brennan, C. W., Verhaak, R. G. W., McKenna, A., Campos, B., Noushmehr, H., Salama, S. R., Zheng, S., Chakravarty, D., Sanborn, J. Z., Berman, S. H., Beroukhim, R., Bernard, B., Wu, C.-J., Genovese, G., Shmulevich, I., Barnholtz-Sloan, J., Zou, L., Vegesna, R., Shukla, S. A., Ciriello, G., Yung, W. K., Zhang, W., Sougnez, C., Mikkelsen, T., Aldape, K., Bigner, D. D., Van Meir, E. G., Prados, M., Sloan, A., Black, K. L., Eschbacher, J., Finocchiaro, G., Friedman, W., Andrews, D. W., Guha, A., Iacocca, M., O'Neill, B. P., Foltz, G., Myers, J., Weisenberger, D. J., Penny, R., Kucherlapati, R., Perou, C. M., Hayes, D. N., Gibbs, R., Marra, M., Mills, G. B., Lander, E., Spellman, P., Wilson, R., Sander, C., Weinstein, J., Meyerson, M., Gabriel, S., Laird, P. W., Haussler, D., Getz, G., Chin, L., Benz, C., Barnholtz-Sloan, J., Barrett, W., Ostrom, Q., Wolinsky, Y., Black, K. L., Bose, B., Boulos, P. T., Boulos, M., Brown, J., Czerinski, C., Eppley, M., Iacocca, M., Kempista, T., Kitko, T., Koyfman, Y., Rabeno, B., Rastogi, P., Sugarman, M., Swanson, P., Yalamanchii, K., Otey, I. P., Liu, Y. S., Xiao, Y., Auman, J. T., Chen, P.-C., Hadjipanayis, A., Lee, E., Lee, S., Park, P. J., Seidman, J., Yang, L., Kucherlapati, R., Kalkanis, S., Mikkelsen, T., Poisson, L. M., Raghunathan, A., Scarpace, L., Bernard, B., Bressler, R., Eakin, A., Iype, L., Kreisberg, R. B., Leinonen, K., Reynolds, S., Rovira, H., Thorsson, V., Shmulevich, I., Annala, M. J., Penny, R., Paulauskis, J., Curley, E., Hatfield, M., Mallery, D., Morris, S., Shelton, T., Shelton, C., Sherman, M., Yena, P., Cuppini, L., DiMeco, F., Eoli, M., Finocchiaro, G., Maderna, E., Pollo, B., Saini, M., Balu, S., Hoadley, K. A., Li, L., Miller, C. R., Shi, Y., Topal, M. D., Wu, J., Dunn, G., Giannini, C., O'Neill, B. P., Aksoy, B. A., Antipin, Y., Borsu, L., Berman, S. H., Brennan, C. W., Cerami, E., Chakravarty, D., Ciriello, G., Gao, J., Gross, B., Jacobsen, A., Ladanyi, M., Lash, A., Liang, Y., Reva,

B., Sander, C., Schultz, N., Shen, R., Socci, N. D., Viale, A., Ferguson, M. L., Chen, Q.-R., Demchok, J. A., Dillon, L. A. L., Shaw, K. R. M., Sheth, M., Tarnuzzer, R., Wang, Z., Yang, L., Davidsen, T., Guyer, M. S., Ozenberger, B. A., Sofia, H. J., Bergsten, J., Eckman, J., Harr, J., Myers, J., Smith, C., Tucker, K., Winemiller, C., Zach, L. A., Ljubimova, J. Y., Eley, G., Ayala, B., Jensen, M. A., Kahn, A., Pihl, T. D., Pot, D. A., Wan, Y., Eschbacher, J., Foltz, G., Hansen, N., Hothi, P., Lin, B., Shah, N., Yoon, J., Lau, C., Berens, M., Ardlie, K., Beroukhim, R., Carter, S. L., Cherniack, A. D., Noble, M., Cho, J., Cibulskis, K., DiCara, D., Frazer, S., Gabriel, S. B., Gehlenborg, N., Gentry, J., Heiman, D., Kim, J., Jing, R., Lander, E. S., Lawrence, M., Lin, P., Mallard, W., Meyerson, M., Onofrio, R. C., Saksena, G., Schumacher, S., Sougnez, C., Stojanov, P., Tabak, B., Voet, D., Zhang, H., Zou, L., Getz, G., Dees, N. N., Ding, L., Fulton, L. L., Fulton, R. S., Kanchi, K.-L., Mardis, E. R., Wilson, R. K., Baylin, S. B., Andrews, D. W., Harshyne, L., Cohen, M. L., Devine, K., Sloan, A. E., VandenBerg, S. R., Berger, M. S., Prados, M., Carlin, D., Craft, B., Ellrott, K., Goldman, M., Goldstein, T., Grifford, M., Haussler, D., Ma, S., Ng, S., Salama, S. R., Sanborn, J. Z., Stuart, J., Swatloski, T., Waltman, P., Zhu, J., Foss, R., Frentzen, B., Friedman, W., McTiernan, R., Yachnis, A., Hayes, D. N., Perou, C. M., Zheng, S., Vegesna, R., Mao, Y., Akbani, R., Aldape, K., Bogler, O., Fuller, G. N., Liu, W., Liu, Y., Lu, Y., Mills, G., Protopopov, A., Ren, X., Sun, Y., Wu, C.-J., Yung, W. K. A., Zhang, W., Zhang, J., Chen, K., Weinstein, J. N., Chin, L., Verhaak, R. G. W., Noushmehr, H., Weisenberger, D. J., Bootwalla, M. S., Lai, P. H., Triche, T. J., Jr., Van Den Berg, D. J., Laird, P. W., Gutmann, D. H., Lehman, N. L., VanMeir, E. G., Brat, D., Olson, J. J., Mastrogianakis, G. M., Devi, N. S., Zhang, Z., Bigner, D., Lipp, E. & McLendon, R. The Somatic Genomic Landscape of Glioblastoma. *Cell* **155,** 462–477 (2013).

53. Nonoguchi, N., Ohta, T., Oh, J.-E., Kim, Y.-H., Kleihues, P. & Ohgaki, H. TERT promoter mutations in primary and secondary glioblastomas. *Acta Neuropathologica* **126,** 931–937 (2013).

54. Simon, M., Hosen, I., Gousias, K., Rachakonda, S., Heidenreich, B., Gessi, M., Schramm, J., Hemminki, K., Waha, A. & Kumar, R. TERT promoter mutations: a novel independent prognostic factor in primary glioblastomas. *Neuro-Oncology* **17,** 45–52 (2015).

55. Heaphy, C. M., Subhawong, A. P., Hong, S.-M., Goggins, M. G., Montgomery, E. A., Gabrielson, E., Netto, G. J., Epstein, J. I., Lotan, T. L., Westra, W. H., Shih, I.-M., Iacobuzio-Donahue, C. A., Maitra, A., Li, Q. K., Eberhart, C. G., Taube, J. M., Rakheja, D., Kurman, R. J., Wu, T. C., Roden, R. B., Argani, P., De Marzo, A. M., Terracciano, L., Torbenson, M. & Meeker, A. K. Prevalence of the Alternative Lengthening of Telomeres Telomere Maintenance Mechanism in Human Cancer Subtypes. *The American Journal of Pathology* **179,** 1608–1615 (2011).

56. Liu, X.-Y., Gerges, N., Korshunov, A., Sabha, N., Khuong-Quang, D.-A., Fontebasso, A. M., Fleming, A., Hadjadj, D., Schwartzentruber, J., Majewski, J., Dong, Z., Siegel, P., Albrecht, S., Croul, S., Jones, D. T., Kool, M., Tonjes, M., Reifenberger, G., Faury, D., Zadeh, G., Pfister, S. & Jabado, N. Frequent ATRX mutations and loss of expression in adult diffuse astrocytic tumors carrying IDH1/IDH2 and TP53 mutations. *Acta Neuropathologica* **124,** 615–625 (2012).

57. Ohgaki, H., Dessen, P., Jourde, B., Horstmann, S., Nishikawa, T., Di Patre, P.-L., Burkhard, C., Schüler, D., Probst-Hensch, N. M., Maiorka, P. C., Baeza, N., Pisani, P., Yonekawa, Y., Yasargil, M. G., Lütolf, U. M. & Kleihues, P. Genetic Pathways to Glioblastoma: A Population-Based Study. *Cancer Research* **64,** 6892–6899 (2004).

58. Parsons, D. W., Jones, S., Zhang, X., Lin, J. C.-H., Leary, R. J., Angenendt, P., Mankoo, P., Carter, H., Siu, I.-M., Gallia, G. L., Olivi, A., McLendon, R., Rasheed, B. A., Keir, S., Nikolskaya, T., Nikolsky, Y., Busam, D. A., Tekleab, H., Diaz, L. A., Hartigan, J., Smith, D. R., Strausberg, R. L., Marie, S. K. N., Shinjo, S. M. O., Yan, H., Riggins, G. J., Bigner, D. D., Karchin, R., Papadopoulos, N., Parmigiani, G., Vogelstein, B., Velculescu, V. E. & Kinzler, K. W. An Integrated Genomic Analysis of Human Glioblastoma Multiforme. *Science* **321,** 1807–1812 (2008).

59. Padfield, E., Ellis, H. P. & Kurian, K. M. Current Therapeutic Advances Targeting EGFR and EGFRvIII in Glioblastoma. *Frontiers in Oncology* **5,** (2015).

60. Olympios, N., Gilard, V., Marguet, F., Clatot, F., Di Fiore, F. & Fontanilles, M. TERT Promoter Alterations in Glioblastoma: A Systematic Review. *Cancers* **13,** (2021).

61. Heaphy, C. M., de Wilde, R. F., Jiao, Y., Klein, A. P., Edil, B. H., Shi, C., Bettegowda, C., Rodriguez, F. J., Eberhart, C. G., Hebbar, S., Offerhaus, G. J., McLendon, R., Rasheed, B. A., He, Y., Yan, H., Bigner, D. D., Oba-Shinjo, S. M., Marie, S. K. N., Riggins, G. J., Kinzler, K. W., Vogelstein, B., Hruban, R. H., Maitra, A., Papadopoulos, N. & Meeker, A. K. Altered Telomeres in Tumors with ATRX and DAXX Mutations. *Science* **333,** 425–425 (2011).

62. Feroz, W. & Sheikh, A. M. A. Exploring the multiple roles of guardian of the genome: P53. *Egyptian Journal of Medical Human Genetics* **21,** 49 (2020).

63. Koul, D. PTEN Signaling pathways in glioblastoma. *Cancer Biology & Therapy* **7,** 1321–1325 (2008).

64. Sherr, C. J. The INK4a/ARF network in tumour suppression. *Nature Reviews Molecular Cell Biology* **2,** 731–737 (2001).

65. Hegi, M. E., Diserens, A.-C., Gorlia, T., Hamou, M.-F., de Tribolet, N., Weller, M., Kros, J. M., Hainfellner, J. A., Mason, W., Mariani, L., Bromberg, J. E. C., Hau, P., Mirimanoff, R. O., Cairncross, J. G., Janzer, R. C. & Stupp, R. MGMT Gene Silencing and Benefit from Temozolomide in Glioblastoma. *N Engl J Med* **352,** 997–1003 (2005).

66. Tentori, L. & Graziani, G. Pharmacological Strategies to Increase the Antitumor Activity of Methylating Agents. *Current Medicinal Chemistry* **9,** 1285–1301 (2002).

67. Stefania D'Atri, Lucio Tentori, Pedro Miguel Lacal, Grazia Graziani, Elena Pagani, Elena Benincasa, Giovanna Zambruno, Enzo Bonmassar, & Josef Jiricny. Involvement of the Mismatch Repair System in Temozolomide-Induced Apoptosis. *Mol Pharmacol* **54,** 334 (1998).

68. Esteller, M. & Herman, J. G. Generating mutations but providing chemosensitivity: the role of O6-methylguanine DNA methyltransferase in human cancer. *Oncogene* **23,** 1–8 (2004).

69. Wong, Q. H.-W., Li, K. K.-W., Wang, W.-W., Malta, T. M., Noushmehr, H., Grabovska, Y., Jones, C., Chan, A. K.-Y., Kwan, J. S.-H., Huang, Q. J.-Q., Wong, G. C.-H., Li, W.-C., Liu, X.-Z., Chen, H., Chan, D. T.-M., Mao, Y., Zhang, Z.-Y., Shi, Z.-F. & Ng, H.-K. Molecular landscape of IDH-mutant primary astrocytoma Grade IV/glioblastomas. *Modern Pathology* **34,** 1245–1260 (2021).

70. Alzial, G., Renoult, O., Paris, F., Gratas, C., Clavreul, A. & Pecqueur, C. Wild-type isocitrate dehydrogenase under the spotlight in glioblastoma. *Oncogene* **41,** 613–621 (2022).

71. Baldewpersad Tewarie, N. M. S., Burgers, I. A. V., Dawood, Y., den Boon, H. C., den Brok, M. G. H. E., Klunder, J. H., Koopmans, K. B., Rademaker, E., van den Broek, H. B., van den Bersselaar, S. M., Witjes, J. J., Van Noorden, C. J. F. & Atai, N. A. NADP+-dependent IDH1R132 mutation and its relevance for glioma patient survival. *Medical Hypotheses* **80,** 728–731 (2013).

72. Xu, W., Yang, H., Liu, Y., Yang, Y., Wang, P., Kim, S.-H., Ito, S., Yang, C., Wang, P., Xiao, M.-T., Liu, L., Jiang, W., Liu, J., Zhang, J., Wang, B., Frye, S., Zhang, Y., Xu, Y., Lei, Q., Guan, K.-L., Zhao, S. & Xiong, Y. Oncometabolite 2-Hydroxyglutarate Is a Competitive Inhibitor of α-Ketoglutarate-Dependent Dioxygenases. *Cancer Cell* **19,** 17–30 (2011).

73. Stupp, R., Mason, W. P., van den Bent, M. J., Weller, M., Fisher, B., Taphoorn, M. J. B., Belanger, K., Brandes, A. A., Marosi, C., Bogdahn, U., Curschmann, J., Janzer, R. C., Ludwin, S. K., Gorlia, T., Allgeier, A., Lacombe, D., Cairncross, J. G., Eisenhauer, E. & Mirimanoff, R. O. Radiotherapy plus Concomitant and Adjuvant Temozolomide for Glioblastoma. *N Engl J Med* **352,** 987–996 (2005).

74. Cabrera, A. R., Kirkpatrick, J. P., Fiveash, J. B., Shih, H. A., Koay, E. J., Lutz, S., Petit, J., Chao, S. T., Brown, P. D., Vogelbaum, M., Reardon, D. A., Chakravarti, A., Wen, P. Y. & Chang, E. Radiation therapy for glioblastoma: Executive summary of an American Society for Radiation Oncology Evidence-Based Clinical Practice Guideline. *Practical Radiation Oncology* **6,** 217–225 (2016).

75. Walker, M. D., Strike, T. A. & Sheline, G. E. An analysis of dose-effect relationship in the radiotherapy of malignant gliomas. *International Journal of Radiation Oncology*Biology*Physics* **5,** 1725–1731 (1979).

76. Salazar, O. M., Philip Rubin, M. D., Feldstein, M. L. & Pizzutiello, R. High dose radiation therapy in the treatment of malignant gliomas: Final Report. *International Journal of Radiation Oncology*Biology*Physics* **5,** 1733–1740 (1979).

77. Lawrence, Y. R., Li, X. A., el Naqa, I., Hahn, C. A., Marks, L. B., Merchant, T. E. & Dicker, A. P. Radiation Dose–Volume Effects in the Brain. *International Journal of Radiation Oncology*Biology*Physics* **76,** S20–S27 (2010).

78. Roa, W., Brasher, P. M. A., Bauman, G., Anthes, M., Bruera, E., Chan, A., Fisher, B., Fulton, D., Gulavita, S., Hao, C., Husain, S., Murtha, A., Petruk, K., Stewart, D., Tai, P., Urtasun, R., Cairncross, J. G. & Forsyth, P. Abbreviated Course of Radiation Therapy in Older Patients With Glioblastoma Multiforme: A Prospective Randomized Clinical Trial. *JCO* **22,** 1583–1588 (2004).

79. Perry, J. R., Laperriere, N., O'Callaghan, C. J., Brandes, A. A., Menten, J., Phillips, C., Fay, M., Nishikawa, R., Cairncross, J. G., Roa, W., Osoba, D., Rossiter, J. P., Sahgal, A., Hirte, H., Laigle-Donadey, F., Franceschi, E., Chinot, O., Golfinopoulos, V., Fariselli, L., Wick, A., Feuvret, L., Back, M., Tills, M., Winch, C., Baumert, B. G., Wick, W., Ding, K. & Mason, W. P. Short-Course Radiation plus Temozolomide in Elderly Patients with Glioblastoma. *N Engl J Med* **376,** 1027–1037 (2017).

80. Malmström, A., Grønberg, B. H., Marosi, C., Stupp, R., Frappaz, D., Schultz, H., Abacioglu, U., Tavelin, B., Lhermitte, B., Hegi, M. E., Rosell, J. & Henriksson, R. Temozolomide versus standard 6-week radiotherapy versus hypofractionated radiotherapy in patients older than 60 years with glioblastoma: the Nordic randomised, phase 3 trial. *The Lancet Oncology* **13,** 916–926 (2012).

81. Murray Brunt, A., Haviland, J. S., Wheatley, D. A., Sydenham, M. A., Alhasso, A., Bloomfield, D. J., Chan, C., Churn, M., Cleator, S., Coles, C. E., Goodman, A., Harnett, A., Hopwood, P., Kirby, A. M.,

Kirwan, C. C., Morris, C., Nabi, Z., Sawyer, E., Somaiah, N., Stones, L., Syndikus, I., Bliss, J. M., Yarnold, J. R., Alhasso, A., Armstrong, A., Bliss, J., Bloomfield, D., Bowen, J., Brunt, M., Chan, C., Chantler, H., Churn, M., Cleator, S., Coles, C., Donovan, E., Goodman, A., Griffin, S., Haviland, J., Hopwood, P., Kirby, A., Kirk, J., Kirwan, C., MacLennan, M., Morris, C., Nabi, Z., Sawyer, E., Sculphur, M., Sinclair, J., Somaiah, N., Stones, L., Sydenham, M., Syndikus, I., Tremlett, J., Venables, K., Wheatley, D. & Yarnold, J. Hypofractionated breast radiotherapy for 1 week versus 3 weeks (FAST-Forward): 5-year efficacy and late normal tissue effects results from a multicentre, non-inferiority, randomised, phase 3 trial. *The Lancet* **395,** 1613–1626 (2020).

82. Dearnaley, D., Syndikus, I., Mossop, H., Khoo, V., Birtle, A., Bloomfield, D., Graham, J., Kirkbride, P., Logue, J., Malik, Z., Money-Kyrle, J., O'Sullivan, J. M., Panades, M., Parker, C., Patterson, H., Scrase, C., Staffurth, J., Stockdale, A., Tremlett, J., Bidmead, M., Mayles, H., Naismith, O., South, C., Gao, A., Cruickshank, C., Hassan, S., Pugh, J., Griffin, C. & Hall, E. Conventional versus hypofractionated high-dose intensity-modulated radiotherapy for prostate cancer: 5-year outcomes of the randomised, non-inferiority, phase 3 CHHiP trial. *The Lancet Oncology* **17,** 1047–1060 (2016).

83. Zhang, J., Fan, M., Liu, D., Zhao, K.-L., Wu, K.-L., Zhao, W.-X., Zhu, Z.-F. & Fu, X.-L. Hypo- or conventionally fractionated radiotherapy combined with chemotherapy in patients with limited stage small cell lung cancer. *Radiation Oncology* **12,** 51 (2017).

84. Jin, J., Tang, Y., Hu, C., Jiang, L.-M., Jiang, J., Li, N., Liu, W.-Y., Chen, S.-L., Li, S., Lu, N.-N., Cai, Y., Li, Y.-H., Zhu, Y., Cheng, G.-H., Zhang, H.-Y., Wang, X., Zhu, S.-Y., Wang, J., Li, G.-F., Yang, J.-L., Zhang, K., Chi, Y., Yang, L., Zhou, H.-T., Zhou, A.-P., Zou, S.-M., Fang, H., Wang, S.-L., Zhang, H.-Z., Wang, X.-S., Wei, L.-C., Wang, W.-L., Liu, S.-X., Gao, Y.-H. & Li, Y.-X. Multicenter, Randomized, Phase III Trial of Short-Term Radiotherapy Plus Chemotherapy Versus Long-Term Chemoradiotherapy in Locally Advanced Rectal Cancer (STELLAR). *J Clin Oncol* **40,** 1681–1692 (2022).

85. Lewis, S., Barry, A. & Hawkins, M. A. Hypofractionation in Hepatocellular Carcinoma – The Effect of Fractionation Size. *Clinical Oncology* **34,** e195–e209 (2022).

86. Overgaard, J., Mohanti, B. K., Begum, N., Ali, R., Agarwal, J. P., Kuddu, M., Bhasker, S., Tatsuzaki, H. & Grau, C. Five versus six fractions of radiotherapy per week for squamous-cell carcinoma of the head and neck (IAEA-ACC study): a randomised, multicentre trial. *The Lancet Oncology* **11,** 553–560 (2010).

87. Viegas, C. M., Araujo, C. M. M., Dantas, M. A., Froimtchuk, M., Oliveira, J. A. F., Marchiori, E. & Souhami, L. Concurrent chemotherapy and hypofractionated twice-daily radiotherapy in cervical cancer patients with stage IIIB disease and bilateral parametrial involvement: A phase I-II study. *International Journal of Radiation Oncology*Biology*Physics* **60,** 1154–1159 (2004).

88. Takanen, S., Bottero, M., Nisticò, P. & Sanguineti, G. A Systematic Review on the Impact of Hypofractionated and Stereotactic Radiotherapy on Immune Cell Subpopulations in Cancer Patients. *Cancers* **14,** (2022).

89. Barlow, M. L., Battaglia, N., Gerber, S. A. & Lord, E. M. Hypofractionated radiotherapy treatment preserves immune function and improves tumor control vs. hyperfractionated treatment. *The Journal of Immunology* **196,** 213.13-213.13 (2016).

90. Zhang, T., Yu, H., Ni, C., Zhang, T., Liu, L., Lv, Q., Zhang, Z., Wang, Z., Wu, D., Wu, P., Chen, G., Wang, L., Wei, Q., Huang, J. & Wang, X. Hypofractionated stereotactic radiation therapy activates the peripheral immune response in operable stage I non-small-cell lung cancer. *Sci Rep* **7,** 4866 (2017).

91. Crocenzi, T., Cottam, B., Newell, P., Wolf, R. F., Hansen, P. D., Hammill, C., Solhjem, M. C., To, Y.-Y., Greathouse, A., Tormoen, G., Jutric, Z., Young, K., Bahjat, K. S., Gough, M. J. & Crittenden, M. R. A hypofractionated radiation regimen avoids the lymphopenia associated with neoadjuvant

chemoradiation therapy of borderline resectable and locally advanced pancreatic adenocarcinoma. *Journal for ImmunoTherapy of Cancer* **4,** 45 (2016).

92. Mun, E. J., Babiker, H. M., Weinberg, U., Kirson, E. D. & Von Hoff, D. D. Tumor-Treating Fields: A Fourth Modality in Cancer Treatment. *Clinical Cancer Research* **24,** 266–275 (2018).
93. Lassman, A. B., Joanta-Gomez, A. E., Pan, P. C. & Wick, W. Current usage of tumor treating fields for glioblastoma. *Neuro-Oncology Advances* **2,** vdaa069 (2020).
94. Grossman, S. A., Ye, X., Lesser, G., Sloan, A., Carraway, H., Desideri, S., Piantadosi, S., & for the NABTT CNS Consortium. Immunosuppression in Patients with High-Grade Gliomas Treated with Radiation and Temozolomide. *Clinical Cancer Research* **17,** 5473–5480 (2011).
95. Rudra, S., Hui, C., Rao, Y. J., Samson, P., Lin, A. J., Chang, X., Tsien, C., Fergus, S., Mullen, D., Yang, D., Thotala, D., Hallahan, D., Campian, J. L. & Huang, J. Effect of Radiation Treatment Volume Reduction on Lymphopenia in Patients Receiving Chemoradiotherapy for Glioblastoma. *International Journal of Radiation Oncology*Biology*Physics* **101,** 217–225 (2018).
96. Yovino, S., Kleinberg, L., Grossman, S. A., Narayanan, M. & Ford, E. The Etiology of Treatment-related Lymphopenia in Patients with Malignant Gliomas: Modeling Radiation Dose to Circulating Lymphocytes Explains Clinical Observations and Suggests Methods of Modifying the Impact of Radiation on Immune Cells. *Cancer Investigation* **31,** 140–144 (2013).
97. Ghosh, S., Huang, J., Inkman, M., Zhang, J., Thotala, S., Tikhonova, E., Miheecheva, N., Frenkel, F., Ataullakhanov, R., Wang, X., DeNardo, D., Hallahan, D. & Thotala, D. Radiation-induced circulating myeloid-derived suppressor cells induce systemic lymphopenia after chemoradiotherapy in patients with glioblastoma. *Science Translational Medicine* **15,** eabn6758
98. Byun, H. K., Kim, N., Yoon, H. I., Kang, S.-G., Kim, S. H., Cho, J., Baek, J. G., Chang, J. H. & Suh, C.-O. Clinical predictors of radiation-induced lymphopenia in patients receiving chemoradiation for

glioblastoma: clinical usefulness of intensity-modulated radiotherapy in the immuno-oncology era. *Radiation Oncology* **14,** 51 (2019).

99. Grossman, S. A., Ellsworth, S., Campian, J., Wild, A. T., Herman, J. M., Laheru, D., Brock, M., Balmanoukian, A. & Ye, X. Survival in Patients With Severe Lymphopenia Following Treatment With Radiation and Chemotherapy for Newly Diagnosed Solid Tumors. *J Natl Compr Canc Netw* **13,** 1225–1231 (2015).
100. Kim, W. J., Dho, Y.-S., Ock, C.-Y., Kim, J. W., Choi, S. H., Lee, S.-T., Kim, I. H., Kim, T. M. & Park, C.-K. Clinical observation of lymphopenia in patients with newly diagnosed glioblastoma. *Journal of Neuro-Oncology* **143,** 321–328 (2019).
101. Mapelli, R., Julita, C., Bianchi, S. P., Gallina, N., Lucchini, R., Midulla, M., Puci, F., Saddi, J., Trivellato, S., Panizza, D., De Ponti, E. & Arcangeli, S. Association between treatment-related lymphopenia and survival in glioblastoma patients following postoperative chemoradiotherapy. *Strahlentherapie und Onkologie* **198,** 448–457 (2022).
102. Pitter, K. L., Tamagno, I., Alikhanyan, K., Hosni-Ahmed, A., Pattwell, S. S., Donnola, S., Dai, C., Ozawa, T., Chang, M., Chan, T. A., Beal, K., Bishop, A. J., Barker, C. A., Jones, T. S., Hentschel, B., Gorlia, T., Schlegel, U., Stupp, R., Weller, M., Holland, E. C. & Hambardzumyan, D. Corticosteroids compromise survival in glioblastoma. *Brain* **139,** 1458–1471 (2016).
103. Shields, L. B. E., Shelton, B. J., Shearer, A. J., Chen, L., Sun, D. A., Parsons, S., Bourne, T. D., LaRocca, R. & Spalding, A. C. Dexamethasone administration during definitive radiation and temozolomide renders a poor prognosis in a retrospective analysis of newly diagnosed glioblastoma patients. *Radiation Oncology* **10,** 222 (2015).
104. Yang, I., Tihan, T., Han, S. J., Wrensch, M. R., Wiencke, J., Sughrue, M. E. & Parsa, A. T. CD8+ T-cell infiltrate in newly diagnosed glioblastoma is associated with long-term survival. *Journal of Clinical Neuroscience* **17,** 1381–1385 (2010).

105. Lohr, J., Ratliff, T., Huppertz, A., Ge, Y., Dictus, C., Ahmadi, R., Grau, S., Hiraoka, N., Eckstein, V., Ecker, R. C., Korff, T., von Deimling, A., Unterberg, A., Beckhove, P. & Herold-Mende, C. Effector T-Cell Infiltration Positively Impacts Survival of Glioblastoma Patients and Is Impaired by Tumor-Derived TGF-β. *Clinical Cancer Research* **17,** 4296–4308 (2011).

106. Kmiecik, J., Poli, A., Brons, N. H. C., Waha, A., Eide, G. E., Enger, P. Ø., Zimmer, J. & Chekenya, M. Elevated CD3+ and CD8+ tumor-infiltrating immune cells correlate with prolonged survival in glioblastoma patients despite integrated immunosuppressive mechanisms in the tumor microenvironment and at the systemic level. *Journal of Neuroimmunology* **264,** 71–83 (2013).

107. Prins, R. M., Soto, H., Konkankit, V., Odesa, S. K., Eskin, A., Yong, W. H., Nelson, S. F. & Liau, L. M. Gene Expression Profile Correlates with T-Cell Infiltration and Relative Survival in Glioblastoma Patients Vaccinated with Dendritic Cell Immunotherapy. *Clinical Cancer Research* **17,** 1603–1615 (2011).

108. Hou, L. C., Veeravagu, A., Hsu, A. R. & Tse, V. C. K. Recurrent glioblastoma multiforme: a review of natural history and management options. *Neurosurgical Focus FOC* **20,** E3 (2006).

109. Lu, V. M., Jue, T. R., McDonald, K. L. & Rovin, R. A. The Survival Effect of Repeat Surgery at Glioblastoma Recurrence and its Trend: A Systematic Review and Meta-Analysis. *World Neurosurgery* **115,** 453-459.e3 (2018).

110. Weller, M., Tabatabai, G., Kästner, B., Felsberg, J., Steinbach, J. P., Wick, A., Schnell, O., Hau, P., Herrlinger, U., Sabel, M. C., Wirsching, H.-G., Ketter, R., Bähr, O., Platten, M., Tonn, J. C., Schlegel, U., Marosi, C., Goldbrunner, R., Stupp, R., Homicsko, K., Pichler, J., Nikkhah, G., Meixensberger, J., Vajkoczy, P., Kollias, S., Hüsing, J., Reifenberger, G., Wick, W., & for the DIRECTOR Study Group. MGMT Promoter Methylation Is a Strong Prognostic Biomarker for Benefit from Dose-Intensified Temozolomide Rechallenge in Progressive Glioblastoma: The DIRECTOR Trial. *Clinical Cancer Research* **21,** 2057–2064 (2015).

111. Wick, W., Puduvalli, V. K., Chamberlain, M. C., van den Bent, M. J., Carpentier, A. F., Cher, L. M., Mason, W., Weller, M., Hong, S., Musib, L., Liepa, A. M., Thornton, D. E. & Fine, H. A. Phase III study of enzastaurin compared with lomustine in the treatment of recurrent intracranial glioblastoma. *J Clin Oncol* **28,** 1168–1174 (2010).

112. Jungk, C., Chatziaslanidou, D., Ahmadi, R., Capper, D., Bermejo, J. L., Exner, J., von Deimling, A., Herold-Mende, C. & Unterberg, A. Chemotherapy with BCNU in recurrent glioma: Analysis of clinical outcome and side effects in chemotherapy-naïve patients. *BMC Cancer* **16,** 81 (2016).

113. Parasramka, S., Talari, G., Rosenfeld, M., Guo, J. & Villano, J. Procarbazine, lomustine and vincristine for recurrent high-grade glioma. *Cochrane Database of Systematic Reviews* (2017). doi:10.1002/14651858.CD011773.pub2

114. Stupp, R., Wong, E. T., Kanner, A. A., Steinberg, D., Engelhard, H., Heidecke, V., Kirson, E. D., Taillibert, S., Liebermann, F., Dbalý, V., Ram, Z., Villano, J. L., Rainov, N., Weinberg, U., Schiff, D., Kunschner, L., Raizer, J., Honnorat, J., Sloan, A., Malkin, M., Landolfi, J. C., Payer, F., Mehdorn, M., Weil, R. J., Pannullo, S. C., Westphal, M., Smrcka, M., Chin, L., Kostron, H., Hofer, S., Bruce, J., Cosgrove, R., Paleologous, N., Palti, Y. & Gutin, P. H. NovoTTF-100A versus physician's choice chemotherapy in recurrent glioblastoma: A randomised phase III trial of a novel treatment modality. *European Journal of Cancer* **48,** 2192–2202 (2012).

115. Kazmi, F., Soon, Y. Y., Leong, Y. H., Koh, W. Y. & Vellayappan, B. Re-irradiation for recurrent glioblastoma (GBM): a systematic review and meta-analysis. *Journal of Neuro-Oncology* **142,** 79–90 (2019).

116. Minniti, G., Niyazi, M., Alongi, F., Navarria, P. & Belka, C. Current status and recent advances in reirradiation of glioblastoma. *Radiation Oncology* **16,** 36 (2021).

117. Imber, B. S., Kanungo, I., Braunstein, S., Barani, I. J., Fogh, S. E., Nakamura, J. L., Berger, M. S., Chang, E. F., Molinaro, A. M., Cabrera, J. R., McDermott, M. W., Sneed, P. K. & Aghi, M. K.

Indications and Efficacy of Gamma Knife Stereotactic Radiosurgery for Recurrent Glioblastoma: 2 Decades of Institutional Experience. *Neurosurgery* **80,** 129–139 (2017).

118. Lee, Y., Auh, S. L., Wang, Y., Burnette, B., Wang, Y., Meng, Y., Beckett, M., Sharma, R., Chin, R., Tu, T., Weichselbaum, R. R. & Fu, Y.-X. Therapeutic effects of ablative radiation on local tumor require CD8+ T cells: changing strategies for cancer treatment. *Blood* **114,** 589–595 (2009).
119. Filatenkov, A., Baker, J., Mueller, A. M. S., Kenkel, J., Ahn, G.-O., Dutt, S., Zhang, N., Kohrt, H., Jensen, K., Dejbakhsh-Jones, S., Shizuru, J. A., Negrin, R. N., Engleman, E. G. & Strober, S. Ablative Tumor Radiation Can Change the Tumor Immune Cell Microenvironment to Induce Durable Complete Remissions. *Clinical Cancer Research* **21,** 3727–3739 (2015).
120. Storozynsky, Q. T., Agopsowicz, K. C., Noyce, R. S., Bukhari, A. B., Han, X., Snyder, N., Umer, B. A., Gamper, A. M., Godbout, R., Evans, D. H. & Hitt, M. M. Radiation combined with oncolytic vaccinia virus provides pronounced antitumor efficacy and induces immune protection in an aggressive glioblastoma model. *Cancer Letters* **562,** 216169 (2023).
121. Stessin, A. M., Clausi, M. G., Zhao, Z., Lin, H., Hou, W., Jiang, Z., Duong, T. Q., Tsirka, S. E. & Ryu, S. Repolarized macrophages, induced by intermediate stereotactic dose radiotherapy and immune checkpoint blockade, contribute to long-term survival in glioma-bearing mice. *Journal of Neuro-Oncology* **147,** 547–555 (2020).
122. Lehrer, E. J., Ruiz-Garcia, H., Nehlsen, A. D., Sindhu, K. K., Estrada, R. S., Borst, G. R., Sheehan, J. P., Quinones-Hinojosa, A. & Trifiletti, D. M. Preoperative Stereotactic Radiosurgery for Glioblastoma. *Biology* **11,** (2022).
123. Lehrer, E. J., Jones, B. M., Sindhu, K. K., Dickstein, D. R., Cohen, M., Lazarev, S., Quiñones-Hinojosa, A., Green, S. & Trifiletti, D. M. A Review of the Role of Stereotactic Radiosurgery and Immunotherapy in the Management of Primary Central Nervous System Tumors. *Biomedicines* **10,** (2022).

124. Shaw, E., Scott, C., Souhami, L., Dinapoli, R., Kline, R., Loeffler, J. & Farnan, N. Single dose radiosurgical treatment of recurrent previously irradiated primary brain tumors and brain metastases: final report of RTOG protocol 90-05. *International Journal of Radiation Oncology*Biology*Physics* **47,** 291–298 (2000).

125. Brown, N. F., Carter, T. J., Ottaviani, D. & Mulholland, P. Harnessing the immune system in glioblastoma. *British Journal of Cancer* **119,** 1171–1181 (2018).

126. Hayflick, L. & Moorhead, P. S. The serial cultivation of human diploid cell strains. *Experimental Cell Research* **25,** 585–621 (1961).

127. Hayflick, L. The limited in vitro lifetime of human diploid cell strains. *Experimental Cell Research* **37,** 614–636 (1965).

128. Hooten, N. N. & Evans, M. K. Techniques to Induce and Quantify Cellular Senescence. *JoVE* e55533 (2017). doi:10.3791/55533

129. González-Gualda, E., Baker, A. G., Fruk, L. & Muñoz-Espín, D. A guide to assessing cellular senescence in vitro and in vivo. *The FEBS Journal* **288,** 56–80 (2021).

130. Calcinotto, A., Kohli, J., Zagato, E., Pellegrini, L., Demaria, M. & Alimonti, A. Cellular Senescence: Aging, Cancer, and Injury. *Physiological Reviews* **99,** 1047–1078 (2019).

131. Coppé, J.-P., Patil, C. K., Rodier, F., Sun, Y., Muñoz, D. P., Goldstein, J., Nelson, P. S., Desprez, P.-Y. & Campisi, J. Senescence-Associated Secretory Phenotypes Reveal Cell-Nonautonomous Functions of Oncogenic RAS and the p53 Tumor Suppressor. *PLOS Biology* **6,** e301 (2008).

132. Davalos, A. R., Coppe, J.-P., Campisi, J. & Desprez, P.-Y. Senescent cells as a source of inflammatory factors for tumor progression. *Cancer and Metastasis Reviews* **29,** 273–283 (2010).

133. Milanovic, M., Fan, D. N. Y., Belenki, D., Däbritz, J. H. M., Zhao, Z., Yu, Y., Dörr, J. R., Dimitrova, L., Lenze, D., Monteiro Barbosa, I. A., Mendoza-Parra, M. A., Kanashova, T., Metzner, M., Pardon, K., Reimann, M., Trumpp, A., Dörken, B., Zuber, J., Gronemeyer, H., Hummel, M., Dittmar, G., Lee, S. &

Schmitt, C. A. Senescence-associated reprogramming promotes cancer stemness. *Nature* **553,** 96–100 (2018).

134. Short, S., Fielder, E., Miwa, S. & von Zglinicki, T. Senolytics and senostatics as adjuvant tumour therapy. *EBioMedicine* **41,** 683–692 (2019).

135. Gorgoulis, V., Adams, P. D., Alimonti, A., Bennett, D. C., Bischof, O., Bishop, C., Campisi, J., Collado, M., Evangelou, K., Ferbeyre, G., Gil, J., Hara, E., Krizhanovsky, V., Jurk, D., Maier, A. B., Narita, M., Niedernhofer, L., Passos, J. F., Robbins, P. D., Schmitt, C. A., Sedivy, J., Vougas, K., von Zglinicki, T., Zhou, D., Serrano, M. & Demaria, M. Cellular Senescence: Defining a Path Forward. *Cell* **179,** 813–827 (2019).

136. Dai, C. Y. & Enders, G. H. p16INK4a can initiate an autonomous senescence program. *Oncogene* **19,** 1613–1622 (2000).

137. Chen, J., Huang, X., Halicka, D., Brodsky, S., Avram, A., Eskander, J., Bloomgarden, N. A., Darzynkiewicz, Z. & Goligorsky, M. S. Contribution of p16INK4a and p21CIP1 pathways to induction of premature senescence of human endothelial cells: permissive role of p53. *American Journal of Physiology-Heart and Circulatory Physiology* **290,** H1575–H1586 (2006).

138. Stein, G. H. & Dulić, V. Molecular Mechanisms for the Senescent Cell Cycle Arrest. *Journal of Investigative Dermatology Symposium Proceedings* **3,** 14–18 (1998).

139. Narita, M., Nuñez, S., Heard, E., Narita, M., Lin, A. W., Hearn, S. A., Spector, D. L., Hannon, G. J. & Lowe, S. W. Rb-Mediated Heterochromatin Formation and Silencing of E2F Target Genes during Cellular Senescence. *Cell* **113,** 703–716 (2003).

140. Acosta, J. C., O'Loghlen, A., Banito, A., Guijarro, M. V., Augert, A., Raguz, S., Fumagalli, M., Da Costa, M., Brown, C., Popov, N., Takatsu, Y., Melamed, J., d'Adda di Fagagna, F., Bernard, D., Hernando, E. & Gil, J. Chemokine Signaling via the CXCR2 Receptor Reinforces Senescence. *Cell* **133,** 1006–1018 (2008).

141. Acosta, J. C., Banito, A., Wuestefeld, T., Georgilis, A., Janich, P., Morton, J. P., Athineos, D., Kang, T.-W., Lasitschka, F., Andrulis, M., Pascual, G., Morris, K. J., Khan, S., Jin, H., Dharmalingam, G., Snijders, A. P., Carroll, T., Capper, D., Pritchard, C., Inman, G. J., Longerich, T., Sansom, O. J., Benitah, S. A., Zender, L. & Gil, J. A complex secretory program orchestrated by the inflammasome controls paracrine senescence. *Nature Cell Biology* **15,** 978–990 (2013).

142. Zglinicki, T. von, Saretzki, G., Ladhoff, J., Fagagna, F. d'Adda di & Jackson, S. P. Human cell senescence as a DNA damage response. *Mechanisms of Ageing and Development* **126,** 111–117 (2005).

143. Passos, J. F., Nelson, G., Wang, C., Richter, T., Simillion, C., Proctor, C. J., Miwa, S., Olijslagers, S., Hallinan, J., Wipat, A., Saretzki, G., Rudolph, K. L., Kirkwood, T. B. L. & von Zglinicki, T. Feedback between p21 and reactive oxygen production is necessary for cell senescence. *Molecular Systems Biology* **6,** 347 (2010).

144. Dou, Z., Xu, C., Donahue, G., Shimi, T., Pan, J.-A., Zhu, J., Ivanov, A., Capell, B. C., Drake, A. M., Shah, P. P., Catanzaro, J. M., Daniel Ricketts, M., Lamark, T., Adam, S. A., Marmorstein, R., Zong, W.-X., Johansen, T., Goldman, R. D., Adams, P. D. & Berger, S. L. Autophagy mediates degradation of nuclear lamina. *Nature* **527,** 105–109 (2015).

145. Freund, A., Laberge, R.-M., Demaria, M. & Campisi, J. Lamin B1 loss is a senescence-associated biomarker. *MBoC* **23,** 2066–2075 (2012).

146. Shah, P. P., Donahue, G., Otte, G. L., Capell, B. C., Nelson, D. M., Cao, K., Aggarwala, V., Cruickshanks, H. A., Rai, T. S., McBryan, T., Gregory, B. D., Adams, P. D. & Berger, S. L. Lamin B1 depletion in senescent cells triggers large-scale changes in gene expression and the chromatin landscape. *Genes Dev* **27,** 1787–1799 (2013).

147. Dou, Z., Ghosh, K., Vizioli, M. G., Zhu, J., Sen, P., Wangensteen, K. J., Simithy, J., Lan, Y., Lin, Y., Zhou, Z., Capell, B. C., Xu, C., Xu, M., Kieckhaefer, J. E., Jiang, T., Shoshkes-Carmel, M., Tanim, K. M.

A. A., Barber, G. N., Seykora, J. T., Millar, S. E., Kaestner, K. H., Garcia, B. A., Adams, P. D. & Berger, S. L. Cytoplasmic chromatin triggers inflammation in senescence and cancer. *Nature* **550,** 402–406 (2017).

148. Glück, S., Guey, B., Gulen, M. F., Wolter, K., Kang, T.-W., Schmacke, N. A., Bridgeman, A., Rehwinkel, J., Zender, L. & Ablasser, A. Innate immune sensing of cytosolic chromatin fragments through cGAS promotes senescence. *Nature Cell Biology* **19,** 1061–1070 (2017).
149. He, S. & Sharpless, N. E. Senescence in Health and Disease. *Cell* **169,** 1000–1011 (2017).
150. Dimri, G. P., Lee, X., Basile, G., Acosta, M., Scott, G., Roskelley, C., Medrano, E. E., Linskens, M., Rubelj, I. & Pereira-Smith, O. A biomarker that identifies senescent human cells in culture and in aging skin in vivo. *Proceedings of the National Academy of Sciences* **92,** 9363–9367 (1995).
151. Debacq-Chainiaux, F., Erusalimsky, J. D., Campisi, J. & Toussaint, O. Protocols to detect senescence-associated beta-galactosidase (SA-βgal) activity, a biomarker of senescent cells in culture and in vivo. *Nature Protocols* **4,** 1798–1806 (2009).
152. Lanz, M. C., Zatulovskiy, E., Swaffer, M. P., Zhang, L., Ilerten, I., Zhang, S., You, D. S., Marinov, G., McAlpine, P., Elias, J. E. & Skotheim, J. M. Increasing cell size remodels the proteome and promotes senescence. *Molecular Cell* **82,** 3255-3269.e8 (2022).
153. Rodier, F., Muñoz, D. P., Teachenor, R., Chu, V., Le, O., Bhaumik, D., Coppé, J.-P., Campeau, E., Beauséjour, C. M., Kim, S.-H., Davalos, A. R. & Campisi, J. DNA-SCARS: distinct nuclear structures that sustain damage-induced senescence growth arrest and inflammatory cytokine secretion. *Journal of Cell Science* **124,** 68–81 (2011).
154. Rodier, F., Coppé, J.-P., Patil, C. K., Hoeijmakers, W. A. M., Muñoz, D. P., Raza, S. R., Freund, A., Campeau, E., Davalos, A. R. & Campisi, J. Persistent DNA damage signalling triggers senescence-associated inflammatory cytokine secretion. *Nature Cell Biology* **11,** 973–979 (2009).

155. Althubiti, M., Lezina, L., Carrera, S., Jukes-Jones, R., Giblett, S. M., Antonov, A., Barlev, N., Saldanha, G. S., Pritchard, C. A., Cain, K. & Macip, S. Characterization of novel markers of senescence and their prognostic potential in cancer. *Cell Death & Disease* **5,** e1528–e1528 (2014).

156. Evangelou, K., Lougiakis, N., Rizou, S. V., Kotsinas, A., Kletsas, D., Muñoz-Espín, D., Kastrinakis, N. G., Pouli, N., Marakos, P., Townsend, P., Serrano, M., Bartek, J. & Gorgoulis, V. G. Robust, universal biomarker assay to detect senescent cells in biological specimens. *Aging Cell* **16,** 192–197 (2017).

157. Laberge, R.-M., Sun, Y., Orjalo, A. V., Patil, C. K., Freund, A., Zhou, L., Curran, S. C., Davalos, A. R., Wilson-Edell, K. A., Liu, S., Limbad, C., Demaria, M., Li, P., Hubbard, G. B., Ikeno, Y., Javors, M., Desprez, P.-Y., Benz, C. C., Kapahi, P., Nelson, P. S. & Campisi, J. MTOR regulates the pro-tumorigenic senescence-associated secretory phenotype by promoting IL1A translation. *Nature Cell Biology* **17,** 1049–1061 (2015).

158. Chien, Y., Scuoppo, C., Wang, X., Fang, X., Balgley, B., Bolden, J. E., Premsrirut, P., Luo, W., Chicas, A., Lee, C. S., Kogan, S. C. & Lowe, S. W. Control of the senescence-associated secretory phenotype by NF-κB promotes senescence and enhances chemosensitivity. *Genes Dev* **25,** 2125–2136 (2011).

159. Lopes-Paciencia, S., Saint-Germain, E., Rowell, M.-C., Ruiz, A. F., Kalegari, P. & Ferbeyre, G. The senescence-associated secretory phenotype and its regulation. *Cytokine* **117,** 15–22 (2019).

160. Kang, T.-W., Yevsa, T., Woller, N., Hoenicke, L., Wuestefeld, T., Dauch, D., Hohmeyer, A., Gereke, M., Rudalska, R., Potapova, A., Iken, M., Vucur, M., Weiss, S., Heikenwalder, M., Khan, S., Gil, J., Bruder, D., Manns, M., Schirmacher, P., Tacke, F., Ott, M., Luedde, T., Longerich, T., Kubicka, S. & Zender, L. Senescence surveillance of pre-malignant hepatocytes limits liver cancer development. *Nature* **479,** 547–551 (2011).

161. Lujambio, A., Akkari, L., Simon, J., Grace, D., Tschaharganeh, D. F., Bolden, J. E., Zhao, Z., Thapar, V., Joyce, J. A., Krizhanovsky, V. & Lowe, S. W. Non-Cell-Autonomous Tumor Suppression by p53. *Cell* **153,** 449–460 (2013).

162. Sagiv, A., Burton, D. G. A., Moshayev, Z., Vadai, E., Wensveen, F., Ben-Dor, S., Golani, O., Polic, B. & Krizhanovsky, V. NKG2D ligands mediate immunosurveillance of senescent cells. *Aging (Albany NY)* **8,** 328–344 (2016).

163. Sagiv, A., Biran, A., Yon, M., Simon, J., Lowe, S. W. & Krizhanovsky, V. Granule exocytosis mediates immune surveillance of senescent cells. *Oncogene* **32,** 1971–1977 (2013).

164. van Tuyn, J., Jaber-Hijazi, F., MacKenzie, D., Cole, J. J., Mann, E., Pawlikowski, J. S., Rai, T. S., Nelson, D. M., McBryan, T., Ivanov, A., Blyth, K., Wu, H., Milling, S. & Adams, P. D. Oncogene-Expressing Senescent Melanocytes Up-Regulate MHC Class II, a Candidate Melanoma Suppressor Function. *Journal of Investigative Dermatology* **137,** 2197–2207 (2017).

165. Storer, M., Mas, A., Robert-Moreno, A., Pecoraro, M., Ortells, M. C., Di Giacomo, V., Yosef, R., Pilpel, N., Krizhanovsky, V., Sharpe, J. & Keyes, W. M. Senescence Is a Developmental Mechanism that Contributes to Embryonic Growth and Patterning. *Cell* **155,** 1119–1130 (2013).

166. Muñoz-Espín, D., Cañamero, M., Maraver, A., Gómez-López, G., Contreras, J., Murillo-Cuesta, S., Rodríguez-Baeza, A., Varela-Nieto, I., Ruberte, J., Collado, M. & Serrano, M. Programmed Cell Senescence during Mammalian Embryonic Development. *Cell* **155,** 1104–1118 (2013).

167. Davaapil, H., Brockes, J. P. & Yun, M. H. Conserved and novel functions of programmed cellular senescence during vertebrate development. *Development* **144,** 106–114 (2017).

168. Villiard, É., Denis, J.-F., Hashemi, F. S., Igelmann, S., Ferbeyre, G. & Roy, S. Senescence gives insights into the morphogenetic evolution of anamniotes. *Biology Open* **6,** 891–896 (2017).

169. Demaria, M., Ohtani, N., Youssef, S. A., Rodier, F., Toussaint, W., Mitchell, J. R., Laberge, R.-M., Vijg, J., Van Steeg, H., Dollé, M. E. T., Hoeijmakers, J. H. J., de Bruin, A., Hara, E. & Campisi, J. An Essential Role for Senescent Cells in Optimal Wound Healing through Secretion of PDGF-AA. *Developmental Cell* **31,** 722–733 (2014).

170. Jun, J.-I. & Lau, L. F. The matricellular protein CCN1 induces fibroblast senescence and restricts fibrosis in cutaneous wound healing. *Nature Cell Biology* **12,** 676–685 (2010).

171. Krizhanovsky, V., Yon, M., Dickins, R. A., Hearn, S., Simon, J., Miething, C., Yee, H., Zender, L. & Lowe, S. W. Senescence of Activated Stellate Cells Limits Liver Fibrosis. *Cell* **134,** 657–667 (2008).

172. Ritschka, B., Storer, M., Mas, A., Heinzmann, F., Ortells, M. C., Morton, J. P., Sansom, O. J., Zender, L. & Keyes, W. M. The senescence-associated secretory phenotype induces cellular plasticity and tissue regeneration. *Genes Dev* **31,** 172–183 (2017).

173. Price, J. S., Waters, J. G., Darrah, C., Pennington, C., Edwards, D. R., Donell, S. T. & Clark, I. M. The role of chondrocyte senescence in osteoarthritis. *Aging Cell* **1,** 57–65 (2002).

174. Minamino, T. & Komuro, I. Vascular Cell Senescence. *Circulation Research* **100,** 15–26 (2007).

175. Martínez-Cué, C. & Rueda, N. Cellular Senescence in Neurodegenerative Diseases. *Frontiers in Cellular Neuroscience* **14,** (2020).

176. Lee, S. & Schmitt, C. A. The dynamic nature of senescence in cancer. *Nature Cell Biology* **21,** 94–101 (2019).

177. Braig, M., Lee, S., Loddenkemper, C., Rudolph, C., Peters, A. H. F. M., Schlegelberger, B., Stein, H., Dörken, B., Jenuwein, T. & Schmitt, C. A. Oncogene-induced senescence as an initial barrier in lymphoma development. *Nature* **436,** 660–665 (2005).

178. Chen, Z., Trotman, L. C., Shaffer, D., Lin, H.-K., Dotan, Z. A., Niki, M., Koutcher, J. A., Scher, H. I., Ludwig, T., Gerald, W., Cordon-Cardo, C. & Paolo Pandolfi, P. Crucial role of p53-dependent cellular senescence in suppression of Pten-deficient tumorigenesis. *Nature* **436,** 725–730 (2005).

179. Bartkova, J., Rezaei, N., Liontos, M., Karakaidos, P., Kletsas, D., Issaeva, N., Vassiliou, L.-V. F., Kolettas, E., Niforou, K., Zoumpourlis, V. C., Takaoka, M., Nakagawa, H., Tort, F., Fugger, K., Johansson, F., Sehested, M., Andersen, C. L., Dyrskjot, L., Ørntoft, T., Lukas, J., Kittas, C., Helleday,

T., Halazonetis, T. D., Bartek, J. & Gorgoulis, V. G. Oncogene-induced senescence is part of the tumorigenesis barrier imposed by DNA damage checkpoints. *Nature* **444,** 633–637 (2006).

180. Eggert, T., Wolter, K., Ji, J., Ma, C., Yevsa, T., Klotz, S., Medina-Echeverz, J., Longerich, T., Forgues, M., Reisinger, F., Heikenwalder, M., Wang, X. W., Zender, L. & Greten, T. F. Distinct Functions of Senescence-Associated Immune Responses in Liver Tumor Surveillance and Tumor Progression. *Cancer Cell* **30,** 533–547 (2016).
181. Demaria, M., O'Leary, M. N., Chang, J., Shao, L., Liu, S., Alimirah, F., Koenig, K., Le, C., Mitin, N., Deal, A. M., Alston, S., Academia, E. C., Kilmarx, S., Valdovinos, A., Wang, B., de Bruin, A., Kennedy, B. K., Melov, S., Zhou, D., Sharpless, N. E., Muss, H. & Campisi, J. Cellular Senescence Promotes Adverse Effects of Chemotherapy and Cancer Relapse. *Cancer Discovery* **7,** 165–176 (2017).
182. Kim, Y. H., Choi, Y. W., Lee, J., Soh, E. Y., Kim, J.-H. & Park, T. J. Senescent tumor cells lead the collective invasion in thyroid cancer. *Nature Communications* **8,** 15208 (2017).
183. Alimirah, F., Pulido, T., Valdovinos, A., Alptekin, S., Chang, E., Jones, E., Diaz, D. A., Flores, J., Velarde, M. C., Demaria, M., Davalos, A. R., Wiley, C. D., Limbad, C., Desprez, P.-Y. & Campisi, J. Cellular Senescence Promotes Skin Carcinogenesis through p38MAPK and p44/42MAPK Signaling. *Cancer Research* **80,** 3606–3619 (2020).
184. Yang, L., Fang, J. & Chen, J. Tumor cell senescence response produces aggressive variants. *Cell Death Discovery* **3,** 17049 (2017).
185. Soto-Gamez, A. & Demaria, M. Therapeutic interventions for aging: the case of cellular senescence. *Drug Discovery Today* **22,** 786–795 (2017).
186. Wang, L., Lankhorst, L. & Bernards, R. Exploiting senescence for the treatment of cancer. *Nature Reviews Cancer* **22,** 340–355 (2022).
187. Williams, G. C. Pleiotropy, Natural Selection, and the Evolution of Senescence. *Science of Aging Knowledge Environment* **2001,** cp13–cp13 (2001).

188. Rodier, F. & Campisi, J. Four faces of cellular senescence. *Journal of Cell Biology* **192,** 547–556 (2011).

189. McInnes, C. J., Damon, I. K., Smith, G. L., McFadden, G., Isaacs, S. N., Roper, R. L., Evans, D. H., Damaso, C. R., Carulei, O., Wise, L. M. & Lefkowitz, E. J. ICTV Virus Taxonomy Profile: Poxviridae 2023. *Journal of General Virology* **104,** (2023).

190. Geddes, A. M. The history of smallpox. *Clinics in Dermatology* **24,** 152–157 (2006).

191. Verardi Paulo H., Aziz Fatema H., Ahmad Shabbir, Jones Leslie A., Beyene Berhanu, Ngotho Rosemary N., Wamwayi Henry M., Yesus Mebratu G., Egziabher Berhe G., & Yilma Tilahun D. Long-Term Sterilizing Immunity to Rinderpest in Cattle Vaccinated with a Recombinant Vaccinia Virus Expressing High Levels of the Fusion and Hemagglutinin Glycoproteins. *Journal of Virology* **76,** 484–491 (2002).

192. Brochier, B., Kieny, M. P., Costy, F., Coppens, P., Bauduin, B., Lecocq, J. P., Languet, B., Chappuis, G., Desmettre, P., Afiademanyo, K., Libois, R. & Pastoret, P.-P. Large-scale eradication of rabies using recombinant vaccinia-rabies vaccine. *Nature* **354,** 520–522 (1991).

193. Rosatte, R., Allan, M., Bachmann, P., Sobey, K., Donovan, D., Davies, J. C., Silver, A., Bennett, K., Brown, L., Stevenson, B., Buchanan, T., Bruce, L., Wandeler, A., Fehlner-Gardiner, C., Beresford, A., Beath, A., Escobar, M., Maki, J. & Schumacher, C. PREVALENCE OF TETRACYCLINE AND RABIES VIRUS ANTIBODY IN RACCOONS, SKUNKS, AND FOXES FOLLOWING AERIAL DISTRIBUTION OF V-RG BAITS TO CONTROL RACCOON RABIES IN ONTARIO, CANADA. *Journal of Wildlife Diseases* **44,** 946–964 (2008).

194. Guo, Z. S. & Bartlett, D. L. Vaccinia as a vector for gene delivery. *Expert Opinion on Biological Therapy* **4,** 901–917 (2004).

195. Guo, Z. S., Lu, B., Guo, Z., Giehl, E., Feist, M., Dai, E., Liu, W., Storkus, W. J., He, Y., Liu, Z. & Bartlett, D. L. Vaccinia virus-mediated cancer immunotherapy: cancer vaccines and oncolytics. *J Immunother Cancer* **7,** 6 (2019).

196. Sánchez-Sampedro, L., Perdiguero, B., Mejías-Pérez, E., García-Arriaza, J., Di Pilato, M. & Esteban, M. The Evolution of Poxvirus Vaccines. *Viruses* **7,** 1726–1803 (2015).

197. Brinkmann, A., Souza, A. R. V., Esparza, J., Nitsche, A. & Damaso, C. R. Re-assembly of nineteenth-century smallpox vaccine genomes reveals the contemporaneous use of horsepox and horsepox-related viruses in the USA. *Genome Biology* **21,** 286 (2020).

198. Damaso, C. R. Revisiting Jenner's mysteries, the role of the Beaugency lymph in the evolutionary path of ancient smallpox vaccines. *The Lancet Infectious Diseases* **18,** e55–e63 (2018).

199. Jacobs, B. L., Langland, J. O., Kibler, K. V., Denzler, K. L., White, S. D., Holechek, S. A., Wong, S., Huynh, T. & Baskin, C. R. Vaccinia virus vaccines: Past, present and future. *Antiviral Research* **84,** 1–13 (2009).

200. Parker, R. F., Bronson, L. H. & Green, R. H. FURTHER STUDIES OF THE INFECTIOUS UNIT OF VACCINIA. *Journal of Experimental Medicine* **74,** 263–281 (1941).

201. Burrell, C. J., Howard, C. R. & Murphy, F. A. in *Fenner and White's Medical Virology (Fifth Edition)* (eds. Burrell, C. J., Howard, C. R. & Murphy, F. A.) 229–236 (Academic Press, 2017). doi:10.1016/B978-0-12-375156-0.00016-3

202. Cyrklaff, M., Risco, C., Fernández, J. J., Jiménez, M. V., Estéban, M., Baumeister, W. & Carrascosa, J. L. Cryo-electron tomography of vaccinia virus. *Proceedings of the National Academy of Sciences* **102,** 2772–2777 (2005).

203. Cyrklaff, M., Linaroudis, A., Boicu, M., Chlanda, P., Baumeister, W., Griffiths, G. & Krijnse-Locker, J. Whole Cell Cryo-Electron Tomography Reveals Distinct Disassembly Intermediates of Vaccinia Virus. *PLOS ONE* **2,** e420 (2007).

204. Prazsák, I., Tombácz, D., Szűcs, A., Dénes, B., Snyder, M. & Boldogkői, Z. Full Genome Sequence of the Western Reserve Strain of Vaccinia Virus Determined by Third-Generation Sequencing. *Genome Announc* **6,** (2018).

205. Goebel, S. J., Johnson, G. P., Perkus, M. E., Davis, S. W., Winslow, J. P. & Paoletti, E. The complete DNA sequence of vaccinia virus. *Virology* **179,** 247–66, 517–563 (1990).

206. Johnson, G. P., Goebel, S. J. & Paoletti, E. An Update on the Vaccinia Virus Genome. *Virology* **196,** 381–401 (1993).

207. Resch, W., Hixson, K. K., Moore, R. J., Lipton, M. S. & Moss, B. Protein composition of the vaccinia virus mature virion. *Virology* **358,** 233–247 (2007).

208. Baroudy, B. M., Venkatesan, S. & Moss, B. Incompletely base-paired flip-flop terminal loops link the two DNA strands of the vaccinia virus genome into one uninterrupted polynucleotide chain. *Cell* **28,** 315–324 (1982).

209. Venkatesan Sundararajan, Gershowitz Alan, & Moss Bernard. Complete Nucleotide Sequences of Two Adjacent Early Vaccinia Virus Genes Located Within the Inverted Terminal Repetition. *Journal of Virology* **44,** 637–646 (1982).

210. Shenouda, M. M., Noyce, R. S., Lee, S. Z., Wang, J. L., Lin, Y.-C., Favis, N. A., Desaulniers, M. A. & Evans, D. H. The mismatched nucleotides encoded in vaccinia virus flip-and-flop hairpin telomeres serve an essential role in virion maturation. *PLOS Pathogens* **18,** e1010392 (2022).

211. Wittek, R. Organization and expression of the poxvirus genome. *Experientia* **38,** 285–297 (1982).

212. Qin Li, Favis Nicole, Famulski Jakub, & Evans David H. Evolution of and Evolutionary Relationships between Extant Vaccinia Virus Strains. *Journal of Virology* **89,** 1809–1824 (2015).

213. Mackett, M. & Archard, L. C. Conservation and Variation in Orthopoxvirus Genome Structure. *Journal of General Virology* **45,** 683–701 (1979).

214. Gubser, C., Hué, S., Kellam, P. & Smith, G. L. Poxvirus genomes: a phylogenetic analysis. *Journal of General Virology* **85,** 105–117 (2004).

215. Smith, G. L., Vanderplasschen, A. & Law, M. The formation and function of extracellular enveloped vaccinia virus. *Journal of General Virology* **83,** 2915–2931 (2002).

216. Hollinshead, M., Vanderplasschen, A., Smith, G. L. & Vaux, D. J. Vaccinia virus intracellular mature virions contain only one lipid membrane. *J Virol* **73,** 1503–1517 (1999).

217. Roberts, K. L. & Smith, G. L. Vaccinia virus morphogenesis and dissemination. *Trends in Microbiology* **16,** 472–479 (2008).

218. Vanderplasschen, A., Mathew, E., Hollinshead, M., Sim, R. B. & Smith, G. L. Extracellular enveloped vaccinia virus is resistant to complement because of incorporation of host complement control proteins into its envelope. *Proceedings of the National Academy of Sciences* **95,** 7544–7549 (1998).

219. Payne L. Polypeptide composition of extracellular enveloped vaccinia virus. *Journal of Virology* **27,** 28–37 (1978).

220. Roper R L, Payne L G, & Moss B. Extracellular vaccinia virus envelope glycoprotein encoded by the A33R gene. *Journal of Virology* **70,** 3753–3762 (1996).

221. Pütz, M. M., Midgley, C. M., Law, M. & Smith, G. L. Quantification of antibody responses against multiple antigens of the two infectious forms of Vaccinia virus provides a benchmark for smallpox vaccination. *Nature Medicine* **12,** 1310–1315 (2006).

222. Vanderplasschen, A., Hollinshead, M. & Smith, G. L. Intracellular and extracellular vaccinia virions enter cells by different mechanisms. *Journal of General Virology* **79,** 877–887 (1998).

223. Vanderplasschen A & Smith G L. A novel virus binding assay using confocal microscopy: demonstration that the intracellular and extracellular vaccinia virions bind to different cellular receptors. *Journal of Virology* **71,** 4032–4041 (1997).

224. Locker, J. K., Kuehn, A., Schleich, S., Rutter, G., Hohenberg, H., Wepf, R. & Griffiths, G. Entry of the Two Infectious Forms of Vaccinia Virus at the Plasma Membane Is Signaling-Dependent for the IMV but Not the EEV. *MBoC* **11,** 2497–2511 (2000).

225. van Eijl, H., Hollinshead, M., Rodger, G., Zhang, W.-H. & Smith, G. L. The vaccinia virus F12L protein is associated with intracellular enveloped virus particles and is required for their egress to the cell surface. *Journal of General Virology* **83,** 195–207 (2002).

226. Blasco R & Moss B. Role of cell-associated enveloped vaccinia virus in cell-to-cell spread. *Journal of Virology* **66,** 4170–4179 (1992).

227. Cudmore, S., Cossart, P., Griffiths, G. & Way, M. Actin-based motility of vaccinia virus. *Nature* **378,** 636–638 (1995).

228. Frischknecht, F., Moreau, V., Röttger, S., Gonfloni, S., Reckmann, I., Superti-Furga, G. & Way, M. Actin-based motility of vaccinia virus mimics receptor tyrosine kinase signalling. *Nature* **401,** 926–929 (1999).

229. Payne, L. G. Significance of extracellular enveloped virus in the in vitro and in vivo dissemination of vaccinia. *J Gen Virol* **50,** 89–100 (1980).

230. Law, M. & Smith, G. L. Antibody Neutralization of the Extracellular Enveloped Form of Vaccinia Virus. *Virology* **280,** 132–142 (2001).

231. DeHaven Brian C., Girgis Natasha M., Xiao Yuhong, Hudson Paul N., Olson Victoria A., Damon Inger K., & Isaacs Stuart N. Poxvirus Complement Control Proteins Are Expressed on the Cell Surface through an Intermolecular Disulfide Bridge with the Viral A56 Protein. *Journal of Virology* **84,** 11245–11254 (2010).

232. Doceul, V., Hollinshead, M., van der Linden, L. & Smith, G. L. Repulsion of Superinfecting Virions: A Mechanism for Rapid Virus Spread. *Science* **327,** 873–876 (2010).

233. Smith, G. L., Benfield, C. T. O., Maluquer de Motes, C., Mazzon, M., Ember, S. W. J., Ferguson, B. J. & Sumner, R. P. Vaccinia virus immune evasion: mechanisms, virulence and immunogenicity. *Journal of General Virology* **94,** 2367–2392 (2013).

234. Potts, K. G., Irwin, C. R., Favis, N. A., Pink, D. B., Vincent, K. M., Lewis, J. D., Moore, R. B., Hitt, M. M. & Evans, D. H. Deletion of F4L (ribonucleotide reductase) in vaccinia virus produces a selective oncolytic virus and promotes anti-tumor immunity with superior safety in bladder cancer models. *EMBO Mol Med* **9,** 638 (2017).

235. McKenzie, R., Kotwal, G. J., Moss, B., Hammer, C. H. & Frank, M. M. Regulation of Complement Activity by Vaccinia Virus Complement-Control Protein. *The Journal of Infectious Diseases* **166,** 1245–1250 (1992).

236. DiPerna, G., Stack, J., Bowie, A. G., Boyd, A., Kotwal, G., Zhang, Z., Arvikar, S., Latz, E., Fitzgerald, K. A. & Marshall, W. L. Poxvirus Protein N1L Targets the I-κB Kinase Complex, Inhibits Signaling to NF-κB by the Tumor Necrosis Factor Superfamily of Receptors, and Inhibits NF-κB and IRF3 Signaling by Toll-like Receptors *. *Journal of Biological Chemistry* **279,** 36570–36578 (2004).

237. Shisler Joanna L. & Jin Xiao-Lu. The Vaccinia Virus K1L Gene Product Inhibits Host NF-κB Activation by Preventing IκBα Degradation. *Journal of Virology* **78,** 3553–3560 (2004).

238. Pallett Mitchell A., Ren Hongwei, Zhang Rui-Yao, Scutts Simon R., Gonzalez Laura, Zhu Zihan, Maluquer de Motes Carlos, & Smith Geoffrey L. Vaccinia Virus BBK E3 Ligase Adaptor A55 Targets Importin-Dependent NF-κB Activation and Inhibits CD8+ T-Cell Memory. *Journal of Virology* **93,** 10.1128/jvi.00051-19 (2019).

239. Liu Ruikang & Moss Bernard. Vaccinia Virus C9 Ankyrin Repeat/F-Box Protein Is a Newly Identified Antagonist of the Type I Interferon-Induced Antiviral State. *Journal of Virology* **92,** 10.1128/jvi.00053-18 (2018).

240. Liu, R., Olano, L. R., Mirzakhanyan, Y., Gershon, P. D. & Moss, B. Vaccinia Virus Ankyrin-Repeat/F-Box Protein Targets Interferon-Induced IFITs for Proteasomal Degradation. *Cell Reports* **29,** 816-828.e6 (2019).

241. Mann, B. A., Huang, J. H., Li, P., Chang, H.-C., Slee, R. B., O'Sullivan, A., Anita, M., Yeh, N., Klemsz, M. J., Brutkiewicz, R. R., Blum, J. S. & Kaplan, M. H. Vaccinia Virus Blocks Stat1-Dependent and Stat1-Independent Gene Expression Induced by Type I and Type II Interferons. *Journal of Interferon & Cytokine Research* **28,** 367–380 (2008).

242. Unterholzner, L., Sumner, R. P., Baran, M., Ren, H., Mansur, D. S., Bourke, N. M., Randow, F., Smith, G. L. & Bowie, A. G. Vaccinia Virus Protein C6 Is a Virulence Factor that Binds TBK-1 Adaptor Proteins and Inhibits Activation of IRF3 and IRF7. *PLOS Pathogens* **7,** e1002247 (2011).

243. Meade, N., Furey, C., Li, H., Verma, R., Chai, Q., Rollins, M. G., DiGiuseppe, S., Naghavi, M. H. & Walsh, D. Poxviruses Evade Cytosolic Sensing through Disruption of an mTORC1-mTORC2 Regulatory Circuit. *Cell* **174,** 1143-1157.e17 (2018).

244. Eaglesham, J. B., Pan, Y., Kupper, T. S. & Kranzusch, P. J. Viral and metazoan poxins are cGAMP-specific nucleases that restrict cGAS–STING signalling. *Nature* **566,** 259–263 (2019).

245. Alcamí, A., Khanna, A., Paul, N. L. & Smith, G. L. Vaccinia virus strains Lister, USSR and Evans express soluble and cell-surface tumour necrosis factor receptors. *Journal of General Virology* **80,** 949–959 (1999).

246. Bahar, M. W., Kenyon, J. C., Putz, M. M., Abrescia, N. G. A., Pease, J. E., Wise, E. L., Stuart, D. I., Smith, G. L. & Grimes, J. M. Structure and Function of A41, a Vaccinia Virus Chemokine Binding Protein. *PLOS Pathogens* **4,** e5 (2008).

247. Alcamí A & Smith G L. Vaccinia, cowpox, and camelpox viruses encode soluble gamma interferon receptors with novel broad species specificity. *Journal of Virology* **69,** 4633–4639 (1995).

248. Symons, J. A., Alcamí, A. & Smith, G. L. Vaccinia virus encodes a soluble type I interferon receptor of novel structure and broad species soecificity. *Cell* **81,** 551–560 (1995).

249. Ren, H., Ferguson, B. J., de Motes, C. M., Sumner, R. P., Harman, L. E. R. & Smith, G. L. Enhancement of CD8+ T-cell memory by removal of a vaccinia virus nuclear factor-κB inhibitor. *Immunology* **145,** 34–49 (2015).

250. Benfield, C. T. O., Ren, H., Lucas, S. J., Bahsoun, B. & Smith, G. L. Vaccinia virus protein K7 is a virulence factor that alters the acute immune response to infection. *J Gen Virol* **94,** 1647–1657 (2013).

251. Walzer, T., Galibert, L. & Smedt, T. D. Poxvirus semaphorin A39R inhibits phagocytosis by dendritic cells and neutrophils. *European Journal of Immunology* **35,** 391–398 (2005).

252. Ng, A., Tscharke, D. C., Reading, P. C. & Smith, G. L. The vaccinia virus A41L protein is a soluble 30 kDa glycoprotein that affects virus virulence. *Journal of General Virology* **82,** 2095–2105 (2001).

253. Gray, R. D. M., Albrecht, D., Beerli, C., Huttunen, M., Cohen, G. H., White, I. J., Burden, J. J., Henriques, R. & Mercer, J. Nanoscale polarization of the entry fusion complex of vaccinia virus drives efficient fusion. *Nature Microbiology* **4,** 1636–1644 (2019).

254. Chung Che-Sheng, Hsiao Jye-Chian, Chang Yuan-Shau, & Chang Wen. A27L Protein Mediates Vaccinia Virus Interaction with Cell Surface Heparan Sulfate. *Journal of Virology* **72,** 1577–1585 (1998).

255. Chiu, W.-L., Lin, C.-L., Yang, M.-H., Tzou, D.-L. M. & Chang, W. Vaccinia virus 4c (A26L) protein on intracellular mature virus binds to the extracellular cellular matrix laminin. *Journal of Virology* **81,** 2149–2157 (2007).

256. Hsiao Jye-Chian, Chung Che-Sheng, & Chang Wen. Vaccinia Virus Envelope D8L Protein Binds to Cell Surface Chondroitin Sulfate and Mediates the Adsorption of Intracellular Mature Virions to Cells. *Journal of Virology* **73,** 8750–8761 (1999).

257. Carter, G. C., Law, M., Hollinshead, M. & Smith, G. L. Entry of the vaccinia virus intracellular mature virion and its interactions with glycosaminoglycans. *Journal of General Virology* **86,** 1279–1290 (2005).

258. Townsley, A. C., Weisberg, A. S., Wagenaar, T. R. & Moss, B. Vaccinia virus entry into cells via a low-pH-dependent endosomal pathway. *Journal of Virology* **80,** 8899–8908 (2006).

259. Mercer, J. & Helenius, A. Vaccinia Virus Uses Macropinocytosis and Apoptotic Mimicry to Enter Host Cells. *Science* **320,** 531–535 (2008).

260. Mercer, J., Knébel, S., Schmidt, F. I., Crouse, J., Burkard, C. & Helenius, A. Vaccinia virus strains use distinct forms of macropinocytosis for host-cell entry. *Proceedings of the National Academy of Sciences* **107,** 9346–9351 (2010).

261. Law, M., Carter, G. C., Roberts, K. L., Hollinshead, M. & Smith, G. L. Ligand-induced and nonfusogenic dissolution of a viral membrane. *Proceedings of the National Academy of Sciences* **103,** 5989–5994 (2006).

262. Schmidt, F. I., Bleck, C. K. E., Helenius, A. & Mercer, J. Vaccinia extracellular virions enter cells by macropinocytosis and acid-activated membrane rupture. *The EMBO Journal* **30,** 3647–3661 (2011).

263. Moss, B. Membrane fusion during poxvirus entry. *Seminars in Cell & Developmental Biology* **60,** 89–96 (2016).

264. Laliberte, J. P., Weisberg, A. S. & Moss, B. The Membrane Fusion Step of Vaccinia Virus Entry Is Cooperatively Mediated by Multiple Viral Proteins and Host Cell Components. *PLOS Pathogens* **7,** e1002446 (2011).

265. Schmidt, F. I., Bleck, C. K. E., Reh, L., Novy, K., Wollscheid, B., Helenius, A., Stahlberg, H. & Mercer, J. Vaccinia Virus Entry Is Followed by Core Activation and Proteasome-Mediated Release of the Immunomodulatory Effector VH1 from Lateral Bodies. *Cell Reports* **4,** 464–476 (2013).

266. Bidgood, S. R., Samolej, J., Novy, K., Collopy, A., Albrecht, D., Krause, M., Burden, J. J., Wollscheid, B. & Mercer, J. Poxviruses package viral redox proteins in lateral bodies and modulate the host oxidative response. *PLOS Pathogens* **18,** e1010614 (2022).

267. Broyles, S. S. Vaccinia virus transcription. *Journal of General Virology* **84,** 2293–2303 (2003).

268. Mallardo, M., Schleich, S. & Locker, J. K. Microtubule-dependent Organization of Vaccinia Virus Core–derivd Early mRNAs into Distinct Cytoplasmic Structures. *Molecular Biology of the Cell* **12,** 3875–3891 (2001).

269. Carter, G. C., Rodger, G., Murphy, B. J., Law, M., Krauss, O., Hollinshead, M. & Smith, G. L. Vaccinia virus cores are transported on microtubules. *Journal of General Virology* **84,** 2443–2458 (2003).

270. Tolonen, N., Doglio, L., Schleich, S. & Locker, J. K. Vaccinia Virus DNA Replication Occurs in Endoplasmic Reticulum-enclosed Cytoplasmic Mini-Nuclei. *MBoC* **12,** 2031–2046 (2001).

271. Mallardo Massimo, Leithe Edward, Schleich Sibylle, Roos Norbert, Doglio Laura, & Krijnse Locker Jacomine. Relationship between Vaccinia Virus Intracellular Cores, Early mRNAs, and DNA Replication Sites. *Journal of Virology* **76,** 5167–5183 (2002).

272. Katsafanas, G. C. & Moss, B. Colocalization of Transcription and Translation within Cytoplasmic Poxvirus Factories Coordinates Viral Expression and Subjugates Host Functions. *Cell Host & Microbe* **2,** 221–228 (2007).

273. Greseth, M. D. & Traktman, P. The Life Cycle of the Vaccinia Virus Genome. *Annu. Rev. Virol.* **9,** 239–259 (2022).

274. Greseth Matthew D., Boyle Kathleen A., Bluma Matthew S., Unger Bethany, Wiebe Matthew S., Soares-Martins Jamaria A., Wickramasekera Nadi T., Wahlberg James, & Traktman Paula. Molecular Genetic and Biochemical Characterization of the Vaccinia Virus I3 Protein, the Replicative Single-Stranded DNA Binding Protein. *Journal of Virology* **86,** 6197–6209 (2012).

275. Kieser, Q., Noyce, R. S., Shenouda, M., Lin, Y.-C. J. & Evans, D. H. Cytoplasmic factories, virus assembly, and DNA replication kinetics collectively constrain the formation of poxvirus recombinants. *PLOS ONE* **15,** e0228028 (2020).

276. Assarsson, E., Greenbaum, J. A., Sundström, M., Schaffer, L., Hammond, J. A., Pasquetto, V., Oseroff, C., Hendrickson, R. C., Lefkowitz, E. J., Tscharke, D. C., Sidney, J., Grey, H. M., Head, S. R., Peters, B. & Sette, A. Kinetic analysis of a complete poxvirus transcriptome reveals an immediate-early class of genes. *Proceedings of the National Academy of Sciences* **105,** 2140–2145 (2008).

277. Baldick C J & Moss B. Characterization and temporal regulation of mRNAs encoded by vaccinia virus intermediate-stage genes. *Journal of Virology* **67,** 3515–3527 (1993).

278. Moss, B. Poxvirus DNA Replication. *Cold Spring Harbor Perspectives in Biology* **5,** (2013).

279. Maruri-Avidal Liliana, Weisberg Andrea S., Bisht Himani, & Moss Bernard. Analysis of Viral Membranes Formed in Cells Infected by a Vaccinia Virus L2-Deletion Mutant Suggests Their Origin from the Endoplasmic Reticulum. *Journal of Virology* **87,** 1861–1871 (2013).

280. Maruri-Avidal Liliana, Weisberg Andrea S., & Moss Bernard. Vaccinia Virus L2 Protein Associates with the Endoplasmic Reticulum near the Growing Edge of Crescent Precursors of Immature Virions and Stabilizes a Subset of Viral Membrane Proteins. *Journal of Virology* **85,** 12431–12441 (2011).

281. Cepeda, V. & Esteban, M. Novel insights on the progression of intermediate viral forms in the morphogenesis of vaccinia virus. *Virus Research* **183,** 23–29 (2014).

282. Morgan, C. The Insertion of DNA into Vaccinia Virus. *Science* **193,** 591–592 (1976).

283. Szajner Patricia, Weisberg Andrea S., Wolffe Elizabeth J., & Moss Bernard. Vaccinia Virus A30L Protein Is Required for Association of Viral Membranes with Dense Viroplasm To Form Immature Virions. *Journal of Virology* **75,** 5752–5761 (2001).

284. Szajner, P., Jaffe, H., Weisberg, A. S. & Moss, B. A complex of seven vaccinia virus proteins conserved in all chordopoxviruses is required for the association of membranes and viroplasm to form immature virions. *Virology* **330,** 447–459 (2004).

285. Chichón, F. J., Rodríguez, M. J., Risco, C., Fraile-Ramos, A., Fernández, J. J., Esteban, M. & Carrascosa, J. L. Membrane remodelling during vaccinia virus morphogenesis. *Biology of the Cell* **101,** 401–414 (2009).

286. Joklik, W. K. & Becker, Y. The replication and coating of vaccinia DNA. *Journal of Molecular Biology* **10,** 452–474 (1964).

287. Byrd, C. M. & Hruby, D. E. Vaccinia virus proteolysis—a review. *Reviews in Medical Virology* **16,** 187–202 (2006).

288. Sanderson, C. M., Hollinshead, M. & Smith, G. L. The vaccinia virus A27L protein is needed for the microtubule-dependent transport of intracellular mature virus particles. *Journal of General Virology* **81,** 47–58 (2000).

289. Tooze, J., Hollinshead, M., Reis, B., Radsak, K. & Kern, H. Progeny vaccinia and human cytomegalovirus particles utilize early endosomal cisternae for their envelopes. *Eur J Cell Biol* **60,** 163–178 (1993).

290. Schmelz M, Sodeik B, Ericsson M, Wolffe E J, Shida H, Hiller G, & Griffiths G. Assembly of vaccinia virus: the second wrapping cisterna is derived from the trans Golgi network. *Journal of Virology* **68,** 130–147 (1994).

291. Sivan Gilad, Weisberg Andrea S., Americo Jeffrey L., & Moss Bernard. Retrograde Transport from Early Endosomes to the trans-Golgi Network Enables Membrane Wrapping and Egress of Vaccinia Virus Virions. *Journal of Virology* **90,** 8891–8905 (2016).

292. Herrero-Martínez, E., Roberts, K. L., Hollinshead, M. & Smith, G. L. Vaccinia virus intracellular enveloped virions move to the cell periphery on microtubules in the absence of the A36R protein. *Journal of General Virology* **86,** 2961–2968 (2005).

293. Hollinshead, M., Rodger, G., Van Eijl, H., Law, M., Hollinshead, R., Vaux, D. J. T. & Smith, G. L. Vaccinia virus utilizes microtubules for movement to the cell surface. *Journal of Cell Biology* **154,** 389–402 (2001).

294. Smith, G. L., Murphy, B. J. & Law, M. Vaccinia Virus Motility. *Annu. Rev. Microbiol.* **57,** 323–342 (2003).

295. Laliberte Jason P. & Moss Bernard. A Novel Mode of Poxvirus Superinfection Exclusion That Prevents Fusion of the Lipid Bilayers of Viral and Cellular Membranes. *Journal of Virology* **88,** 9751–9768 (2014).

296. Wagenaar Timothy R. & Moss Bernard. Expression of the A56 and K2 Proteins Is Sufficient To Inhibit Vaccinia Virus Entry and Cell Fusion. *Journal of Virology* **83,** 1546–1554 (2009).

297. Beerli, C., Yakimovich, A., Kilcher, S., Reynoso, G. V., Fläschner, G., Müller, D. J., Hickman, H. D. & Mercer, J. Vaccinia virus hijacks EGFR signalling to enhance virus spread through rapid and directed infected cell motility. *Nature Microbiology* **4,** 216–225 (2019).

298. Turvey, S. E. & Broide, D. H. Innate immunity. *Journal of Allergy and Clinical Immunology* **125,** S24–S32 (2010).

299. Neefjes, J., Jongsma, M. L. M., Paul, P. & Bakke, O. Towards a systems understanding of MHC class I and MHC class II antigen presentation. *Nature Reviews Immunology* **11,** 823–836 (2011).

300. Wagner, S., Mullins, C. S. & Linnebacher, M. Colorectal cancer vaccines: Tumor-associated antigens vs neoantigens. *World J Gastroenterol* **24,** 5418–5432 (2018).

301. Andersen, M. H., Schrama, D., thor Straten, P. & Becker, J. C. Cytotoxic T Cells. *Journal of Investigative Dermatology* **126,** 32–41 (2006).

302. Merad, M., Sathe, P., Helft, J., Miller, J. & Mortha, A. The Dendritic Cell Lineage: Ontogeny and Function of Dendritic Cells and Their Subsets in the Steady State and the Inflamed Setting. *Annu. Rev. Immunol.* **31,** 563–604 (2013).

303. Vatner, R. E. & Janssen, E. M. STING, DCs and the link between innate and adaptive tumor immunity. *Molecular Immunology* **110,** 13–23 (2019).

304. Hildner, K., Edelson, B. T., Purtha, W. E., Diamond, M., Matsushita, H., Kohyama, M., Calderon, B., Schraml, B. U., Unanue, E. R., Diamond, M. S., Schreiber, R. D., Murphy, T. L. & Murphy, K. M. Batf3 Deficiency Reveals a Critical Role for CD8α+ Dendritic Cells in Cytotoxic T Cell Immunity. *Science* **322,** 1097–1100 (2008).

305. McNab, F., Mayer-Barber, K., Sher, A., Wack, A. & O'Garra, A. Type I interferons in infectious disease. *Nature Reviews Immunology* **15,** 87–103 (2015).

306. Zitvogel, L., Galluzzi, L., Kepp, O., Smyth, M. J. & Kroemer, G. Type I interferons in anticancer immunity. *Nature Reviews Immunology* **15,** 405–414 (2015).

307. Medrano, R. F. V., Hunger, A., Mendonça, S. A., Barbuto, J. A. M. & Strauss, B. E. Immunomodulatory and antitumor effects of type I interferons and their application in cancer therapy. *Oncotarget; Vol 8, No 41* (2017). at <https://www.oncotarget.com/article/19531/text/>

308. Platanias, L. C. Mechanisms of type-I- and type-II-interferon-mediated signalling. *Nature Reviews Immunology* **5,** 375–386 (2005).

309. Le Bon, A. & Tough, D. F. Links between innate and adaptive immunity via type I interferon. *Current Opinion in Immunology* **14,** 432–436 (2002).

310. Diamond, M. S., Kinder, M., Matsushita, H., Mashayekhi, M., Dunn, G. P., Archambault, J. M., Lee, H., Arthur, C. D., White, J. M., Kalinke, U., Murphy, K. M. & Schreiber, R. D. Type I interferon is selectively required by dendritic cells for immune rejection of tumors. *Journal of Experimental Medicine* **208,** 1989–2003 (2011).

311. Fuertes, M. B., Kacha, A. K., Kline, J., Woo, S.-R., Kranz, D. M., Murphy, K. M. & Gajewski, T. F. Host type I IFN signals are required for antitumor CD8+ T cell responses through CD8α+ dendritic cells. *Journal of Experimental Medicine* **208,** 2005–2016 (2011).

312. Klarquist, J., Hennies, C. M., Lehn, M. A., Reboulet, R. A., Feau, S. & Janssen, E. M. STING-Mediated DNA Sensing Promotes Antitumor and Autoimmune Responses to Dying Cells. *The Journal of Immunology* **193,** 6124–6134 (2014).

313. Razavi, S.-M., Lee, K. E., Jin, B. E., Aujla, P. S., Gholamin, S. & Li, G. Immune Evasion Strategies of Glioblastoma. *Frontiers in Surgery* **3,** (2016).

314. Nduom, E. K., Weller, M. & Heimberger, A. B. Immunosuppressive mechanisms in glioblastoma. *Neuro-Oncology* **17,** vii9–vii14 (2015).

315. Hambardzumyan, D., Gutmann, D. H. & Kettenmann, H. The role of microglia and macrophages in glioma maintenance and progression. *Nature Neuroscience* **19,** 20–27 (2016).

316. De Boeck, A., Ahn, B. Y., D'Mello, C., Lun, X., Menon, S. V., Alshehri, M. M., Szulzewsky, F., Shen, Y., Khan, L., Dang, N. H., Reichardt, E., Goring, K.-A., King, J., Grisdale, C. J., Grinshtein, N., Hambardzumyan, D., Reilly, K. M., Blough, M. D., Cairncross, J. G., Yong, V. W., Marra, M. A., Jones, S. J. M., Kaplan, D. R., McCoy, K. D., Holland, E. C., Bose, P., Chan, J. A., Robbins, S. M. & Senger, D. L. Glioma-derived IL-33 orchestrates an inflammatory brain tumor microenvironment that accelerates glioma progression. *Nature Communications* **11,** 4997 (2020).

317. Andaloussi, A. E. & Lesniak, M. S. An increase in CD4+ CD25+ FOXP3+ regulatory T cells in tumor-infiltrating lymphocytes of human glioblastoma multiforme. *Neuro-oncology* **8,** 234–243 (2006).

318. Dubinski, D., Wölfer, J., Hasselblatt, M., Schneider-Hohendorf, T., Bogdahn, U., Stummer, W., Wiendl, H. & Grauer, O. M. CD4+ T effector memory cell dysfunction is associated with the accumulation of granulocytic myeloid-derived suppressor cells in glioblastoma patients. *Neuro-Oncology* **18,** 807–818 (2016).

319. Chang, A. L., Miska, J., Wainwright, D. A., Dey, M., Rivetta, C. V., Yu, D., Kanojia, D., Pituch, K. C., Qiao, J., Pytel, P., Han, Y., Wu, M., Zhang, L., Horbinski, C. M., Ahmed, A. U. & Lesniak, M. S. CCL2 Produced by the Glioma Microenvironment Is Essential for the Recruitment of Regulatory T Cells and Myeloid-Derived Suppressor Cells. *Cancer Research* **76,** 5671–5682 (2016).

320. Lindau, D., Gielen, P., Kroesen, M., Wesseling, P. & Adema, G. J. The immunosuppressive tumour network: myeloid-derived suppressor cells, regulatory T cells and natural killer T cells. *Immunology* **138,** 105–115 (2013).

321. Hao, C., Chen, G., Zhao, H., Li, Y., Chen, J., Zhang, H., Li, S., Zhao, Y., Chen, F., Li, W. & Jiang, W. G. PD-L1 Expression in Glioblastoma, the Clinical and Prognostic Significance: A Systematic Literature Review and Meta-Analysis. *Frontiers in Oncology* **10,** (2020).

322. Ransohoff, R. M. & Engelhardt, B. The anatomical and cellular basis of immune surveillance in the central nervous system. *Nature Reviews Immunology* **12,** 623–635 (2012).

323. Louveau, A., Smirnov, I., Keyes, T. J., Eccles, J. D., Rouhani, S. J., Peske, J. D., Derecki, N. C., Castle, D., Mandell, J. W., Lee, K. S., Harris, T. H. & Kipnis, J. Structural and functional features of central nervous system lymphatic vessels. *Nature* **523,** 337–341 (2015).

324. Liau, L. M., Ashkan, K., Brem, S., Campian, J. L., Trusheim, J. E., Iwamoto, F. M., Tran, D. D., Ansstas, G., Cobbs, C. S., Heth, J. A., Salacz, M. E., D'Andre, S., Aiken, R. D., Moshel, Y. A., Nam, J. Y., Pillainayagam, C. P., Wagner, S. A., Walter, K. A., Chaudhary, R., Goldlust, S. A., Lee, I. Y., Bota, D. A., Elinzano, H., Grewal, J., Lillehei, K., Mikkelsen, T., Walbert, T., Abram, S., Brenner, A. J., Ewend, M. G., Khagi, S., Lovick, D. S., Portnow, J., Kim, L., Loudon, W. G., Martinez, N. L., Thompson, R. C., Avigan, D. E., Fink, K. L., Geoffroy, F. J., Giglio, P., Gligich, O., Krex, D., Lindhorst, S. M., Lutzky, J., Meisel, H.-J., Nadji-Ohl, M., Sanchin, L., Sloan, A., Taylor, L. P., Wu, J. K., Dunbar, E. M., Etame, A. B., Kesari, S., Mathieu, D., Piccioni, D. E., Baskin, D. S., Lacroix, M., May, S.-A., New, P. Z., Pluard, T. J., Toms, S. A., Tse, V., Peak, S., Villano, J. L., Battiste, J. D., Mulholland, P. J., Pearlman, M. L.,

Petrecca, K., Schulder, M., Prins, R. M., Boynton, A. L. & Bosch, M. L. Association of Autologous Tumor Lysate-Loaded Dendritic Cell Vaccination With Extension of Survival Among Patients With Newly Diagnosed and Recurrent Glioblastoma: A Phase 3 Prospective Externally Controlled Cohort Trial. *JAMA Oncology* **9,** 112–121 (2023).

325. Arrieta, V. A., Dmello, C., McGrail, D. J., Brat, D. J., Lee-Chang, C., Heimberger, A. B., Chand, D., Stupp, R. & Sonabend, A. M. Immune checkpoint blockade in glioblastoma: from tumor heterogeneity to personalized treatment. *J Clin Invest* **133,** (2023).
326. Luksik, A. S., Yazigi, E., Shah, P. & Jackson, C. M. CAR T Cell Therapy in Glioblastoma: Overcoming Challenges Related to Antigen Expression. *Cancers (Basel)* **15,** (2023).
327. Shoaf, M. L. & Peters, K. B. Clinical Trials of Oncolytic Viruses in Glioblastoma. *Advances in Oncology* **2,** 139–158 (2022).
328. Bausart, M., Préat, V. & Malfanti, A. Immunotherapy for glioblastoma: the promise of combination strategies. *Journal of Experimental & Clinical Cancer Research* **41,** 35 (2022).
329. Cloughesy, T. F., Petrecca, K., Walbert, T., Butowski, N., Salacz, M., Perry, J., Damek, D., Bota, D., Bettegowda, C., Zhu, J.-J., Iwamoto, F., Placantonakis, D., Kim, L., Elder, B., Kaptain, G., Cachia, D., Moshel, Y., Brem, S., Piccioni, D., Landolfi, J., Chen, C. C., Gruber, H., Rao, A. R., Hogan, D., Accomando, W., Ostertag, D., Montellano, T. T., Kheoh, T., Kabbinavar, F. & Vogelbaum, M. A. Effect of Vocimagene Amiretrorepvec in Combination With Flucytosine vs Standard of Care on Survival Following Tumor Resection in Patients With Recurrent High-Grade Glioma: A Randomized Clinical Trial. *JAMA Oncology* **6,** 1939–1946 (2020).
330. Desjardins, A., Gromeier, M., Herndon, J. E., Beaubier, N., Bolognesi, D. P., Friedman, A. H., Friedman, H. S., McSherry, F., Muscat, A. M., Nair, S., Peters, K. B., Randazzo, D., Sampson, J. H., Vlahovic, G., Harrison, W. T., McLendon, R. E., Ashley, D. & Bigner, D. D. Recurrent Glioblastoma Treated with Recombinant Poliovirus. *N Engl J Med* **379,** 150–161 (2018).

331. Frampton, J. E. Teserpaturev/G47Δ: First Approval. *BioDrugs* **36,** 667–672 (2022).

332. Dock, G. THE INFLUENCE OF COMPLICATING DISEASES UPON LEUKAEMIA.: CASES OF TUBERCULOSIS AND LEUKOEMIA. MISCELLANEOUS INFECTIONS. CHANGES IN THE RED BLOOD CORPUSCLES. QUALITATIVE CHANGES IN THE BLOOD, ESPECIALLY IN THE LEUKOCYTES. WHEN DOES THE CHANGE OCCUR? THE EFFECTS OF VARIOUS PROCESSES OTHER THAN INFECTION ON LEUKOEMIA. BIBLIOGRAPHY. *The American Journal of the Medical Sciences (1827-1924)* **127,** 563 (1904).

333. Bierman, H. R., Crile, D. M., Dod, K. S., Kelly, K. H., Petrakis, N. I., White, L. P. & Shimkin, M. B. Remissions in leukemia of childhood following acute infectious disease. Staphylococcus and streptococcus, varicella, and feline panleukopenias. *Cancer* **6,** 591–605 (1953).

334. Pasquinucci, G. POSSIBLE EFFECT OF MEASLES ON LEUKÆMIA. *The Lancet* **297,** 136 (1971).

335. Mota, H. C. Infantile Hodgkin's disease: remission after measles. *Br Med J* **2,** 421 (1973).

336. Taqi, A. M., Abdurrahman, M. B., Yakubu, A. M. & Fleming, A. F. REGRESSION OF HODGKIN'S DISEASE AFTER MEASLES. *The Lancet* **317,** 1112 (1981).

337. Hoster, H. A., Zanes, R. P., Jr. & von Haam, E. Studies in Hodgkin's Syndrome: IX. The Association of "Viral" Hepatitis and Hodgkin's Disease (A Preliminary Report). *Cancer Research* **9,** 473–480 (1949).

338. Kelly, E. & Russell, S. J. History of Oncolytic Viruses: Genesis to Genetic Engineering. *Molecular Therapy* **15,** 651–659 (2007).

339. Martuza, R. L., Malick, A., Markert, J. M., Ruffner, K. L. & Coen, D. M. Experimental Therapy of Human Glioma by Means of a Genetically Engineered Virus Mutant. *Science* **252,** 854–856 (1991).

340. Ma, R., Li, Z., Chiocca, E. A., Caligiuri, M. A. & Yu, J. The emerging field of oncolytic virus-based cancer immunotherapy. *Trends in Cancer* **9,** 122–139 (2023).

341. Lichty, B. D., Breitbach, C. J., Stojdl, D. F. & Bell, J. C. Going viral with cancer immunotherapy. *Nature Reviews Cancer* **14,** 559 (2014).

342. Russell, S. J., Peng, K.-W. & Bell, J. C. Oncolytic virotherapy. *Nature Biotechnology* **30,** 658 (2012).

343. Guo, Z. S., Liu, Z. & Bartlett, D. L. Oncolytic Immunotherapy: Dying the Right Way is a Key to Eliciting Potent Antitumor Immunity. *Frontiers in Oncology* **4,** (2014).

344. Heinrich, B., Klein, J., Delic, M., Goepfert, K., Engel, V., Geberzahn, L., Lusky, M., Erbs, P., Preville, X. & Moehler, M. Immunogenicity of oncolytic vaccinia viruses JX-GFP and TG6002 in a human melanoma in vitro model: studying immunogenic cell death, dendritic cell maturation and interaction with cytotoxic T lymphocytes. *Onco Targets Ther* **10,** 2389–2401 (2017).

345. Galluzzi, L., Buqué, A., Kepp, O., Zitvogel, L. & Kroemer, G. Immunogenic cell death in cancer and infectious disease. *Nature Reviews Immunology* **17,** 97–111 (2017).

346. Galluzzi, L., Vitale, I., Warren, S., Adjemian, S., Agostinis, P., Martinez, A. B., Chan, T. A., Coukos, G., Demaria, S., Deutsch, E., Draganov, D., Edelson, R. L., Formenti, S. C., Fucikova, J., Gabriele, L., Gaipl, U. S., Gameiro, S. R., Garg, A. D., Golden, E., Han, J., Harrington, K. J., Hemminki, A., Hodge, J. W., Hossain, D. M. S., Illidge, T., Karin, M., Kaufman, H. L., Kepp, O., Kroemer, G., Lasarte, J. J., Loi, S., Lotze, M. T., Manic, G., Merghoub, T., Melcher, A. A., Mossman, K. L., Prosper, F., Rekdal, Ø., Rescigno, M., Riganti, C., Sistigu, A., Smyth, M. J., Spisek, R., Stagg, J., Strauss, B. E., Tang, D., Tatsuno, K., van Gool, S. W., Vandenabeele, P., Yamazaki, T., Zamarin, D., Zitvogel, L., Cesano, A. & Marincola, F. M. Consensus guidelines for the definition, detection and interpretation of immunogenic cell death. *J Immunother Cancer* **8,** (2020).

347. de Vries, C. R., Kaufman, H. L. & Lattime, E. C. Oncolytic viruses: focusing on the tumor microenvironment. *Cancer Gene Therapy* **22,** 169 (2015).

348. Saha, D., Martuza, R. L. & Rabkin, S. D. Macrophage Polarization Contributes to Glioblastoma Eradication by Combination Immunovirotherapy and Immune Checkpoint Blockade. *Cancer Cell* **32,** 253-267.e5 (2017).

349. Hou, W., Sampath, P., Rojas, J. J. & Thorne, S. H. Oncolytic Virus-Mediated Targeting of PGE2 in the Tumor Alters the Immune Status and Sensitizes Established and Resistant Tumors to Immunotherapy. *Cancer Cell* **30,** 108–119 (2016).

350. Liu, Z., Ravindranathan, R., Kalinski, P., Guo, Z. S. & Bartlett, D. L. Rational combination of oncolytic vaccinia virus and PD-L1 blockade works synergistically to enhance therapeutic efficacy. *Nature Communications* **8,** 14754 (2017).

351. Fend, L., Remy-Ziller, C., Foloppe, J., Kempf, J., Cochin, S., Barraud, L., Accart, N., Erbs, P., Fournel, S. & Préville, X. Oncolytic virotherapy with an armed vaccinia virus in an orthotopic model of renal carcinoma is associated with modification of the tumor microenvironment. *OncoImmunology* **5,** e1080414 (2016).

352. van den Bossche, W. B. L., Kleijn, A., Teunissen, C. E., Voerman, J. S. A., Teodosio, C., Noske, D. P., van Dongen, J. J. M., Dirven, C. M. F. & Lamfers, M. L. M. Oncolytic virotherapy in glioblastoma patients induces a tumor macrophage phenotypic shift leading to an altered glioblastoma microenvironment. *Neuro-Oncology* **20,** 1494–1504 (2018).

353. Angelova, L. A., Barf, M., Geletneky, K., Unterberg, A. & Rommelaere, J. Immunotherapeutic Potential of Oncolytic H-1 Parvovirus: Hints of Glioblastoma Microenvironment Conversion towards Immunogenicity. *Viruses* **9,** (2017).

354. Umer, B. A., Noyce, R. S., Franczak, B. C., Shenouda, M. M., Kelly, R. G., Favis, N. A., Desaulniers, M., Baldwin, T. A., Hitt, M. M. & Evans, D. H. Deciphering the Immunomodulatory Capacity of Oncolytic Vaccinia Virus to Enhance the Immune Response to Breast Cancer. *Cancer Immunology Research* **8,** 618–631 (2020).

355. Breitbach, C. J., Paterson, J. M., Lemay, C. G., Falls, T. J., McGuire, A., Parato, K. A., Stojdl, D. F., Daneshmand, M., Speth, K., Kirn, D., McCart, J. A., Atkins, H. & Bell, J. C. Targeted Inflammation

During Oncolytic Virus Therapy Severely Compromises Tumor Blood Flow. *Molecular Therapy* **15,** 1686–1693 (2007).

356. Breitbach, C. J., Arulanandam, R., De Silva, N., Thorne, S. H., Patt, R., Daneshmand, M., Moon, A., Ilkow, C., Burke, J., Hwang, T.-H., Heo, J., Cho, M., Chen, H., Angarita, F. A., Addison, C., McCart, J. A., Bell, J. C. & Kirn, D. H. Oncolytic Vaccinia Virus Disrupts Tumor-Associated Vasculature in Humans. *Cancer Research* **73,** 1265–1275 (2013).
357. Krishnamurthy Sateesh, Takimoto Toru, Scroggs Ruth Ann, & Portner Allen. Differentially Regulated Interferon Response Determines the Outcome of Newcastle Disease Virus Infection in Normal and Tumor Cell Lines. *Journal of Virology* **80,** 5145–5155 (2006).
358. Coffey, M. C., Strong, J. E., Forsyth, P. A. & Lee, P. W. K. Reovirus Therapy of Tumors with Activated Ras Pathway. *Science* **282,** 1332–1334 (1998).
359. Anderson, B. D., Nakamura, T., Russell, S. J. & Peng, K.-W. High CD46 Receptor Density Determines Preferential Killing of Tumor Cells by Oncolytic Measles Virus. *Cancer Research* **64,** 4919–4926 (2004).
360. Aref, S., Castleton, A. Z., Bailey, K., Burt, R., Dey, A., Leongamornlert, D., Mitchell, R. J., Okasha, D. & Fielding, A. K. Type 1 Interferon Responses Underlie Tumor-Selective Replication of Oncolytic Measles Virus. *Molecular Therapy* **28,** 1043–1055 (2020).
361. Farassati, F., Yang, A.-D. & Lee, P. W. K. Oncogenes in Ras signalling pathway dictate host-cell permissiveness to herpes simplex virus 1. *Nature Cell Biology* **3,** 745–750 (2001).
362. Kawashima, T., Kagawa, S., Kobayashi, N., Shirakiya, Y., Umeoka, T., Teraishi, F., Taki, M., Kyo, S., Tanaka, N. & Fujiwara, T. Telomerase-Specific Replication-Selective Virotherapy for Human Cancer. *Clinical Cancer Research* **10,** 285–292 (2004).

363. Bach, P., Abel, T., Hoffmann, C., Gal, Z., Braun, G., Voelker, I., Ball, C. R., Johnston, I. C. D., Lauer, U. M., Herold-Mende, C., Mühlebach, M. D., Glimm, H. & Buchholz, C. J. Specific Elimination of CD133+ Tumor Cells with Targeted Oncolytic Measles Virus. *Cancer Research* **73,** 865–874 (2013).

364. Wang, Z., Liu, W., Wang, L., Gao, P., Li, Z., Wu, J., Zhang, H., Wu, H., Kong, W., Yu, B. & Yu, X. Enhancing the antitumor activity of an engineered TRAIL-coated oncolytic adenovirus for treating acute myeloid leukemia. *Signal Transduction and Targeted Therapy* **5,** 40 (2020).

365. de Graaf, J. F., de Vor, L., Fouchier, R. A. M. & van den Hoogen, B. G. Armed oncolytic viruses: A kick-start for anti-tumor immunity. *Cytokine & Growth Factor Reviews* **41,** 28–39 (2018).

366. First Oncolytic Viral Therapy for Melanoma. *Cancer Discovery* **6,** 6–6 (2016).

367. Heo, J., Reid, T., Ruo, L., Breitbach, C. J., Rose, S., Bloomston, M., Cho, M., Lim, H. Y., Chung, H. C., Kim, C. W., Burke, J., Lencioni, R., Hickman, T., Moon, A., Lee, Y. S., Kim, M. K., Daneshmand, M., Dubois, K., Longpre, L., Ngo, M., Rooney, C., Bell, J. C., Rhee, B.-G., Patt, R., Hwang, T.-H. & Kirn, D. H. Randomized dose-finding clinical trial of oncolytic immunotherapeutic vaccinia JX-594 in liver cancer. *Nature Medicine* **19,** 329–336 (2013).

368. Moehler, M., Heo, J., Lee, H. C., Tak, W. Y., Chao, Y., Paik, S. W., Yim, H. J., Byun, K. S., Baron, A., Ungerechts, G., Jonker, D., Ruo, L., Cho, M., Kaubisch, A., Wege, H., Merle, P., Ebert, O., Habersetzer, F., Blanc, J. F., Rosmorduc, O., Lencioni, R., Patt, R., Leen, A. M., Foerster, F., Homerin, M., Stojkowitz, N., Lusky, M., Limacher, J. M., Hennequi, M., Gaspar, N., McFadden, B., De Silva, N., Shen, D., Pelusio, A., Kirn, D. H., Breitbach, C. J. & Burke, J. M. Vaccinia-based oncolytic immunotherapy Pexastimogene Devacirepvec in patients with advanced hepatocellular carcinoma after sorafenib failure: a randomized multicenter Phase IIb trial (TRAVERSE). *OncoImmunology* **8,** 1615817 (2019).

369. Guo, Z. S., Lotze, M. T., Zhu, Z., Storkus, W. J. & Song, X.-T. Bi- and Tri-Specific T Cell Engager-Armed Oncolytic Viruses: Next-Generation Cancer Immunotherapy. *Biomedicines* **8,** (2020).

370. Komarova, S., Kawakami, Y., Stoff-Khalili, M. A., Curiel, D. T. & Pereboeva, L. Mesenchymal progenitor cells as cellular vehicles for delivery of oncolytic adenoviruses. *Molecular Cancer Therapeutics* **5,** 755–766 (2006).

371. Su, Y., Su, C. & Qin, L. Current landscape and perspective of oncolytic viruses and their combination therapies. *Translational Oncology* **25,** 101530 (2022).

372. Sivanandam, V., LaRocca, C. J., Chen, N. G., Fong, Y. & Warner, S. G. Oncolytic Viruses and Immune Checkpoint Inhibition: The Best of Both Worlds. *Molecular Therapy - Oncolytics* **13,** 93–106 (2019).

373. Fend, L., Yamazaki, T., Remy, C., Fahrner, C., Gantzer, M., Nourtier, V., Préville, X., Quéméneur, E., Kepp, O., Adam, J., Marabelle, A., Pitt, J. M., Kroemer, G. & Zitvogel, L. Immune Checkpoint Blockade, Immunogenic Chemotherapy or IFN-α Blockade Boost the Local and Abscopal Effects of Oncolytic Virotherapy. *Cancer Research* **77,** 4146–4157 (2017).

374. LaRocca, C. J. & Warner, S. G. Oncolytic viruses and checkpoint inhibitors: combination therapy in clinical trials. *Clinical and Translational Medicine* **7,** 35 (2018).

375. Garber, K. China Approves World's First Oncolytic Virus Therapy For Cancer Treatment. *JNCI: Journal of the National Cancer Institute* **98,** 298–300 (2006).

376. Todo, T., Ito, H., Ino, Y., Ohtsu, H., Ota, Y., Shibahara, J. & Tanaka, M. Intratumoral oncolytic herpes virus G47Δ for residual or recurrent glioblastoma: a phase 2 trial. *Nature Medicine* **28,** 1630–1639 (2022).

377. van Putten, E. H. P., Kleijn, A., van Beusechem, V. W., Noske, D., Lamers, C. H. J., de Goede, A. L., Idema, S., Hoefnagel, D., Kloezeman, J. J., Fueyo, J., Lang, F. F., Teunissen, C. E., Vernhout, R. M., Bakker, C., Gerritsen, W., Curiel, D. T., Vulto, A., Lamfers, M. L. M. & Dirven, C. M. F. Convection Enhanced Delivery of the Oncolytic Adenovirus Delta24-RGD in Patients with Recurrent GBM: A Phase I Clinical Trial Including Correlative Studies. *Clinical Cancer Research* **28,** 1572–1585 (2022).

378. Gállego Pérez-Larraya, J., Garcia-Moure, M., Labiano, S., Patiño-García, A., Dobbs, J., Gonzalez-Huarriz, M., Zalacain, M., Marrodan, L., Martinez-Velez, N., Puigdelloses, M., Laspidea, V., Astigarraga, I., Lopez-Ibor, B., Cruz, O., Oscoz Lizarbe, M., Hervas-Stubbs, S., Alkorta-Aranburu, G., Tamayo, I., Tavira, B., Hernandez-Alcoceba, R., Jones, C., Dharmadhikari, G., Ruiz-Moreno, C., Stunnenberg, H., Hulleman, E., van der Lugt, J., Idoate, M. Á., Diez-Valle, R., Esparragosa Vázquez, I., Villalba, M., de Andrea, C., Núñez-Córdoba, J. M., Ewald, B., Robbins, J., Fueyo, J., Gomez-Manzano, C., Lang, F. F., Tejada, S. & Alonso, M. M. Oncolytic DNX-2401 Virus for Pediatric Diffuse Intrinsic Pontine Glioma. *N Engl J Med* **386,** 2471–2481 (2022).

379. Nguyen, H.-M. & Saha, D. The Current State of Oncolytic Herpes Simplex Virus for Glioblastoma Treatment. *Oncolytic Virother* **10,** 1–27 (2021).

380. Markert, J. M., Liechty, P. G., Wang, W., Gaston, S., Braz, E., Karrasch, M., Nabors, L. B., Markiewicz, M., Lakeman, A. D., Palmer, C. A., Parker, J. N., Whitley, R. J. & Gillespie, G. Y. Phase Ib Trial of Mutant Herpes Simplex Virus G207 Inoculated Pre-and Post-tumor Resection for Recurrent GBM. *Molecular Therapy* **17,** 199–207 (2009).

381. Bernstock, J. D., Bag, A. K., Fiveash, J., Kachurak, K., Elsayed, G., Chagoya, G., Gessler, F., Valdes, P. A., Madan-Swain, A., Whitley, R., Markert, J. M., Gillespie, G. Y., Johnston, J. M. & Friedman, G. K. Design and Rationale for First-in-Human Phase 1 Immunovirotherapy Clinical Trial of Oncolytic HSV G207 to Treat Malignant Pediatric Cerebellar Brain Tumors. *Human Gene Therapy* **31,** 1132–1139 (2020).

382. Waters, A. M., Johnston, J. M., Reddy, A. T., Fiveash, J., Madan-Swain, A., Kachurak, K., Bag, A. K., Gillespie, G. Y., Markert, J. M. & Friedman, G. K. Rationale and Design of a Phase 1 Clinical Trial to Evaluate HSV G207 Alone or with a Single Radiation Dose in Children with Progressive or Recurrent Malignant Supratentorial Brain Tumors. *Human Gene Therapy Clinical Development* **28,** 7–16 (2017).

383. Lauer, U. M., Schell, M., Beil, J., Berchtold, S., Koppenhöfer, U., Glatzle, J., Königsrainer, A., Möhle, R., Nann, D., Fend, F., Pfannenberg, C., Bitzer, M. & Malek, N. P. Phase I Study of Oncolytic Vaccinia Virus GL-ONC1 in Patients with Peritoneal Carcinomatosis. *Clinical Cancer Research* **24,** 4388–4398 (2018).

384. Mell, L. K., Brumund, K. T., Daniels, G. A., Advani, S. J., Zakeri, K., Wright, M. E., Onyeama, S.-J., Weisman, R. A., Sanghvi, P. R., Martin, P. J. & Szalay, A. A. Phase I Trial of Intravenous Oncolytic Vaccinia Virus (GL-ONC1) with Cisplatin and Radiotherapy in Patients with Locoregionally Advanced Head and Neck Carcinoma. *Clin Cancer Res* **23,** 5696–5702 (2017).

385. Zeh, H. J., Downs-Canner, S., McCart, J. A., Guo, Z. S., Rao, U. N. M., Ramalingam, L., Thorne, S. H., Jones, H. L., Kalinski, P., Wieckowski, E., O'Malley, M. E., Daneshmand, M., Hu, K., Bell, J. C., Hwang, T.-H., Moon, A., Breitbach, C. J., Kirn, D. H. & Bartlett, D. L. First-in-man Study of Western Reserve Strain Oncolytic Vaccinia Virus: Safety, Systemic Spread, and Antitumor Activity. *Molecular Therapy* **23,** 202–214 (2015).

386. Xia, Z.-J., Chang, J.-H., Zhang, L., Jiang, W.-Q., Guan, Z.-Z., Liu, J.-W., Zhang, Y., Hu, X.-H., Wu, G.-H., Wang, H.-Q., Chen, Z.-C., Chen, J.-C., Zhou, Q.-H., Lu, J.-W., Fan, Q.-X., Huang, J.-J. & Zheng, X. [Phase III randomized clinical trial of intratumoral injection of E1B gene-deleted adenovirus (H101) combined with cisplatin-based chemotherapy in treating squamous cell cancer of head and neck or esophagus]. *Ai Zheng* **23,** 1666–1670 (2004).

387. Greig, S. L. Talimogene Laherparepvec: First Global Approval. *Drugs* **76,** 147–154 (2016).

388. Foloppe, J., Kempf, J., Futin, N., Kintz, J., Cordier, P., Pichon, C., Findeli, A., Vorburger, F., Quemeneur, E. & Erbs, P. The Enhanced Tumor Specificity of TG6002, an Armed Oncolytic Vaccinia Virus Deleted in Two Genes Involved in Nucleotide Metabolism. *Molecular Therapy - Oncolytics* **14,** 1–14 (2019).

389. Cono, J., 1962-, Casey, C. G. & Bell, D. M. Smallpox vaccination and adverse reactions; guidance for clinicians. (2003). at <https://stacks.cdc.gov/view/cdc/6773>

390. Belongia, E. A. & Naleway, A. L. Smallpox vaccine: the good, the bad, and the ugly. *Clin Med Res* **1,** 87–92 (2003).

391. Wein, L. M., Wu, J. T. & Kirn, D. H. Validation and Analysis of a Mathematical Model of a Replication-competent Oncolytic Virus for Cancer Treatment: Implications for Virus Design and Delivery. *Cancer Research* **63,** 1317–1324 (2003).

392. Kirn, D. H., Wang, Y., Liang, W., Contag, C. H. & Thorne, S. H. Enhancing Poxvirus Oncolytic Effects through Increased Spread and Immune Evasion. *Cancer Research* **68,** 2071–2075 (2008).

393. Berwin, B., Reed, R. C. & Nicchitta, C. V. Virally Induced Lytic Cell Death Elicits the Release of Immunogenic GRP94/gp96 *. *Journal of Biological Chemistry* **276,** 21083–21088 (2001).

394. Guo, Z. S., Naik, A., O'Malley, M. E., Popovic, P., Demarco, R., Hu, Y., Yin, X., Yang, S., Zeh, H. J., Moss, B., Lotze, M. T. & Bartlett, D. L. The Enhanced Tumor Selectivity of an Oncolytic Vaccinia Lacking the Host Range and Antiapoptosis Genes SPI-1 and SPI-2. *Cancer Research* **65,** 9991–9998 (2005).

395. Tappe, K. A., Budida, R., Stankov, M. V., Frenz, T., R. Shah, H., Volz, A., Sutter, G., Kalinke, U. & Behrens, G. M. N. Immunogenic cell death of dendritic cells following modified vaccinia virus Ankara infection enhances CD8+ T cell proliferation. *European Journal of Immunology* **48,** 2042–2054 (2018).

396. Smith, G. L. & Moss, B. Infectious poxvirus vectors have capacity for at least 25 000 base pairs of foreign DNA. *Gene* **25,** 21–28 (1983).

397. Gammon, D. B., Gowrishankar, B., Duraffour, S., Andrei, G., Upton, C. & Evans, D. H. Vaccinia Virus–Encoded Ribonucleotide Reductase Subunits Are Differentially Required for Replication and Pathogenesis. *PLOS Pathogens* **6,** e1000984 (2010).

398. Liu, Z., Ge, Y., Wang, H., Ma, C., Feist, M., Ju, S., Guo, Z. S. & Bartlett, D. L. Modifying the cancer-immune set point using vaccinia virus expressing re-designed interleukin-2. *Nature Communications* **9,** 4682 (2018).

399. Liu, Z., Ravindranathan, R., Li, J., Kalinski, P., Guo, Z. S. & Bartlett, D. L. CXCL11-Armed oncolytic poxvirus elicits potent antitumor immunity and shows enhanced therapeutic efficacy. *OncoImmunology* **5,** e1091554 (2016).

400. Kowalsky, S. J., Liu, Z., Feist, M., Berkey, S. E., Ma, C., Ravindranathan, R., Dai, E., Roy, E. J., Guo, Z. S. & Bartlett, D. L. Superagonist IL-15-Armed Oncolytic Virus Elicits Potent Antitumor Immunity and Therapy That Are Enhanced with PD-1 Blockade. *Molecular Therapy* **26,** 2476–2486 (2018).

401. Gujar, S., Pol, J. G. & Kroemer, G. Heating it up: Oncolytic viruses make tumors 'hot' and suitable for checkpoint blockade immunotherapies. *OncoImmunology* **7,** e1442169 (2018).

402. Irwin, C. R., Hitt, M. M. & Evans, D. H. Targeting Nucleotide Biosynthesis: A Strategy for Improving the Oncolytic Potential of DNA Viruses. *Frontiers in Oncology* **7,** (2017).

403. Bitter, E. E., Townsend, M. H., Erickson, R., Allen, C. & O'Neill, K. L. Thymidine kinase 1 through the ages: a comprehensive review. *Cell & Bioscience* **10,** 138 (2020).

404. Nordlund, P. & Reichard, P. Ribonucleotide Reductases. *Annu. Rev. Biochem.* **75,** 681–706 (2006).

405. Björklund, S., Skog, S., Tribukait, B. & Thelander, L. S-phase-specific expression of mammalian ribonucleotide reductase R1 and R2 subunit mRNAs. *Biochemistry* **29,** 5452–5458 (1990).

406. Engström, Y., Eriksson, S., Jildevik, I., Skog, S., Thelander, L. & Tribukait, B. Cell cycle-dependent expression of mammalian ribonucleotide reductase. Differential regulation of the two subunits. *Journal of Biological Chemistry* **260,** 9114–9116 (1985).

407. Chabes, A. L., Björklund, S. & Thelander, L. S Phase-specific Transcription of the Mouse Ribonucleotide Reductase R2 Gene Requires Both a Proximal Repressive E2F-binding Site and an Upstream Promoter Activating Region *. *Journal of Biological Chemistry* **279,** 10796–10807 (2004).

408. Weir J P & Moss B. Nucleotide sequence of the vaccinia virus thymidine kinase gene and the nature of spontaneous frameshift mutations. *Journal of Virology* **46,** 530–537 (1983).

409. Tengelsen, L. A., Slabaugh, M. B., Bibler, J. K. & Hruby, D. E. Nucleotide sequence and molecular genetic analysis of the large subunit of ribonucleotide reductase encoded by vaccinia virus. *Virology* **164,** 121–131 (1988).

410. Slabaugh M, Roseman N, Davis R, & Mathews C. Vaccinia virus-encoded ribonucleotide reductase: sequence conservation of the gene for the small subunit and its amplification in hydroxyurea-resistant mutants. *Journal of Virology* **62,** 519–527 (1988).

411. Aye, Y., Li, M., Long, M. J. C. & Weiss, R. S. Ribonucleotide reductase and cancer: biological mechanisms and targeted therapies. *Oncogene* **34,** 2011–2021 (2015).

412. Shao, C., Wang, P., Liao, B., Gong, S. & Wu, N. Multi-Omics Integration Analysis of TK1 in Glioma: A Potential Biomarker for Predictive, Preventive, and Personalized Medical Approaches. *Brain Sci* **13,** (2023).

413. Sun, H., Yang, B., Zhang, H., Song, J., Zhang, Y., Xing, J., Yang, Z., Wei, C., Xu, T., Yu, Z., Xu, Z., Hou, M., Ji, M. & Zhang, Y. RRM2 is a potential prognostic biomarker with functional significance in glioma. *Int J Biol Sci* **15,** 533–543 (2019).

414. Potts, K. G., Irwin, C. R., Favis, N. A., Pink, D. B., Vincent, K. M., Lewis, J. D., Moore, R. B., Hitt, M. M. & Evans, D. H. Deletion of F4L (ribonucleotide reductase) in vaccinia virus produces a selective oncolytic virus and promotes anti-tumor immunity with superior safety in bladder cancer models. *EMBO Molecular Medicine* **9,** 638–654 (2017).

415. Barani, I. J. & Larson, D. A. in *Current Understanding and Treatment of Gliomas* (eds. Raizer, J. & Parsa, A.) 49–73 (Springer International Publishing, 2015). doi:10.1007/978-3-319-12048-5_4

416. van Herk, M. Errors and margins in radiotherapy. *Seminars in Radiation Oncology* **14,** 52–64 (2004).

417. Moghaddasi, L., Bezak, E. & Marcu, L. G. Current challenges in clinical target volume definition: Tumour margins and microscopic extensions. *Acta Oncologica* **51,** 984–995 (2012).

418. Han, X., Xue, X., Zhou, H. & Zhang, G. A molecular view of the radioresistance of gliomas. *Oncotarget* **8,** 100931–100941 (2017).

419. Storozynsky, Q. & Hitt, M. M. The Impact of Radiation-Induced DNA Damage on cGAS-STING-Mediated Immune Responses to Cancer. *International Journal of Molecular Sciences* **21,** (2020).

420. Walle, T., Martinez Monge, R., Cerwenka, A., Ajona, D., Melero, I. & Lecanda, F. Radiation effects on antitumor immune responses: current perspectives and challenges. *Ther Adv Med Oncol* **10,** 1758834017742575 (2018).

421. Lichty, B. D., Breitbach, C. J., Stojdl, D. F. & Bell, J. C. Going viral with cancer immunotherapy. *Nature Reviews Cancer* **14,** 559–567 (2014).

422. Hou, W., Sampath, P., Rojas, J. J. & Thorne, S. H. Oncolytic Virus-Mediated Targeting of PGE2 in the Tumor Alters the Immune Status and Sensitizes Established and Resistant Tumors to Immunotherapy. *Cancer Cell* **30,** 108–119 (2016).

423. Advani, S. J., Buckel, L., Chen, N. G., Scanderbeg, D. J., Geissinger, U., Zhang, Q., Yu, Y. A., Aguilar, R. J., Mundt, A. J. & Szalay, A. A. Preferential Replication of Systemically Delivered Oncolytic Vaccinia Virus in Focally Irradiated Glioma Xenografts. *Clinical Cancer Research* **18,** 2579–2590 (2012).

424. Buckel, L., Advani, S. J., Frentzen, A., Zhang, Q., Yu, Y. A., Chen, N. G., Ehrig, K., Stritzker, J., Mundt, A. J. & Szalay, A. A. Combination of fractionated irradiation with anti-VEGF expressing vaccinia virus therapy enhances tumor control by simultaneous radiosensitization of tumor associated endothelium. *International Journal of Cancer* **133,** 2989–2999 (2013).

425. Timiryasova, T. M., Gridley, D. S., Chen, B., Andres, M. L., Dutta-Roy, R., Miller, G., Bayeta, E. J. M. & Fodor, I. Radiation Enhances the Anti-tumor Effects of Vaccinia-p53 Gene Therapy in Glioma. *Technol Cancer Res Treat* **2,** 223–235 (2003).

426. Jeon, H.-Y., Kim, J.-K., Ham, S. W., Oh, S.-Y., Kim, J., Park, J.-B., Lee, J.-Y., Kim, S.-C. & Kim, H. Irradiation induces glioblastoma cell senescence and senescence-associated secretory phenotype. *Tumor Biology* **37,** 5857–5867 (2016).

427. Salam, R., Saliou, A., Bielle, F., Bertrand, M., Antoniewski, C., Carpentier, C., Alentorn, A., Capelle, L., Sanson, M., Huillard, E., Bellenger, L., Guégan, J. & Le Roux, I. Cellular senescence in malignant cells promotes tumor progression in mouse and patient Glioblastoma. *Nature Communications* **14,** 441 (2023).

428. Kim, J.-A., Seong, R.-K. & Shin, O. S. Enhanced Viral Replication by Cellular Replicative Senescence. *in* **16,** 286–295 (2016).

429. Hsieh, T.-H., Tsai, T.-T., Chen, C.-L., Shen, T.-J., Jhan, M.-K., Tseng, P.-C. & Lin, C.-F. Senescence in Monocytes Facilitates Dengue Virus Infection by Increasing Infectivity. *Frontiers in Cellular and Infection Microbiology* **10,** (2020).

430. Siebels Svenja, Czech-Sioli Manja, Spohn Michael, Schmidt Claudia, Theiss Juliane, Indenbirken Daniela, Günther Thomas, Grundhoff Adam, & Fischer Nicole. Merkel Cell Polyomavirus DNA Replication Induces Senescence in Human Dermal Fibroblasts in a Kap1/Trim28-Dependent Manner. *mBio* **11,** e00142-20 (2020).

431. AbuBakar, S., Shu, M.-H., Johari, J. & Wong, P.-F. Senescence affects endothelial cells susceptibility to dengue virus infection. *Int J Med Sci* **11,** 538–544 (2014).

432. Baz-Martínez, M., Da Silva-Álvarez, S., Rodríguez, E., Guerra, J., El Motiam, A., Vidal, A., García-Caballero, T., González-Barcia, M., Sánchez, L., Muñoz-Fontela, C., Collado, M. & Rivas, C. Cell senescence is an antiviral defense mechanism. *Scientific Reports* **6,** 37007 (2016).

433. Seoane, R., Vidal, S., Bouzaher, Y. H., El Motiam, A. & Rivas, C. The Interaction of Viruses with the Cellular Senescence Response. *Biology* **9,** (2020).

434. Weiland, T., Lampe, J., Essmann, F., Venturelli, S., Berger, A., Bossow, S., Berchtold, S., Schulze-Osthoff, K., Lauer, U. M. & Bitzer, M. Enhanced killing of therapy-induced senescent tumor cells by oncolytic measles vaccine viruses. *International Journal of Cancer* **134,** 235–243 (2014).

435. Elsherbiny, M. E., Chen, H., Emara, M. & Godbout, R. ω-3 and ω-6 Fatty Acids Modulate Conventional and Atypical Protein Kinase C Activities in a Brain Fatty Acid Binding Protein Dependent Manner in Glioblastoma Multiforme. *Nutrients* **10,** (2018).

436. Zemp, F. J., Lun, X., McKenzie, B. A., Zhou, H., Maxwell, L., Sun, B., Kelly, J. J. P., Stechishin, O., Luchman, A., Weiss, S., Cairncross, J. G., Hamilton, M. G., Rabinovich, B. A., Rahman, M. M., Mohamed, M. R., Smallwood, S., Senger, D. L., Bell, J., McFadden, G. & Forsyth, P. A. Treating brain tumor–initiating cells using a combination of myxoma virus and rapamycin. *Neuro-Oncology* **15,** 904–920 (2013).

437. Reilly, K. M., Loisel, D. A., Bronson, R. T., McLaughlin, M. E. & Jacks, T. Nf1;Trp53 mutant mice develop glioblastoma with evidence of strain-specific effects. *Nature Genetics* **26,** 109–113 (2000).

438. Pisklakova, A., McKenzie, B., Zemp, F., Lun, X., Kenchappa, R. S., Etame, A. B., Rahman, M. M., Reilly, K., Pilon-Thomas, S., McFadden, G., Kurz, E. & Forsyth, P. A. M011L-deficient oncolytic myxoma virus induces apoptosis in brain tumor-initiating cells and enhances survival in a novel immunocompetent mouse model of glioblastoma. *Neuro-Oncology* **18,** 1088–1098 (2016).

439. Marumoto, T., Tashiro, A., Friedmann-Morvinski, D., Scadeng, M., Soda, Y., Gage, F. H. & Verma, I. M. Development of a novel mouse glioma model using lentiviral vectors. *Nature Medicine* **15,** 110–116 (2009).

440. Cheema, T. A., Wakimoto, H., Fecci, P. E., Ning, J., Kuroda, T., Jeyaretna, D. S., Martuza, R. L. & Rabkin, S. D. Multifaceted oncolytic virus therapy for glioblastoma in an immunocompetent cancer stem cell model. *Proceedings of the National Academy of Sciences* **110,** 12006–12011 (2013).

441. Jung, H., Wang, S.-Y., Yang, I.-W., Hsueh, D.-W., Yang, W.-J., Wang, T.-H. & Wang, H.-S. Detection and treatment of mycoplasma contamination in cultured cells. *Chang Gung Med J* **26,** 250–258 (2003).

442. Mohamed, A., Clements, D. R., Gujar, S. A., Lee, P. W., Smiley, J. R. & Shmulevitz, M. Single Amino Acid Differences between Closely Related Reovirus T3D Lab Strains Alter Oncolytic Potency In Vitro and In Vivo. *J Virol* **94,** (2020).

443. Stojdl, D. F., Lichty, B. D., tenOever, B. R., Paterson, J. M., Power, A. T., Knowles, S., Marius, R., Reynard, J., Poliquin, L., Atkins, H., Brown, E. G., Durbin, R. K., Durbin, J. E., Hiscott, J. & Bell, J. C. VSV strains with defects in their ability to shutdown innate immunity are potent systemic anti-cancer agents. *Cancer Cell* **4,** 263–275 (2003).

444. Diallo, J.-S., Vähä-Koskela, M., Le Boeuf, F. & Bell, J. in *Oncolytic Viruses: Methods and Protocols* (eds. Kirn, D. H., Liu, T.-C. & Thorne, S. H.) 127–140 (Humana Press, 2012). doi:10.1007/978-1-61779-340-0_10

445. Repetto, G., del Peso, A. & Zurita, J. L. Neutral red uptake assay for the estimation of cell viability/cytotoxicity. *Nature Protocols* **3,** 1125–1131 (2008).

446. Bommareddy, P. K., Lowe, D. B., Kaufman, H. L., Rabkin, S. D. & Saha, D. Multi-parametric flow cytometry staining procedure for analyzing tumor-infiltrating immune cells following oncolytic herpes simplex virus immunotherapy in intracranial glioblastoma. *J Biol Methods* **6,** e112 (2019).

447. Omuro, A. & DeAngelis, L. M. Glioblastoma and Other Malignant Gliomas: A Clinical Review. *JAMA* **310,** 1842–1850 (2013).

448. Samson, A., West, E. J., Carmichael, J., Scott, K. J., Turnbull, S., Kuszlewicz, B., Dave, R. V., Peckham-Cooper, A., Tidswell, E., Kingston, J., Johnpulle, M., da Silva, B., Jennings, V. A., Bendjama, K., Stojkowitz, N., Lusky, M., Prasad, K., Toogood, G. J., Auer, R., Bell, J., Twelves, C. J., Harrington, K. J., Vile, R. G., Pandha, H., Errington-Mais, F., Ralph, C., Newton, D. J., Anthoney, A., Melcher, A. A.

& Collinson, F. Neoadjuvant Intravenous Oncolytic Vaccinia Virus Therapy Promotes Anticancer Immunity in Patients. *Cancer Immunol Res* **10,** 745–756 (2022).

449. Breitbach, C. J., Bell, J. C., Hwang, T.-H., Kirn, D. H. & Burke, J. The emerging therapeutic potential of the oncolytic immunotherapeutic Pexa-Vec (JX-594). *Oncolytic Virother* **4,** 25–31 (2015).
450. Lu, V. M., Shah, A. H., Vallejo, F. A., Eichberg, D. G., Luther, E. M., Shah, S. S., Komotar, R. J. & Ivan, M. E. Clinical trials using oncolytic viral therapy to treat adult glioblastoma: a progress report. *Neurosurgical Focus FOC* **50,** E3 (2021).
451. Ottolino-Perry, K., Diallo, J.-S., Lichty, B. D., Bell, J. C. & Andrea McCart, J. Intelligent Design: Combination Therapy With Oncolytic Viruses. *Molecular Therapy* **18,** 251–263 (2010).
452. Garcia, C. A., Bhargav, A. G., Brooks, M., Suárez-Meade, P., Mondal, S. K., Zarco, N., ReFaey, K., Jentoft, M., Middlebrooks, E. H., Snuderl, M., Carrano, A., Guerrero-Cazares, H., Schiapparelli, P., Sarabia-Estrada, R. & Quiñones-Hinojosa, A. Functional Characterization of Brain Tumor-Initiating Cells and Establishment of GBM Preclinical Models that Incorporate Heterogeneity, Therapy, and Sex Differences. *Molecular Cancer Therapeutics* **20,** 2585–2597 (2021).
453. Buller, R. M. L., Smith, G. L., Cremer, K., Notkins, A. L. & Moss, B. Decreased virulence of recombinant vaccinia virus expression vectors is associated with a thymidine kinase-negative phenotype. *Nature* **317,** 813–815 (1985).
454. Claes, A., Idema, A. J. & Wesseling, P. Diffuse glioma growth: a guerilla war. *Acta Neuropathologica* **114,** 443–458 (2007).
455. Meng, W., Palmer, J. D., Siedow, M., Haque, S. J. & Chakravarti, A. Overcoming Radiation Resistance in Gliomas by Targeting Metabolism and DNA Repair Pathways. *International Journal of Molecular Sciences* **23,** (2022).
456. Mittal, A., Nenwani, M., Sarangi, I., Achreja, A., Lawrence, T. S. & Nagrath, D. Radiotherapy-induced metabolic hallmarks in the tumor microenvironment. *Trends in Cancer* **8,** 855–869 (2022).

457. Seyfried, T. N., El-Abbadi, M. & Roy, M. L. Ganglioside distribution in murine neural tumors. *Molecular and Chemical Neuropathology* **17,** 147–167 (1992).

458. Binello, E., Qadeer, Z. A., Kothari, H. P., Emdad, L. & Germano, I. M. Stemness of the CT-2A Immunocompetent Mouse Brain Tumor Model: Characterization In Vitro. *J Cancer* **3,** 166–174 (2012).

459. Martínez, R. M. M. and A. *Standardization of an orthotopic mouse brain tumor model following transplantation of CT-2A astrocytoma cells*. *Histology and histopathology, vol. 22, nº12 (2007)* (Murcia: F. Hernández, 2007). at <http://hdl.handle.net/10201/28516>

460. Khalsa, J. K., Cheng, N., Keegan, J., Chaudry, A., Driver, J., Bi, W. L., Lederer, J. & Shah, K. Immune phenotyping of diverse syngeneic murine brain tumors identifies immunologically distinct types. *Nature Communications* **11,** 3912 (2020).

461. Han, S., Zhang, C., Li, Q., Dong, J., Liu, Y., Huang, Y., Jiang, T. & Wu, A. Tumour-infiltrating CD4+ and CD8+ lymphocytes as predictors of clinical outcome in glioma. *British Journal of Cancer* **110,** 2560–2568 (2014).

462. Humphries, W., Wei, J., Sampson, J. H. & Heimberger, A. B. The Role of Tregs in Glioma-Mediated Immunosuppression: Potential Target for Intervention. *Neurosurgery Clinics* **21,** 125–137 (2010).

463. Quezada, S. A., Peggs, K. S., Simpson, T. R. & Allison, J. P. Shifting the equilibrium in cancer immunoediting: from tumor tolerance to eradication. *Immunological Reviews* **241,** 104–118 (2011).

464. Sayour, E. J., McLendon, P., McLendon, R., De Leon, G., Reynolds, R., Kresak, J., Sampson, J. H. & Mitchell, D. A. Increased proportion of FoxP3+ regulatory T cells in tumor infiltrating lymphocytes is associated with tumor recurrence and reduced survival in patients with glioblastoma. *Cancer Immunology, Immunotherapy* **64,** 419–427 (2015).

465. Hambardzumyan, D., Gutmann, D. H. & Kettenmann, H. The role of microglia and macrophages in glioma maintenance and progression. *Nature Neuroscience* **19,** 20–27 (2016).

466. Lun, X. Q., Jang, J.-H., Tang, N., Deng, H., Head, R., Bell, J. C., Stojdl, D. F., Nutt, C. L., Senger, D. L., Forsyth, P. A. & McCart, J. A. Efficacy of Systemically Administered Oncolytic Vaccinia Virotherapy for Malignant Gliomas Is Enhanced by Combination Therapy with Rapamycin or Cyclophosphamide. *Clinical Cancer Research* **15,** 2777–2788 (2009).

467. Radaelli, E., Ceruti, R., Patton, V., Russo, M., Degrassi, A., Croci, V., Caprera, F., Stortini, G., Scanziani, E. & Pesenti, E. Immunohistopathological and neuroimaging characterization of murine orthotopic xenograft models of glioblastoma multiforme recapitulating the most salient features of human disease. (2009).

468. Candolfi, M., Curtin, J. F., Nichols, W. S., Muhammad, AKM. G., King, G. D., Pluhar, G. E., McNiel, E. A., Ohlfest, J. R., Freese, A. B., Moore, P. F., Lerner, J., Lowenstein, P. R. & Castro, M. G. Intracranial glioblastoma models in preclinical neuro-oncology: neuropathological characterization and tumor progression. *Journal of Neuro-Oncology* **85,** 133–148 (2007).

469. Mansfield, D., Pencavel, T., Kyula, J. N., Zaidi, S., Roulstone, V., Thway, K., Karapanagiotou, L., Khan, A. A., McLaughlin, M., Touchefeu, Y., Seth, R., Melcher, A. A., Vile, R. G., Pandha, H. S. & Harrington, K. J. Oncolytic Vaccinia virus and radiotherapy in head and neck cancer. *Oral Oncology* **49,** 108–118 (2013).

470. Dai, M. H., Liu, S. L., Chen, N. G., Zhang, T. P., You, L., Q. Zhang, F., Chou, T. C., Szalay, A. A., Fong, Y. & Zhao, Y. P. Oncolytic vaccinia virus in combination with radiation shows synergistic antitumor efficacy in pancreatic cancer. *Cancer Letters* **344,** 282–290 (2014).

471. Wilkinson, M. J., Smith, H. G., McEntee, G., Kyula-Currie, J., Pencavel, T. D., Mansfield, D. C., Khan, A. A., Roulstone, V., Hayes, A. J. & Harrington, K. J. Oncolytic vaccinia virus combined with

radiotherapy induces apoptotic cell death in sarcoma cells by down-regulating the inhibitors of apoptosis. *Oncotarget* **7,** 81208–81222 (2016).

472. Wilkinson, M. J., Smith, H. G., Pencavel, T. D., Mansfield, D. C., Kyula-Currie, J., Khan, A. A., McEntee, G., Roulstone, V., Hayes, A. J. & Harrington, K. J. Isolated limb perfusion with biochemotherapy and oncolytic virotherapy combines with radiotherapy and surgery to overcome treatment resistance in an animal model of extremity soft tissue sarcoma. *International Journal of Cancer* **139,** 1414–1422 (2016).
473. Kyula, J. N., Khan, A. A., Mansfield, D., Karapanagiotou, E. M., McLaughlin, M., Roulstone, V., Zaidi, S., Pencavel, T., Touchefeu, Y., Seth, R., Chen, N. G., Yu, Y. A., Zhang, Q., Melcher, A. A., Vile, R. G., Pandha, H. S., Ajaz, M., Szalay, A. A. & Harrington, K. J. Synergistic cytotoxicity of radiation and oncolytic Lister strain vaccinia in V600D/EBRAF mutant melanoma depends on JNK and TNF-α signaling. *Oncogene* **33,** 1700–1712 (2014).
474. Chen, W.-Y., Chen, Y.-L., Lin, H.-W., Chang, C.-F., Huang, B.-S., Sun, W.-Z. & Cheng, W.-F. Stereotactic body radiation combined with oncolytic vaccinia virus induces potent anti-tumor effect by triggering tumor cell necroptosis and DAMPs. *Cancer Letters* **523,** 149–161 (2021).
475. Cui, X., Morales, R.-T. T., Qian, W., Wang, H., Gagner, J.-P., Dolgalev, I., Placantonakis, D., Zagzag, D., Cimmino, L., Snuderl, M., Lam, R. H. W. & Chen, W. Hacking macrophage-associated immunosuppression for regulating glioblastoma angiogenesis. *Biomaterials* **161,** 164–178 (2018).
476. Woroniecka, K., Chongsathidkiet, P., Rhodin, K., Kemeny, H., Dechant, C., Farber, S. H., Elsamadicy, A. A., Cui, X., Koyama, S., Jackson, C., Hansen, L. J., Johanns, T. M., Sanchez-Perez, L., Chandramohan, V., Yu, Y.-R. A., Bigner, D. D., Giles, A., Healy, P., Dranoff, G., Weinhold, K. J., Dunn, G. P. & Fecci, P. E. T-Cell Exhaustion Signatures Vary with Tumor Type and Are Severe in Glioblastoma. *Clinical Cancer Research* **24,** 4175–4186 (2018).

477. Saha, D., Martuza, R. L. & Rabkin, S. D. Macrophage Polarization Contributes to Glioblastoma Eradication by Combination Immunovirotherapy and Immune Checkpoint Blockade. *Cancer Cell* **32,** 253-267.e5 (2017).

478. Liu, C. J., Schaettler, M., Blaha, D. T., Bowman-Kirigin, J. A., Kobayashi, D. K., Livingstone, A. J., Bender, D., Miller, C. A., Kranz, D. M., Johanns, T. M. & Dunn, G. P. Treatment of an aggressive orthotopic murine glioblastoma model with combination checkpoint blockade and a multivalent neoantigen vaccine. *Neuro-Oncology* **22,** 1276–1288 (2020).

479. Nair, S., Mazzoccoli, L., Jash, A., Govero, J., Bais, S. S., Hu, T., Fontes-Garfias, C. R., Shan, C., Okada, H., Shresta, S., Rich, J. N., Shi, P.-Y., Diamond, M. S. & Chheda, M. G. Zika virus oncolytic activity requires CD8+ T cells and is boosted by immune checkpoint blockade. *JCI Insight* **6,** 144619 (2021).

480. Liljedahl, E., Konradsson, E., Gustafsson, E., Jonsson, K. F., Olofsson, J. K., Ceberg, C. & Redebrandt, H. N. Long-term anti-tumor effects following both conventional radiotherapy and FLASH in fully immunocompetent animals with glioblastoma. *Scientific Reports* **12,** 1–12 (2022).

481. Maksoud, S. The DNA Double-Strand Break Repair in Glioma: Molecular Players and Therapeutic Strategies. *Molecular Neurobiology* **59,** 5326–5365 (2022).

482. Lhuillier, C., Rudqvist, N.-P., Elemento, O., Formenti, S. C. & Demaria, S. Radiation therapy and anti-tumor immunity: exposing immunogenic mutations to the immune system. *Genome Medicine* **11,** 40 (2019).

483. Udayakumar, T. S., Betancourt, D. M., Ahmad, A., Tao, W., Totiger, T. M., Patel, M., Marples, B., Barber, G. & Pollack, A. Radiation Attenuates Prostate Tumor Antiviral Responses to Vesicular Stomatitis Virus Containing IFNb, Resulting in Pronounced Antitumor Systemic Immune Responses.

484. Martinez-Velez, N., Marigil, M., García-Moure, M., Gonzalez-Huarriz, M., Aristu, J. J., Ramos-García, L.-I., Tejada, S., Díez-Valle, R., Patiño-García, A., Becher, O. J., Gomez-Manzano, C., Fueyo, J. & Alonso, M. M. Delta-24-RGD combined with radiotherapy exerts a potent antitumor effect in

diffuse intrinsic pontine glioma and pediatric high grade glioma models. *Acta Neuropathol Commun* **7,** 64 (2019).

485. Buonfiglioli, A. & Hambardzumyan, D. Macrophages and microglia: the cerberus of glioblastoma. *Acta Neuropathologica Communications* **9,** 54 (2021).

486. Amoozgar, Z., Kloepper, J., Ren, J., Tay, R. E., Kazer, S. W., Kiner, E., Krishnan, S., Posada, J. M., Ghosh, M., Mamessier, E., Wong, C., Ferraro, G. B., Batista, A., Wang, N., Badeaux, M., Roberge, S., Xu, L., Huang, P., Shalek, A. K., Fukumura, D., Kim, H.-J. & Jain, R. K. Targeting Treg cells with GITR activation alleviates resistance to immunotherapy in murine glioblastomas. *Nature Communications* **12,** 2582 (2021).

487. de Groot, J., Penas-Prado, M., Alfaro-Munoz, K., Hunter, K., Pei, B. L., O'Brien, B., Weathers, S.-P., Loghin, M., Kamiya Matsouka, C., Yung, W. K. A., Mandel, J., Wu, J., Yuan, Y., Zhou, S., Fuller, G. N., Huse, J., Rao, G., Weinberg, J. S., Prabhu, S. S., McCutcheon, I. E., Lang, F. F., Ferguson, S. D., Sawaya, R., Colen, R., Yadav, S. S., Blando, J., Vence, L., Allison, J., Sharma, P. & Heimberger, A. B. Window-of-opportunity clinical trial of pembrolizumab in patients with recurrent glioblastoma reveals predominance of immune-suppressive macrophages. *Neuro-Oncology* **22,** 539–549 (2020).

488. Fukuhara, H., Ino, Y. & Todo, T. Oncolytic virus therapy: A new era of cancer treatment at dawn. *Cancer Science* **107,** 1373–1379 (2016).

489. Prasanna, P. G., Citrin, D. E., Hildesheim, J., Ahmed, M. M., Venkatachalam, S., Riscuta, G., Xi, D., Zheng, G., Deursen, J. van, Goronzy, J., Kron, S. J., Anscher, M. S., Sharpless, N. E., Campisi, J., Brown, S. L., Niedernhofer, L. J., O'Loghlen, A., Georgakilas, A. G., Paris, F., Gius, D., Gewirtz, D. A., Schmitt, C. A., Abazeed, M. E., Kirkland, J. L., Richmond, A., Romesser, P. B., Lowe, S. W., Gil, J., Mendonca, M. S., Burma, S., Zhou, D. & Coleman, C. N. Therapy-Induced Senescence: Opportunities to Improve Anticancer Therapy. *JNCI: Journal of the National Cancer Institute* **113,** 1285–1298 (2021).

490. Rodier, F. & Campisi, J. Four faces of cellular senescence. *Journal of Cell Biology* **192,** 547–556 (2011).

491. Beltzig, L., Schwarzenbach, C., Leukel, P., Frauenknecht, K. B. M., Sommer, C., Tancredi, A., Hegi, M. E., Christmann, M. & Kaina, B. Senescence Is the Main Trait Induced by Temozolomide in Glioblastoma Cells. *Cancers* **14,** (2022).

492. Sundar, S. J., Shakya, S., Barnett, A., Wallace, L. C., Jeon, H., Sloan, A., Recinos, V. & Hubert, C. G. Three-dimensional organoid culture unveils resistance to clinical therapies in adult and pediatric glioblastoma. *Translational Oncology* **15,** 101251 (2022).

493. Touchefeu, Y., Vassaux, G. & Harrington, K. J. Oncolytic viruses in radiation oncology. *Radiotherapy and Oncology* **99,** 262–270 (2011).

494. Lun, X., Chan, J., Zhou, H., Sun, B., Kelly, J. J., Stechishin, O. O., Bell, J. C., Parato, K., Hu, K., Vaillant, D., Wang, J., Liu, T.-C., Breitbach, C., Kirn, D., Senger, D. L. & Forsyth, P. A. Efficacy and Safety/Toxicity Study of Recombinant Vaccinia Virus JX-594 in Two Immunocompetent Animal Models of Glioma. *Molecular Therapy* **18,** 1927–1936 (2010).

495. Tkacheva, A. V., Sivolobova, G. F., Grazhdantseva, A. A., Shevelev, O. B., Razumov, I. A., Zavjalov, E. L., Loktev, V. B. & Kochneva, G. V. Targeted Therapy of Human Glioblastoma Combining the Oncolytic Properties of Parvovirus H-1 and Attenuated Strains of the Vaccinia Virus. *Molecular Genetics, Microbiology and Virology* **34,** 140–147 (2019).

496. Quick, Q. A. & Gewirtz, D. A. An accelerated senescence response to radiation in wild-type p53 glioblastoma multiforme cells. *Journal of Neurosurgery JNS* **105,** 111–118 (2006).

497. Zanoni, M., Sarti, A. C., Zamagni, A., Cortesi, M., Pignatta, S., Arienti, C., Tebaldi, M., Sarnelli, A., Romeo, A., Bartolini, D., Tosatto, L., Adinolfi, E., Tesei, A. & Di Virgilio, F. Irradiation causes senescence, ATP release, and P2X7 receptor isoform switch in glioblastoma. *Cell Death & Disease* **13,** 80 (2022).

498. Zhang, X., Ye, C., Sun, F., Wei, W., Hu, B. & Wang, J. Both Complexity and Location of DNA Damage Contribute to Cellular Senescence Induced by Ionizing Radiation. *PLOS ONE* **11,** e0155725 (2016).

499. Zhang, L., Cheng, F., Wei, Y., Zhang, L., Guo, D., Wang, B. & Li, W. Inhibition of TAZ contributes radiation-induced senescence and growth arrest in glioma cells. *Oncogene* **38,** 2788–2799 (2019).

500. Wali, A. & Strayer, D. S. Infection with Vaccinia Virus Alters Regulation of Cell Cycle Progression. *DNA and Cell Biology* **18,** 837–843 (1999).

501. Yoo, N.-K., Pyo, C.-W., Kim, Y., Ahn, B.-Y. & Choi, S.-Y. Vaccinia virus-mediated cell cycle alteration involves inactivation of tumour suppressors associated with Brf1 and TBP. *Cellular Microbiology* **10,** 583–592 (2008).

502. Sherley, J. L. & Kelly, T. J. Regulation of human thymidine kinase during the cell cycle. *J Biol Chem* **263,** 8350–8358 (1988).

503. Bjoerklund, S., Skog, S., Tribukait, B. & Thelander, L. S-Phase-specific expression of mammalian ribonucleotide reductase R1 and R2 subunit mRNAs. *Biochemistry* **29,** 5452–5458 (1990).

504. Chabes, A. & Thelander, L. Controlled Protein Degradation Regulates Ribonucleotide Reductase Activity in Proliferating Mammalian Cells during the Normal Cell Cycle and in Response to DNA Damage and Replication Blocks*. *Journal of Biological Chemistry* **275,** 17747–17753 (2000).

505. Parato, K. A., Breitbach, C. J., Le Boeuf, F., Wang, J., Storbeck, C., Ilkow, C., Diallo, J.-S., Falls, T., Burns, J., Garcia, V., Kanji, F., Evgin, L., Hu, K., Paradis, F., Knowles, S., Hwang, T.-H., Vanderhyden, B. C., Auer, R., Kirn, D. H. & Bell, J. C. The Oncolytic Poxvirus JX-594 Selectively Replicates in and Destroys Cancer Cells Driven by Genetic Pathways Commonly Activated in Cancers. *Molecular Therapy* **20,** 749–758 (2012).

506. Tanaka, H., Arakawa, H., Yamaguchi, T., Shiraishi, K., Fukuda, S., Matsui, K., Takei, Y. & Nakamura, Y. A ribonucleotide reductase gene involved in a p53-dependent cell-cycle checkpoint for DNA damage. *Nature* **404,** 42–49 (2000).

507. BASLER, C. F. & GARCÍA-SASTRE, A. VIRUSES AND THE TYPE I INTERFERON ANTIVIRAL SYSTEM: INDUCTION AND EVASION. *International Reviews of Immunology* **21,** 305–337 (2002).

508. Deng, L., Zeng, Q., Wang, M., Cheng, A., Jia, R., Chen, S., Zhu, D., Liu, M., Yang, Q., Wu, Y., Zhao, X., Zhang, S., Liu, Y., Yu, Y., Zhang, L. & Chen, X. Suppression of NF-κB Activity: A Viral Immune Evasion Mechanism. *Viruses* **10,** (2018).

509. Chien, Y., Scuoppo, C., Wang, X., Fang, X., Balgley, B., Bolden, J. E., Premsrirut, P., Luo, W., Chicas, A., Lee, C. S., Kogan, S. C. & Lowe, S. W. Control of the senescence-associated secretory phenotype by NF-κB promotes senescence and enhances chemosensitivity. *Genes Dev* **25,** 2125–2136 (2011).

510. Rovillain, E., Mansfield, L., Caetano, C., Alvarez-Fernandez, M., Caballero, O. L., Medema, R. H., Hummerich, H. & Jat, P. S. Activation of nuclear factor-kappa B signalling promotes cellular senescence. *Oncogene* **30,** 2356–2366 (2011).

511. Schoggins, J. W., Wilson, S. J., Panis, M., Murphy, M. Y., Jones, C. T., Bieniasz, P. & Rice, C. M. A diverse range of gene products are effectors of the type I interferon antiviral response. *Nature* **472,** 481–485 (2011).

512. Haller, O., Stertz, S. & Kochs, G. The Mx GTPase family of interferon-induced antiviral proteins. *Microbes and Infection* **9,** 1636–1643 (2007).

513. Perng, Y.-C. & Lenschow, D. J. ISG15 in antiviral immunity and beyond. *Nature Reviews Microbiology* **16,** 423–439 (2018).

514. Sun, S.-C., Ganchi, P. A., Ballard, D. W. & Greene, W. C. NF-κB Controls Expression of Inhibitor IκBα: Evidence for an Inducible Autoregulatory Pathway. *Science* **259,** 1912–1915 (1993).

515. Liu, T., Zhang, L., Joo, D. & Sun, S.-C. NF-κB signaling in inflammation. *Signal Transduction and Targeted Therapy* **2,** 17023 (2017).

516. Liao, E.-C., Hsu, Y.-T., Chuah, Q.-Y., Lee, Y.-J., Hu, J.-Y., Huang, T.-C., Yang, P.-M. & Chiu, S.-J. Radiation induces senescence and a bystander effect through metabolic alterations. *Cell Death & Disease* **5,** e1255–e1255 (2014).

517. Elbakrawy, E., Kaur Bains, S., Bright, S., AL-Abedi, R., Mayah, A., Goodwin, E. & Kadhim, M. Radiation-Induced Senescence Bystander Effect: The Role of Exosomes. *Biology* **9,** (2020).

518. Leu, J.-D., Wang, C.-Y., Lo, C.-C., Lin, M.-Y., Chang, C.-Y., Hung, W.-C., Lin, S.-T., Wang, B.-S. & Lee, Y.-J. Involvement of c-Myc in low dose radiation-induced senescence enhanced migration and invasion of unirradiated cancer cells. *Aging (Albany NY)* **13,** 22208–22231 (2021).

519. Antelo-Iglesias, L., Picallos-Rabina, P., Estévez-Souto, V., Da Silva-Álvarez, S. & Collado, M. The role of cellular senescence in tissue repair and regeneration. *Mechanisms of Ageing and Development* **198,** 111528 (2021).

520. Freund, A., Orjalo, A. V., Desprez, P.-Y. & Campisi, J. Inflammatory networks during cellular senescence: causes and consequences. *Trends in Molecular Medicine* **16,** 238–246 (2010).

521. Xue, W., Zender, L., Miething, C., Dickins, R. A., Hernando, E., Krizhanovsky, V., Cordon-Cardo, C. & Lowe, S. W. Senescence and tumour clearance is triggered by p53 restoration in murine liver carcinomas. *Nature* **445,** 656–660 (2007).

522. Baker, D. J., Perez-Terzic, C., Jin, F., Pitel, K. S., Niederländer, N. J., Jeganathan, K., Yamada, S., Reyes, S., Rowe, L., Hiddinga, H. J., Eberhardt, N. L., Terzic, A. & van Deursen, J. M. Opposing roles for p16Ink4a and p19Arf in senescence and ageing caused by BubR1 insufficiency. *Nature Cell Biology* **10,** 825–836 (2008).

523. Baker, D. J., Wijshake, T., Tchkonia, T., LeBrasseur, N. K., Childs, B. G., van de Sluis, B., Kirkland, J. L. & van Deursen, J. M. Clearance of p16Ink4a-positive senescent cells delays ageing-associated disorders. *Nature* **479,** 232–236 (2011).

524. Mavrogonatou, E., Pratsinis, H. & Kletsas, D. The role of senescence in cancer development. *Seminars in Cancer Biology* **62,** 182–191 (2020).

525. Jeon, H.-Y., Ham, S. W., Kim, J.-K., Jin, X., Lee, S. Y., Shin, Y. J., Choi, C.-Y., Sa, J. K., Kim, S. H., Chun, T., Jin, X., Nam, D.-H. & Kim, H. Ly6G+ inflammatory cells enable the conversion of cancer cells to cancer stem cells in an irradiated glioblastoma model. *Cell Death & Differentiation* **26,** 2139–2156 (2019).

526. Reddel, R. R. Senescence: an antiviral defense that is tumor suppressive? *Carcinogenesis* **31,** 19–26 (2010).

527. Basisty, N., Kale, A., Jeon, O. H., Kuehnemann, C., Payne, T., Rao, C., Holtz, A., Shah, S., Sharma, V., Ferrucci, L., Campisi, J. & Schilling, B. A proteomic atlas of senescence-associated secretomes for aging biomarker development. *PLOS Biology* **18,** e3000599 (2020).

528. Ember, S. W. J., Ren, H., Ferguson, B. J. & Smith, G. L. Vaccinia virus protein C4 inhibits NF-κB activation and promotes virus virulence. *J Gen Virol* **93,** 2098–2108 (2012).

529. Neidel, S., Ren, H., Torres, A. A. & Smith, G. L. NF-κB activation is a turn on for vaccinia virus phosphoprotein A49 to turn off NF-κB activation. *Proceedings of the National Academy of Sciences* **116,** 5699–5704 (2019).

530. Sumner, R. P., Maluquer de Motes, C., Veyer, D. L. & Smith, G. L. Vaccinia virus inhibits NF-κB-dependent gene expression downstream of p65 translocation. *J Virol* **88,** 3092–3102 (2014).

531. Shiravand, Y., Khodadadi, F., Kashani, S. M., Hosseini-Fard, S. R., Hosseini, S., Sadeghirad, H., Ladwa, R., O'Byrne, K. & Kulasinghe, A. Immune Checkpoint Inhibitors in Cancer Therapy. *Current Oncology* **29,** 3044–3060 (2022).

532. Zeng, J., See, A. P., Phallen, J., Jackson, C. M., Belcaid, Z., Ruzevick, J., Durham, N., Meyer, C., Harris, T. J., Albesiano, E., Pradilla, G., Ford, E., Wong, J., Hammers, H.-J., Mathios, D., Tyler, B., Brem, H., Tran, P. T., Pardoll, D., Drake, C. G. & Lim, M. Anti-PD-1 Blockade and Stereotactic

Radiation Produce Long-Term Survival in Mice With Intracranial Gliomas. *International Journal of Radiation Oncology*Biology*Physics* **86,** 343–349 (2013).

533. Kim, J. E., Patel, M. A., Mangraviti, A., Kim, E. S., Theodros, D., Velarde, E., Liu, A., Sankey, E. W., Tam, A., Xu, H., Mathios, D., Jackson, C. M., Harris-Bookman, S., Garzon-Muvdi, T., Sheu, M., Martin, A. M., Tyler, B. M., Tran, P. T., Ye, X., Olivi, A., Taube, J. M., Burger, P. C., Drake, C. G., Brem, H., Pardoll, D. M. & Lim, M. Combination Therapy with Anti-PD-1, Anti-TIM-3, and Focal Radiation Results in Regression of Murine Gliomas. *Clinical Cancer Research* **23,** 124–136 (2017).
534. Lee, Y. S., Lee, W. S., Kim, C. W., Lee, S. J., Yang, H., Kong, S. J., Ning, J., Yang, K.-M., Kang, B., Kim, W. R., Chon, H. J. & Kim, C. Oncolytic vaccinia virus reinvigorates peritoneal immunity and cooperates with immune checkpoint inhibitor to suppress peritoneal carcinomatosis in colon cancer. *J Immunother Cancer* **8,** (2020).
535. Ge, Y., Wang, H., Ren, J., Liu, W., Chen, L., Chen, H., Ye, J., Dai, E., Ma, C., Ju, S., Guo, Z. S., Liu, Z. & Bartlett, D. L. Oncolytic vaccinia virus delivering tethered IL-12 enhances antitumor effects with improved safety. *J Immunother Cancer* **8,** (2020).
536. Sun, Y., Zhang, Z., Zhang, C., Zhang, N., Wang, P., Chu, Y., Chard Dunmall, L. S., Lemoine, N. R. & Wang, Y. An effective therapeutic regime for treatment of glioma using oncolytic vaccinia virus expressing IL-21 in combination with immune checkpoint inhibition. *Molecular Therapy - Oncolytics* **26,** 105–119 (2022).
537. Jhawar, S. R., Wang, S.-J., Thandoni, A., Bommareddy, P. K., Newman, J. H., Marzo, A. L., Kuzel, T. M., Gupta, V., Reiser, J., Daniels, P., Schiff, D., Mitchell, D., LeBoeuf, N. R., Simmons, C., Goyal, S., Lasfar, A., Guevara-Patino, J. A., Haffty, B. G., Kaufman, H. L., Silk, A. W. & Zloza, A. Combination oncolytic virus, radiation therapy, and immune checkpoint inhibitor treatment in anti-PD-1-refractory cancer. *J Immunother Cancer* **11,** (2023).

538. Johnson, D. B., Nebhan, C. A., Moslehi, J. J. & Balko, J. M. Immune-checkpoint inhibitors: long-term implications of toxicity. *Nature Reviews Clinical Oncology* **19,** 254–267 (2022).

539. Sterner, R. C. & Sterner, R. M. CAR-T cell therapy: current limitations and potential strategies. *Blood Cancer Journal* **11,** 69 (2021).

540. O'Rourke, D. M., Nasrallah, M. P., Desai, A., Melenhorst, J. J., Mansfield, K., Morrissette, J. J. D., Martinez-Lage, M., Brem, S., Maloney, E., Shen, A., Isaacs, R., Mohan, S., Plesa, G., Lacey, S. F., Navenot, J.-M., Zheng, Z., Levine, B. L., Okada, H., June, C. H., Brogdon, J. L. & Maus, M. V. A single dose of peripherally infused EGFRvIII-directed CAR T cells mediates antigen loss and induces adaptive resistance in patients with recurrent glioblastoma. *Science Translational Medicine* **9,** eaaa0984 (2017).

541. DeSelm, C., Palomba, M. L., Yahalom, J., Hamieh, M., Eyquem, J., Rajasekhar, V. K. & Sadelain, M. Low-Dose Radiation Conditioning Enables CAR T Cells to Mitigate Antigen Escape. *Molecular Therapy* **26,** 2542–2552 (2018).

542. Moon, E. K., Wang, L.-C. S., Bekdache, K., Lynn, R. C., Lo, A., Thorne, S. H. & Albelda, S. M. Intra-tumoral delivery of CXCL11 via a vaccinia virus, but not by modified T cells, enhances the efficacy of adoptive T cell therapy and vaccines. *OncoImmunology* **7,** e1395997 (2018).

543. Cohen, J. IL-12 Deaths: Explanation and a Puzzle. *Science* **270,** 908–908 (1995).

544. Schwartz, R. N., Stover, L. & Dutcher, J. P. Managing toxicities of high-dose interleukin-2. *Oncology (Williston Park)* **16,** 11–20 (2002).

545. Liu, J., Cao, S., Kim, S., Chung, E. Y., Homma, Y., Guan, X., Jimenez, V. & Ma, X. Interleukin-12: an update on its immunological activities, signaling and regulation of gene expression. *Curr Immunol Rev* **1,** 119–137 (2005).

546. Jackaman, C., Bundell, C. S., Kinnear, B. F., Smith, A. M., Filion, P., van Hagen, D., Robinson, B. W. S. & Nelson, D. J. IL-2 Intratumoral Immunotherapy Enhances CD8+ T Cells That Mediate Destruction

of Tumor Cells and Tumor-Associated Vasculature: A Novel Mechanism for IL-2 1. *The Journal of Immunology* **171,** 5051–5063 (2003).

547. Bradley, L. M., Haynes, L. & Swain, S. L. IL-7: maintaining T-cell memory and achieving homeostasis. *Trends in Immunology* **26,** 172–176 (2005).

548. Li, J., O'Malley, M., Urban, J., Sampath, P., Guo, Z. S., Kalinski, P., Thorne, S. H. & Bartlett, D. L. Chemokine Expression From Oncolytic Vaccinia Virus Enhances Vaccine Therapies of Cancer. *Molecular Therapy* **19,** 650–657 (2011).

549. Rojas, J. J., Sampath, P., Bonilla, B., Ashley, A., Hou, W., Byrd, D. & Thorne, S. H. Manipulating TLR Signaling Increases the Anti-tumor T Cell Response Induced by Viral Cancer Therapies. *Cell Rep* **15,** 264–273 (2016).

550. McKelvey, K. J., Hudson, A. L., Donaghy, H., Stoner, S. P., Wheeler, H. R., Diakos, C. I. & Howell, V. M. Differential effects of radiation fractionation regimens on glioblastoma. *Radiation Oncology* **17,** 17 (2022).

551. Vanpouille-Box, C., Alard, A., Aryankalayil, M. J., Sarfraz, Y., Diamond, J. M., Schneider, R. J., Inghirami, G., Coleman, C. N., Formenti, S. C. & Demaria, S. DNA exonuclease Trex1 regulates radiotherapy-induced tumour immunogenicity. *Nature Communications* **8,** 15618 (2017).

552. Grapin, M., Richard, C., Limagne, E., Boidot, R., Morgand, V., Bertaut, A., Derangere, V., Laurent, P.-A., Thibaudin, M., Fumet, J. D., Crehange, G., Ghiringhelli, F. & Mirjolet, C. Optimized fractionated radiotherapy with anti-PD-L1 and anti-TIGIT: a promising new combination. *Journal for ImmunoTherapy of Cancer* **7,** 160 (2019).

553. Bertho, A., Iturri, L. & Prezado, Y. in *International Review of Cell and Molecular Biology* (eds. Mirjolet, C. & Galluzzi, L.) **376,** 37–68 (Academic Press, 2023).

554. Matuszak, N., Suchorska, W. M., Milecki, P., Kruszyna-Mochalska, M., Misiarz, A., Pracz, J. & Malicki, J. FLASH radiotherapy: an emerging approach in radiation therapy. *Rep Pract Oncol Radiother* **27,** 344–351 (2022).

555. Prezado, Y. Divide and conquer: spatially fractionated radiation therapy. *Expert Reviews in Molecular Medicine* **24,** e3 (2022).

556. Eggold, J. T., Chow, S., Melemenidis, S., Wang, J., Natarajan, S., Loo, P. E., Manjappa, R., Viswanathan, V., Kidd, E. A., Engleman, E., Dorigo, O., Loo, B. W. & Rankin, E. B. Abdominopelvic FLASH Irradiation Improves PD-1 Immune Checkpoint Inhibition in Preclinical Models of Ovarian Cancer. *Molecular Cancer Therapeutics* **21,** 371–381 (2022).

557. Iturri, L., Bertho, A., Lamirault, C., Juchaux, M., Gilbert, C., Espenon, J., Sebrie, C., Jourdain, L., Pouzoulet, F., Verrelle, P., De Marzi, L. & Prezado, Y. Proton FLASH Radiation Therapy and Immune Infiltration: Evaluation in an Orthotopic Glioma Rat Model. *International Journal of Radiation Oncology*Biology*Physics* **116,** 655–665 (2023).

558. Bertho, A., Iturri, L., Brisebard, E., Juchaux, M., Gilbert, C., Ortiz, R., Sebrie, C., Jourdain, L., Lamirault, C., Ramasamy, G., Pouzoulet, F. & Prezado, Y. Evaluation of the Role of the Immune System Response After Minibeam Radiation Therapy. *International Journal of Radiation Oncology*Biology*Physics* **115,** 426–439 (2023).

559. Andrew J. Johnsrud, Samir V. Jenkins, A. Jamshidi-Parsian, Charles M. Quick, Edvaldo P. Galhardo, Ruud P.M. Dings, Kieng B. Vang, Ganesh Narayanasamy, Issam Makhoul, & Robert J. Griffin. Evidence for Early Stage Anti-Tumor Immunity Elicited by Spatially Fractionated Radiotherapy-Immunotherapy Combinations. *Radiation Research* **194,** 688–697 (2020).

560. Seoane, R., Vidal, S., Bouzaher, Y. H., El Motiam, A. & Rivas, C. The Interaction of Viruses with the Cellular Senescence Response. *Biology* **9,** (2020).

561. d'Adda di Fagagna, F. Living on a break: cellular senescence as a DNA-damage response. *Nature Reviews Cancer* **8,** 512–522 (2008).

562. Lilley, C. E., Schwartz, R. A. & Weitzman, M. D. Using or abusing: viruses and the cellular DNA damage response. *Trends in Microbiology* **15,** 119–126 (2007).

563. Luftig, M. A. Viruses and the DNA Damage Response: Activation and Antagonism. *Annu. Rev. Virol.* **1,** 605–625 (2014).

564. Stracker, T. H., Carson, C. T. & Weitzman, M. D. Adenovirus oncoproteins inactivate the Mre11–Rad50–NBS1 DNA repair complex. *Nature* **418,** 348–352 (2002).

565. Nikitin, P. A., Yan, C. M., Forte, E., Bocedi, A., Tourigny, J. P., White, R. E., Allday, M. J., Patel, A., Dave, S. S., Kim, W., Hu, K., Guo, J., Tainter, D., Rusyn, E. & Luftig, M. A. An ATM/Chk2-mediated DNA damage-responsive signaling pathway suppresses Epstein-Barr virus transformation of primary human B cells. *Cell Host Microbe* **8,** 510–522 (2010).

566. Hristova, D. B., Lauer, K. B. & Ferguson, B. J. Viral interactions with non-homologous end-joining: a game of hide-and-seek. *J Gen Virol* **101,** 1133–1144 (2020).

567. Burma, S. & Chen, D. J. Role of DNA–PK in the cellular response to DNA double-strand breaks. *DNA Repair* **3,** 909–918 (2004).

568. Musiani, D., Giambruno, R., Massignani, E., Ippolito, M. R., Maniaci, M., Jammula, S., Manganaro, D., Cuomo, A., Nicosia, L., Pasini, D. & Bonaldi, T. PRMT1 Is Recruited via DNA-PK to Chromatin Where It Sustains the Senescence-Associated Secretory Phenotype in Response to Cisplatin. *Cell Rep* **30,** 1208-1222.e9 (2020).

569. Ferguson, B. J., Mansur, D. S., Peters, N. E., Ren, H. & Smith, G. L. DNA-PK is a DNA sensor for IRF-3-dependent innate immunity. *eLife* **1,** e00047 (2012).

570. Peters, N. E., Ferguson, B. J., Mazzon, M., Fahy, A. S., Krysztofinska, E., Arribas-Bosacoma, R., Pearl, L. H., Ren, H. & Smith, G. L. A Mechanism for the Inhibition of DNA-PK-Mediated DNA Sensing by a Virus. *PLOS Pathogens* **9,** e1003649 (2013).

571. Scutts, S. R., Ember, S. W., Ren, H., Ye, C., Lovejoy, C. A., Mazzon, M., Veyer, D. L., Sumner, R. P. & Smith, G. L. DNA-PK Is Targeted by Multiple Vaccinia Virus Proteins to Inhibit DNA Sensing. *Cell Rep* **25,** 1953-1965.e4 (2018).

572. Postigo, A., Ramsden, A. E., Howell, M. & Way, M. Cytoplasmic ATR Activation Promotes Vaccinia Virus Genome Replication. *Cell Rep* **19,** 1022–1032 (2017).

573. Gameiro, S. R., Ardiani, A., Kwilas, A. & Hodge, J. W. Radiation-induced survival responses promote immunogenic modulation to enhance immunotherapy in combinatorial regimens. *OncoImmunology* **3,** e28643 (2014).

574. Reits, E. A., Hodge, J. W., Herberts, C. A., Groothuis, T. A., Chakraborty, M., K.Wansley, E., Camphausen, K., Luiten, R. M., de Ru, A. H., Neijssen, J., Griekspoor, A., Mesman, E., Verreck, F. A., Spits, H., Schlom, J., van Veelen, P. & Neefjes, J. J. Radiation modulates the peptide repertoire, enhances MHC class I expression, and induces successful antitumor immunotherapy. *Journal of Experimental Medicine* **203,** 1259–1271 (2006).

575. Gameiro, S. R., Malamas, A. S., Bernstein, M. B., Tsang, K. Y., Vassantachart, A., Sahoo, N., Tailor, R., Pidikiti, R., Guha, C. P. & Hahn, S. M. Tumor cells surviving exposure to proton or photon radiation share a common immunogenic modulation signature, rendering them more sensitive to T cell–mediated killing. *International Journal of Radiation Oncology* Biology* Physics* **95,** 120–130 (2016).

576. Garnett, C. T., Palena, C., Chakarborty, M., Tsang, K.-Y., Schlom, J. & Hodge, J. W. Sublethal Irradiation of Human Tumor Cells Modulates Phenotype Resulting in Enhanced Killing by Cytotoxic T Lymphocytes. *Cancer Research* **64,** 7985–7994 (2004).

577. Chakraborty, M., Abrams, S. I., Camphausen, K., Liu, K., Scott, T., Coleman, C. N. & Hodge, J. W. Irradiation of Tumor Cells Up-Regulates Fas and Enhances CTL Lytic Activity and CTL Adoptive Immunotherapy. *The Journal of Immunology* **170,** 6338–6347 (2003).

578. Gameiro, S. R., Jammeh, M. L., Wattenberg, M. M., Tsang, K. Y., Ferrone, S. & Hodge, J. W. Radiation-induced immunogenic modulation of tumor enhances antigen processing and calreticulin exposure, resulting in enhanced T-cell killing. *Oncotarget* **5,** 403–416 (2014).

579. Slavin-Chiorini, D. C., Catalfamo, M., Kudo-Saito, C., Hodge, J. W., Schlom, J. & Sabzevari, H. Amplification of the lytic potential of effector/memory CD8+ cells by vector-based enhancement of ICAM-1 (CD54) in target cells: implications for intratumoral vaccine therapy. *Cancer Gene Therapy* **11,** 665–680 (2004).